The Dissertation Committee for A.R.M. Nabiul Afrooz Certifies that this is the Approved

Version of the Following Dissertation:

AGGREGATION AND DEPOSITION OF GOLD NANOPARTICLES IN SINGULAR AND BINARY PARTICLE SYSTEMS: ROLE OF SIZE, SHAPE, AND ENVIRONMENTAL CHARACTERISTICS

Committee:

Navid B. Saleh, Supervisor

Desmond F. Lawler

Howard M. Liljestrand

Mary J. Kirisits

Brian A. Korgel

Aggregation and Deposition of Gold Nanoparticles in Singular and Binary Particle Systems: Role of Size, Shape, and Environmental Characteristics

by

A.R.M. Nabiul Afrooz, B.E.; M.E.

Dissertation
Presented to the Faculty of the Graduate School of
The University of Texas at Austin
In Partial Fulfillment
Of the Requirements for the Degree of

Doctor of Philosophy

The University of Texas at Austin
May 2015

Dedication

My Late Aunt, Momena Khatun

Acknowledgements

First and foremost, I would like to thank God for giving me the strength and patience to achieve the ultimate goal in my graduate studies. In the course of achieving this feat, I am indebted to several people for their selfless contribution in various ways. I would never have been able to finish my dissertation without their help and support.

I would like to express my deep gratitude and sincerest appreciation to my PhD supervisor, Dr. Navid Saleh, for his invaluable guidance, tremendous support, great patience and mentorship in the course of this research project. I am indebted to him forever for his continuous caring and encouragement in my life since the very first day I came to the USA for my graduate studies. I have learnt zillions from him, about research and life, throughout my PhD studies. I am blessed to have him as my PhD advisor in my academic journey.

I would also like to thank all the members of my dissertation committee. I am grateful to Dr. Desmond Lawler for his help and suggestions in designing the transport experiments and drafting the dissertation. My PhD studies would remain incomplete without attending his "Physico-chemical Treatment Processes" course and the discussions I was privileged to have with him during my early days at UT. His magical personality and words greatly inspired me every time I entered his room. And I thank Dr. Howard Liljestrand for his help during the admission process to the PhD program in Environmental Engineering at UT. I highly appreciate his feedback and recommendations to improve the writings and handing me a sample dissertation for proper formatting. I appreciate Dr. Mary J Kirisits's careful review of my PhD proposal and excellent feedback on the writings to that improve the final dissertation a lot. She was always supportive to me and my work. Finally, I would like to express my gratitude Dr. Brian A Korgel for taking the time to go through the dissertation carefully and insightful comments to improve the writing. I feel

honored to have Drs. Lynn Katz and Maria Juenger in my PhD Qualifying Examination committee and would like to acknowledge their input in broadening my core knowledge of Environmental Engineering.

I would extend my acknowledgement to the people who helped me in various material characterization techniques performed in the course of this research project. Especially, Dr. Haijun Qiang from Clemson University and Dr. Jervis Karalee from UT Austin for HRTEM. Dr. Iftheker Khan from University of Rhode-Island for cryo-TEM imaging. Dr. Richard Piner for Raman Spectroscopy. I also thank Zhengwang (Lisa) He for helping to get TOC data. Many thanks to Ms. RoseAnna Goewey, Mr. Charles Perego, Mr. Lamont Prosser, Mr. Danny Quiroz, and Mr. Phil Tomlin to make my life easier at UT Austin.

I am grateful to the current and past members of SusNWaTr research group. Especially Dr. Iftheker Khan and Nirupam for their assistance, advice and suggestions over the past 5 years. Thanks to Jaime for the amazing experimental schematics and to Stetson, without whom working in the lab could not be as fun as it was. Special word of thanks to my good friend, Dipesh, for helping me in the lab in finishing up the final project of the following dissertation. I also thank all the members of EWRE research group, specifically Anne, Bryant, Farith, Gustavo, Sarah, Sedat, SH, Sooyon, Sungmin, Emily, and Tongren, for making my days at UT exhilarating.

Thanks to my biggest supporter, my family, for their love and prayers during this process. Thanks to my parents for believing in me and doing all that they have done to encourage me in my life-long learning, including my pursuit of doctoral degree. Very special thanks extended to my loving wife, Sumaia, for being there through it all. She was always there to inspire me at the time of my toughest struggle and deepest frustrations.

Aggregation and Deposition of Gold Nanoparticles in Singular and Binary Particle Systems: Role of Size, Shape, and Environmental Characteristics

A.R.M. Nabiul Afrooz, Ph.D

The University of Texas at Austin, 2015

Supervisor: Navid B Saleh

Engineered nanomaterials (ENMs) are used in numerous applications due to their unique advantages. Gold nanomaterials (AuNMs) are one such functional ENM, which are utilized as model nanoparticles due to their controlled properties. AuNMs can be synthesized with highly uniform size and shape, where increase in the anisotropy gives rise to novel properties; e.g., unique Plasmon resonance, shape dependent physico-chemical properties, and quantum confinement, etc. These advantages have popularized the use of AuNMs in a wide range of applications in sensing, drug delivery, and photodynamic therapies. Increased use of these ENMs calls for systematic evaluation of the AuNMs to assess the effect of their size and shape on fate and transport in aquatic environment.

The natural environment, due to the presence of natural colloids and potential presence of secondary ENMs, presents additional system complexities in studying ENM fate and transport. This dissertation was designed to address two major data gaps: i.e., roles of i) anisotropy and ii) presence of secondary particles on aggregation and deposition of AuNMs. Poly-acrylic acid (PAA) coated uniform-sized gold nanospheres (AuNS) and nanorods (AuNR) are utilized as model nanoparticles. The first part of this research investigated the effect of shape of AuNMs on their

aggregation and deposition in singular particulate system under relevant ionic strengths. The second part of this dissertation focused on investigation of the effects of a secondary nanoparticle, i.e., pluronic acid modified single-walled carbon nanotubes (PA-SWNTs), on aggregation and filtration of AuNSs under a wide range of ionic strength.

Effects of shape of AuNMs on their aggregation kinetics were investigated by employing time resolved dynamic light scattering (TRDLS) in a wide range of mono- and di-valent electrolyte conditions. Aggregation histories were obtained for the AuNSs and AuNRs in presence of a wide range of NaCl and $CaCl_2$ conditions. The critical coagulation concentrations (CCCs), computed from the stability plots of the AuNMs, were used to compare the aggregation propensity of the PAA coated AuNSs with the AuNRs. The deposition kinetics was monitored using the quartz crystal microbalance with dissipation (QCM-D) technique for a range of NaCl concentrations. Deposition rates determined were used to understand the effects of shape of the AuNMs on their deposition kinetics. Experimental findings suggest that the shape of nanomaterials can influence interfacial properties and result in unique aggregation and deposition behavior under typical aquatic conditions

Effects of AuNS size on their aggregation behavior was investigated using citrate stabilized 30 nm and 60 nm sized National Institute of Standards and Technology (NIST) standard particles in biological media. Continuous size evolution of AuNS aggregates was monitored over a 24 h period employing DLS and static light scattering (SLS). Electrokinetic measurements, UV-vis spectroscopy, and electron microscopy were performed for material characterization. The findings from this study indicate that initial differences in AuNS sizes diminish over time as the particles aggregate under the influence of elevated ionic strength in the media. The results from this study

will likely influence characterization and experimental design considerations for *in vitro* nano-toxicity studies.

The effects of the presence of a secondary particle, PA-SWNTs, on hetero-aggregation behavior of PAA coated AuNS were systematically studied over a wide range of mono- and di-valent electrolyte conditions. PA modification of SWNTs made them stable in the entire range of electrolyte concentration where SWNT-SWNT aggregation has been eliminated via steric interaction. Hetero-aggregation mechanisms of AuNS were deciphered utilizing electron microscopy and electrokinetics. Experimental results suggest that the AuNS aggregates faster in hetero-dispersion in presence of PA-SWNT than in homo-disperstion at elevated ionic strength. However, hetero-rates are slower in case of low ionic strength cases. Techniques developed in this study can be can be adopted elsewhere to assess hetero-aggregation of a wider set of ENMs, hence achieving reliability in nanoparticle environmental exposure and risk.

Co-transport of AuNS in presence of PA-SWNTs through saturated porous media was also assessed using bench-scale column experiments under a wide range of aquatic conditions (1-100 mM NaCl). Homogenous AuNS suspensions were utilized as control to compare their breakthrough properties with those of the AuNS hetero-dispersions (in presence of PA-SWNTs). This study also assessed the role of pre-coating of the collectors (with PA-SWNTs) on AuNS' mobility to understand the order of introduction of the secondary particles. The study results demonstrate that the presence of secondary particles and the order in which these are introduced to the experimental system strongly influence AuNS mobility. Thus ENM can be highly mobile or can get strongly filtered out, depending on the secondary PA-SWNT and background environmental conditions.

This research not only evaluates the role of material attributes in their fate and transport but also extends to assess the role of environmental complexities on the same. The research findings enhance our current understanding of environmental interaction of the ENMs and call for further studies, incorporating additional complexities (i.e., material and system), to assess the fate, transport, and effects of the ENMs in the natural environment.

Table of Contents

List of Tables

List of Figures

Chapter 1

Background and Introduction

1.1 Introduction

Inspired by molecular engineering and guided by Richard Feynman's vision, the nanotechnology revolution has enabled material scientists and engineers to take control over atomistic manipulation. Such tremendous capacity of nano-scale engineering has become evident by the discovery of geodesic structures, i.e., fullerenes in 1985. Since then engineered nanomaterials (ENM) have become the primary building blocks of new technologies, guiding and shaping the directions of numerous commercial and service product lines with an estimated market value of $26 billion in 2014, and projected to reach $64.2 billion by 2019[1]. The nanotechnology revolution, alongside the technological advancement, poses risk of exposing new class of contaminants (i.e., ENMs) to the environment following unique fate and transport processes. Broadly, this dissertation focuses on the effect of ENMs' physico-chemical properties and environmental complexities on the fate and transport of ENMs.

1.2 Environmental Release of the Engineered Nanoparticles

ENMs are defined as materials with at least one dimension between 1-100 nm, possessing unique properties compared to their bulk counterpart. This novel material-class with superior physical, chemical, electrical, and biological properties are now ubiquitously used in a large number of consumer products ranging in a wide category of appliances: automotive, electronics, personal care, cleaning, construction, home furnishing, and textiles[2]. ENMs have also been used in various other applications, which include but are not limited to coatings, drug delivery, solar cells, and sensors[3]. Unlike bulk materials, nanomaterials' size and shape have distinct effect on their properties that inspired interest and subsequent control over these attributes to tune ENMs properties. For instance, rod-like NMs[4-10], i.e., tubes, wires, rods, and whiskers, with large

diameter to length ratio (i.e., aspect ratio) present unique optical[11], thermal[12], and electrical[13] properties and impart multifunctionality in a wide range of applications[5, 14-16].

Carbonaceous nanomaterials (e.g., single-walled and multiwalled carbon nanotubes), with diameters in the nano-scale and lengths in microns, are known to be the first and primary anisotropic nano-scale materials[17-19]. Anisotropic carbonaceous NMs are widely used[20] in antimicrobial coatings[21], conducting films[22], microelectronics[23], energy storage[24], and biotechnology[25]. Anisotropic metallic NMs on the other hand, i.e., metallic nanorods and nanowires[5, 26, 27], are widely used in energy sectors and biomedical applications. For example, silver nanorods are used in antimicrobial applications[28], while zinc-oxide rods are utilized in hydrogen storage[14], field emission devices[29, 30], solar cells[31-33], and sensing applications[34-37]. Rod-shaped titanium dioxides are used in photo-electrochemical applications[38-42], while gold nanorods (AuNRs) are used in biological sensing, drug, and gene delivery[43-49]. Anisotropic ENMs are gaining increasing interests as material scientists are mastering their abilities to 'dial in' desired optical, chemical, and electronic properties by gaining control over their aspect ratio.

Such widespread usage of and continued interests in anisotropic NMs indicate that these materials will be released in the natural environment. Hence appropriate attention to assess their environmental health and safety (EHS) and risk assessment is highly desired. Environmental release of any ENM may occur intentionally, e.g., via their usage in environmental remediation or during the manufacturing process, or unintentionally, e.g., accidental or inappropriate disposal of NMs from consumer products. Upon release at different stages of their life cycle, ENMs are likely to participate in various physical (e.g., aggregation and disaggregation, sedimentation and resuspension, deposition and release), chemical (e.g., dissolution, sorption, redox, surface coating replacement), and biological (e.g., uptake, bio-macromolecule-ENM interaction, and

microorganism-mediated chemical transformation) processes[50]. These fate and transport processes are also known to influence subsequent environmental transformation of ENMs. Therefore, reliable nano-EHS necessitates systematic assessment of environmental fate and transport of ENMs as a function of material attributes as well as environmental parameters.

1.3 Aggregation and Deposition of Nanoparticles

Natural water typically consists of several dissolved species and ions. The ionic strength of the natural water varies on the basis of its source. In general, freshwater ionic strength ranges between 1-10 mM, while potable or drinking water ionic strength has 1-20 mM range, with seawater having ionic strength of greater than 700 mM[51]. In the presence of such ionic species, randomly moving (under the influence of Brownian diffusion) charged nanoparticles usually experience electrical double layer compression, followed by particle-particle attachment. This attachment process is an interplay between attractive van der Waals (VDW) attraction and repulsive electrostatic double layer forces[52]. Such (irreversible) agglomeration of multiple particles, commonly termed as aggregation, is the physico-chemical process that all ENM will undergo when released in natural and engineered aquatic environments. This particle-particle attachment process has been studied systematically over the past half-a-century by environmental engineers and colloidal scientists with an interest to remove particulate contaminants from water in water and wastewater treatment plants[53]. Aggregation of ENMs will not only modulate particle size over time but will also influence their settling, mobility, bioavailability, and toxicity in aquatic and soil systems[54, 55].

Groundwater aquifer and marine sediments are the two most likely sinks of ENMs in the natural environment. In these micro-environments, ENMs interact with natural surfaces (e.g., soil or collector grains) and can get deposited or removed from the water streams. Elemental composition and surface chemistry of the ENMs, aggregation state, ionic strength of the pore

water, physical and geo-chemical nature of the porous media, pore water velocity, and redox-state and pH are factors known to influence ENM deposition in natural porous media. ENMs' mobility and persistence in the porous media determines their potential exposure to the soil and benthic organisms. Moreover, understanding ENM's deposition through the porous media is extremely important in assessing their removal mechanism during conventional sand filtration processes and also in predicting their transport during groundwater and soil remediation application.

Aggregation and deposition behavior of ENMs are the key piece of the complex puzzle of nano-EHS. Despite considerable improvement in understanding aggregation and deposition processes in the lab-scale clean systems, the role of material attributes (size, shape, surface functionality) and environmental complexities (i.e., presence of other particulate matter, bio- and geo-macromolecules, collector heterogeneity) are understudied[54, 56]. These environmental and material complexities are likely to influence ENMs' aggregation, deposition, and transformation in the natural environment[57], thus demanding complete mechanistic understanding of such influences through experimental and theoretical investigations.

1.3.1 Role of Anisotropy on Aggregation and Deposition

Classical Derjaguin-Landau-Verwey-Overbeek (DLVO) theory is generally used to predict ENMs' aggregation and deposition behavior[58-65]. In addition, clean-bed filtration theory (CFT) is utilized to predict NM mobility in porous environmental systems[60, 62, 64, 65]. However, rod-shaped NMs, due to their anisotropic geometry, violate most fundamental assumptions of these theoretical formulations and experimental predictions, exhibiting unknown aggregation rates[66], fractal structures,[67] and unique filtration mechanisms[68].

Classical colloidal literature bears evidence of particle geometry playing a significant role in modulating aggregation propensity[69], deposition mechanism[70], and surface interaction[71]. Extent

of VDW attraction has been described to be stronger between the anisotropic particles because of greater number of atoms in close proximity in a rod shaped particle compared to a spherical one[71]. Shape of a colloid also influences the effective drag force acting on the particle in the aqueous suspensions[72]. However, systematic assessment of variation of geometric parameters on ENM interaction is scarce. To date, studies on fate and transport of anisotropic NMs have mostly been limited to carbon nanotubes (with little to no control over aspect ratio within the same sample) [62, 64, 73-78], with unresolved mechanisms for aggregation and deposition of these materials. Inspired by colloidal evidences, some recent studies[79, 80] reported shape-dependent aggregation characteristics of ENMs in environmentally relevant solution chemistry. While our knowledge and understanding about aggregation behavior is expanding, detailed mechanistic understanding of the shape-effect on aggregation and deposition is yet to be discerned.

1.3.2 Role of Secondary Particles on Aggregation and Deposition

Natural environmental conditions are typically simulated by varying pH, ionic strength, and natural organic matter in the experimental studies. Though the natural aquatic environments can contain naturally occurring particles or previously released ENMs, nano-EHS studies are lacking in evaluating the role of such secondary particulate entities. Colloidal aggregation literature has put considerable focus in understanding interaction between dissimilar (with respect to charge, size, shape, and elemental composition) particles[81, 82]. Extension of these studies to ENM aggregation and deposition has been limited. Introduction of environmental complexity with secondary particles in ENM aggregation processes is challenging due to the difficulty in distinguishing between primary and secondary particles using the common experimental tools. ENM deposition assessment on the other hand has also been limited to single particle systems with continued challenges in theoretical and mechanistic understanding of these processes.

Complexity of natural systems arises from the presence of pre-existing colloids that cause altered aggregation (hetero-aggregation) behavior and also can alter particle transport through porous media (co-transport). The hetero-aggregation problem has primarily been addressed in studies relevant to chemical applications (e.g., toners, advanced ceramics, core-shell composites, etc.) or in case of natural waters containing clay or other colloids, using symmetric spherical colloids[83-87]. Additionally, complexity and heterogeneity of natural aqueous systems is well known in the literature to have significant impact on ENM behavior[63, 68, 74, 88, 89]. In earlier ENM studies, NOM has been widely used as an effort to mimic the effect of system complexity on the aggregation and deposition behavior of ENMs[56, 90]. Some recent studies[90-93] also reported the effect of bacteria and biofilm on the aggregation and deposition of NMs. However, the number of systematic studies evaluating aggregation and deposition behavior of ENMs in presence of a secondary NM is small. Therefore, a critical data gap also exists in understanding hetero-aggregation/co-deposition behavior of NMs in representative aqueous or subsurface environments. Consequently, reliability issues emanate regarding ENMs' aggregation and deposition data from the large gap between the conditions used in such studies and those that exist in the natural environment.

1.4 Problem Statement and Significance

Systematic evaluation of environmental behavior of anisotropic ENMs calls for uniformity in particle geometry, which requires careful control in the synthesis process. Gold nanomaterials (AuNMs) are among the few ENMs, where control over synthesizing highly uniform particles (in terms of size and shape) has been achieved[94, 95]. Gold enjoys many advantages over other metallic nanoparticles: it is considerably less redox-active, chemically very stable, and has low background in natural waters; making it easy to detect either optically or by inductively-coupled plasma mass

spectrometry (ICP-MS). For these reasons, AuNMs have often been used as a model in fundamental studies of nano-EHS.

Even though isotropic (gold nanospheres, AuNS) and anisotropic (AuNR) nanoparticles are assumed to be safe to use has led to their incorporation in a number of biomedical applications[96], recent *in vitro* and *in vivo* findings have demonstrated significant toxic responses of AuNMs in model biological systems[77, 96-106 98, 101, 107-109]. Cellular necrosis and apoptosis may occur at certain doses depending on AuNR aspect ratio[100, 101]. Moreover, AuNRs have been shown to bind to DNA, causing conformational changes that affect transcription[110]. AuNRs have also been found to induce inflammatory response and apoptosis in the liver of higher vertebrates such as mice[77, 96, 97]. The toxicological potential of AuNRs together with their advantages as model NMs provide support for their usage in systematic and mechanistic studies to better understand potential risks associated with anisotropic ENMs in general.

As noted earlier, a data gap in reliable fate and transport properties (incorporating the material and system complexities) of ENMs make exposure analyses difficult and to date have resulted in a lack of regulation of NM usage[111, 112]. Evaluation of the aggregation and deposition of AuNRs could potentially address the data gap in the ENMs' fate and transport literature in terms of material complexity. However, any complete risk assessment of AuNMs must incorporate environmental complexities in the experimental design. Therefore, there is a critical need for systematic research in understanding the role of anisotropy and environmental complexity on the fate and transport of AuNMs.

1.5 Research Objectives

Appreciating the aforementioned data gap, this dissertation aims to achieve three specific goals: first, investigating the role of size and shape on the aggregation and deposition behavior of

AuNMs; second, assessing the role of secondary entity on aggregation kinetics of AuNMs, i.e., hetero-aggregation; and third, transport of AuNMs through porous media in presence of a pre-existing NM (e.g., carbon nanotube), i.e., co-transport. AuNSs in combination with nonionic polymer, pluronic acid coated single-walled carbon nanotubes (PA-SWNTs) are used to evaluate such aggregation and transport behavior in binary particulate systems and under a wide range of environmentally relevant conditions.

1.6 Research Hypotheses

Hypothesis 1: Size and shape of AuNMs will influence their aggregation and deposition in aquatic environment

Hypothesis 2: Presence of secondary NMs (e.g., PA-SWNT) will alter AuNS aggregation behavior

Hypothesis 3: Transport of AuNS through porous media will be influenced by the secondary particles, e.g., PA-SWNTs' presence

1.7 Approach and Methodology

In this research AuNMs are used to assess the role of anisotropy and system complexity on the aggregation and deposition of the nanoparticles. SWNTs are used as the secondary NMs. Accomplishment of the stated research goals involves successful completion of the tasks outlined below.

Task 1. a) Role of shape on aggregation and deposition kinetics of AuNM

b) Role of preliminary size in the aggregation of AuNS under high salinity

Task 2. Hetero-aggregation of AuNS in presence of PA-SWNT

Task 3. Co-transport of AuNS in presence of PA-SWNT

1.8 Organization of the Dissertation

The dissertation is organized in six chapters and four appendices. The body consists of chapters 2, 3, 4, and 5, which comprise of the materials prepared for publication in peer reviewed journals of Chemosphere, Journal of Nanoparticle Research, and Environmental Science and Technology. Chapter 1 presents the introduction to this dissertation with a brief overview on ENMs' aggregation and deposition, data gap, problem statement and significance, research objective, and hypotheses.

Chapter 2 presents research results that test the first hypothesis; i.e., studying the influence of shape on the aggregation and deposition, employing PAA coated AuNSs and AuNRs. Dynamic light scattering (DLS) and quartz-crystal-microbalance with dissipation (QCM-D) were used for aggregation and deposition study, respectively. This work was led by A. R. M. Nabiul Afrooz and co-authored by Sean T. Sivalapalan, Catherine J. Murphy, Saber M. Hussain, John J. Schlager, and Navid B. Saleh and was published in *Chemosphere* in December 2012, with a title[113] "Spheres vs. Rods: The Shape of Gold Nanoparticles Influences Aggregation and Deposition Behavior".

Chapter 3 is considered a continuation of the evaluation of the first hypothesis. This study provides an insight on the effect of ENMs' preliminary diameter on their aggregation behavior under high salinity condition. PAA-coated AuNSs were exposed to cell culture media to monitor their aggregate size and structure over 24 h. This work was led by A. R. M. Nabiul Afrooz and co-authored by Saber M. Hussain and Navid B. Saleh and was published in *Journal of Nanoparticle Research* in December 2014, with the title[114] "Aggregate size and structure determination of nanomaterials- Importance of dynamic evolution".

Chapter 4 presents the task performed to test the second hypothesis. It presents a novel technique to assess influence of a secondary ENMs on AuNS aggregation using DLS and transmission electron microscopy (TEM). PAA-coated AuNS and PA-SWNTs have been used to

study hetero-aggregation of AuNSs under a wide range of ionic strength. Effect of natural organic matter (NOM) on hetero-aggregation of AuNSs was also presented. This work was led by A. R. M. Nabiul Afrooz and co-authored by Iftheker A. Khan, Saber M. Hussain, and Navid B. Saleh and was published in *Environmental Science and Technology* in January 2013, with the title[115] "Mechanistic Hetero-aggregation of Gold Nanoparticles in a Wide Range of Solution Chemistry".

Chapter 5 presents a systematic study to investigate the final hypothesis. This chapter presents experimental results of PAA-coated AuNS transport through saturated porous media in presence of PA-SWNTs. This study also evaluates effects of coated collectors with PA-SWNTs (already filtered out SWNTs) on AuNS transport. The effects of NOM on co-transport of AuNS-SWNT has been assessed. This article will be submitted for publication and will be led by A. R. M. Nabiul Afrooz and co-authored by Dipesh Das, Catherine J. Murphy, Peter Vikesland, and Navid B. Saleh. The tentative title of the manuscript is "Co-transport of Gold Nanoparticles with Single-Walled Carbon Nanotubes in Saturated Porous Media".

The final chapter (Chapter 6) presents the summary, conclusions, environmental implications, and future recommendations relevant to ENM fate, transport, and toxicity.

1.8 Literature Cited

1. Research, B. *Nanotechnology: A Realistic Market Assessment*; 2014.
2. CPI Nanoparticle consumer products inventory http://www.nanotechproject.org/cpi/browse/categories/ (Feb 26),
3. Pérez, J.; Bax, L.; Escolano, C. *Roadmap Report on Nanoparticles*; Willems & van den Wildenberg sl: Barcelona, Spain, 2005; pp 26-28.
4. Salem, A. K.; Searson, P. C.; Leong, K. W., Multifunctional nanorods for gene delivery. *Nat Mater* **2003,** *2*, (10), 668-671.
5. Murphy, C. J.; Thompson, L. B.; Alkilany, A. M.; Sisco, P. N.; Boulos, S. P.; Sivapalan, S. T.; Yang, J. A.; Chernak, D. J.; Huang, J., The Many Faces of Gold Nanorods. *The Journal of Physical Chemistry Letters* **2010**, 2867-2875.
6. Richter, G.; Hillerich, K.; Gianola, D. S.; MoÌˆnig, R.; Kraft, O.; Volkert, C. A., Ultrahigh Strength Single Crystalline Nanowhiskers Grown by Physical Vapor Deposition. *Nano Letters* **2009,** *9*, (8), 3048-3052.
7. Yang, P.; Yan, R.; Fardy, M., Semiconductor Nanowire: What's Next? *Nano Letters* **2010,** *10*, (5), 1529-1536.
8. Yuzvinsky, T. D.; Mickelson, W.; Aloni, S.; Begtrup, G. E.; Kis, A.; Zettl, A., Shrinking a Carbon Nanotube. *Nano Letters* **2006,** *6*, (12), 2718-2722.
9. Khan, I. A.; Ferguson, P. L.; Sabo-Attwood, T.; Saleh, N. B. In *Systematic change in chirality affects aggregation kinetics of single-walled carbon nanotubes* 240th ACS National Meeting, Boston, MA, 2010; Boston, MA, 2010.
10. Murphy, C. J.; San, T. K.; Gole, A. M.; Orendorff, C. J.; Gao, J. X.; Gou, L.; Hunyadi, S. E.; Li, T., Anisotropic metal nanoparticles: Synthesis, assembly, and optical applications. *J. Phys. Chem. B* **2005,** *109*, (29), 13857-13870.
11. Pérez-Juste, J.; Pastoriza-Santos, I.; Liz-Marzán, L. M.; Mulvaney, P., Gold nanorods: Synthesis, characterization and applications. *Coordination Chemistry Reviews* **2005,** *249*, (17-18), 1870-1901.
12. Yang, B.; Han, Z. H., Temperature-dependent thermal conductivity of nanorod-based nanofluids. *Appl. Phys. Lett.* **2006,** *89*, (8), 3.
13. Kwak, C. H.; Kim, B. H.; Park, C. I.; Seo, S. Y.; Kim, S. H.; Han, S. W., Structural and electrical properties of ZnO nanorods and Ti buffer layers. *Appl. Phys. Lett.* **2010,** *96*, (5), 3.
14. Wan, Q.; Lin, C. L.; Yu, X. B.; Wang, T. H., Room-temperature hydrogen storage characteristics of ZnO nanowires. *Appl. Phys. Lett.* **2004,** *84*, (1), 124-126.
15. Huynh, W. U.; Dittmer, J. J.; Alivisatos, A. P., Hybrid nanorod-polymer solar cells. *Science* **2002,** *295*, (5564), 2425-2427.
16. Chang, W.-S.; Ha, J. W.; Slaughter, L. S.; Link, S., Plasmonic nanorod absorbers as orientation sensors. *Proceedings of the National Academy of Sciences* **2010,** *107*, (7), 2781-2786.
17. Iijima, S.; Ichihashi, T., Single-shell carbon nanotubes of 1-nm diameter. *Nature* **1993,** *363*, (6430), 603-605.
18. Mani, R. C.; Li, X.; Sunkara, M. K.; Rajan, K., Carbon Nanopipettes. *Nano Letters* **2003,** *3*, (5), 671-673.
19. *Consumer product inventories*; Woodrow Wilson International Center for Scholars: Washington, DC, 2010.
20. De Volder, M. F.; Tawfick, S. H.; Baughman, R. H.; Hart, A. J., Carbon nanotubes: present and future commercial applications. *Science* **2013,** *339*, (6119), 535-539.

21. Beigbeder, A.; Degee, P.; Conlan, S. L.; Mutton, R. J.; Clare, A. S.; Pettitt, M. E.; Callow, M. E.; Callow, J. A.; Dubois, P., Preparation and characterisation of silicone-based coatings filled with carbon nanotubes and natural sepiolite and their application as marine fouling-release coatings. *Biofouling* **2008,** *24*, (4), 291-302.
22. Wu, Z.; Chen, Z.; Du, X.; Logan, J. M.; Sippel, J.; Nikolou, M.; Kamaras, K.; Reynolds, J. R.; Tanner, D. B.; Hebard, A. F., Transparent, conductive carbon nanotube films. *Science* **2004,** *305*, (5688), 1273-1276.
23. Ionescu, A. M.; Riel, H., Tunnel field-effect transistors as energy-efficient electronic switches. *Nature* **2011,** *479*, (7373), 329-337.
24. Dai, L.; Chang, D. W.; Baek, J. B.; Lu, W., Carbon nanomaterials for advanced energy conversion and storage. *Small* **2012,** *8*, (8), 1130-1166.
25. De La Zerda, A.; Zavaleta, C.; Keren, S.; Vaithilingam, S.; Bodapati, S.; Liu, Z.; Levi, J.; Smith, B. R.; Ma, T.-J.; Oralkan, O., Carbon nanotubes as photoacoustic molecular imaging agents in living mice. *Nature nanotechnology* **2008,** *3*, (9), 557-562.
26. Xiang, J.; Lu, W.; Hu, Y.; Wu, Y.; Yan, H.; Lieber, C. M., Ge/Si nanowire heterostructures as high-performance field-effect transistors. *Nature* **2006,** *441*, (7092), 489-493.
27. Tian, B.; Zheng, X.; Kempa, T. J.; Fang, Y.; Yu, N.; Yu, G.; Huang, J.; Lieber, C. M., Coaxial silicon nanowires as solar cells and nanoelectronic power sources. *Nature* **2007,** *449*, (7164), 885-889.
28. Akhavan, O.; Ghaderi, E., Enhancement of antibacterial properties of Ag nanorods by electric field. *Sci. Technol. Adv. Mater.* **2009,** *10*, (1).
29. Dev, A.; Kar, S.; Chakrabarti, S.; Chaudhuri, S., Optical and field emission properties of ZnO nanorod arrays synthesized on zinc foils by the solvothermal route. *Nanotechnology* **2006,** *17*, (5), 1533-1540.
30. Yoon, S. H.; Yang, H.; Kim, Y. S., Synthesis of ZnO nanorods and their application to hybrid plasma display panels for reduction of discharge voltages. *J. Ceram. Process. Res.* **2007,** *8*, (4), 261-265.
31. Jiang, X. X.; Chen, F.; Xu, H.; Yang, L. G.; Qiu, W. M.; Shi, M. M.; Wang, M.; Chen, H. Z., Template-free synthesis of vertically aligned CdS nanorods and its application in hybrid solar cells. *Sol. Energy Mater. Sol. Cells* **2010,** *94*, (2), 338-344.
32. Na, S. I.; Kim, S. S.; Hong, W. K.; Park, J. W.; Jo, J.; Nah, Y. C.; Lee, T.; Kim, D. Y., Fabrication of TiO2 nanotubes by using electrodeposited ZnO nanorod template and their application to hybrid solar cells. *Electrochim. Acta* **2008,** *53*, (5), 2560-2566.
33. Yin, Z. Y.; Wu, S. X.; Zhou, X. Z.; Huang, X.; Zhang, Q. C.; Boey, F.; Zhang, H., Electrochemical Deposition of ZnO Nanorods on Transparent Reduced Graphene Oxide Electrodes for Hybrid Solar Cells. *Small* **2010,** *6*, (2), 307-312.
34. Fang, F.; Futter, J.; Markwitz, A.; Kennedy, J., UV and humidity sensing properties of ZnO nanorods prepared by the arc discharge method. *Nanotechnology* **2009,** *20*, (24).
35. Fulati, A.; Ali, S. M. U.; Riaz, M.; Amin, G.; Nur, O.; Willander, M., Miniaturized pH Sensors Based on Zinc Oxide Nanotubes/Nanorods. *Sensors* **2009,** *9*, (11), 8911-8923.
36. Ogata, K.; Koike, K.; Sasa, S.; Inoue, M.; Yano, M., ZnO nanorod arrays on n-type Si(111) substrates for pH measurements. *J. Vac. Sci. Technol. B* **2009,** *27*, (3), 1684-1687.
37. Water, W.; Chen, S. E., Using ZnO nanorods to enhance sensitivity of liquid sensor. *Sens. Actuator B-Chem.* **2009,** *136*, (2), 371-375.
38. Adachi, M.; Jiu, J.; Isoda, S., Synthesis of morphology-controlled titania nanocrystals and application for dye-sensitized solar cell's. *Curr. Nanosci.* **2007,** *3*, (4), 285-295.

39. Bao, S. J.; Bao, Q. L.; Li, C. M.; Dong, Z. L., Novel porous anatase TiO2 nanorods and their high lithium electroactivity. *Electrochem. Commun.* **2007,** *9*, (5), 1233-1238.
40. Kislyuk, V. V.; Dimitriev, O. P., Nanorods and nanotubes for solar cells. *J. Nanosci. Nanotechnol.* **2008,** *8*, (1), 131-148.
41. Wei, Q. S.; Hirota, K.; Tajima, K.; Hashimoto, K., Design and synthesis of TiO2 nanorod assemblies and their application for photovoltaic devices. *Chem. Mat.* **2006,** *18*, (21), 5080-5087.
42. Yao, Q. H.; Liu, J. F.; Peng, Q.; Wang, X.; Li, Y. D., Nd-doped TiO2 nanorods: Preparation and application in dye-sensitized solar cells. *Chem.-Asian J.* **2006,** *1*, (5), 737-741.
43. Chanda, N.; Shukla, R.; Katti, K. V.; Kannan, R., Gastrin releasing protein receptor specific gold nanorods: Breast and prostate tumor avid nanovectors for molecular imaging. *Nano Lett.* **2009,** *9*, (5), 1798-1805.
44. Ding, H.; Yong, K. T.; Roy, I.; Pudavar, H. E.; Law, W. C.; Bergey, E. J.; Prasad, P. N., Gold nanorods coated with multilayer polyelectrolyte as contrast agents for multimodal imaging. *J. Phys. Chem. C* **2007,** *111*, (34), 12552-12557.
45. Durr, N. J.; Larson, T.; Smith, D. K.; Korgel, B. A.; Sokolov, K.; Ben-Yakar, A., Two-photon luminescence imaging of cancer cells using molecularly targeted gold nanorods. *Nano Lett.* **2007,** *7*, (4), 941-945.
46. Eghtedari, M.; Liopo, A. V.; Copland, J. A.; Oraevslty, A. A.; Motamedi, M., Engineering of Hetero-Functional Gold Nanorods for the in vivo Molecular Targeting of Breast Cancer Cells. *Nano Lett.* **2009,** *9*, (1), 287-291.
47. El-Sayed, I. H.; Huang, X. H.; El-Sayed, M. A., Surface plasmon resonance scattering and absorption of anti-EGFR antibody conjugated gold nanoparticles in cancer diagnostics: Applications in oral cancer. *Nano Lett.* **2005,** *5*, (5), 829-834.
48. Huff, T. B.; Tong, L.; Zhao, Y.; Hansen, M. N.; Cheng, J. X.; Wei, A., Hyperthermic effects of gold nanorods on tumor cells. *Nanomedicine* **2007,** *2*, (1), 125-132.
49. Kawano, T.; Niidome, Y.; Mori, T.; Katayama, Y.; Niidome, T., PNIPAM Gel-Coated Gold Nanorods, for Targeted Delivery Responding to a Near-Infrared Laser. *Bioconjugate Chem.* **2009,** *20*, (2), 209-212.
50. Mueller, N. C.; Nowack, B., Exposure modeling of engineered nanoparticles in the environment. *Environmental Science & Technology* **2008,** *42*, (12), 4447-4453.
51. Ibanez, J. G.; Hernandez-Esparza, M.; Doria-Serrano, C.; Fregoso-Infante, A.; Singh, M. M., *Environmental chemistry: fundamentals*. Springer Science & Business Media: 2010.
52. Saleh, N. B.; Afrooz, A. R. M. N.; Aich, N.; Plazas-Tuttle, J., Aggregation kinetics and fractal dimensions of nanomaterials in environmental systems. In *Engineered nanoparticles and the environment: Biophysico-chemical processes and biotoxicity*, 2015.
53. Lawler, D.; Benjamin, M., *Water Quality Engineering: Physical-Chemical Treatment Processes*. McGraw-Hill: 2003.
54. Hotze, E. M.; Phenrat, T.; Lowry, G. V., Nanoparticle aggregation: challenges to understanding transport and reactivity in the environment. *Journal of environmental quality* **2010,** *39*, (6), 1909-1924.
55. Borm, P.; Klaessig, F. C.; Landry, T. D.; Moudgil, B.; Pauluhn, J.; Thomas, K.; Trottier, R.; Wood, S., Research strategies for safety evaluation of nanomaterials, part V: role of dissolution in biological fate and effects of nanoscale particles. *Toxicological Sciences* **2006,** *90*, (1), 23-32.

56. Petosa, A. R.; Jaisi, D. P.; Quevedo, I. R.; Elimelech, M.; Tufenkji, N., Aggregation and deposition of engineered nanomaterials in aquatic environments: role of physico-chemical interactions. *Environmental science & technology* **2010,** *44*, (17), 6532-6549.
57. Lowry, G.; Casman, E., Nanomaterial transport, transformation, and fate in the environment. In *Nanomaterials: risks and benefits*, Springer: 2009; pp 125-137.
58. Chen, K. L.; Elimelech, M., Aggregation and deposition kinetics of fullerene (C-60) nanoparticles. *Langmuir* **2006,** *22*, (26), 10994-11001.
59. Chen, K. L.; Elimelech, M., Influence of humic acid on the aggregation kinetics of fullerene (C-60) nanoparticles in monovalent and divalent electrolyte solutions. *J. Colloid Interface Sci.* **2007,** *309*, (1), 126-134.
60. Chen, K. L.; Mylon, S. E.; Elimelech, M., Aggregation kinetics of alginate-coated hematite nanoparticles in monovalent and divalent electrolytes. *Environ. Sci. Technol.* **2006,** *40*, (5), 1516-1523.
61. Chen, K. L.; Smith, B. A.; Ball, W. P.; Fairbrother, D. H., Assessing the colloidal properties of engineered nanoparticles in water: case studies from fullerene C-60 nanoparticles and carbon nanotubes. *Environ. Chem.* **2009,** *7*, (1), 10-27.
62. Chen, Q.; Saltiel, C.; Manickavasagam, S.; Schadler, L. S.; Siegel, R. W.; Yang, H. C., Aggregation behavior of single-walled carbon nanotubes in dilute aqueous suspension. *J. Colloid Interface Sci.* **2004,** *280*, (1), 91-97.
63. Saleh, N.; Kim, H. J.; Phenrat, T.; Matyjaszewski, K.; Tilton, R. D.; Lowry, G. V., Ionic strength and composition affect the mobility of surface-modified Fe-0 nanoparticles in water-saturated sand columns. *Environ. Sci. Technol.* **2008,** *42*, (9), 3349-3355.
64. Saleh, N. B.; Pfefferle, L. D.; Elimelech, M., Aggregation kinetics of multiwalled carbon nanotubes in aquatic systems: Measurements and environmental implications. *Environ. Sci. Technol.* **2008,** *42*, (21), 7963-7969.
65. Saleh, N. B.; Pfefferle, L. D.; Elimelech, M., Influence of Biomacromolecules and Humic Acid on the Aggregation Kinetics of Single-Walled Carbon Nanotubes. *Environmental Science & Technology* **2010,** *44*, (7), 2412-2418.
66. Puisto, A.; Illa, X.; Mohtaschemi, M.; Alava, M., Modeling the viscosity and aggregation of suspensions of highly anisotropic nanoparticles. *The European Physical Journal E: Soft Matter and Biological Physics* **2012,** *35*, (1), 1-7.
67. Mohraz, A.; Moler, D. B.; Ziff, R. M.; Solomon, M. J., Effect of Monomer Geometry on the Fractal Structure of Colloidal Rod Aggregates. *Physical Review Letters* **2004,** *92*, (15), 155503.
68. Bradford, S. A.; Yates, S. R.; Bettahar, M.; Simunek, J., Physical factors affecting the transport and fate of colloids in saturated porous media. *Water Resour. Res.* **2002,** *38*, (12).
69. Klein, R.; Meakin, P., Universality in colloid aggregation. *Nature* **1989,** *339*.
70. Okubo, T.; Aotani, S., Microscopic observation of ordered colloids in sedimentation equilibrium and the importance of Debye-screening length. 8. Unsymmetrical ordering and inclusion of anisotropic particles. *Colloid and Polymer Science* **1988,** *266*, (11), 1049-1057.
71. Vold, M. J., Van der Waals' attraction between anisometric particles. *Journal of Colloid Science* **1954,** *9*, (5), 451-459.
72. Youngren, G.; Acrivos, A., Stokes flow past a particle of arbitrary shape: a numerical method of solution. *Journal of fluid Mechanics* **1975,** *69*, (02), 377-403.

73. Saleh, N. B.; Pfefferle, L. D.; Elimelech, M., Influence of biomacromolecules and humic acid on the aggregation kinetics of single-walled carbon nanotubes. *Environ. Sci. Technol.* **2010,** *44*, (7), 2412-2418.
74. Jaisi, D. P.; Elimelech, M., Single-walled carbon nanotubes exhibit limited transport in soil columns. *Environ. Sci. Technol.* **2009,** *43*, (24), 9161-9166.
75. Liu, X. Y.; O'Carroll, D. M.; Petersen, E. J.; Huang, Q. G.; Anderson, C. L., Mobility of multiwalled carbon nanotubes in porous media. *Environ. Sci. Technol.* **2009,** *43*, (21), 8153-8158.
76. Smith, B.; Wepasnick, K.; Schrote, K. E.; Bertele, A. H.; Ball, W. P.; O'Melia, C.; Fairbrother, D. H., Colloidal properties of aqueous suspensions of acid-treated, multi-walled carbon nanotubes. *Environ. Sci. Technol.* **2009,** *43*, (3), 819-825.
77. Smith, B.; Wepasnick, K.; Schrote, K. E.; Cho, H. H.; Ball, W. P.; Fairbrother, D. H., Influence of surface oxides on the colloidal stability of multi-walled carbon nanotubes: A structure-property relationship. *Langmuir* **2009,** *25*, (17), 9767-9776.
78. Tian, Y.; Gao, B.; Batista, C. S.; Ziegler, K. J., Transport of engineered nanoparticles in saturated porous media. *J Nanopart Res* **2010,** *12*, 2371-2380.
79. Keller, A. A.; Wang, H.; Zhou, D.; Lenihan, H. S.; Cherr, G.; Cardinale, B. J.; Miller, R.; Ji, Z., Stability and aggregation of metal oxide nanoparticles in natural aqueous matrices. *Environmental Science & Technology* **2010,** *44*, (6), 1962-1967.
80. Zhou, D.; Keller, A. A., Role of morphology in the aggregation kinetics of ZnO nanoparticles. *Water research* **2010,** *44*, (9), 2948-2956.
81. Islam, A.; Chowdhry, B.; Snowden, M., Hetero-aggregation in colloidal dispersions. *Advances in colloid and interface science* **1995,** *62*, (2), 109-136.
82. Lin, W.; Kobayashi, M.; Skarba, M.; Mu, C.; Galletto, P.; Borkovec, M., Hetero-aggregation in binary mixtures of oppositely charged colloidal particles. *Langmuir* **2006,** *22*, (3), 1038-1047.
83. Yates, P. D.; Franks, G. V.; Jameson, G. J., Orthokinetic Hetero-aggregation with nanoparticles: Effect of particle size ratio on aggregate properties. *Colloids and Surfaces a-Physico-chemical and Engineering Aspects* **2008,** *326*, (1-2), 83-91.
84. Kim, A. Y.; Berg, J. C., Fractal Hetero-aggregation of Oppositely Charged Colloids. *Journal of Colloid and Interface Science* **2000,** *229*, (2), 607-614.
85. James, R. O.; Homola, A.; Healy, T. W., Heterocoagulation of amphoteric latex colloids. *Journal of the Chemical Society, Faraday Transactions 1: Physical Chemistry in Condensed Phases* **1977,** *73*, 1436-1445.
86. Kitano, H.; Iwai, S.; Ise, N.; Okubo, T., Kinetic analysis of association processes between oppositely charged polymer latex particles. *Journal of the American Chemical Society* **1987,** *109*, (22), 6641-6644.
87. Fern; aacute; ndez-Barbero, A.; Vincent, B., Charge Hetero-aggregation between hard and soft particles. *Physical Review E* **2000,** *63*, (1), 011509.
88. Saleh, N.; Phenrat, T.; Sirk, K.; Dufour, B.; Ok, J.; Sarbu, T.; Matyjaszewski, K.; Tilton, R. D.; Lowry, G. V., Adsorbed Triblock Copolymers Deliver Reactive Iron Nanoparticles to the Oil/Water Interface. *Nano Letters* **2005,** *5*, (12), 2489-2494.
89. Sun, N.; Elimelech, M.; Sun, N.-Z.; Ryan, J. N., A novel two-dimensional model for colloid transport in physically and geochemically heterogeneous porous media. *Journal of Contaminant Hydrology* **2001,** *49*, (3-4), 173-199.

90. Chowdhury, I.; Cwiertny, D. M.; Walker, S. L., Combined factors influencing the aggregation and deposition of nano-TiO2 in the presence of humic acid and bacteria. *Environmental science & technology* **2012,** *46*, (13), 6968-6976.
91. Yang, H.; Tong, M.; Kim, H., Effect of Carbon Nanotubes on the Transport and Retention of Bacteria in Saturated Porous Media. *Environmental science & technology* **2013,** *47*, (20), 11537-11544.
92. Tong, M.; Ding, J.; Shen, Y.; Zhu, P., Influence of biofilm on the transport of fullerene (C 60) nanoparticles in porous media. *water research* **2010,** *44*, (4), 1094-1103.
93. Lerner, R. N.; Lu, Q.; Zeng, H.; Liu, Y., The effects of biofilm on the transport of stabilized zerovalent iron nanoparticles in saturated porous media. *Water research* **2012,** *46*, (4), 975-985.
94. Murphy, C. J. S., T. K.; Gole, A.; Orendorff, C. J.; Gao, J.; Gou, L.; Hunyadi, S. Li, T, Anisotropic Metal Nanoparticles: Synthesis, Assembly, and Optical Applications, . [a Top Five ACS article by citations, National Chemistry Week, 2007]. *J. Phys. Chem. B* **2005,** *109*, 13857-13870.
95. Gou, L. M., C. J., Fine-Tuning the shape of gold nanorods *Chem. Mat.* **2005,** *17*, 3668-3672.
96. Cho, W. S.; Kim, S.; Han, B. S.; Son, W. C.; Jeong, J., Comparison of gene expression profiles in mice liver following intravenous injection of 4 and 100 nm-sized PEG-coated gold nanoparticles. *Toxicol. Lett.* **2009,** *191*, (1), 96-102.
97. Akiyama, Y.; Mori, T.; Katayama, Y.; Niidome, T., The effects of PEG grafting level and injection dose on gold nanorod biodistribution in the tumor-bearing mice. *J. Control. Release* **2009,** *139*, (1), 81-84.
98. Goodman, C. M.; McCusker, C. D.; Yilmaz, T.; Rotello, V. M., Toxicity of gold nanoparticles functionalized with cationic and anionic side chains. *Bioconjugate Chem.* **2004,** *15*, (4), 897-900.
99. Merchant, B., Gold, the Noble Metal and the Paradoxes of its Toxicology. *Biologicals* **1998,** *26*, (1), 49-59.
100. Pan, Y.; Neuss, S.; Leifert, A.; Fischler, M.; Wen, F.; Simon, U.; Schmid, G.; Brandau, W.; Jahnen-Dechent, W., Size-dependent cytotoxicity of gold nanoparticles. *Small* **2007,** *3*, (11), 1941-1949.
101. Tong, L.; Cheng, J. X., Gold nanorod-mediated photothermolysis induces apoptosis of macrophages via damage of mitochondria. *Nanomedicine* **2009,** *4*, (3), 265-276.
102. Root, S. W.; Andrews, G. A.; Kniseley, R. M.; Tyor, M. P., The distribution and radiation effects of intravenously administered colloidal Au198 in man. *Cancer* **1954,** *7*, (5), 856-866.
103. Alkilany, A. M.; Murphy, C. J., Toxicity and cellular uptake of gold nanoparticles: what we have learned so far? *J Nanopart Res* **2010,** *12*, (7), 2313-2333.
104. Kang, S.; Mauter, M. S.; Elimelech, M., Microbial Cytotoxicity of Carbon-Based Nanomaterials: Implications for River Water and Wastewater Effluent. *Environmental Science & Technology* **2009,** *43*, (7), 2648-2653.
105. Kang, S.; Pinault, M.; Pfefferle, L. D.; Elimelech, M., Single-walled carbon nanotubes exhibit strong antimicrobial activity. *Langmuir* **2007,** *23*, (17), 8670-8673.
106. Vecitis, C. D.; Zodrow, K. R.; Kang, S.; Elimelech, M., Electronic-Structure-Dependent Bacterial Cytotoxicity of Single-Walled Carbon Nanotubes. *Acs Nano* **2010,** *ASAP*.

107. Hauck, T. S.; Ghazani, A. A.; Chan, W. C. W., Assessing the effect of surface chemistry on gold nanorod uptake, toxicity, and gene expression in mammalian cells. *Small* **2008,** *4*, (1), 153-159.
108. Patra, C. R.; Moneim, S. S. A.; Wang, E.; Dutta, S.; Patra, S.; Eshed, M.; Mukherjee, P.; Gedanken, A.; Shah, V. H.; Mukhopadhyay, D., In vivo toxicity studies of europium hydroxide nanorods in mice. *Toxicol. Appl. Pharmacol.* **2009,** *240*, (1), 88-98.
109. Wang, S. G.; Lu, W. T.; Tovmachenko, O.; Rai, U. S.; Yu, H. T.; Ray, P. C., Challenge in understanding size and shape dependent toxicity of gold nanomaterials in human skin keratinocytes. *Chem. Phys. Lett.* **2008,** *463*, (1-3), 145-149.
110. Goodman, C. M.; Chari, N. S.; Han, G.; Hong, R.; Ghosh, P.; Rotello, V. M., DNA-binding by functionalized gold nanoparticles: Mechanism and structural requirements. *Chemical Biology & Drug Design* **2006,** *67*, (4), 297-304.
111. Colvin, V. L., The potential environmental impact of engineered nanomaterials. *Nature Biotech* **2003,** *21*, 166-1170.
112. Wiesner, M. R.; Bottero, J.-Y., *Environmental Nanotechnology: Applications and Impacts of Nanomaterials*. McGraw-Hill Companies: New York, NY, 2007.
113. Afrooz, A. R. M. N.; Sivalapalan, S. T.; Murphy, C. J.; Hussain, S. M.; Schlager, J. J.; Saleh, N. B., Spheres vs. rods: The shape of gold nanoparticles influences aggregation and deposition behavior. *Chemosphere* **2013,** *91*, (1), 93-98.
114. Afrooz, A. R. M. N.; Hussain, S.; Saleh, N., Aggregate size and structure determination of nanomaterials in physiological media: importance of dynamic evolution. *Journal of Nanoparticle Research* **2014,** *16*, (12), 1-7.
115. Afrooz, A. R. M. N.; Khan, I. A.; Hussain, S. M.; Saleh, N. B., Mechanistic Hetero-aggregation of Gold Nanoparticles in a Wide Range of Solution Chemistry. *Environmental Science & Technology* **2013,** *47*, (4), 1853-1860.

Chapter 2

Spheres vs. Rods: The Shape of Gold Nanoparticles Influences Aggregation and Deposition Behavior[1]

[1]Afrooz, A. N., Sivalapalan, S. T., Murphy, C. J., Hussain, S. M., Schlager, J. J., & Saleh, N. B. (2013). Spheres vs. rods: The shape of gold nanoparticles influences aggregation and deposition behavior. *Chemosphere*, 91(1), 93-98.
Contributions of the Co-Authors: S.T.S: AuNM Synthesis and TEM; C.J.M: Co-PI; S.M.H and J.J.S: Intellectual Contributions in Manuscript Preparation

Abstract

The influence of shape on nanomaterial aggregation and deposition was systematically studied with PAA coated uniform-sized AuNSs and AuNRs. Time resolved dynamic light scattering was employed to study their aggregation kinetics in a wide range of mono- and di-valent electrolyte conditions. Results indicated that PAA coated AuNSs have higher aggregation propensity compared to anisotropic PAA coated AuNRs, as observed through critical coagulation concentration (CCC). The CCC values were estimated as 50 mM NaCl and 1.8 mM $CaCl_2$ for AuNS, which showed substantial increase to 250 mM NaCl and 7 mM $CaCl_2$ for anisotropic AuNRs. Though electrokinetic behavior showed similar surface potential for the spherical and rod-shaped materials, the geometric differences between the samples have likely resulted in unique conformation of the PAA coatings, leading to different magnitudes of steric hindrances and hence yielding the observed aggregation behavior. The deposition kinetics was monitored using the quartz crystal microbalance with dissipation technique. AuNRs showed relatively slower deposition compared to AuNSs for low electrolytes concentrations. With the increase in electrolyte concentration, the differences in deposition rates between spheres and rods diminished. The results from this study showed that the shape of nanomaterials can influence interfacial properties and result in unique aggregation and deposition behavior under typical aquatic conditions.

Keywords: Gold nanorods; gold nanospheres; shape; aggregation; deposition; poly (acrylic acid); conformation

2.1 Introduction

Rod-like nanomaterials [1, 2] with high aspect ratio (length to diameter ratio) have unique optical [3], thermal [4], and electrical [5] properties—thus considered an exciting material class exhibiting multi-functionality in many applications [1]. Presently, carbonaceous nanomaterials (e.g., single-walled and multiwalled carbon nanotubes) are the most widely produced anisotropic nanostructures [6], followed closely by metallic nanorods and nanowires [1, 7]. Due to concerns about fibrous 'asbestos-like' structure, there has been significant attention directed toward environmental implications and biocompatibility of anisotropic carbon nanostructures. However, a considerable lack in such studies for metallic anisotropic materials still exists.

AuNMs are identified as one of the dominant ones within the plasmon-resonant functional material class—used for biological imaging and image-guided non-invasive therapies [8]. Anisotropic AuNMs, i.e., AuNRs, yield unique optical properties relevant to biological applications, e.g., drug delivery, contrast agents [9, 10]. However, recent *in vitro* and *in vivo* findings have demonstrated toxicity of AuNRs [11, 12]. Cellular necrosis and apoptosis may occur at certain doses depending on AuNR size [13]. These anisotropic nanomaterials have also been shown to induce inflammatory response and apoptosis in the liver of higher vertebrates, such as mice. Such reports not only highlight necessity of fate and transport studies of AuNR but also indicate the need for careful evaluation of aggregation behavior to enumerate toxicity mechanisms with anisotropic gold.

Spherical colloids have been used for decades for studying fundamental interfacial interactions [14, 15]. Moreover, particle geometry is a key parameter influencing their behavior [16]. In addition, physico-chemical properties, aggregation propensity, and surface interaction of colloids are known to be substantially altered by the change in colloid shape; i.e., from spheres to

cylinders [17, 18]. Despite such evidence, there are a paucity of studies that systematically evaluates shape effects of nanomaterials on their environmental behavior and toxicity. A recent review on experimental aggregation and deposition studies of engineered nanomaterials is a testament to this reality, where an exhaustive list of implication literature is presented with no evidence of shape-effect studies [19]. Fundamental studies on the shape-effect on aggregation propensity in biological exposure conditions are also lacking [9]. There are only a handful of studies [20, 21] that systematically evaluated the role of shape on aggregation and deposition of nanoparticles.

The objective of this study is to investigate the effect of AuNM shape on aggregation and deposition behavior in a wide range of mono- and di-valent electrolyte conditions. The ability to uniformly synthesize AuNSs and AuNRs enables such systematic evaluation. AuNM morphology is evaluated with transmission electron microscopy (TEM), while their plasmon-resonance signature is identified with UV-Vis spectroscopy. The aggregation kinetics are systematically studied using a time resolved dynamic light scattering technique (TRDLS). Deposition behavior is evaluated with the interfacial Quartz Crystal Microbalance with Dissipation (QCM-D) technique. This study evaluates the role of shape on AuNM aggregation and deposition, where the mechanisms are enumerated with electrokinetic measurements and role of geometry on surface coating conformation.

2.2 Materials and Methods:

2.2.1 Synthesis and Sample Preparation

AuNSs with 12 nm diameter at 2 nM concentration and AuNRs with same diameter and an aspect ratio of 5 (i.e., 12 × 60 nm dimensions) at 0.2 nM strength were prepared using a seed mediated approach. The details of synthesis have been discussed elsewhere [22, 23]. For this study the protocol is essentially controlled reduction of gold salts in aqueous solution at room temperature in the

presence of a "structure-directing" cationic surfactant; e.g., cetyltrimethyl-ammonium bromide, CTAB [24]. After purification by dialysis and centrifugation, a bilayer of CTAB remained on the AuNM surfaces, rendering positive surface charge to the particles and thus preventing aggregation [25]. Overcoating the AuNMs with anionic polymers such as poly (acrylic acid), PAA, switches the surface charge to a negative potential. Colloidal suspension of AuNS was prepared with a dilution factor of 75 while the AuNR was used at the original synthesized concentration.

2.2.2 Surface Properties—Morphology, Chemistry, and Electrokinetics

AuNM morphology and physical attributes (shape and size uniformity) was probed with electron microscopy, employing a JEOL 2100F TEM. The aqueous dispersions of AuNMs were placed on 200-mesh (0.075 mm) copper grids coated with carbon-Formvar (Electron Microscopy Science) and dried at room temperature. Images were obtained at 200 kV accelerating voltage. Upon synthesis, Plasmon resonance spectra were obtained on a Cary 500 UV-Vis-NIR spectrophotometer. In addition, electrophoretic measurements, to ensure effective surface overcoating from with PAA, were performed on a Brookhaven ZetaPALS instrument. After shipping from Illinois to South Carolina, AuNS and AuNR stability were verified optically with an Agilent 8453 UV-Vis spectrometer (Santa Clara, CA). For such measurements, 3 mL of AuNM suspensions at 10-fold dilution were added to a 5 mm path-length quartz cuvette. Spectral response for the UV and visual wavelength range (200 to 1100 nm) was collected. Multiple runs were performed to ensure reproducibility. Further surface characterization was performed with electrokinetic measurements, measuring electrophoretic mobility (EPM) by a Malvern Zetasizer (Malvern Instruments, Worcestershire, UK). 1 mL AuNM suspension (with dilution factor 75 and 1 for AuNS and AuNR, respectively) was injected into the polycarbonate capillary cell (DTS

1060C), ensuring no air-bubble intrusion. At least 20 measurements, with triplicate samples, were recorded at 22 °C.

2.2.3 Aggregation Kinetics

The aggregation kinetics was studied using TRDLS. A robust light scattering precision instrument (ALV/CGS-3, Langen, Germany), equipped with a 22 mW HeNe laser at 632 nm (equivalent to 800 mW laser at 532 nm) and a highly sensitive High QE APD detector with photomultipliers, was used. Detailed procedures regarding TRDLS has been described elsewhere [26, 27]. In brief, 2 mL volume of 3.01×10^{12} mL^{-1} number-particle of AuNS or AuNR was injected to a rigorously cleaned glass vial (Supelco, Bellefonte, PA). A pre-measured amount of electrolyte solution, to achieve 1-200 mM NaCl and 0.1-7.6 mM $CaCl_2$ for AuNS and 1 to 550 mM NaCl and 0.1 to 20 mM $CaCl_2$ for AuNR, was introduced to initiate aggregation. Scattered light intensity was detected with a photon-detector, positioned at 90° from the incident laser. The hydrodynamic radii (HR) profile was generated using auto-correlation function and cumulant analysis. A gradual increase of HR was plotted against time to obtain initial aggregation rates for each salt concentration. The estimated rates were normalized with the favorable aggregation slope. Further details on the formulae used for such computation is presented as SM-1 in supplementary material (SM) section.

2.2.4 Interfacial Deposition

Deposition experiments were performed using a Q-sense E4 (Q-sense, Västra Frölunda, Sweden) QCM-D. A pre-cleaned (with 2% hellmanex solution) silica quartz crystal was first treated in a plasma chamber for 20 min [28]. Upon establishment of inherent frequency and dissipation for the quartz crystal (F&D), the crystal was equilibrated with the background electrolyte solution of concern to establish a stable baseline. AuNM suspensions at 6.02×10^{14} mL^{-1} number-particle was then introduced to the flow-through chamber at identical background chemistry. A range of

mono-valent electrolyte, i.e., 10-1000 mM NaCl, was used to evaluate deposition behavior. Deposition of particles on the crystal was monitored with the change in vibrational frequency of the crystal in the third overtone [28]. The frequency profile was recorded with Q-soft 401 software and initial deposition slopes were estimated to obtain deposition rates of the AuNMs at each electrolyte condition.

2.3 Results and Discussion

2.3.1 AuNM Characteristics

Representative TEM micrographs of the AuNS and AuNR are presented in Fig. 2.1. Figure 1a shows uniform sized spheres with relatively rounded edges. Slight angularity is noticed in some of the spherical features.

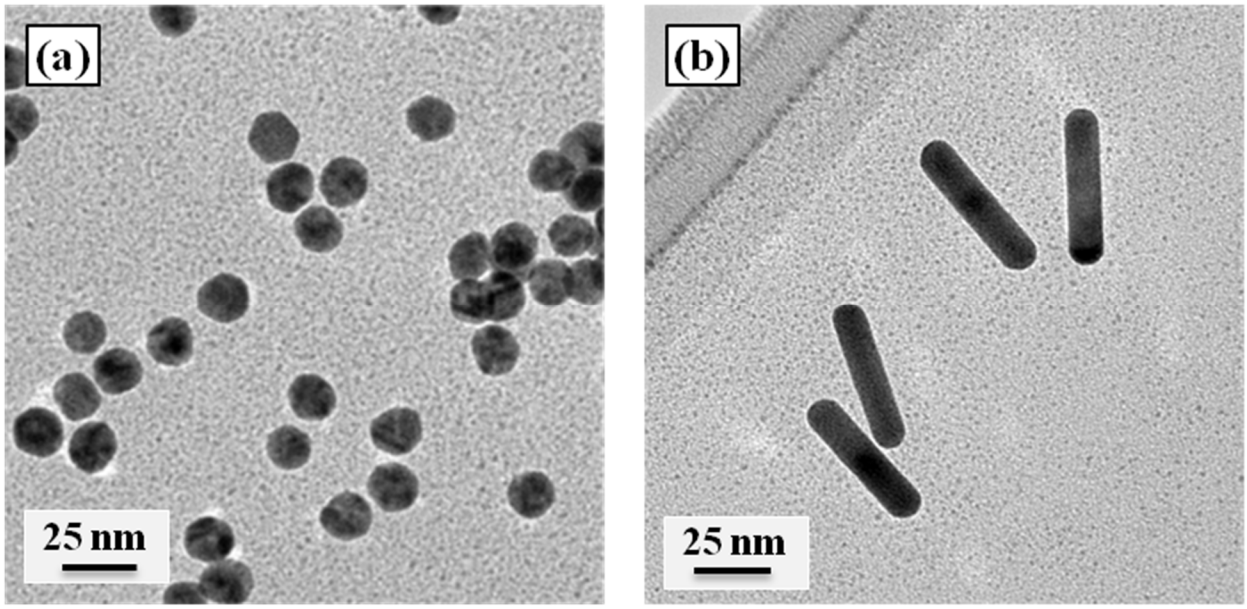

FIGURE 2.1. Representative TEM micrographs of (a) AuNS and (b) AuNR. Scale bars are 25 nm.

A high degree of uniformity is observed for the synthesized AuNS showing 12±0.5 nm diameters. For AuNR, similar degree of uniformity in rod diameter and length is observed (Fig. 2.1b). The rods are observed to be near identical with 12±0.8 nm × 60±2 nm dimensions. The rod edges are observed as symmetrically rounded.

Plasmon resonance of AuNS and AuNR is probed with UV-Vis spectroscopy as presented in Fig. 2.2. The AuNSs show characteristic localized surface plasmon resonance (LSPR) at 520-540 nm wavelength range (Fig. 2.2a). AuNRs exhibit two LSPR peaks—first one near 520 nm, corresponding to the resonance from the shorter dimension of the rods (transverse), where the second peak at 830 nm corresponds to response from the longitudinal axis (Fig. 2.2b). These results are consistent with literature presented LSPR peaks that report 520 nm for AuNS [29] and 518 and 860 nm for transverse and longitudinal AuNR axes, respectively [30].

The surface potentials of the AuNMs are presented in Figure 2.3 for a range of mono- and divalent electrolyte concentrations. The EPM values of AuNS showed a gradual decrease from – (2.95±0.04) × 10^{-8} to – (0.74±0.02) × 10^{-8} m^2 V^{-1} s^{-1} with an increase of NaCl concentration from 3 to 100 mM. In the case of AuNRs, EPM values were reduced from – (2.88±0.17) × 10^{-8} to – (0.29±0.01) × 10^{-8} m^2 V^{-1} s^{-1} for a similar increase in NaCl concentration. The negative surface potential demonstrates effective overcoating of AuNM surfaces with PAA. For divalent Ca^{2+}, approximately one and half log leftward shift was observed for EPM sensitivity; as expected with multi-valent counterions. A gradual decrease from – (2.86±0.28) × 10^{-8} to – (0.55±0.23) × 10^{-8} and – (2.32±0.19) × 10^{-8} to – (0.28±0.32) × 10^{-8} m^2 V^{-1} s^{-1} was observed for AuNS and AuNR, respectively. Similar electrokinetic behavior, i.e., reported ζ-potential of -(36.9±6.6) mV, is observed in earlier literature for PAA coated 12 nm AuNS [31]; whereas, PAA coated AuNR exhibited -33 mV [32].

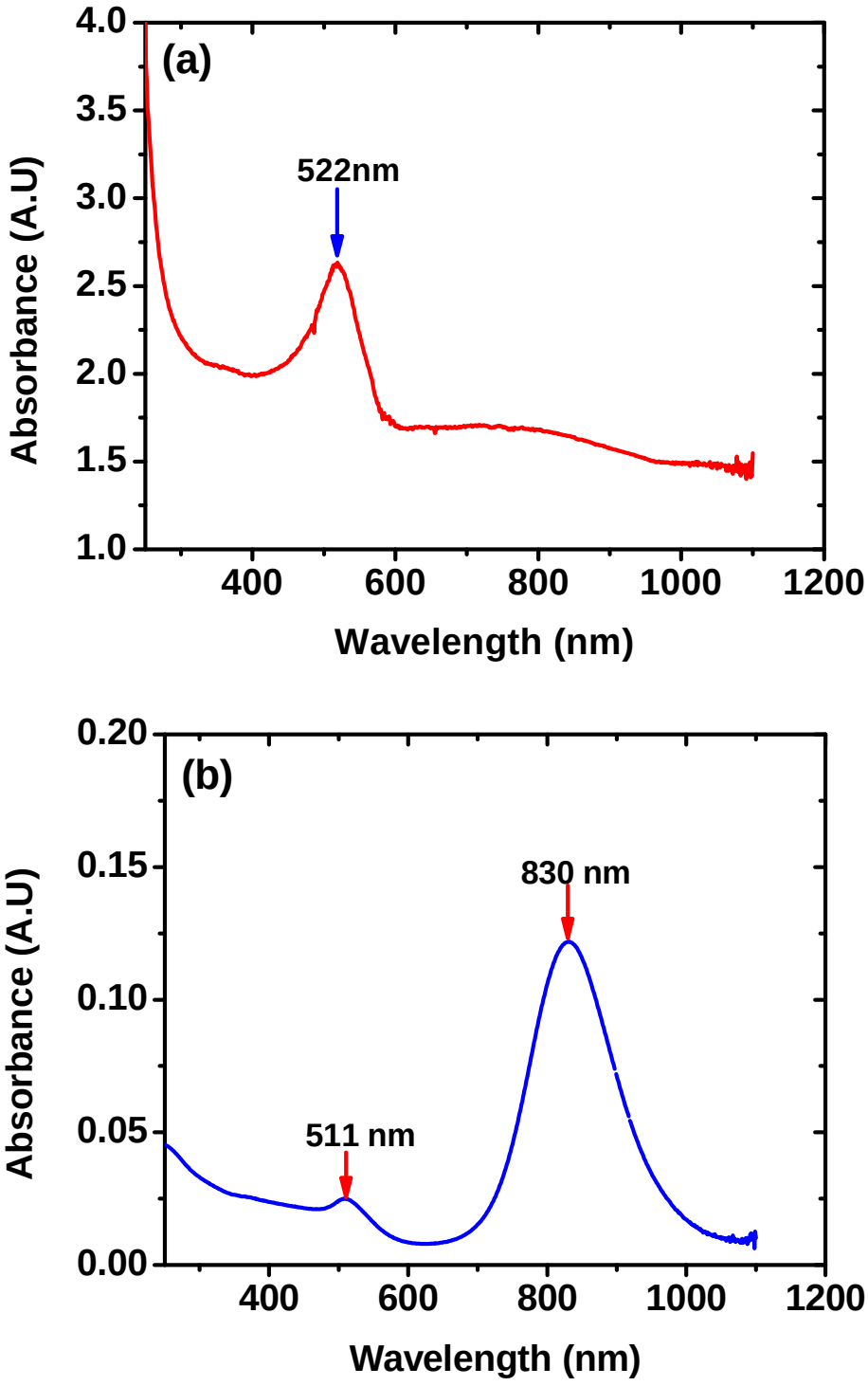

FIGURE 2.2. Characteristic UV-Vis spectra of (a) AuNS and (b) AuNR showing the LPSRs for both shapes.

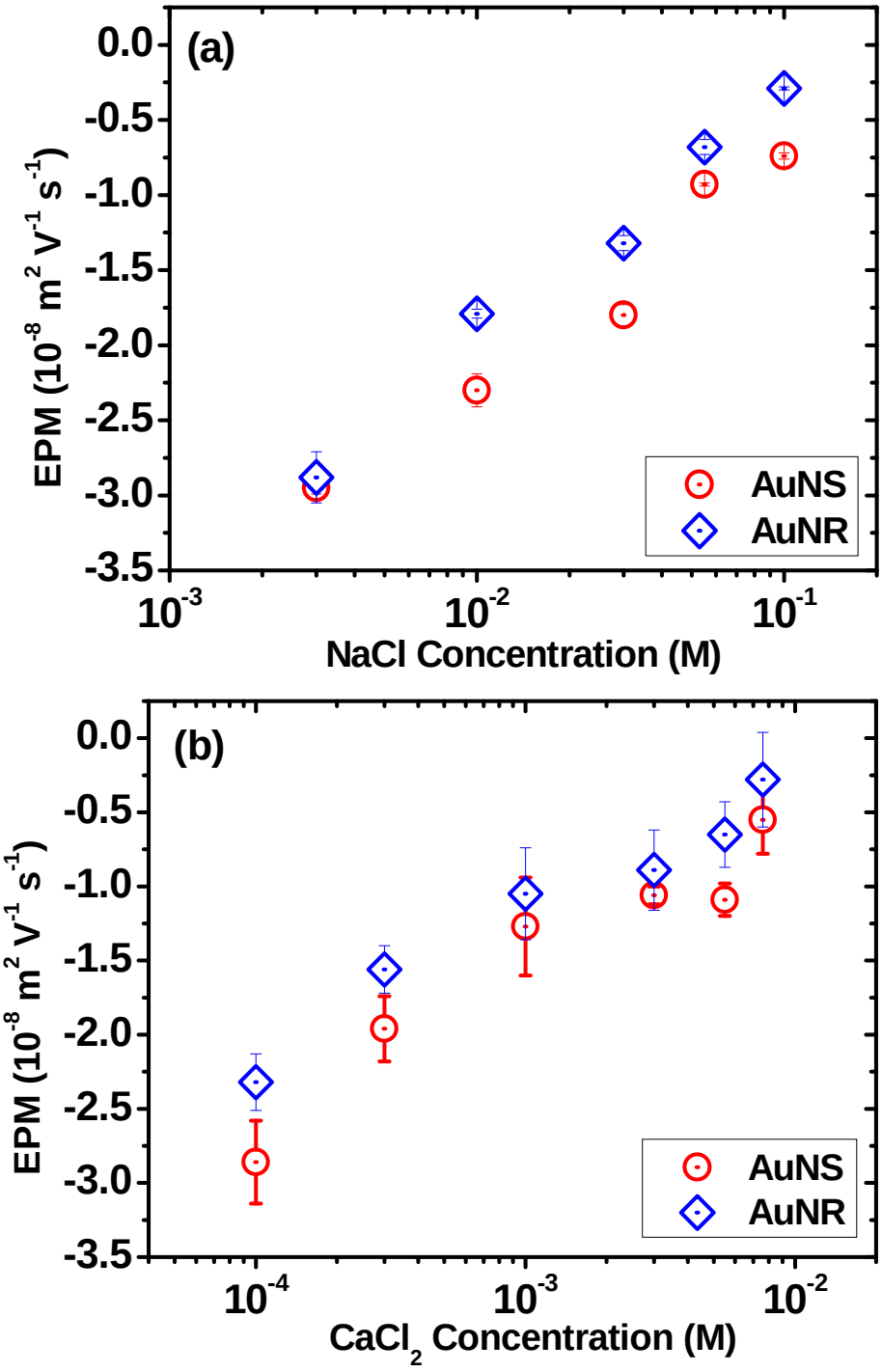

FIGURE 2.3. Electrophoretic mobility (EPM) of AuNS and AuNR with (a) monovalent NaCl and (b) divalent $CaCl_2$. The measurements were performed at 22 °C.

2.3.2 AuNM Aggregation Kinetics

Figure 4 presents stability profiles of the AuNMs for mono- and di-valent electrolyte scenarios. Overall, the AuNSs show classical Derjaguin-Landau-Verwey-Overbeek type aggregation behavior with defined unfavorable or reaction limited (RLCA) and favorable or diffusion limited aggregation (DLCA) regimes. In the case of AuNRs, both aggregation regimes exist, although the regime switch is more abrupt compared to AuNSs. In addition, the AuNRs show higher stability compared to the AuNSs, where this effect is more profound with mono-valent electrolyte case. The attachment efficiencies computed from raw aggregation profiles (Fig. A-1) show a gradual increase with the increase in NaCl concentration for AuNS. The regime confluence, quantified with critical coagulation concentration (CCC), show relatively lower stability for AuNS—50 mM NaCl in this case. The anisotropic AuNRs show a steeper response in the RLCA regime, though exhibit a half log right-shift to initiating the regime (Fig. 2.4a). The estimated CCC for AuNR is ~250 mM NaCl with a less defined regime confluence. CCC values of 70 mM NaCl for citrate-coated 30 nm AuNSs have been reported [33] earlier. Significantly higher stabilities were reported for 1,1-mercaptoundecanoic acid coated 28 nm AuNSs yielding a CCC of 200 mM NaCl [33].

Similar aggregation behavior is observed with divalent cations, however with a 1.5-2.0 log left-shift, compared to monovalent NaCl. The stability ratios, computed from aggregation profiles (Fig. A-2), are presented in form of stability plots in Fig. 2.4b. Overall, differences in aggregation between AuNS and AuNR appear to have minimized with divalent cations. AuNSs show relatively lower stability compared to AuNRs in the RLCA regime; such differences largely diminish in higher salt conditions, i.e., in the DLCA regime. The CCC values are estimated as 1.8 and 7 mM for AuNS and AuNR, respectively. Though the literature includes at least one comparative

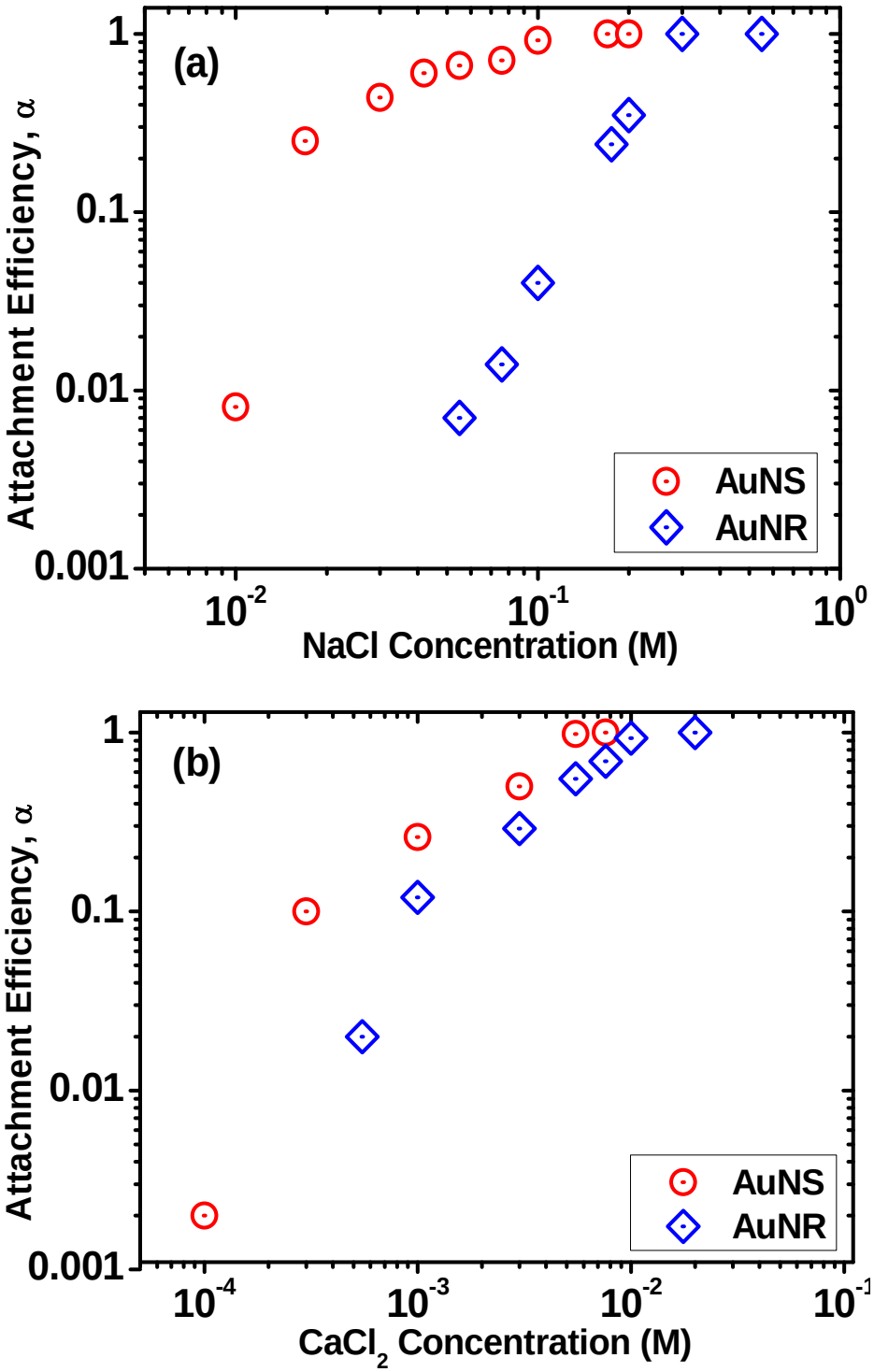

FIGURE 2.4. Stability plots of AuNS and AuNRs with (a) monovalent NaCl and (b) divalent $CaCl_2$. The measurements were performed at 20 °C.

aggregate formation study in the presence of various divalent metallic salts [34], to our knowledge, this is the first quantitative study of AuNM aggregation as a function of divalent cations.

2.3.3 Mechanism of Aggregation

The aggregation behavior differences for spheres and rods occurred primarily due to steric interaction and physical packing uniqueness, in RLCA and DLCA regimes, respectively. It is well known in the literature that polyelectrolyte conformation on interfaces is highly influenced by surface curvature [35]. In this study, the AuNSs possess higher curvature compared to the AuNRs with flat longitudinal surfaces. Such differences will likely alter PAA conformation on these surfaces, resulting in a relatively compressed PAA layer for AuNSs compared to an extended brush-like layer for AuNRs. Thus higher steric interaction alongside with a relatively higher electrokinetic contribution from the AuNR surfaces resulted in their enhanced stability at the RLCA regime. At the DLCA regime, where polyelectrolytes have most likely undergone charge screening with high amount of cations, the stabilization for AuNRs had likely occurred from physical packing hindrances as observed in for uncharged random-packing cases [36-38]—rods are known to possess higher hindrances, thus less packing density, compared to spheres. Electrosteric interactions at the RLCA regime and physical hindrances to packing in the DLCA regime are identified as the key mechanisms for the shape effects on aggregation.

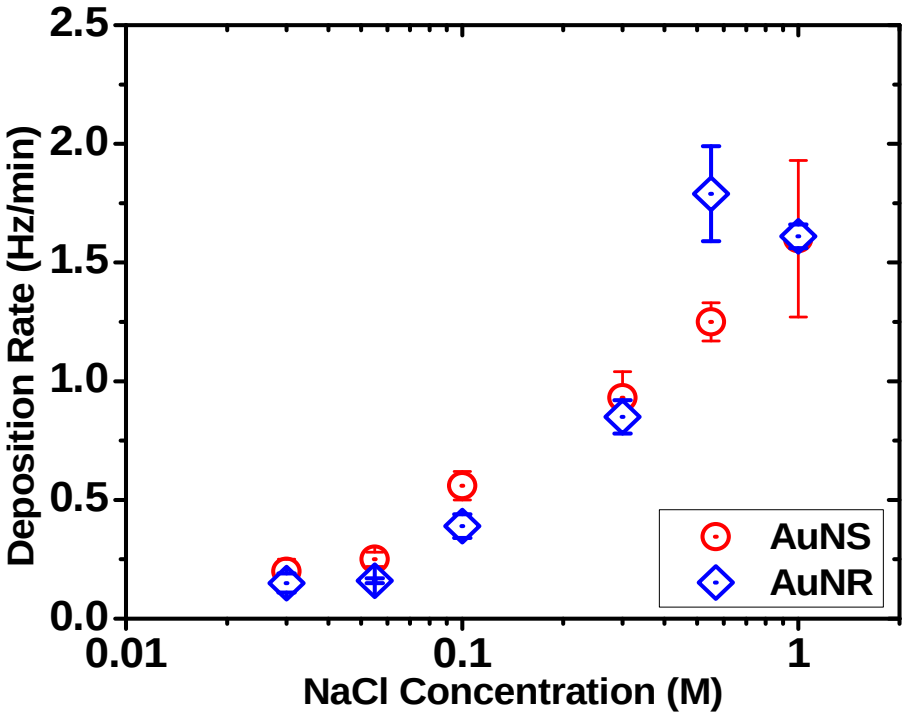

FIGURE 2.5. Deposition rates of AuNMs onto a silica coated quartz crystal in the presence of NaCl. Deposition rates are expressed as the rates of normalized frequency shift at the third overtone. Each data point represents the mean of triplicate measurements conducted at the same experimental conditions, and the error bars represent standard deviations. Measurements were carried out at 20 °C.

2.3.4 Deposition Behavior

Interfacial deposition rates of AuNMs, evaluated with QCM-D, are presented in Figure 2.5. The deposition rates are computed from frequency profiles (Fig. A-3). Both AuNSs and AuNRs show relatively similar deposition behavior under a range of NaCl concentrations; however, AuNRs show slightly lower deposition rates compared to AuNSs up to 100 mM. Deposition rates of AuNS vary from 0.2 to 1.6 Hz min^{-1} for AuNS; whereas for AuNR, this variation is from 0.04 to 1.61 Hz min^{-1}. Compared to the aggregation behavior, the differences in deposition rates between AuNS and AuNR are less profound for the lower NaCl concentrations. Such differences might have occurred not only from the interfacial chemical differences but also from relative packing of AuNRs onto quartz deposition surface, compared to AuNS cases. The absence of PAA coatings

on the quartz crystals have also caused a reduced steric hindrance to deposition for rods, which was otherwise observed in the aggregation study. Previous literature also reported less profound interfacial interaction during deposition, when compared to aggregation; e.g., for fullerenes [39].

2.4 Conclusions

This article presents a systematic study probing the effects of shape on aggregation and deposition behavior of uniformly synthesized AuNMs. Results indicate that anisotropic nanorods have higher stability compared to nanospheres and thus are likely to be more mobile in environmental systems. Relatively higher stability of AuNRs also can have unique implications in their interaction with biological entities. As AuNRs are identified as more potent to manifest deleterious effects to environmental and biological systems, further systematic studies are necessary for carefully evaluation of their fate, transport, and toxicity behavior.

2.5 Literature Cited

1. Murphy, C. J.; Thompson, L. B.; Alkilany, A. M.; Sisco, P. N.; Boulos, S. P.; Sivapalan, S. T.; Yang, J. A.; Chernak, D. J.; Huang, J., The many faces of gold nanorods. *J. Phys. Chem. Lett.* **2010**, 2867-2875.
2. Salem, A. K.; Searson, P. C.; Leong, K. W., Multifunctional nanorods for gene delivery. *Nat. Mater.* **2003,** *2*, (10), 668-671.
3. Pérez-Juste, J.; Pastoriza-Santos, I.; Liz-Marzán, L. M.; Mulvaney, P., Gold nanorods: Synthesis, characterization and applications. *Coordin. Chem. Rev.* **2005,** *249*, (17-18), 1870-1901.
4. Yang, B.; Han, Z. H., Temperature-dependent thermal conductivity of nanorod-based nanofluids. *Appl. Phys. Lett.* **2006,** *89*, (8), 3.
5. Kwak, C. H.; Kim, B. H.; Park, C. I.; Seo, S. Y.; Kim, S. H.; Han, S. W., Structural and electrical properties of ZnO nanorods and Ti buffer layers. *Appl. Phys. Lett.* **2010,** *96*, (5), 3.
6. Iijima, S.; Ichihashi, T., Single-shell carbon nanotubes of 1-nm diameter. *Nature* **1993,** *363*, (6430), 603-605.
7. Tian, B.; Zheng, X.; Kempa, T. J.; Fang, Y.; Yu, N.; Yu, G.; Huang, J.; Lieber, C. M., Coaxial silicon nanowires as solar cells and nanoelectronic power sources. *Nature* **2007,** *449*, (7164), 885-889.
8. Huff, T. B.; Hansen, M. N.; Zhao, Y.; Cheng, J.-X.; Wei, A., Controlling the cellular uptake of gold nanorods. *Langmuir* **2007,** *23*, (4), 1596-1599.
9. Huang, X.; Neretina, S.; El-Sayed, M. A., Gold nanorods: From synthesis and properties to biological and biomedical applications. *Adv. Mater.* **2009,** *21*, (48), 4880-4910.
10. Jain, P. K.; Lee, K. S.; El-Sayed, I. H.; El-Sayed, M. A., Calculated absorption and scattering properties of gold nanoparticles of different size, shape, and composition: Applications in biological imaging and biomedicine. *J. Phy. Chem. B.* **2006,** *110*, (14), 7238-7248.
11. Hauck, T. S.; Ghazani, A. A.; Chan, W. C. W., Assessing the effect of surface chemistry on gold nanorod uptake, toxicity, and gene expression in mammalian cells. *Small* **2008,** *4*, (1), 153-159.
12. Patra, C. R.; Moneim, S. S. A.; Wang, E.; Dutta, S.; Patra, S.; Eshed, M.; Mukherjee, P.; Gedanken, A.; Shah, V. H.; Mukhopadhyay, D., In vivo toxicity studies of europium hydroxide nanorods in mice. *Toxicol. Appl. Pharmacol.* **2009,** *240*, (1), 88-98.
13. Pan, Y.; Neuss, S.; Leifert, A.; Fischler, M.; Wen, F.; Simon, U.; Schmid, G.; Brandau, W.; Jahnen-Dechent, W., Size-dependent cytotoxicity of gold nanoparticles. *Small* **2007,** *3*, (11), 1941-1949.
14. Leunissen, M. E.; Christova, C. G.; Hynninen, A. P.; Royall, C. P.; Campbell, A. I.; Imhof, A.; Dijkstra, M.; van Roij, R.; van Blaaderen, A., Ionic colloidal crystals of oppositely charged particles. *Nature* **2005,** *437*, (7056), 235-240.
15. Vanzanten, J. H.; Elimelech, M., Determination of absolute coagulation rate constants by multiangle light-scattering. *J. Colloid Interf. Sci.* **1992,** *154*, (1), 1-7.
16. Onsager, L., The effects of shape on the interaction of colloidal particles. *Ann. NY. Acad. Sci.* **1949,** *51*, (4), 627-659.
17. Bhattacharjee, S.; Chen, J. Y.; Elimelech, M., DLVO interaction energy between spheroidal particles and a flat surface. *Colloids and Surfaces A.* **2000,** *165*, (1-3), 143-156.

18. Hunter, R. J., *Foundations of colloid science*. Oxford University Press: New York, NY, 1995; Vol. 1.
19. Petosa , A. R.; J aisi, D.; Q ue vedo , I.; E limelech , M.; T ufenkji , N., Aggregation and deposition of engineered nanomaterials in aquatic environments: Role of physico-chemical interactions. *Environ. Sci. Technol.* **2010,** *44*, 6532–6549.
20. Mulvihill, M. J.; Habas, S. E.; Jen-La Plante, H.; Wan, J.; Mokari, T., Influence of size, shape, and surface coating on the stability of aqueous suspensions of CdSe nanoparticles. *Chem. Mater.* **2010,** *22*, (18), 5251-5257.
21. Zhou, D. X.; Keller, A. A., Role of morphology in the aggregation kinetics of ZnO nanoparticles. *Water Res.* **2010,** *44*, (9), 2948-2956.
22. Jana, N. R.; Gearheart, L.; Murphy, C. J., Seed-mediated growth approach for shape-controlled synthesis of spheroidal and rod-like gold nanoparticles using a surfactant template. *Adv. Mater.* **2001,** *13*, (18), 1389-1393.
23. Jana, N. R.; Gearheart, L.; Murphy, C. J., Seeding growth for size control of 5-40 nm diameter gold nanoparticles. *Langmuir* **2001,** *17*, (22), 6782-6786.
24. Jana, N. R.; Gearheart, L.; Murphy, C. J., Wet chemical synthesis of high aspect ratio cylindrical gold nanorods. *J. Phys. Chem. B.* **2001,** *105*, (19), 4065-4067.
25. Gao, J. X.; Bender, C. M.; Murphy, C. J., Dependence of the gold nanorod aspect ratio on the nature of the directing surfactant in aqueous solution. *Langmuir* **2003,** *19*, (21), 9065-9070.
26. Saleh, N. B.; Pfefferle, L. D.; Elimelech, M., Aggregation kinetics of multiwalled carbon nanotubes in aquatic systems: Measurements and environmental implications. *Environ. Sci. Technol.* **2008,** *42*, (21), 7963-7969.
27. Saleh, N. B.; Pfefferle, L. D.; Elimelech, M., Influence of biomacromolecules and humic acid on the aggregation kinetics of single-walled carbon nanotubes. *Environ. Sci. Technol.* **2010,** *44*, (7), 2412-2418.
28. Saleh, N.; Kim, H.-J.; Phenrat, T.; Matyjaszewski, K.; Tilton, R. D.; Lowry, G. V., Ionic strength and composition affect the mobility of surface-modified Fe-0 nanoparticles in water-saturated sand columns. *Environ. Sci.Technol.* **2008,** *42*, (9), 3349-3355.
29. Haiss, W.; Thanh, N. T. K.; Aveyard, J.; Fernig, D. G., Determination of size and concentration of gold nanoparticles from UV-Vis spectra. *Anal. Chem.* **2007,** *79*, (11), 4215-4221.
30. Murphy, C. J.; San, T. K.; Gole, A. M.; Orendorff, C. J.; Gao, J. X.; Gou, L.; Hunyadi, S. E.; Li, T., Anisotropic metal nanoparticles: Synthesis, assembly, and optical applications. *J. Phys. Chem. B* **2005,** *109*, (29), 13857-13870.
31. Deng, Z.; Liang, M.; Toth, I.; Monteiro, M.; Minchin, F., Molecular interaction of Poly(acrylic acid) gold nanoparticles with human fibrinogen. *ACS Nano* **2012**.
32. Wang, J.; Dong, B.; Chen, B.; Jiang, Z.; Song, H., Selective photothermal therapy for breast cancer with targeting peptide modified gold nanorods. *Dalton T.* **2012,** *41*, (36), 11134-11144.
33. Liu, J. F.; Legros, S.; Ma, G. B.; Veinot, J. G. C.; von der Kammer, F.; Hofmann, T., Influence of surface functionalization and particle size on the aggregation kinetics of engineered nanoparticles. *Chemosphere* **2012,** *87*, (8), 918-924.
34. Yang, Y. I.; Choi, I.; Hong, S.; Lee, S.; Kang, T.; Lee, H.; Yi, J., Selective aggregation of polyanion-coated gold nanorods induced by divalent metal ions in an aqueous solution. *J. Nanosci. Nanotechno.* **2010,** *10*, (5), 3538-3542.

35. Furusawa, K.; Shou, Z.; Nagahashi, N., Polymer adsorption on fine particles - the effects of particle-size and its stability. *Colloid Polym. Sci.* **1992,** *270*, (3), 212-218.
36. Kyrylyuk, A. V.; Philipse, A. P., Effect of particle shape on the random packing density of amorphous solids. *Phys. Status Solidi A.* **2011,** *208*, (10), 2299-2302.
37. Kyrylyuk, A. V. W., Alan. Philipse Albert P. In *Random packings of Rod-Sphere mixtures simulated by mechanical contraction method* 6th International Conference on Micromechanics of Granular Media, Golden, Colorado., 2009; M. Nakagawa, S. L., Ed. 2009.
38. Rudge, J. F.; Holness, M. B.; Smith, G. C., Quantitative textural analysis of packings of elongate crystals. *Contrib. Mineral. Petr.* **2008,** *156*, (4), 413-429.
39. Chen, K. L.; Elimelech, M., Aggregation and deposition kinetics of fullerene (C-60) nanoparticles. *Langmuir* **2006,** *22*, (26), 10994-11001.

Chapter 3

Aggregate Size and Structure Determination of Nanomaterials in Physiological Media: Importance of Dynamic Evolution[2]

[2]Afrooz, A. N., Hussain, S. M., & Saleh, N. B. (2014). Aggregate size and structure determination of nanomaterials in physiological media: importance of dynamic evolution. *Journal of Nanoparticle Research*, 16(12), 1-7.
Contributions of the Co-Author: S.M.H: Co-PI

Abstract

Most *in-vitro* nanotoxicological assays are performed after 24 h exposure. However, in determining size and shape effect of nanoparticles in toxicity assays, initial characterization data is generally used to describe experimental outcome. The dynamic size and structure of aggregates are typically ignored in these studies. This brief communication reports dynamic evolution of aggregation characteristics of gold nanoparticles. The study finds that gradual increase in aggregate size of AuNS occurs up to 6 h duration; beyond this time period, the aggregation process deviates from gradual to a more abrupt behaviour as large networks are formed. Results of the study also show that aggregated clusters possess unique structural conformation depending on nominal diameter of the nanoparticles. The differences in fractal dimensions of the AuNS samples likely occurred due to geometric differences, causing larger packing propensities for smaller sized particles. Both such observations can have profound influence on dosimetry for *in vitro* nanotoxicity analyses.

Keywords: gold nanoparticles; dynamic light scattering; static light scattering; network structure; in vitro

3.1 Introduction

Toxicity concerns in regard to ENMs have emanated from early history of particulate toxicity[1-3]. Initial evaluation and quantitation of toxic potential at the nano-scale has followed molecular toxicity principles and protocols, where physico-chemical characterization of ENMs received minor attention. However, over time, for better understanding of toxicity mechanisms, nanotoxicologists gave considerable attention to careful evaluation of size, shape, aggregation propensity, dissolution, oxidative radical production capabilities, and other physico-chemical properties[4]. Among this set of parameters, dynamic aggregation propensity, not only convoluted delineation of toxicity mechanisms, but more so caused uncertainties in determining effective dosage; necessitating accurate determination of aggregate cluster size and shape, delivered to the cellular or organelle hosts [5, 6].

Though definitional controversies exist between the US national nanotechnology initiative's (NNI's) and that of the more recent one's from European Union's Scientific Committee on Emerging and Newly Identified Health Risks (SCENIHR)[7], ENMs are defined to possess a finite size (1-100nm) bounded by a conglomerate of molecules. At this scale, quantum mechanical forces dominate and 'diffusion' serves as the driving parameter for particulate transport in a fluid phase. Thus ENM, when introduced to a fluid, undergoes diffusional transport and inevitable collisions between the particulate entities, resulting in subsequent agglomeration or aggregation. Thus aggregated cluster formation has confounded nano-safety evaluation by presenting challenges of dynamic agglomeration, making the dose consideration in nanotoxicology questionable. Moreover, nanotoxicity literature presents conflicting evidence with regard to size-dependence on toxicity [1, 8, 9]. Realizing these challenges, i.e., effective dose determination and precise interpretation of geometry dependent toxic responses of ENMs, recent studies urged

determination of time-dependent concentration of ENMs in a dose-response assay [10, 11]. The state-of-the-art nano-safety literature only considers primary ENM size in exposure fluid matrices leaving the inevitable aggregation impact unaddressed[12, 13].It is also well known that aggregation properties of ENMs are influenced by ENM shape, surface functionalities, and exposure medium properties [14-16]. Furthermore, classical colloidal literature has identified that aggregation of nano-scale entities will not only evolve with time, but will also possess an internal structure; that too depends on material physico-chemical properties and surrounding fluid chemistry[17]. The aggregation dynamics and structure will both influence diffusion and sedimentation of ENMs and thus necessitate systematic evaluation of such parameters for delineation of toxicity mechanism or accurate dose determination in nano-safety studies.

A significant number of the nanotoxicity studies gave considerable attention to size characterization, but the majority of them ignored the time dependent evolution of aggregate size for the duration of the exposure. The objective of this study is to present a new insight onto aggregation of AuNS in presence of biological media through continuous monitoring of the aggregate size and structure. In this study time dependent aggregate size and structure evolution were evaluated using dynamic and static light scattering (DLS/SLS). Electrophoresis, UV-vis spectroscopy, and electron microscopy were performed for material characterization. The findings from this study will likely influence nanomaterial characterization for *in vitro* toxicity studies.

3.2 Materials and methods

3.2.1 Sample Preparation

Monodisperse AuNS were procured from National Institute of Standard and Technology (NIST) possessing nominal diameter of 30 and 60 nm (reference material RM-8012 and RM-8013, respectively). For measurements in presence of de-ionized (DI) water, stock nanoparticle

suspension (50 mg/L) was vortexed for 10 s and diluted 20 times to obtain 2.5 mg/L concentration. This value is in the range of commonly used concentration in published toxicity studies[18, 19] . On the other hand, for measurements in presence of media, similar dilution of the stock suspension was performed using the exposure media (RPMI solution with 1% streptomycin in presence of 10% fetal bovine serum, FBS).This solution chemistry was used for all subsequent electro-kinetic and light scattering measurements.

3.2.2 Transmission Electron Microscopy

High resolution transmission electron microscopy (HRTEM) was performed with a Hitachi H-9500 (Hitachi High Technologies America Inc., Pleasanton, CA) to evaluate the morphology of gold nanospheres (AuNSs) in DI water. Prepared 2.5 mg/L AuNS suspensions were diluted by a factor of two to achieve desired particle concentration and were placed on the carbon formvar TEM grid and dried at 60°C. An accelerated voltage of 30 kV was used to adequately image the aggregates.

3.2.3 Zeta-potential Measurement

Zeta-potential of 30 and 60 nm AuNSs in DI, exposure media, with 1% streptomycin and 10 % FBS were determined using Malvern zetasizer (Malvern Instruments Ltd, Worcestershire, UK). 1 mL sample of prepared AuNS suspension was injected into the polycarbonate capillary cell (DTS 1060C) ensuring zero air bubble introduction. At least 20 measurements were recorded for each of the conditions to ensure measurement reproducibility.

3.2.4 Dynamic Light Scattering

State-of-the-art DLS goniometer system (ALV-CGS/3, ALV-GmbH, Langen, Germany) was employed to carefully monitor the aggregation profiles, collecting average hydrodynamic radii in 15 s interval. Detailed measurement protocol has been described elsewhere [16]. In brief, 2 mL

AuNS sample at 2.5 mg/L concentration in biological media with serum (RPMI-1640 + 1% Penicillin-streptomycin+ 10% FBS) was placed in a previously cleaned borosilicate vial. A 632.8 nm laser was shined through the sample and scattered light was collected at an angle of 90°. AuNS size data were collected through the software interface attained by data processing with an attached auto-correlator.. Hydrodynamic radii of the particles were then plotted against measurement time. All measurements were carried out at a temperature of 37 °C to simulate a typical cell culture condition.

3.2.5 Static Light Scattering

The ALV-CGS/3 goniometer system (ALV-GmbH, Langen, Germany) was also used to carry out angle-dependent SLS of the AuNSs. Stock suspensions of AuNSs were diluted to 2.5 mg/L in the media was added to the borosilicate glass vial quiscently left for 1 h to undergo initial aggregation. Upon reaching quasi-equilibrium in the aggregation process, angle-dependent sattering was started. Scattered intensity for an angular range of 12.5° to 100° were collected in 0.5° increment. Aggregate structure was measured in every 2 h for 24 h duration at 37 °C. Measurements were performed in triplicates for reproducibility. Fractal dimension of the aggregate was computed by plotting a log-log profile of scattering intensity against the wave vector magnitude. Slope of the fractal regime profile was computed using linear fit, which represented the fractal dimension (D_f).

3.3 Results and Discussion

3.3.1 Morphological and Electro-kinetic Characterization of the Nanoparticles

TEM micrographs in Figure 3.1 show that the AuNSs are nearly spherical and relatively uniform in size. Diameter of the nanoparticles observed in TEM varied from 25-32 nm to 45-65 nm for 30 and 60 nm diameter AuNSs, respectively. Initial sizes of the nanoparticles in DI water were further confirmed using DLS measurements. Figure B-1 shows relatively stable average size profile for

both the AuNSs, indicating high stability of the gold suspensions. Characteristic Plasmon resonance of the AuNS is confirmed with UV-Vis spectroscopy as shown in Figure B-2. Both AuNSs showed well-defined characteristic peaks at 524 and 532 nm for 30 and 60 nm particles, respectively.

Surface potential as a function of background solution chemistry is presented in Figure B-3. AuNS show negative surface charge in DI water and zeta-potential values are found to be –(30.65 ± 4.18) and –(46.22 ± 7.89) mV for 30 and 60 nm, respectively. However, in presence of exposure media, the values are reduced to – (8.84 ± 3.19) and – (15.29 ± 3.39) mV, respectively. It is noteworthy, that addition of streptomycin and FBS didn't influence the surface potential of the AuNS's substantially; i.e. resulting in values of – (9.82± 3.42) and – (11.99± 5.69) mV, respectively. The reduction in zeta-potential is likely due to electrostatic screening in presence of high amount of mono- and di-valent electrolyte in the exposure media. Such behavior was consistently observed in prior studies [20].

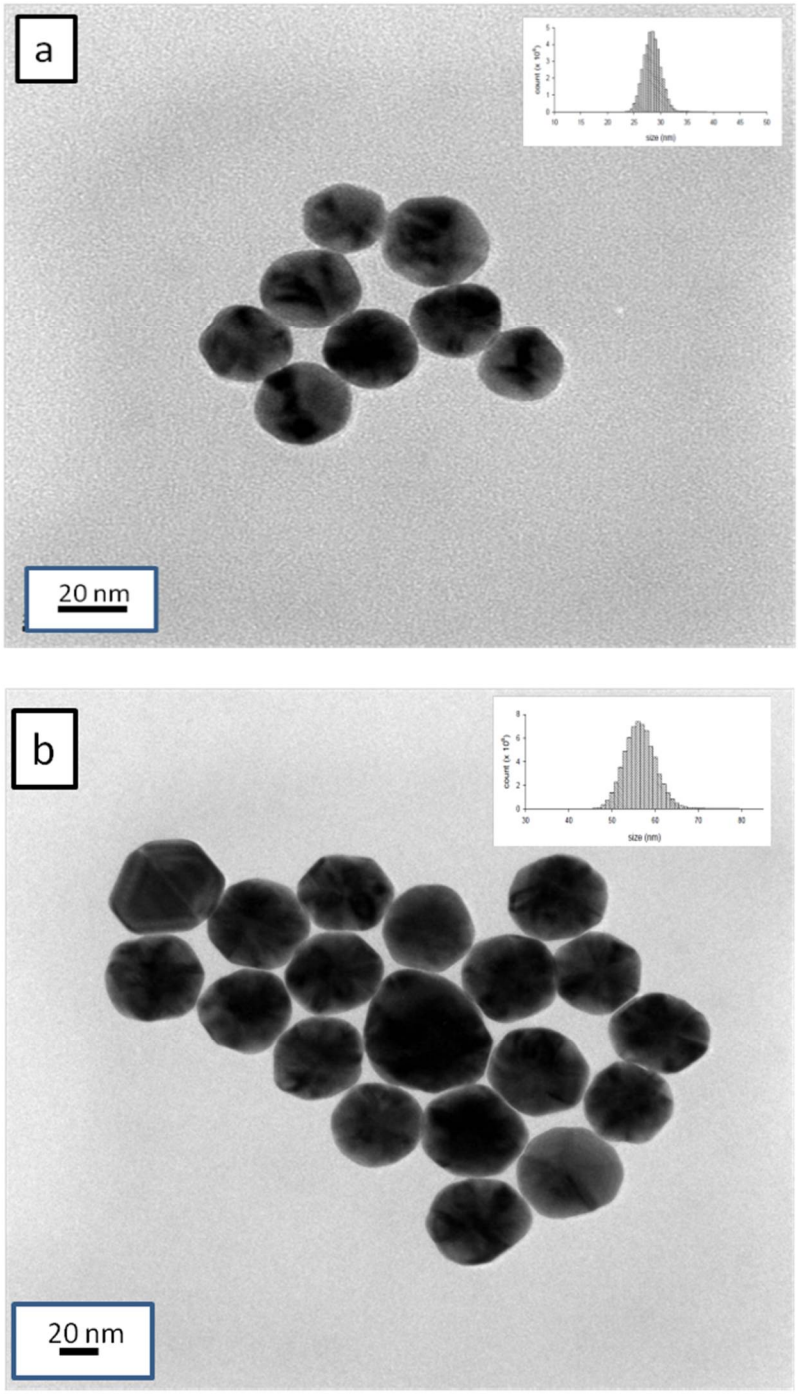

FIGURE 3.1 Transmission electron microscope (TEM) images of gold nanoparticles demonstrating rounded morphologies and corresponding size histograms. a) 30 nm sample, b) 60 nm sample

3.3.2 Aggregate Sizes of the Nanoparticles in the Culture Media

Figure 3.2 presents dynamic aggregation profiles of the AuNSs over a time period of 24 h. The initial aggregation pattern shows classical cluster formation with time; i.e., formation of dimers, trimers, tetramers, etc. Such gradual increase in cluster size, which likely results from particle collisions via electrostatic screening, continued until 6 h, beyond which the average size data started to show significant scatter. The classical size evolution profile up to this time period consistently showed noticeable cluster-size differences for the two particle types; e.g., at 6 h, 30 and 60 nm AuNS formed 331±65 and 526±86 nm clusters, respectively. From 6-24 h period, the observed scatter in average size data bears unique significance. Based on the fundamentals of particulate scattering[21], such deviation in size in short time increment (15 s) can be interpreted as a wide particle network; where light is scattered from a smaller segment of the network at an instant, when at the next instant the scattering occurs from a much larger cluster. This large variation in size or 'scatter' widened for this 6-24 h period. The dynamic aggregation profiles signify that cluster-size differences diminished beyond 6 h period thus can have profound impact on effective dose for *in vitro* studies; i.e., gradual nano-scale AuNS will mostly be suspended up to 6 h time period, whereas sudden and significant settling of larger sized AuNS clusters will likely occur at and beyond this critical time. Thus an overall dose determination for nanomaterials with no consideration of variation of the effective dosage over time is likely compromising the mechanistic evaluation of most nanotoxicity. Such accurate dose determination issues have been otherwise observed as a challenge in earlier nanotoxicity literature[6, 8].

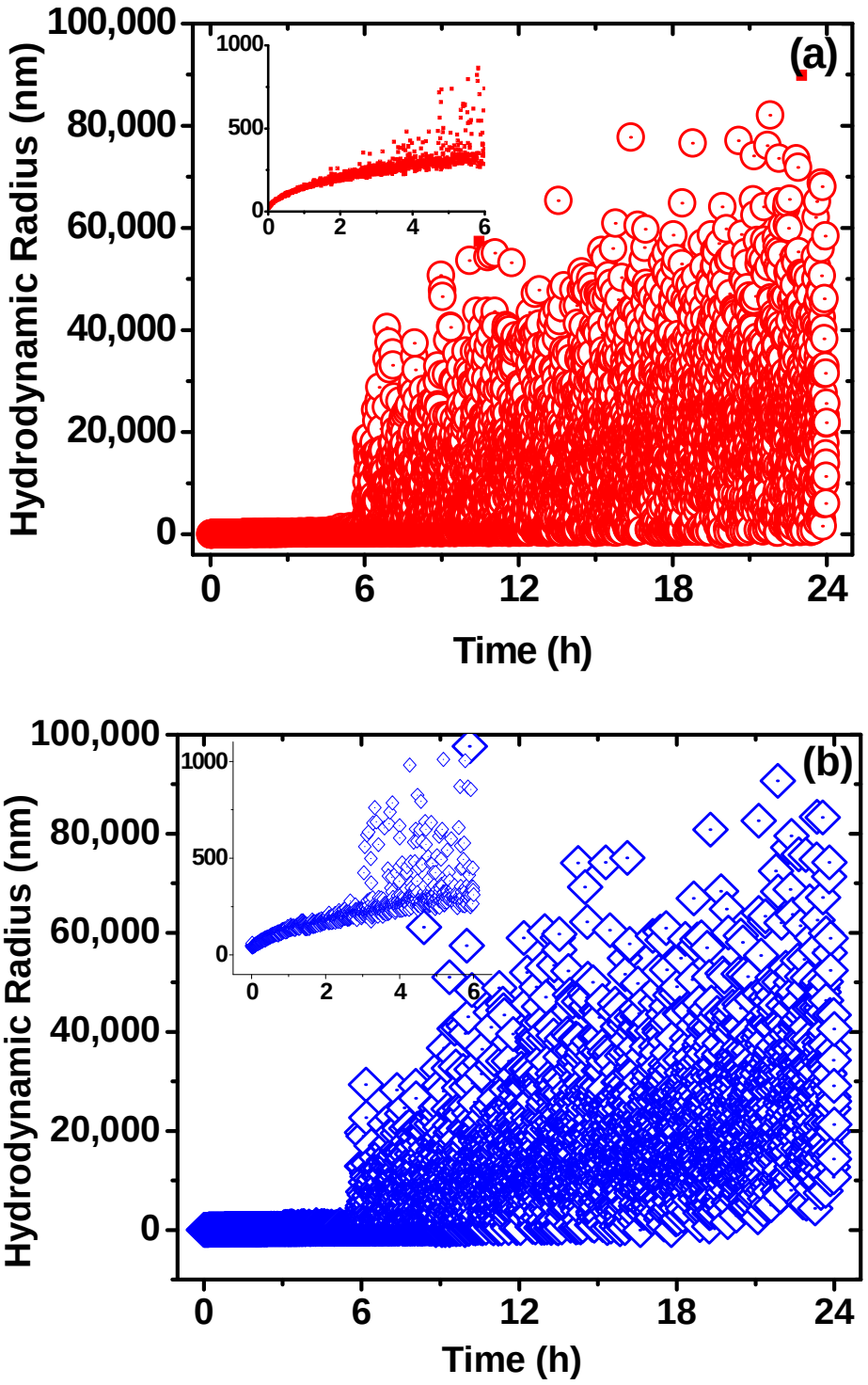

FIGURE 3.2 Aggregation characteristics of gold nanoparticles in physiological condition consisting RPMI media a) 30 nm samples, b) 60 nm samples

3.3.3 Aggregate Structures of the Nanoparticles in the Culture Media

Aggregate structural conformation was also studied via SLS as shown in Figure 3.3. Angle-dependent scattering data I (q) was plotted with wave vector, q for the entire scattering regime. The linear fractal regime data was then analyzed employing classical fractal theory[22]. Using linear fit of the fractal regime I vs q to determine fractal dimension D_f. The theoretical relationships relevant to fractal dimension and the wave vector are presented by Equations I and II).

$$I \propto q^{-D_f} \quad \text{..... (I)}$$

$$q = \frac{4\pi\eta \sin\frac{\theta}{2}}{\lambda} \quad \text{..... (II)}$$

where, θ is used to express scattering angle, while λ stands for laser wavelength. D_f values thus determined for 30 and 60 nm AuNSs over 24 h period are presented in Figure 3.3. The D_f values presented here were estimated from statistical fit from the scattering data, shown in Figure B-4. The D_f for 30 nm AuNS showed consistency over the entire exposure period, which varied between 2.79±0.01 and 2.72±0.03 (Table B-1). The values indicate relatively compact structural conformation for the 30 nm AuNS. It is to be noted that D_f values closer to the numerical value 3.0 represents a more compact structure with little internal porosity, whereas, D_f values near 1.0 represents a more loose internal structure with large internal porosity. However, the 60 nm AuNSs showed relatively lower D_f, with an increasing trend for the exposure period of 12 to 24 h; i.e., 1.99±0.13 to 2.62±0.02 (Table B-2). The dynamic aggregation and packing of 60 nm AuNSs thus will likely result in an evolving structural conformation of the clusters that varies from relatively loose packing toward compact conformation with the progression in time. A two-way ANOVA analysis (Table B-3) showed significant effect of size of the particle ($p<0.001$) and the time of measurement ($p=0.0035$) on the structure of the nanoparticle aggregates. However, relatively

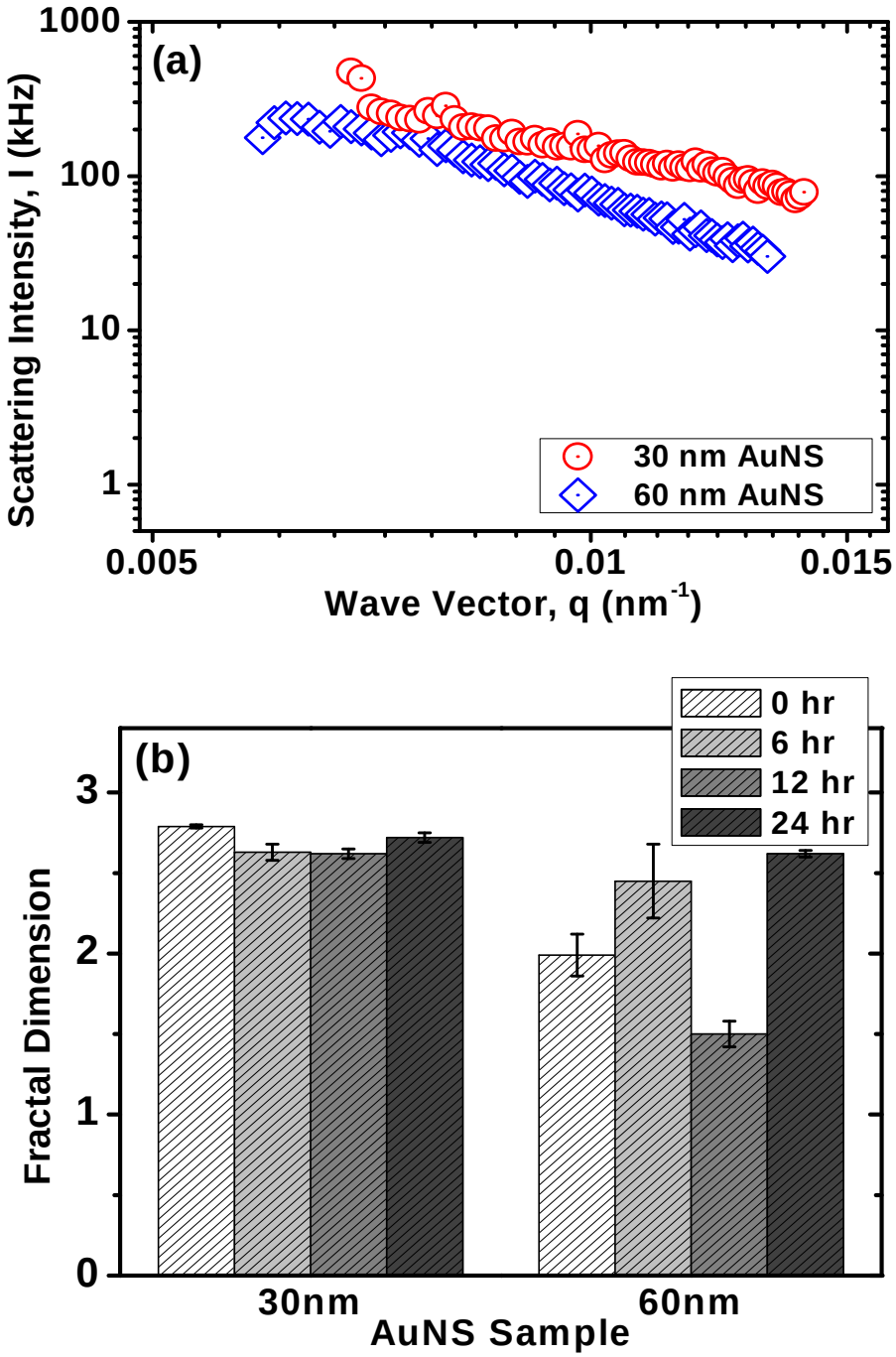

FIGURE 3.3 Angle dependent static light scattering (SLS) measurement of gold nanoparticles. a) Raw data for fractal dimension (D_f) calculation, b) Bar chart showing $D_f$over 24 h period for different sizes of nanoparticles. A two-way ANOVA analysis showed significant difference among individual observations

lower p-value for 60 nm particles indicates larger variability of D_f over time. The deviation from the increasing trend of D_f after 6 h time period for this case reinforces the complex structure formation at longer exposure periods. Eventually, after long exposure times, both particle types reach rather compact structural form and lose size specific differences in aggregation. Thus differences in cluster formation of the 30 and 60 nm AuNSs will not only show diminished differences for overall size, but also for structural conformation.

The mechanism for both dynamic aggregation behavior and cluster conformation of the AuNSs lacks presentation of direct evidence in this article. However, the hypothetical explanation of the observed behavior is outlined as follows. The initial aggregation behavior as shown in Figure 3.3 (until the 6 h mark) can easily be explained by the size differences between the two particles. The cluster size evolution and sizes attained up to this point thus reflect the initial size difference of these particles. The network formation of the AuNSs, however, indicates a critical size attainment of the clusters near to the 6 h time period; where the grown clusters served as critical nucleating size for fast growth of aggregate networks. As observed in the zeta-potential values, low electrokinetic energy barrier resulted in short ranged particle interaction, which likely had caused accelerated aggregation to form large networked structure. This process of large networked formation is similar to 'aggregative nucleation' process, where individual particles or clusters are coerced to already aggregated clusters[23]. This mechanism is known as non-classical nucleation of cluster formation compared to the classical LaMer mechanism[24]. In addition to this process, protein (from the FBS) possess charged moieties, which is likely to induce bridging by divalent calcium ion (from the RPMI), could also contribute to such network formation. However, in order to support any such hypothesis, systematic studies involving multiple biological media in presence of a range of protein structures should be performed.

The differences in the networked structure of D_f between the two AuNS samples, likely resulted from geometric size differences causing unique packing propensities; larger the AuNSs higher was the resistance to packing, when compared to the smaller counterpart[25]. It should be noted that, Figure 3b lacks in capturing a defined trend for Df over time. This further confirms the complexity of formed particle network beyond the 6 hour period. SLS experiments collect localized scattering information, which can be considered as average measurements of the overall particle sample at a time point. Since Figure 3.2 has shown abrupt alteration of particle size beyond 6 hour time period, and a likely formation of particle network, the localized SLS measurement thus was unable to capture the actual fractal dimension of these network structures. This data thus further highlights the complexity of these network formation and reinforces the observations from Figure 3.2.

3.4 Conclusions

Time-dependent aggregation and D_f measurements thus highlight the importance of dynamic evaluation of these properties for nanomaterials in physiological conditions. Most of the toxicological studies consider 24 h as the time period for collection and analysis of biological assays. Nanotoxicology literature has reported multi-micron sized aggregate formation at the end of exposure time-period when size was evaluated in relevant biological media; e.g., magnetite particles in RPMI (2.2±0.6 μm) (Schulze et al. 2008), polystyrene in Krebs-Ringer-modified buffer (~4 μm) (Wiogo et al. 2011), titanium in Dulbecco's Modified Eagle's Medium (DMEM) (2.37±0.16 μm) (Long et al. 2006), titanium in RPMI (1.8±0.4 μm) (Long et al. 2007). Conceptually, nano-toxicological studies to date assume that these aggregates are discrete entities of a certain size and settle following Stokes's law in the *in vitro* exposure well. However, the findings in this study—i.e., possible formation of network structure and thus a completely different

mode of settling (zone setting)—show that these reported sizes have likely painted an inaccurate picture of nanoparticle exposure for *in vitro* studies. A singular time-point size assessment likely captures a "snapshot" of the true aggregation state; i.e., a single time-point measurement does not capture large size variability (in short time interval) and can lead to wrong assessment of *in vitro* mechanisms.

The continuous measurement of size evolution of AuNSs indicates that important size information (which can result in altered effective dosage of nanoparticles) can be lost if singular size data point is utilized in such analysis. As found in this study, formation of networked structure after 6 h may necessitate a reconsideration of re-designing the cell viability studies that use 24 h time point as exposure period. Accurate assessment of nanotoxicity mechanisms will either require continuous evaluation of particle size over time, intermediate time point for toxicity assays, or inverted in vitro approach, where effective dosage of nanoparticles will only be influenced by diffusion and not by aggregation and subsequent sedimentation (Cho et al. 2011).Thus continuous measurement of particle size evolution is necessary to better understand nano-bio interaction, particularly in cases of *in vitro* exposures.

3.5 Literature Cited

1. Oberdorster, G.; Maynard, A.; Donaldson, K.; Castranova, V.; Fitzpatrick, J.; Ausman, K.; Carter, J.; Karn, B.; Kreyling, W.; Lai, D.; Olin, S.; Monteiro-Riviere, N.; Warheit, D.; Yang, H.; Toxicity, I. R. F. R. S. I. N.; Screening Working, G., Principles for characterizing the potential human health effects from exposure to nanomaterials: elements of a screening strategy. *Particle and fibre toxicology* **2005,** *2*, 8-8.
2. Kante, B.; Couvreur, P.; Dubois-Krack, G.; De Meester, C.; Guiot, P.; Roland, M.; Mercier, M.; Speiser, P., Toxicity of polyalkylcyanoacrylate nanoparticles I: Free nanoparticles. *Journal of pharmaceutical sciences* **1982,** *71*, (7), 786-790.
3. Allison, A. C., Lysosomes and toxicity of particulate pollutants. *Archives of Internal Medicine* **1971,** *128*, (1), 131-&.
4. Nel, A. E.; Maedler, L.; Velegol, D.; Xia, T.; Hoek, E. M. V.; Somasundaran, P.; Klaessig, F.; Castranova, V.; Thompson, M., Understanding biophysico-chemical interactions at the nano-bio interface. *Nature Materials* **2009,** *8*, (7), 543-557.
5. Pasquini, L. M.; Hashmi, S. M.; Sommer, T. J.; Elimelech, M.; Zimmerman, J. B., Impact of Surface Functionalization on Bacterial Cytotoxicity of Single-Walled Carbon Nanotubes. *Environmental Science & Technology* **2012,** *46*, (11), 6297-6305.
6. Nel, A.; Xia, T.; Madler, L.; Li, N., Toxic potential of materials at the nanolevel. *Science* **2006,** *311*, (5761), 622-627.
7. POTOČNIK, J., Commission Recommendation of 18 October 2011 on the definition of nanomaterial Text with EEA relevance. *Official Journal of the European Union* **2011,** *275*, 38-40.
8. Oberdorster, G.; Oberdorster, E.; Oberdorster, J., Nanotoxicology: An emerging discipline evolving from studies of ultrafine particles. *Environmental Health Perspectives* **2005,** *113*, (7), 823-839.
9. Oberdorster, G.; Stone, V.; Donaldson, K., Toxicology of nanoparticles: A historical perspective. *Nanotoxicology* **2007,** *1*, (1), 2-25.
10. Cho, E. C.; Zhang, Q.; Xia, Y., The effect of sedimentation and diffusion on cellular uptake of gold nanoparticles. *Nature Nanotechnology* **2011,** *6*, (6), 385-391.
11. Lison, D.; Thomassen, L. C. J.; Rabolli, V.; Gonzalez, L.; Napierska, D.; Seo, J. W.; Kirsch-Volders, M.; Hoet, P.; Kirschhock, C. E. A.; Martens, J. A., Nominal and effective dosimetry of silica nanoparticles in cytotoxicity assays. *Toxicol. Sci.* **2008,** *104*, (1), 155-162.
12. Kim, T.-H.; Kim, M.; Park, H.-S.; Shin, U. S.; Gong, M.-S.; Kim, H.-W., Size-dependent cellular toxicity of silver nanoparticles. *Journal of Biomedical Materials Research Part A* **2012,** *100A*, (4), 1033-1043.
13. Clément, L.; Hurel, C.; Marmier, N., Toxicity of TiO2 nanoparticles to cladocerans, algae, rotifers and plants – Effects of size and crystalline structure. *Chemosphere* **2013,** *90*, (3), 1083-1090.
14. Zhou, D.; Keller, A. A., Role of morphology in the aggregation kinetics of ZnO nanoparticles. *Water Research* **2010,** *44*, (9), 2948-2956.
15. Phenrat, T.; Saleh, N.; Sirk, K.; Kim, H.-J.; Tilton, R. D.; Lowry, G. V., Stabilization of aqueous nanoscale zerovalent iron dispersions by anionic polyelectrolytes: adsorbed anionic polyelectrolyte layer properties and their effect on aggregation and sedimentation. *Journal of Nanoparticle Research* **2008,** *10*, (5), 795-814.

16. Saleh, N. B.; Pfefferle, L. D.; Elimelech, M., Influence of Biomacromolecules and Humic Acid on the Aggregation Kinetics of Single-Walled Carbon Nanotubes. *Environmental Science & Technology* **2010,** *44*, (7), 2412-2418.
17. Weitz, D. A.; Oliveria, M., Fractal structures formed by kinetic aggregation of aqueous gold colloids. *Physical Review Letters* **1984,** *52*, (16), 1433-1436.
18. Hauck, T. S.; Ghazani, A. A.; Chan, W. C., Assessing the effect of surface chemistry on gold nanorod uptake, toxicity, and gene expression in mammalian cells. *Small* **2008,** *4*, (1), 153-159.
19. Shukla, R.; Bansal, V.; Chaudhary, M.; Basu, A.; Bhonde, R. R.; Sastry, M., Biocompatibility of gold nanoparticles and their endocytotic fate inside the cellular compartment: a microscopic overview. *Langmuir* **2005,** *21*, (23), 10644-10654.
20. Afrooz, A. R. M. N.; Khan, I. A.; Hussain, S. M.; Saleh, N. B., Mechanistic Hetero-aggregation of Gold Nanoparticles in a Wide Range of Solution Chemistry. *Environmental Science & Technology* **2013,** *47*, (4), 1853-1860.
21. Pecora, R., *Dynamic light scattering: Applications of photon correlation spectroscopy*. Springer-Verlag New York, LLC: 1985.
22. Lin, M. Y.; Lindsay, H. M.; Weitz, D. A.; Ball, R. C.; Klein, R.; Meakin, P., Universality in colloid aggregation. *Nature* **1989,** *339*, (6223), 360-362.
23. Shields, S. P.; Richards, V. N.; Buhro, W. E., Nucleation control of size and dispersity in aggregative nanoparticle growth. A study of the coarsening kinetics of thiolate-capped gold nanocrystals. *Chemistry of Materials* **2010,** *22*, (10), 3212-3225.
24. Lamer, V. K.; Dinegar, R. H., Theory, production and mechanism of formation of monodispersed hydrosols. *Journal of the American Chemical Society* **1950,** *72*, (11), 4847-4854.
25. Wu, H., Lattuada, M., Morbidelli, M., Dependence of fractal dimension of DLCA clusters on size of primary particles. *Advances in Colloid and Interface Science* **2013**.

Chapter 4

Mechanistic Hetero-aggregation of Gold Nanoparticles in a Wide Range of Solution Chemistry[3]

[3]Afrooz, A. N., Khan, I. A., Hussain, S. M., & Saleh, N. B. (2013). Mechanistic heteroaggregation of gold nanoparticles in a wide range of solution chemistry. *Environmental Science & Technology*, 47(4), 1853-1860.
Contributions of the Co-Authors: I.A.K: Characterization of the Materials, PA Functionalization of SWNT, Aggregation Data Plotting; S.M.H: Co-PI

Abstract

Hetero-aggregation behavior of AuNS in presence of PA modified single-walled carbon nanotubes (PA-SWNTs), was systematically studied for a wide range of mono- and di-valent (NaCl and $CaCl_2$) electrolyte conditions. Homo-aggregation rates of AuNS were also determined to delineate hetero-aggregation mechanisms. Time resolved DLS was employed to monitor aggregation. The homo-aggregation of AuNS showed classical DLVO type behavior with defined reaction limited (RLCA) and diffusion limited (DLCA) aggregation regimes. PA-SWNTs homo-aggregation on the other hand showed no response with electrolyte increase. AuNS hetero-aggregation rates on the other hand, showed regime dependent response. At low electrolyte or RLCA regime, AuNS hetero-aggregation showed significantly slower rates, compared to its homo-aggregation behavior; while, enhanced hetero-aggregation was observed for DLCA regime. The key mechanisms of hetero-aggregation of AuNS are identified as 'obstruction to collision' at RLCA regime and 'facilitating enhanced attachment' at DLCA regime, manifested by the presence of PA-SWNTs. Presence of Suwannee River humic acid (SRHA) also showed aggregation enhancement for both homo- and hetero-systems, in presence of divalent Ca^{2+} ions. Bridging between SRHA molecules is identified as the key mechanism for increased aggregation rate. The findings of this study are relevant, particularly to co-existence of engineered nanomaterials. The strategy of using non-aggregating PA-SWNTs is a novel experimental strategy that can be adopted elsewhere to further the hetero-aggregation studies for a wider set of particles and surface coatings.

Keywords: Hetero-aggregation; co-existence; gold nanoparticles; single-walled carbon nanotubes; pluronic

4.1 Introduction

Unique advantages at the nano-scale have encouraged research and commercialization of ENMs and nano-laden products. Safety concerns on nanotechnology thus increasing, necessitate realistic prediction of their fate and transport [1] and mechanistic evaluation of their toxicity [2]. In the fate and transport literature, aggregation propensity is systematically studied using classical colloidal techniques and under environmentally relevant background conditions [3-6]. In nano-toxicity studies aggregation is mostly evaluated in control settings with little relevance to the actual exposure conditions [7]. However, most of such studies concentrate on singular particulate systems with little emphasis on the influence of secondary particulate matter—that are highly relevant to biological and aquatic systems containing particulate biological entities and naturally occurring colloids; e.g., proteins, particulate organic matter, clay, and other inorganic particles [8-10]. In addition, co-existence of ENMs also presents a binary particulate scenario in environmental settings [11]. Understanding aggregation behavior in heterogeneous environment is thus of immense importance that will allow for reliable evaluation of ENM fate and nano-bio interaction mechanisms.

Particle-particle interaction in a singular system, i.e., homo-aggregation, is primarily influenced by diffusion potential at the colloidal scale and particle collision radius [12-14]. Experimental and theoretical studies are well established on the fundamentals of homo-aggregation theory and mechanisms for a variation of their surface properties, background solution chemistry, and other physico-chemical attributes [10, 13, 15-17]. In a more complex natural or biological setting, aggregation occurs in presence of other dissimilar particles—in terms of chemical composition, electrical charge, size, or shape—and is termed as hetero-aggregation [18-22]. Hetero-aggregation of ENMs is identified as an important phenomenon not only in biological and natural systems but also in engineered processes; e.g., separation technology [23], coating processes

[24], food and biotechnological processes [12, 18], ceramic industries [25], and composites or core-shell materials [24]. Nanomaterial interaction in such hetero-systems is also likely to be influenced by physico-chemical properties and background chemical conditions. However, the state-of-the-art ENM fate and transport, mechanistic nano-bio interaction, and particle processing literature have paid little attention to systematically evaluate hetero-aggregation as a function of such key parameters.

Classical colloidal studies focused on resolving short- and long-ranged interfacial interaction issues [26, 27] and developed DLVO models (with necessary extensions) to predict and analyze colloidal stability [28]. These models are later applied for homo-aggregation analyses of ENMs as a function of particle size, geometry, chemical composition, crystal structures, and surface coatings [10, 15-17]. On the contrary, colloidal hetero-aggregation studies showed a limited focus with the use of asymmetric colloidal systems only; i.e., soft and/or hard colloids with opposite surface potential [19, 29-36]. Such classical hetero-aggregation studies present aggregation rate determination at different electrolyte conditions and evaluate mechanisms with theoretical DLVO predictions and its Hogg–Healey–Fuerstenau (HHF) approximation [18, 19, 33, 35, 37, 38]. Overall, the hetero-mixtures in such studies showed less stability compared to their homogeneous suspensions at similar electrolyte conditions [38, 39]. It is noteworthy that hetero-aggregates, i.e., aggregated clusters with more than one colloidal identity, are found to be formed at both low and high electrolyte concentration ranges [29, 35, 36, 40]. Electrostatic attraction between oppositely charged entities though dominate at the low range, the mechanism of aggregation get obscured with complexities in the higher electrolyte range—arising from simultaneous electrostatic screening of both the charged entities as well as competitive attachment of similar and dissimilar colloids [35]. Attempts have been made to address such complexities by subtracting the homo-

aggregation rates from simultaneous homo-hetero-aggregation ones [29, 35]. However, these challenges become more profound in case of ENMs, which possess inherent complexities in their physico-chemical attributes. The focus for hetero-aggregation of ENMs thus got further limited to extremely low electrolyte cases (0.1 mM NaCl) where the key parameter remains to be the relative concentrations of the binary entities [41]. The key data gap in classical colloid literature is the lack of techniques or strategies for hetero-aggregation, applicable to like-charged particles and for a wide range of electrolytes. In addition, the strategies of simultaneous homo/hetero studies to decipher hetero-mechanisms also fail to apply to more complex ENM systems. Thus systematic evaluation of ENM hetero-aggregation in a wide range of electrolytes requires a novel strategy that can employ light scattering as an effective and singular detection technique.

The objective of this study is to establish light scattering as a single analytical technique that can determine aggregation behavior and enumerate aggregation mechanisms of AuNSs in a binary system; i.e., in presence of PA coated single-walled carbon nanotubes (PA-SWNTs). Due to unique spectral signature, chemical stability, and low background concentration, AuNS is used as a model nanomaterial,—with size dependent plasmon resonance—which leaves room for future expansion of this technique to address a wider set of natural colloids and ENMs. PA-SWNTs is used as a secondary entity on the premise of co-existence of nanomaterials [11]; while choice of PA is based on the likelihood of similar non-ionic organic matter presence in the natural environment [42, 43]. In this study, PA surface modification enabled a physical presence of SWNTs as secondary tubular entities with no response (i.e., aggregation response) to electrolytes and thus allowed the use of light scattering as a singular technique to evaluate hetero-aggregation of AuNS in a wide range of electrolytes. The physico-chemical properties of AuNS and PA-SWNTs are characterized using UV-vis and Raman spectroscopy, TEM, and electrophoretic measurements. Time-resolved

dynamic light scattering is used to evaluate aggregation behavior of AuNS with mono- and divalent electrolytes in both homo- and hetero-aggregation scenarios. The aggregation data are analyzed using classical stability theory while mechanisms of aggregation are enumerated using TEM, electrokinetic properties, and classical colloid and polyelectrolyte literature.

4.2 Materials and Methods

4.2.1 Preparation of the AuNS Suspension

Aqueous suspension of poly (acrylic acid) stabilized AuNSs with 10 nm primary particle diameter were procured from Nanopartz Inc. (Loveland, CO). Manufacturer reported the concentration of AuNS to be 4.0 g/L as determined by inductively coupled plasma mass spectrometry (ICPMS) method at pH 7.0. The AuNS stock suspension was vortexed for 30 s and diluted 200 times to perform aggregation studies and physico-chemical characterizations.

4.2.2 PA-SWNT Preparation

To perform surface functionalization with PA F127 (Sigma Aldrich), CoMoCat SWNTs (SG65) were procured from SouthWest NanoTechnologies Inc. (SWeNT, Norman, OK). A 0.02% (w/v) stock solution of PA was prepared in deionized water (resistivity ~18.2 MΩ-cm). SWNTs were added to 50 mL of surfactant solution to yield 105±5 mg/L initial concentration (SWNT: PA=1:2). The suspension was then subjected to tip sonication (S-4000, Misonix) for 30 min with ice cooling, and an average energy input of 45±5 kJ was maintained. The dispersion was allowed to stand for 24 h and subsequently subjected to centrifuge for 1 h at ~10,900 ×g (Sorvall RC 5C plus, Thermo-Fisher, MA). The supernatant was decanted to collect the PA-SWNT stock for all subsequent measurements.

4.2.3 Characterization of AuNS and PA-SWNTs

The AuNSs and PA-SWNTs were characterized to determine their chemical signatures as well as to evaluate the key physico-chemical properties. TEM imaging was performed to evaluate morphology of individual nanomaterials as well as to enumerate hetero-aggregation mechanisms. UV-vis and Raman Spectroscopy were performed to study AuNS characteristic signature and SWNT defects and extent of oxidation, respectively. Electrophoretic mobility measurements were performed for the entire range of solution conditions to evaluate electrostatic interaction for delineation of aggregation mechanisms.

TEM was performed with a Hitachi H-9500 (Hitachi High Technologies America Inc., Pleasanton, CA) to evaluate size, shape, and physical morphology of AuNS and PA-SWNTs. A few drops of previously prepared nanomaterial suspension were placed on the carbon formvar TEM grid and dried at 60 °C. An accelerating voltage of 30 kV was used. For hetero-aggregation cases, a few drops of the AuNS and PA-SWNT mixture with relevant electrolytes were added to the TEM grids and imaged following previously mentioned protocol.

UV-vis spectroscopy was performed on an Agilent 8453 UV-vis system (Santa Clara, CA) to evaluate the characteristic plasmon resonance of AuNS. 3 mL of AuNS suspension at a dilution of 200 were added to a 5 mm path-length quartz cuvette and a spectral response was collected spanning between 300 to 800 nm wavelength ranges. The structural signature of SWNTs, both pristine and PA- modified, was determined using Raman spectroscopy on a LabRam confocal Raman spectrometer (JY Horiba, HORIBA Instruments Inc., Irvine, CA), equipped with a liquid nitrogen-cooled CCD detector and a He/Ne (632.817 nm) laser for excitation. The spectra presented here is the average of at least 5 scans with integration times of 120 s for each.

Surface potentials of AuNS and PA-SWNTs were measured with Malvern Zetasizer (Malvern Instruments Ltd, Worcestershire, UK). For each condition, 1 mL sample was injected into the polycarbonate capillary cell (DTS 1060C) ensuring no air bubble introduction. At least 20 measurements were recorded for each condition using multiple replicate sample analysis to ensure reproducibility. Entire range of experimental ionic strength for NaCl and $CaCl_2$ was considered; while Suwannee River humic acid (SRHA) was added to appropriate dilution to evaluate role of NOM on electrokinetic behavior.

4.2.4 Solution Chemistry

All aggregation experiments, (e.g., homo- and hetero-aggregation) were performed in the presence of mono-valent (NaCl) and di-valent ($CaCl_2$) electrolyte solutions (BDH Chemicals, Dubai, UAE) over a wide concentration range, i.e., 1 mM to 550 mM NaCl and 0.1 mM to 30 mM $CaCl_2$. The pH of the stock suspension was unadjusted (ambient) and determined to be 6.5±0.05. All reagent solutions were filtered with 0.45 μm inorganic membrane filters (VWR international LLC, Radnor, PA, USA).

SRHA (Standard II, International Humic Substances Society) was used as a model NOM. A 410 mg/L SRHA stock was prepared and subsequently filtered with 0.22 μm cellulose acetate membrane filter (Corning Inc., Corning, NY). The pH of SRHA was adjusted to 6.5 by adding NaOH and was stored at 4 °C in the dark. A diluted stock of SRHA at 2.5 mg/L TOC, relevant to most natural surface waters [16], was used for aggregation and electrokinetic experiments.

4.2.5 Dynamic Light Scattering Measurement

TRDLS was utilized to determine evolution of hydrodynamic radius with time. A 22 mW 632 nm HeNe laser incorporated ALV/CGS-3 compact goniometer system (ALV-Laser GmbH, Langen/Hessen, Germany) with QE APD detector (photomultipliers of 1:25 sensitivity) was

employed to monitor size evolution in every 15 s for at least 50 min. Detailed procedure of TRDLS has been described elsewhere [16, 17]. In brief, 2 mL of AuNS suspension at 20 mg/L concentration is used for both homo- and hetero-aggregation measurements. It is critical to maintain uniform concentration for all the measurements to draw appropriate comparisons between aggregation rates. The equal concentration was ensured not only through carefully controlling the dilutions but also monitoring the raw scattering intensity over time. For the hetero-aggregation studies AuNS suspensions at identical concentration to the singular systems, i.e., 20 mg/L, were added to PA-SWNTs at 1 mg/L concentration. The borosilicate vials used to evaluate aggregation behavior were thoroughly cleaned prior to measurements [16, 17]. The singular and binary suspensions were then added with electrolyte solutions at appropriate dilutions and vortexed for 10 s before inserting to toluene-filled sample housing. Scattered light was collected at 90° and analyzed using auto cross-correlator to calculate average hydrodynamic radii. For each electrolyte condition, initial aggregation rate was estimated from linear regression of aggregate size vs. time data; up to 30% increase of aggregates size from initial sizes measured by DLS [17, 41]. Homo- and hetero-aggregation rates were the key parameters determined to draw comparisons and mechanisms of the singular and binary systems. However, attachment efficiencies (α) were determined only in case of homo-aggregation using equation 1. The inability to achieve a favorable aggregation rate, even at near-saline conditions, restricted estimation of α value for hetero-aggregation.

Attachment efficiency 'α' is represented as follows [16, 17];

$$\alpha = \frac{\left[\frac{dR_0(t)}{dt}\right]_{\{t \to 0\}}}{\left[\frac{dR_0(t)}{dt}\right]_{\{t \to 0, fav\}}} \quad \text{......} (1)$$

where, α is the attachment efficiency, and t is the time of aggregation. All TRDLS measurements were conducted at 20±0.5 °C and at least duplicate samples were tested to obtain significant reproducibility.

4.3 Results and Discussion

4.3.1 Morphological and Chemical Characterization

AuNS and PA-SWNTs were characterized with TEM to evaluate their physical morphology. Figure 4.1(a) shows spherical structures with angular features for some of the entities. The AuNS size, as determined from TEM, ranges from 10-20 nm; with most of the AuNS found to be near 10 nm size with having spherical geometry.

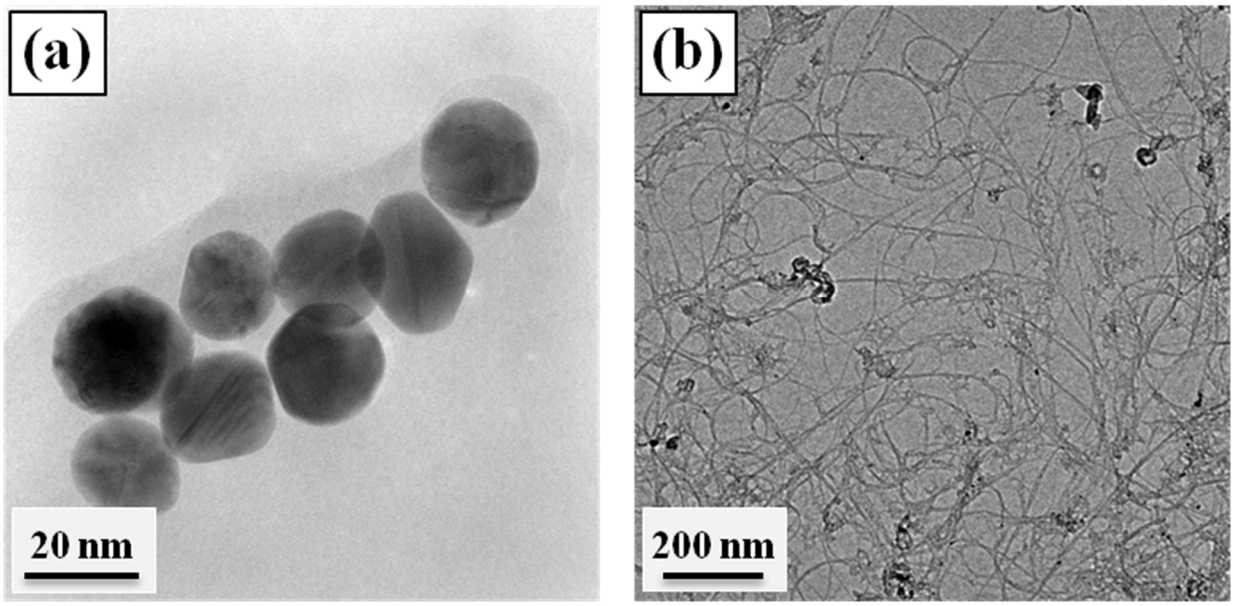

FIGURE 4.1. Representative TEM micrographs of a) AuNS and b) PA-SWNTs in DI water.

The PA-SWNTs morphology on the other hand, show dispersed tubes that are relatively long with high degree of debundling (Figure 4.1b). Amorphous features, likely to be pluronic coatings, are observed throughout the micrographs. These features also appear to be closely associated with the SWNTs. In addition, a few spherical dark objects are consistently observed in the micrographs that are likely to be catalyst clusters, used during synthesis [17]. Such debundling

and declustering of carbon structures due to PA modification, e.g., in case of graphene, was observed elsewhere [44].

The chemical surface properties of AuNS and PA-SWNTs are evaluated with UV-vis and Raman spectroscopy, respectively. Figure C-1a shows absorbance spectrum of AuNS. A broad absorbance band is observed between 450-600 nm wavelengths. Such behavior occurs from collective oscillation of conductive electrons at the interface of metallic particles and its surroundings, resulting in Plasmon resonance at a specific wavelength; i.e., 522 nm with 0.44 absorbance, in this case. The resonance wavelength is consistent with the literature reported values [45], that show peaks near 520 nm for 10 nm AuNS [45]. Surface characteristics of pristine and PA-SWNTs on the other hand, is probed with Raman spectroscopy, as shown in Figure C-1b. The Raman spectrum of pristine SWNTs shows defined peaks at 1320 and 1590 cm^{-1}, known as defect mode or 'D' band and high energy graphitic 'G' band, respectively. The D and G band show similar peaks at 1310 and 1593 cm^{-1} for PA-SWNTs. However, the D/G ratio is estimated as 0.21±0.01 for pristine case, which slightly decreased to 0.16±0.01 upon PA modification. The decline in D/G ratio reflects on surface coverage by PA molecules, which likely have caused partial shielding of surface defects. Such low defect levels on the surfaces of the SWNTs are comparable to literature reported values that shows a D/G range of 0.05 to 0.21 [46]. Lowering of surface defects due to non-covalent surface modification is also observed earlier in the literature [47]. In addition, Figure S1b also shows defined peaks at 2620 and 2595 cm^{-1}, which represent double Raman resonance of SWNTs. The occurrence of G' bands is consistent with literature reporting [46], while defined peaks—of the second harmonic response—reaffirms low extent of defects on SWNT and PA-SWNT surfaces.

4.3.2 Electrokinetic Properties

Electrokinetic properties of AuNS and PA-SWNTS with mono- and di-valent electrolytes are presented in Figure 4.2. The EPMs are measured at each salt concentration for AuNS, whereas, only a subset of low and high electrolyte concentrations are used for non-ionic PA-SWNTs. Figure 4.2a shows presence of negative surface potential on AuNS surfaces for the entire range of electrolytes. It confirms surface presence of PAA; which has negative carboxyl functionalities along its polymeric backbone [48]. The EPM values showed gradual decrease with the increase in NaCl and $CaCl_2$ concentrations, with a ~1.5 log concentration separation. In presence of NaCl (0.01-0.55 M) and $CaCl_2$ (0.0003-0.03 M), the EPM varied from $-(1.83\pm0.01) \times 10^{-8}$ to $-(0.70\pm0.02) \times 10^{-8}$ and from $-(1.51\pm0.04) \times 10^{-8}$ to $-(0.27\pm0.18) \times 10^{-8}$ $m^2V^{-1}S^{-1}$, respectively, for the lower and higher end of electrolyte concentrations. The decrease in EPM follows classical electrostatic screening of surface charges along the backbone of the attached polyelectrolytes, due to increased cation presence [49]. Literature values show both negative [50] and positive [51] surface potentials for AuNS, depending on the type of surface coating. Relatively high EPM are reported in case of citric acid (CA) and mercaptoundecanoic acid (MDA) modified AuNS with values of $-(3.29\pm0.16) \times 10^{-8}$ and $-(3.55\pm0.55) \times 10^{-8}$ $m^2V^{-1}S^{-1}$, respectively [50]. The relatively higher EPM values in such cases likely have resulted from a higher coverage of relatively smaller molecular weight surface coatings, compared to that of PAA.

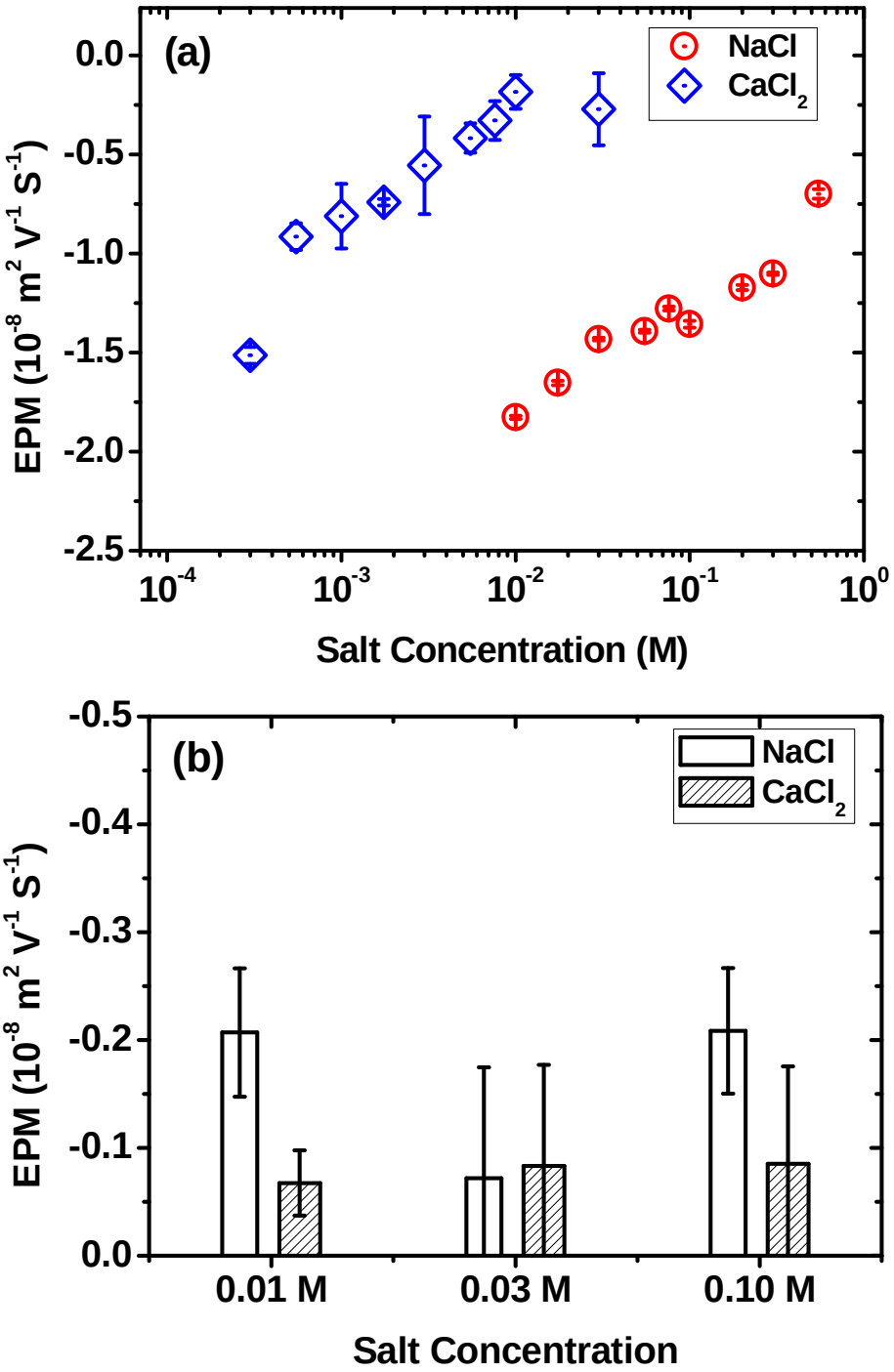

FIGURE 4.2. Electrophoretic mobility (EPM) of (a) AuNS and (b) PA-SWNTs with mono- and di-valent salts (NaCl and $CaCl_2$). Measurements were carried out at a pH of ~6.5 and a temperature of 20 °C.

Figure 4.2b shows EPM of PA-SWNTs with 10, 30, and 100 mM NaCl and $CaCl_2$. It is well-known that SWNTs acquire negative surface potential in water during mechanochemical suspension procedures [17]. The non-ionic PA modification in this study dominated the SWNT surface chemistry as demonstrated by negligible EPM values varying between $-(0.32\pm0.33) \times 10^{-8}$ to $-(0.05\pm0.19) \times 10^{-8}\ m^2V^{-1}S^{-1}$. The presence of $CaCl_2$ showed relatively lower EPM compared to NaCl cases, however, with high standard deviation between replicate measurements. Overall, such lower magnitude of surface potential with non-ionic PA F127 modification of SWNTs is observed elsewhere in the literature [52]; with reported zeta-potential of –(18.40±7.6) mV. Similar surface potential is also observed for non-ionic triton-x modified graphene and multiwalled carbon nanotubes, showing values of -28 mV and -30 mV, respectively.

4.3.3 Homo- and Hetero-Aggregation Kinetics

Figure 4.3 presents homo- and hetero-aggregation rates, systematically measured for a wide range of mono- and di-valent electrolytes. The attachment efficiencies (α) are only computed for homo-aggregation of AuNS (Figure C-2); hetero-aggregation rates did not reach plateau at the diffusion limited regime and thus disallowed estimation of their α values. The homo-aggregation rates, estimated from aggregation profiles (Figure C-3), show gradual increase—from 0.0004 to 0.3072 nm/s—with the increase in mono-valent NaCl concentration (Figure 4.3a). The homo-aggregation behavior of AuNS is better manifested in its stability plot (Figure C-2a) that shows typical DLVO type behavior with well-defined aggregation regimes; i.e., reaction limited (RLCA) or unfavorable and diffusion limited (DLCA) or favorable regimes. Similar trend of homo-aggregation rates (Figure 4.3b) and α values (Figure C-2b) are observed with $CaCl_2$, showing defined RLCA and DLCA regimes. High sensitivity to both Na^+ and Ca^{2+} at RLCA regime is observed from electrokinetic behavior (Figure 4.2a) as well as from the steep sloped stability profiles of AuNS

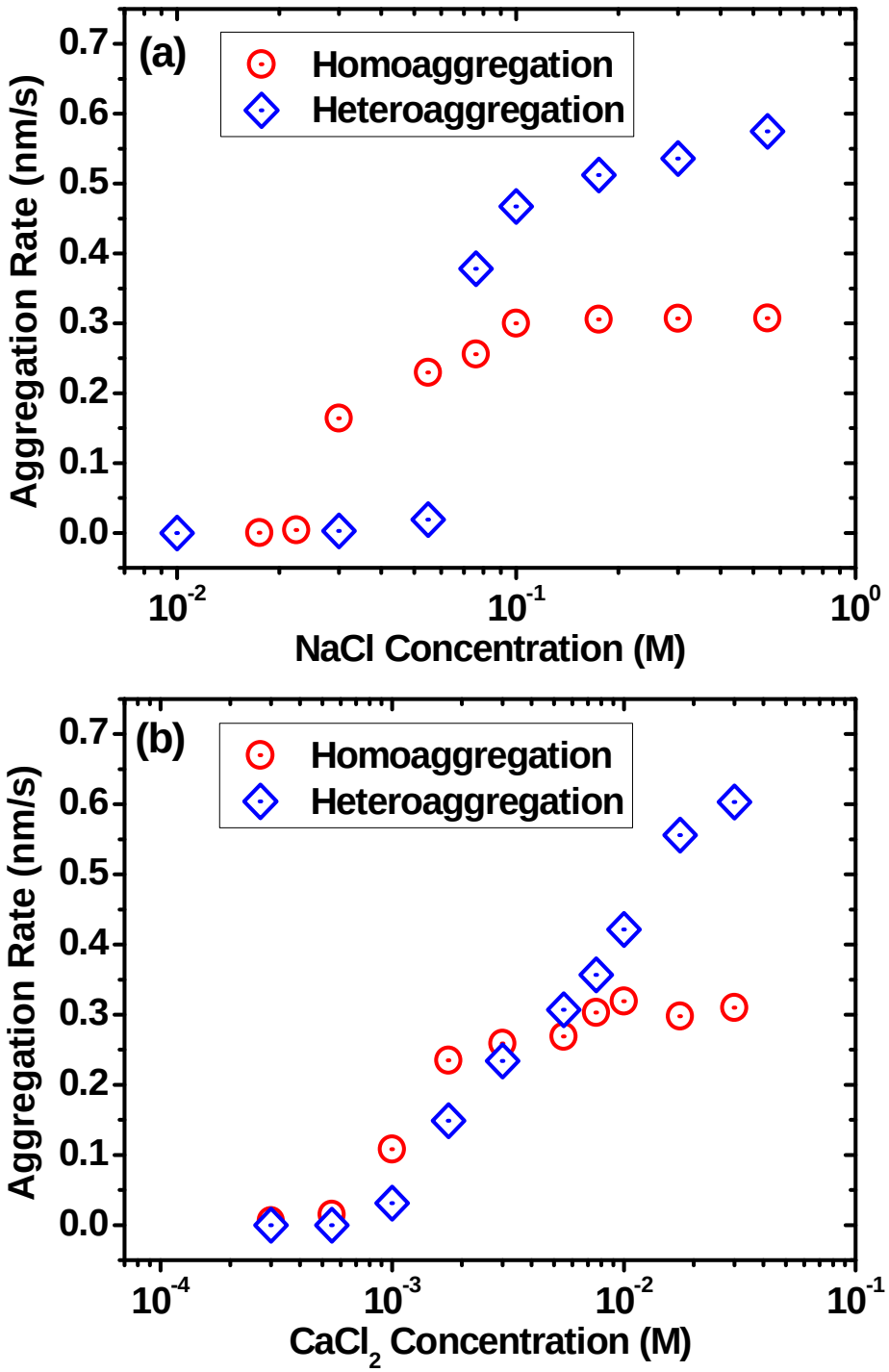

FIGURE 4.3. Initial aggregation rates of homo- and hetero-aggregation of AuNS with (a) NaCl and (b) $CaCl_2$. Measurements were carried out at pH of ~6.5 and a temperature of 20 °C.

(Figure C-2). Such responses to salt not only signify reduced electrostatic interaction between AuNS but also reflect on the conformational change of the polyelectrolytes.

At low electrolyte conditions, PAA brushes are known to be fully extended, while they contract sharply with increase in cation presence [49]. Initial AuNS particle size data qualitatively reflects on such conformational change; where, initial diameter of 15±1 nm at DI water increases to less than 20 nm with an addition of 10 mM NaCl (less than the diameter of a dimer). A combination of lowered electrostatic repulsion along with significantly lower steric contribution from contracted polyelectrolyte brushes has likely contributed to aggregation of AuNS. The CCC for homo-aggregation of AuNS is determined as 57.5 mM NaCl and 3.3 mM $CaCl_2$. Literature reported values show similar CCC (70 mM NaCl) for CA modified AuNS, while MDA modification resulted in significantly higher CCC (200 mM NaCl) [50].

Hetero-aggregation rates of AuNS show regime specific behavior (Figure 4.3). At low electrolyte conditions, the AuNSs aggregate at a substantially lower rate in presence of PA-SWNTs, compared to its homo-aggregation. The hetero-rates are estimated from hetero-aggregation profiles as presented in Figure C-4. While the AuNS respond to added electrolyte, PA modified SWNTs shows no aggregation—even with the addition of 1 M NaCl or 55 mM $CaCl_2$; Such response from PA-SWNTs is demonstrated with near-equal hydrodynamic radii—101±4 nm at 1 M NaCl compared to 98±4 nm in DI water (Figure C-5),—and nearly unchanged EPM values (Figure 2b). For AuNS hetero-aggregation however, the rates varied from 0.003-0.019 and 0.031-0.234 nm/s for [NaCl] of 30-55 mM and [$CaCl_2$] of 1-3 mM, respectively. These values are substantially lower compared to homo-rates of 0.164-0.230 and 0.108-0.259 nm/s under similar [NaCl] and [$CaCl_2$], respectively. The hetero-rates demonstrate enhanced aggregation near and beyond the CCC values for both mono- and di-valent electrolytes. For [NaCl] of 76-550 mM and

[$CaCl_2$] of 5.5-30 mM, the hetero-rates varied from 0.378-0.575 and 0.307-0.603 nm/s, respectively with no signs of plateau; whereas, homo-rates plateaued at these conditions with values of 0.256-0.307 and 0.269-0.310 nm/s, respectively. Literature reported 2.37 and 1.33 times higher hetero-rates—compared to homo-aggregation rates—for silica and polystyrene latex duo under RLCA and DLCA conditions, respectively [19]. Similarly, colloids with oppositely charged polyelectrolytes showed enhanced aggregation at RLCA regime due to polymer bridging [40]. Relatively higher enhancement of hetero-rates at RLCA—compared to DLCA regime—can be explained with higher favorable interaction between oppositely charged colloids (with lower electrostatic screening) at low electrolyte conditions (compared to higher ones). The only reported ENM hetero-aggregation study showed effects of hematite and multiwalled carbon nanotube relative ratio on hetero-rates; where the maximum hetero rate of 0.28 nm/s was achieved at multiwalled:hematite of 0.0316 [41]. However, this study has failed to present hetero-aggregation results at electrolyte conditions beyond 0.1 mM NaCl. This study thus presents the first reported hetero-aggregation rates of ENMs for both RLCA and DLCA regimes. The mechanisms of aggregation are discussed in the following subsection.

4.3.4 Mechanisms of Hetero-aggregation

Presence of PA-SWNTs alters aggregation behavior of AuNS substantially, for the entire range of electrolytes. The key mechanisms driving hetero-aggregation are based on the interplay between electrostatic interaction of AuNS at each cation concentration, conformational changes of PAA coatings at AuNS surfaces, and the physical presence of non-aggregating PA-SWNTs. At low mono- and di-valent cation concentrations, i.e., at RLCA regime, gradual electrostatic screening and contraction of polyelectrolyte layer thickness [49] initiate AuNS aggregation. It is our conjecture that in such conditions, the physical presence of PA-SWNTs likely act as hindrance to AuNS

collision, thus resulting in relatively lower values of hetero-aggregation rates as compared to those of homo-aggregation.

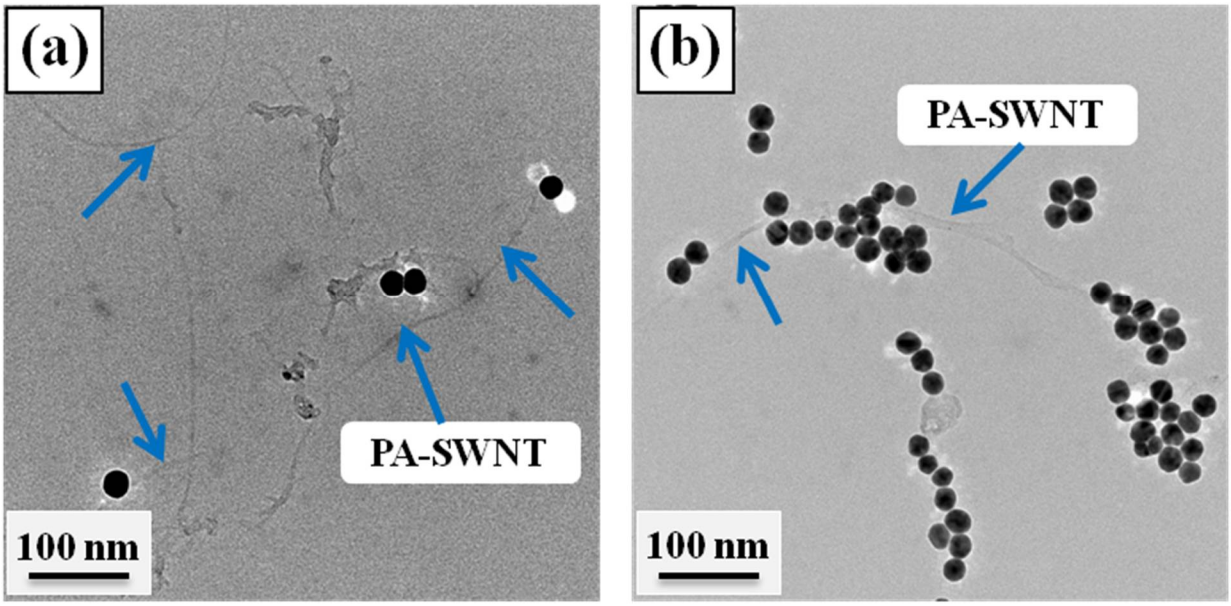

FIGURE 4.4. Representative TEM micrographs of hetero-aggregates at (a) DI water and with (b) 100 mM NaCl. The DI water case represents reaction limited (RLCA) regime while 100 mM NaCl serves as the diffusion limited (DLCA) regime.

Such physical hindrance provided by PA-SWNTs is observed in the representative TEM micrograph, as presented in Figure 4.4a. AuNSs are seen to be either entrapped within curved PA-SWNT segments or attached to the tubular structures. The role of PA-SWNTs transfer from hindrance to facilitation of aggregation in higher electrolyte conditions, i.e., in DLCA regime. The enhanced aggregation of AuNS as observed in such conditions, most likely result from utilization of PA-SWNTs as additional attachment surfaces. It is well-known in the colloid literature that charged colloidal entities act as 'sticky particles'—with higher attachment propensity due to screened electrostatic interaction—in favorable DLCA regimes [53]. AuNSs are likely to demonstrate similar 'sticky' behavior, where PA-SWNTs serve as facilitator to attachment and thus result in enhanced hetero-aggregation. Such phenomenon is observed in the TEM micrograph

as presented in Figure 4b. It shows aggregated AuNS with a preferential clustering along the backbone of PA-SWNTs. Upon substantial electrostatic screening, the AuNS not only attach to each other but also to PA-SWNTs. Subsequent attachment of AuNS to already attached entities on PA-SWNT surfaces can explain the continual increase in hetero-rates even at near saline conditions. Thus the key mechanisms of hetero-aggregation of AuNS are hypothesized as 'obstruction to collision' at RLCA regime and 'facilitating enhanced attachment' at DLCA regime, manifested by the presence of PA-SWNTs. However, this study lacks absolute proof of the validity of this hypothesis because of the inherent perturbation (i.e., drying) induced in the TEM imaging process. Cryo-TEM imaging of the samples may eliminate such sample perturbation during microscopy, and has already been attempted (C-6). However the presence of the SWNTs in the hetero-dispersion is not distinctly visible in the micrographs, possibly due to large dimensional difference between 10 nm diameter AuNS and 1 nm diameter dispersed PA-SWNTs. Cryo-TEM image presented in the appendix is yet not conclusive, hence highlights the need for further experimentation to definitely prove the hetero-aggregation mechanism proposed in this study.

4.3.5 Role of Natural Organic Matter (NOM) on Hetero-aggregation

Presence of SRHA as representative NOM also altered AuNS aggregation at 10 mM ionic strength; i.e., mixed electrolyte condition with 7 mM NaCl and 1 mM $CaCl_2$. At this condition with no SRHA presence, AuNS aggregation profiles show relatively linear increase of aggregate size (Figure 5a) with a slightly lower hetero-rate of 0.064±0.004 nm/s compared to a homo-rate of 0.146±0.007 nm/s (Figure 4.5b). In presence of SRHA however, both the homo- and hetero-rates showed substantial increase with values of 0.298±0.040 nm/s and 0.351±0.013 nm/s, respectively (Figure 4.5b). Moreover, the overall ultimate sizes of aggregates are also found to be higher with SRHA for both homo- and hetero-aggregation (Figure 4.5a). It is also observed that electrokinetic

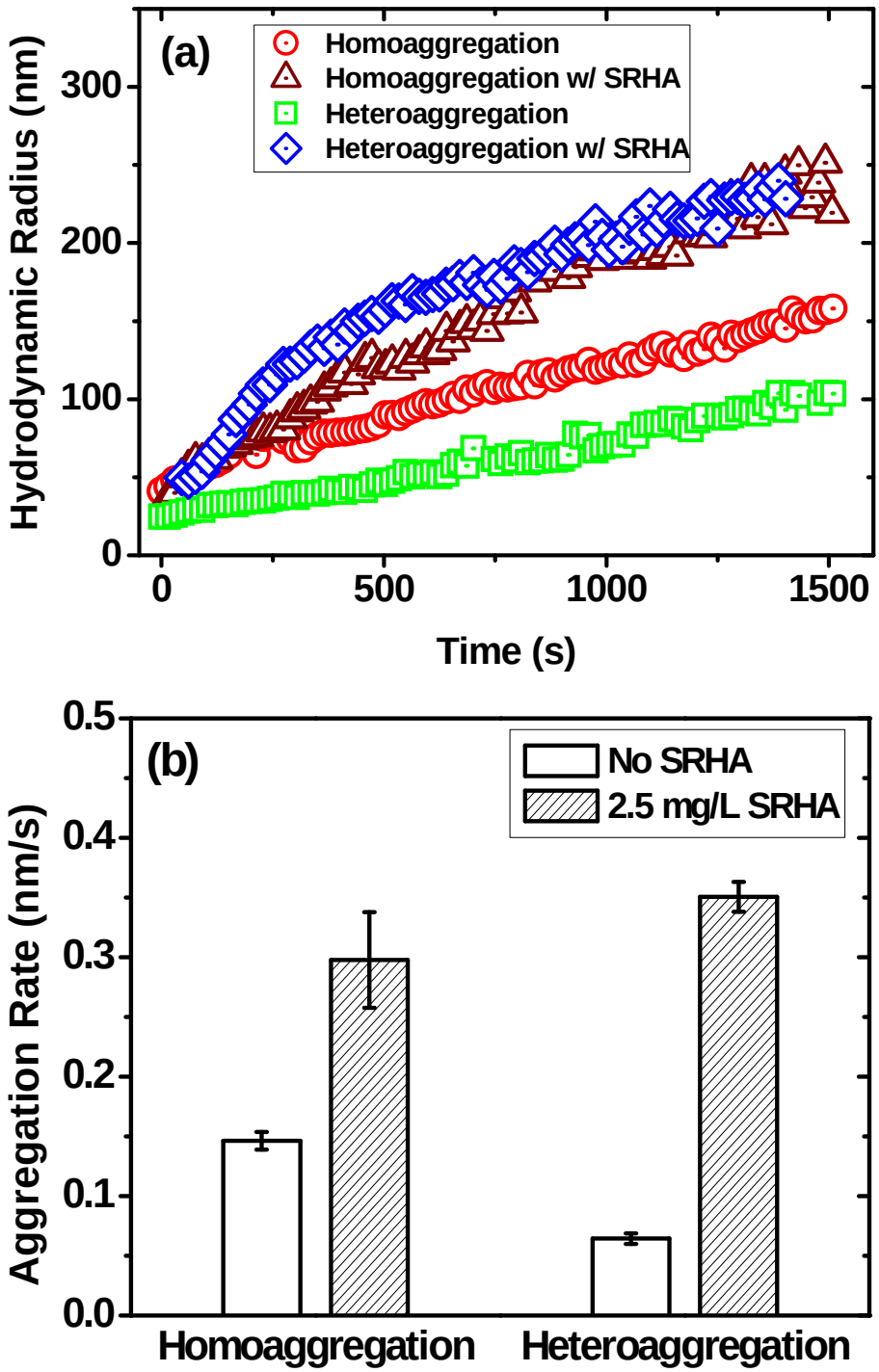

FIGURE 4.5. (a) Aggregation profile and (b) aggregate rate plot for homo- and hetero-aggregation of AuNS in presence of 7 mM NaCl + 1 mM $CaCl_2$ and with and without the presence of Suwannee River humic acid (SRHA). Measurements were carried out at pH of ~6.5 and a temperature of 20 °C.

behavior of AuNS and PA-SWNTs at these conditions are not substantially enhanced with SRHA addition (Figure C-6). The altered aggregation behavior is thus unlikely to be influenced by electrokinetic properties of either material.

SRHA average molecular weight of ~1490 Da [54] is substantially lower compared to both poly (acrylic acid) at >5000 Da and pluronic F127 at 12,600 Da. Therefore, replacement of either of these higher molecular weight surface coatings with SRHA is highly unlikely; as observed in well-known molecular weight dependent surface attachment literature of polymers and surfactants [55]. Lack of enhancement in EPM values with SRHA addition for both AuNS and PA-SWNTs (Figure C-6) can thus be explained. The SRHA, being unsuccessful in replacing either of the polymeric coatings, will likely remain in continuous aqueous phase and potentially serve as additional surfaces for interaction. The presence of Ca^{2+} ions can also result in bridging between SRHA molecules and thus generate aggregated SRHA entities [56]. Presence of SRHA and Ca^{2+} are thus likely to increase collisions between AuNS and/or PA-SWNTs and have resulted in enhanced aggregation for both homo- and hetero-aggregation scenarios.

4.4 Environmental Implications

ENMs, such as AuNS, upon release will encounter particulate entities—either naturally occurring colloids or other ENMs (such as, PA-SWNTs)—and thus will be exposed to a binary particulate environment. Aggregation behavior of AuNS, as determined in this study, shows slower hetero-rates at low electrolyte conditions, indicating to higher mobility under such typical aquatic conditions. In presence of high electrolytes, relevant to marine or estuarine environment, AuNS will likely undergo enhanced hetero-aggregation and thus will generate larger aggregates with potentially faster settling or deposition in such areas. NOM, such as SRHA, can also increase aggregation rates with divalent cation presence, resulting in slower mobility through the aqueous

systems. The findings of this study are relevant particularly to co-existence of ENMs. In addition, the strategy of using non-aggregating PA-SWNTs is a novel experimental strategy that can be adopted elsewhere to further the hetero-aggregation studies for a wider set of particles and surface coatings. The results from this study shows importance of hetero-aggregation in environmental fate and thus will likely invoke interest in the scientific community to systematically evaluate hetero-rates of ENMs in a wide range of electrolytes—potentially with a combination approach of scattering and Plasmon resonance techniques.

4.5 Literature Cited

1. Klaine, S. J.; Alvarez, P. J. J.; Batley, G. E.; Fernandes, T. F.; Handy, R. D.; Lyon, D. Y.; Mahendra, S.; McLaughlin, M. J.; Lead, J. R., Nanomaterials in the environment: Behavior, fate, bioavailability, and effects. *Environmental Toxicology and Chemistry* **2008,** *27*, (9), 1825-1851.
2. Nel, A. E.; Maedler, L.; Velegol, D.; Xia, T.; Hoek, E. M. V.; Somasundaran, P.; Klaessig, F.; Castranova, V.; Thompson, M., Understanding biophysico-chemical interactions at the nano-bio interface. *Nature Materials* **2009,** *8*, (7), 543-557.
3. Denkov, N. D.; Velev, O. D.; Kralchevsky, P. A.; Ivanov, I. B.; Yoshimura, H.; Nagayama, K., Mechanism of formation of 2-dimensional crystals from latex-particles on substrates. *Langmuir* **1992,** *8*, (12), 3183-3190.
4. Grabar, K. C.; Smith, P. C.; Musick, M. D.; Davis, J. A.; Walter, D. G.; Jackson, M. A.; Guthrie, A. P.; Natan, M. J., Kinetic control of interparticle spacing in Au colloid-based surfaces: Rational nanometer-scale architecture. *Journal of the American Chemical Society* **1996,** *118*, (5), 1148-1153.
5. Halperin, A.; Tirrell, M.; Lodge, T. P., Tethered chains in polymer microstructures. *Advances in Polymer Science* **1992,** *100*, 31-71.
6. Mattoussi, H.; Mauro, J. M.; Goldman, E. R.; Anderson, G. P.; Sundar, V. C.; Mikulec, F. V.; Bawendi, M. G., Self-assembly of CdSe-ZnS quantum dot bioconjugates using an engineered recombinant protein. *Journal of the American Chemical Society* **2000,** *122*, (49), 12142-12150.
7. Mukhopadhyay, A.; Grabinski, C.; Afrooz, A. R. M. N.; Saleh, N. B.; Hussain, S., Effect of Gold Nanosphere Surface Chemistry on Protein Adsorption and Cell Uptake In Vitro. *Applied Biochemistry and Biotechnology* **2012,** *167*, (2), 327-337.
8. Gustafsson, O.; Gschwend, P. M., Aquatic colloids: Concepts, definitions, and current challenges. *Limnology and Oceanography* **1997,** *42*, (3), 519-528.
9. Means, J. C.; Wijayaratne, R., Role of natural colloids in the transport of hydrophobic pollutants. *Science* **1982,** *215*, (4535), 968-970.
10. Petosa, A. R.; Jaisi, D. P.; Quevedo, I. R.; Elimelech, M.; Tufenkji, N., Aggregation and Deposition of Engineered Nanomaterials in Aquatic Environments: Role of Physico-chemical Interactions. *Environmental Science & Technology* **2010,** *44*, (17), 6532-6549.
11. Nowack, B.; Bucheli, T. D., Occurrence, behavior and effects of nanoparticles in the environment. *Environmental Pollution* **2007,** *150*, (1), 5-22.
12. Buffle, J.; Wilkinson, K. J.; Stoll, S.; Filella, M.; Zhang, J. W., A generalized description of aquatic colloidal interactions: The three-colloidal component approach. *Environmental Science & Technology* **1998,** *32*, (19), 2887-2899.
13. Li, D.; Kaner, R. B., Shape and aggregation control of nanoparticles: Not shaken, not stirred. *Journal of the American Chemical Society* **2006,** *128*, (3), 968-975.
14. Lin, M. Y.; Lindsay, H. M.; Weitz, D. A.; Klein, R.; Ball, R. C.; Meakin, P., Universal diffusion-limited colloid aggregation. *Journal of Physics-Condensed Matter* **1990,** *2*, (13), 3093-3113.
15. Bagwe, R. P.; Hilliard, L. R.; Tan, W. H., Surface modification of silica nanoparticles to reduce aggregation and nonspecific binding. *Langmuir* **2006,** *22*, (9), 4357-4362.
16. Saleh, N. B.; Pfefferle, L. D.; Elimelech, M., Aggregation Kinetics of Multiwalled Carbon Nanotubes in Aquatic Systems: Measurements and Environmental Implications. *Environmental Science & Technology* **2008,** *42*, (21), 7963-7969.

17. Saleh, N. B.; Pfefferle, L. D.; Elimelech, M., Influence of Biomacromolecules and Humic Acid on the Aggregation Kinetics of Single-Walled Carbon Nanotubes. *Environmental Science & Technology* **2010,** *44*, (7), 2412-2418.
18. Bradley, M., Mat Lazim, A., Eastoe, J., Stimulus-Responsive Hetero-aggregation of colloidal dispersions: Reversible systems and composite materials. *Polymers* **2011,** *3*, 1036-1050.
19. Lin, W.; Kobayashi, M.; Skarba, M.; Nu, C. D.; Galletto, P.; Borkovec, M., Hetero-aggregation in binary mixtures of oppositely charged colloidal particles. *Langmuir* **2006,** *22*, (3), 1038-1047.
20. Lopez-Lopez, J. M.; Schmitt, A.; Moncho-Jorda, A.; Hidalgo-Alvarez, R., Electrostatic Hetero-aggregation regimes in colloidal suspensions. *Advances in Colloid and Interface Science* **2009,** *147-48*, 186-204.
21. Rubio, J.; Souza, M. L.; Smith, R. W., Overview of flotation as a wastewater treatment technique. *Minerals Engineering* **2002,** *15*, (3), 139-155.
22. Ouali, L.; Stoll, S.; Pefferkorn, E.; Elaissari, A.; Lanet, V.; Pichot, C.; Mandrand, B., Coagulation of antibody-sensitized latexes in the presence of antigen. *Polymers for Advanced Technologies* **1995,** *6*, (7), 541-546.
23. Ito, H.; Hayashi, H.; Sasaki, H., Rapid separation of oil particles from low-concentrated O/W emulsions in the presence of anionic surfactants using fibrous slag. *Journal of Colloid and Interface Science* **2002,** *252*, (1), 214-221.
24. Bandini, P.; Prestidge, C. A.; Ralston, J., Colloidal iron oxide slime coatings and galena particle flotation. *Minerals Engineering* **2001,** *14*, (5), 487-497.
25. DiFeo, A.; Finch, J. A., Sphalerite/silica interactions: model predictions. *International Journal of Mineral Processing* **2002,** *64*, (4), 219-227.
26. Derjaguin, B.; Landau, L., Theory of the stability of strongly charged lyophobic sols and of the adhesion of strongly charged-particles in solutions of electrolytes. *Progress in Surface Science* **1993,** *43*, (1-4), 30-59.
27. Verwey, E. J. W., Theory of the stability of lyophobic colloids. *Journal of Physical and Colloid Chemistry* **1947,** *51*, (3), 631-636.
28. Elimelech, M.; Omelia, C. R., Effect of electrolyte type on the electrophoretic mobility of polystyrene latex colloids. *Colloids and Surfaces* **1990,** *44*, 165-178.
29. Findlay, A. D.; Thompson, D. W.; Tipping, E., The aggregation of silica and haematite particles dispersed in natural water samples. *Colloids and Surfaces a-Physico-chemical and Engineering Aspects* **1996,** *118*, (1-2), 97-105.
30. Holthoff, H.; Schmitt, A.; FernandezBarbero, A.; Borkovec, M.; CabrerizoVilchez, M. A.; Schurtenberger, P.; HidalgoAlvarez, R., Measurement of absolute coagulation rate constants for colloidal particles: Comparison of single and multiparticle light scattering techniques. *Journal of Colloid and Interface Science* **1997,** *192*, (2), 463-470.
31. Islam, A. M.; Chowdhry, B. Z.; Snowden, M. J., Hetero-aggregation in colloidal dispersions. *Advances in Colloid and Interface Science* **1995,** *62*, (2-3), 109-136.
32. Lopez-Lopez, J. M.; Moncho-Jorda, A.; Schmitt, A.; Hidalgo-Alvarez, R., Formation and structure of stable aggregates in binary diffusion-limited cluster-cluster aggregation processes. *Physical Review E* **2005,** *72*, (3).
33. Puertas, A. M.; Fernandez-Barbero, A.; de las Nieves, F. J., Kinetics of colloidal Hetero-aggregation . *Physica a-Statistical Mechanics and Its Applications* **2002,** *304*, (3-4), 340-354.

34. Puertas, A. M.; Maroto, J. A.; Fernandez-Barbero, A.; De las Nieves, F. J., On the kinetics of Hetero-aggregation versus electrolyte concentration: comparison between simulation and experiment. *Colloids and Surfaces a-Physico-chemical and Engineering Aspects* **1999,** *151*, (3), 473-481.
35. Yu, W. L.; Borkovec, M., Distinguishing Hetero-aggregation from homoaggregation in mixed binary particle suspensions by multiangle static and dynamic light scattering. *Journal of Physical Chemistry B* **2002,** *106*, (51), 13106-13110.
36. Yu, W. L.; Matijevic, E.; Borkovec, M., Absolute Hetero-aggregation rate constants by multiangle static and dynamic light scattering. *Langmuir* **2002,** *18*, (21), 7853-7860.
37. Jia, J.; Jia, Z.; Iwata, S., Bimodal colloidal mixtures: From fast to slow aggregation regions. *Journal of Colloid and Interface Science* **2011,** *362*, (2), 633-637.
38. Puertas, A. M.; Fernandez-Barbero, A.; De Las Nieves, F. J., Charged colloidal Hetero-aggregation kinetics. *Journal of Chemical Physics* **2001,** *114*, (1), 591-595.
39. Hall, R. J.; Pinkrah, V. T.; Chowdhry, B. Z.; Snowden, M. J., Hetero-aggregation studies of mixed cationic co-polymer/anionic homopolymer microgel dispersions. *Colloids and Surfaces a-Physico-chemical and Engineering Aspects* **2004,** *233*, (1-3), 25-38.
40. Bouyer, F.; Robben, A.; Yu, W. L.; Borkovec, M., Aggregation of colloidal particles in the presence of oppositely charged polyelectrolytes: Effect of surface charge heterogeneities. *Langmuir* **2001,** *17*, (17), 5225-5231.
41. Huynh, K. A., McCaffery,J.M, Chen, K.L., Hetero-aggregation of multiwalled Carbon nanotubes and hematite nanoparticles: rates and mechanisms. *Environ. Sci. Technol.* **2012**.
42. Chefetz, B.; Deshmukh, A. P.; Hatcher, P. G.; Guthrie, E. A., Pyrene sorption by natural organic matter. *Environmental Science & Technology* **2000,** *34*, (14), 2925-2930.
43. Torrents, A.; Jayasundera, S., The sorption of nonionic pesticides onto clays and the influence of natural organic carbon. *Chemosphere* **1997,** *35*, (7), 1549-1565.
44. Seo, J.-W. T.; Green, A. A.; Antaris, A. L.; Hersam, M. C., High-Concentration Aqueous Dispersions of Graphene Using Nonionic, Biocompatible Block Copolymers. *The Journal of Physical Chemistry Letters 2*, (9), 1004-1008.
45. Haiss, W.; Thanh, N. T. K.; Aveyard, J.; Fernig, D. G., Determination of Size and Concentration of Gold Nanoparticles from UV-Vis Spectra. *Analytical Chemistry* **2007,** *79*, (11), 4215-4221.
46. Shen, K.; Curran, S.; Xu, H.; Rogelj, S.; Jiang, Y.; Dewald, J.; Pietrass, T., Single-Walled Carbon Nanotube Purification, Pelletization, and Surfactant-Assisted Dispersion:A Combined TEM and Resonant Micro-Raman Spectroscopy Study. *The Journal of Physical Chemistry B* **2005,** *109*, (10), 4455-4463.
47. Vaisman, L.; Wagner, H. D.; Marom, G., The role of surfactants in dispersion of carbon nanotubes. *Advances in Colloid and Interface Science* **2006,** *128â€“130*, (0), 37-46.
48. Wu, T.; Gong, P.; Szleifer, I.; VlcÌŒek, P.; Å ubr, V.; Genzer, J., Behavior of Surface-Anchored Poly(acrylic acid) Brushes with Grafting Density Gradients on Solid Substrates: 1. Experiment. *Macromolecules* **2007,** *40*, (24), 8756-8764.
49. Treat, N. D.; Ayres, N.; Boyes, S. G.; Brittain, W. J., A Facile Route to Poly(acrylic acid) Brushes Using Atom Transfer Radical Polymerization. *Macromolecules* **2005,** *39*, (1), 26-29.
50. Liu, J.; Legros, S.; Ma, G.; Veinot, J. G. C.; von der Kammer, F.; Hofmann, T., Influence of surface functionalization and particle size on the aggregation kinetics of engineered nanoparticles. *Chemosphere* **2012,** *87*, (8), 918-924.

51. Murphy, R. J.; Pristinski, D.; Migler, K.; Douglas, J. F.; Prabhu, V. M., Dynamic light scattering investigations of nanoparticle aggregation following a light-induced pH jump. *Journal of Chemical Physics* **2010,** *132*, (19).
52. White, B.; Banerjee, S.; O'Brien, S.; Turro, N. J.; Herman, I. P., Zeta-potential measurements of surfactant-wrapped individual single-walled carbon nanotubes. *Journal of Physical Chemistry C* **2007,** *111*, (37), 13684-13690.
53. Carpineti, M.; Ferri, F.; Giglio, M.; Paganini, E.; Perini, U., Salt-induced fast aggregation of polystyrene latex. *Phys Rev A* **1990,** *42*, (12), 7347-7354.
54. Wang, Y.; Combe, C.; Clark, M. M., The effects of pH and calcium on the diffusion coefficient of humic acid. *J. Membr. Sci.* **2001,** *183*, (1), 49-60.
55. Xu, H.; Schlenoff, J. B., Kinetics, isotherms, and competition in polymer adsorption using the quartz crystal microbalance. *Langmuir* **1994,** *10*, (1), 241-245.
56. Yoon, S. H.; Lee, C.-H.; Kim, K.-J.; Fane, A. G., Effect of calcium ion on the fouling of nanofilter by humic acid in drinking water production. *Water Res* **1998,** *32*, 2180-2186.

Chapter 5

Gold Nanoparticles' Transport Through Saturated Porous Media in Presence of Single-walled Carbon Nanotubes[4]

[4]Afrooz, A. R. M. N., Das, D., Murphy, C.J., Vikesland, P., & Saleh, N.B. Co-transport of gold nanospheres with single-walled carbon nanotubes in saturated porous media. (*in preparation*)
Contributions of the Co-Authors: D.D: Characterization of the Materials; C.J.M and P.V: Co-PIs

Abstract

ENM transport through porous media is typically assessed in a controlled environment. Presence of a secondary particle, though environmentally realistic, is rarely considered to evaluate ENM transport behavior. This is one of the first studies to systematically assess the role of a secondary nanoparticle (i.e., PA-SWNTs) on AuNS transport through saturated porous media and under a wide range of aquatic conditions (1-100 mM NaCl). Homogenous AuNS suspensions are utilized as control to compare their breakthrough properties with those of the AuNS hetero-dispersions (in presence of PA-SWNTs). Though AuNS homo-dispersion showed classical ionic strength-dependent transport behavior, presence of PA-SWNTs nearly eliminated the ionic strength effects and made the AuNSs highly mobile. This study also assessed the role of pre-coating of the collectors (with PA-SWNTs) on AuNS' mobility to understand the order of introduction of the secondary particles. Pre-existence of the secondary particles in the porous media transport enhances filtration of primary AuNSs. The study results demonstrate that the presence of secondary particles and the order in which these are introduced to the experimental system, strongly influences AuNS mobility. Thus ENM can be highly mobile or can get strongly filtered out, depending on the secondary PA-SWNT and background environmental chemistry.

Keywords: Co-transport; porous media; gold nanoparticles; single-walled carbon nanotubes; pluronic

5.1 Introduction

Increased use of ENMs makes their environmental release, i.e., intentional as remedial agents, accidental from manufacturing processes, or inevitable at the end of life of ENM-containing products[1-4], highly likely. Regardless of routes of release and exposure[5-7], sediments and porous subsurface are identified as the likely environmental sinks[8, 9] for these ENMs, where they undergo subsequent transport and transformation[10]. Fate and transport, the primary processes dictating ENM exposure and risks, are at the center of nano EHS research[11], which devotes most of its efforts in determining appropriate fate descriptors (deposition rate and efficiency or transport distance) via breakthrough studies[12-22] or by studying deposition onto polished crystal surfaces[23-31]. Although reliable prediction of ENM transport is the ultimate goal of nano-EHS studies, most, if not all, are performed in clean and controlled environmental platforms.

State-of-the-art ENM transport studies have systematically evaluated the effects of various material properties and background chemistries for a wide set of nanoparticles[32]; e.g., fullerenes (nC_{60}), carbon nanotubes (CNTs), nano-scale zero valent iron (nZVI), titanium dioxide (TiO_2), zinc oxide (ZnO), and silver nanoparticles (AgNP). Influence of solution chemistry (pH[33], ionic strength[14], organic matter[31]), ENM characteristics (size and size distribution[17], concentration[17], shape[34], surface charge[35], synthesis method[36], surface coating[37], and magnetic properties[38]), collector properties (grain size distribution[39]), and operating conditions (flow velocity[13] and flow direction[40]) on their mobility also have been reported. In addition to the aforementioned experimental investigations, efforts have been made to predict and validate ENM transport theoretically employing clean-bed filtration theory (CFT)[41, 42]. However, such experimental and theoretical studies of ENMs in homogeneous and single particulate systems have little transferability to the realistic natural environment where presence of natural particles and other

ENMs is common[43]. A critical need thus exists to assessing the influence of system complexity on ENMs' transport.

Most common attempts to simulate system complexity involve investigation of the effects of physical (surface roughness[44] and shape[45]) and geo-chemical (surface charge[46], surface coating[47], and mineralogical compositions[48]) heterogeneities of the collectors, mostly focusing on colloid transport. Although collectors' shape has been reported to influence the single collector efficiency almost by a factor of 2, effects of surface roughness of the collectors proved to be insignificant for colloid deposition[45]. Similarly, the degree of favorable surface charge distribution (patchwise) of the collectors has been correlated with the degree of colloid deposition, both experimentally[49] and theoretically[50]. Recent efforts have also been made to understand various ENMs' (e.g., nZVI, nC_{60}, TiO_2) transport through natural soil, e.g., through ultisol[51], appling[52] and 11 other soil[53] types. Soil texture and mineralogical compositions are found to accelerate or decelerate the deposition of the ENMs in a soil column depending on the specific interaction between the ENMs and the natural collectors.[51-53]. Furthermore, the role of pre-coating[21, 32, 47, 54] of the collector surfaces with NOM, clay or biofilm has been investigated, where ENM transport is reported to decrease due to competition between the ENMs and the NOMs for the attachment sites or to increase due to the availability of increased surface sites of the collectors for NM deposition[36, 54]. Such altered interfacial interaction of the ENM may also occur due to the presence of a secondary particle in the suspensions[55-57]. However, understanding the influences of such secondary particles on ENM transport (co-transport) is limited.

The primary parameter considered in the ENM co-transport literature is the presence of bacteria, where enhanced mobility has been reported for TiO_2[36, 58] when compared to TiO_2 only transport. On the other hand, bacterial transport in presence of CNT has also been reported[59],

where reduced microbial mobility at high ionic strength condition occurred (25-100 mM) in presence of CNTs. Such evidence suggest that particle transport through porous media is significantly influenced by the presence of a secondary particulate entity (co-transport); where the underlying mechanism is likely higher collision and facilitated filtration. However, studies reporting ENM co-transport is scarce in fate and transport literature. To date, only two such studies report ENM co-transport of TiO_2 and multiwalled carbon nanotube[60] and TiO_2 and nC_{60}[61], respectively. Both of these studies were performed at low ionic strength (0.1-10 mM). These studies reported significant differences in the mobility of the primary particles in singular and binary matrices with strong pH and ionic strength dependence. The persistent data gap in ENM co-transport is deciphering filtration mechanisms under the influence of the following parameters: a wide range of environmentally relevant ionic strength, the order of addition of the secondary particles, and presence of NOM.

The objective of this study is to investigate transport of a model nanoparticle, i.e., AuNSs, in presence of a secondary ENM, single-walled carbon nanotube (SWNT), over a wide range of ionic strength. In order to mechanistically assess the filtration mechanisms, inherent SWNT-SWNT interaction at elevated ionic strength is eliminated via PA functionalization[55]. A range of PA concentration is used to generate PA-SWNTs with desirable stability; i.e., highly stable suspensions are utilized for co-transport studies, whereas, SWNTs with lower stability are used to pre-coat the collector surfaces. Hetero- dispersion of AuNSs and SWNTs are used in transport studies through saturated packed bed of sand. The ionic strength is varied over a wide range (1-100 mM NaCl). This study also investigates the effect of pre-coating of the collectors (by less stable PA-SWNTs) on AuNS mobility. This is a first-of-its-kind study to mechanistically assess co-transport of AuNSs over a wide range of ionic strength. This study is the first step to attain a

more reliable assessment of ENM co-transport through porous media under a wide range of environmental conditions

5.2 Materials and Methods

5.2.1 Preparation of AuNS Suspensions

Poly (acrylic acid) or PAA-coated AuNS suspension at a concentration of 50 mg/L was procured from Nanopartz Inc. (Loveland, CO). The supplier reported nominal diameter of the AuNS of 10 nm. Procured AuNSs were diluted 4 times to achieve a concentration of 12.5 mg/L for all transport experiments.

5.2.2 Preparation of PA-SWNTs

Dry SWNTs, produced by high pressure carbon monoxide dispropornation or HipCO method[62] was obtained from Tubes at Rice (Houston, TX). The supplier reported average diameter and length of the SWNTs were 1.03 nm (a range of 0.7-1.45 nm) and 0.93 µm (a range of 0.1-2.6 µm), respectively. Commercially available PA F-127 was obtained from Sigma Aldrich (St. Louise, MO) and 0.02, 0.1, 1, and 10% (w/v) PA solution was prepared using filtered (0.45 µm inorganic membrane filters, VWR international LLC, Radnor, PA) deionized (DI) water (Millipore, Darmstadt, Germany). The PA solutions were prepared by magnetic stirring for 1 h at room temperature.

10 mg of procured SWNTs was added to 100 mL (0.02, 0.1, 1, and 10%) of PA solution and sonicated in an ice bath for 1 h employing a S-4000 ultrasonicator (Misonix, Inc. Farmingdale,NY) at a controlled input energy of 100–105 kJ. The sonicated samples were quiescently left aside for 24 h and the supernatant was decanted and centrifuged at 12000 ×g for 1 h with a Beckman Coulter (Brea, CA) centrifuge. The supernatant of the centrifuged samples was then decanted and used for subsequent experiments.

5.2.3 Solution Chemistry

All transport experiments were performed in the presence of monovalent (NaCl) at 1, 10, 30, and 100 mM concentration. NaCl stock of 5 M was purchased from a commercial source (BDH Chemicals, Dubai, UAE) and diluted with filtered DI water to obtain the solution of appropriate ionic strength. The pH of the salt solutions was unadjusted (ambient) and determined to be 6.56 ± 0.04.

5.2.4 Characterization of AuNSs and PA-SWNTs

Physical morphology of the AuNSs and SWNTs was characterized using a JEOL 2010F Transmission Electron Microscope (TEM) at the Texas Material Institute. Copper-carbon TEM grids were prepared using the NM suspensions at desired particle concentrations and dried at 60 °C for 15 min. Bright field imaging and high-resolution (HR) microscopy techniques were utilized to investigate the particle size and shape. An open source software, i.e., imageJ was used to determine the particle size distribution from the TEM micrographs.

DLS was employed to characterize the size of the NMs in the experimental matrices. Details of the DLS technique has been described elsewhere[63]. Briefly, 2 mL of NM suspension was added into a clean borosilicate glass vial under chosen solution chemistry. A 632.8 nm laser was shined through the vial and scattered light was detected at 90° and converted to hydrodynamic radii (HR) employing an auto-correlator and cumulant analysis. HR data were collected every 10 s for 30 min duration.

To assess and confirm the chemical identity of the AuNS, an Agilent 8454 UV-vis spectrophotometer (Santa Clara, CA) was used. AuNS suspensions were prepared and injected using a 1 mL syringe to a flow through cell of 300 µL volume. Spectral response was collected for the entire UV and visible range (200-1100 nm).

Electrokinetic characterization, i.e., electrophoretic mobility (EPM) of the NMs in their homo- and heterogeneous dispersion states were evaluated using Malvern Zetasizer (Malvern Instruments Ltd., Worcestershire, UK) at pH 6.7±0.1 and at a temperature of 20 °C. For each condition, 800 µL sample was injected into the disposable capillary cell (DTS 1070) ensuring that the sample is in contact with the electrodes without any air bubble introduction. Four different cells were used for AuNS, PA-SWNT (0.02%), PA-SWNT (5%), and AuNS-PA-SWNT (5%) suspensions. Cells were flushed 10 times with DI water between each measurement. 3 replicates were taken for every measurement to ensure reproducibility. NaCl concentrations of 1, 10, 30 and 100 mM were considered for all the suspensions.

5.2.5 Column Experiment

2.5 cm diameter and 10 cm long, Kontes Glass columns (Kimble Chase, Vineland, NJ) were packed with Ottawa sand (Fischer Scientific, Waltham, MA). The 20-30 mesh sand was carefully washed and cleaned following a detailed cleaning protocol described elsewhere[12]. In brief, the Ottawa sand was saturated in DI water overnight and then boiled for 10 min followed by bath sonication and subsequent washing to remove impurities and colloids. Sonication procedure involved multiple sonication-rinsing cycles (10 min sonication and 2 min rinsing). Each sonicated batch was rinsed thrice and the supernatant was decanted prior to the next cycle of sonication. A total of 15 such sonication-rinsing cycles were used to remove all suspended impurities. The cleaned sand was then soaked overnight in concentrated hydrochloric acid (HCl), to remove any metallic impurities. The sand collectors were then washed with DI until the pH reached 6.5 following by an additional cycle of soaking with 50 mM $CaCl_2$. Additional 5 cycles of sonication-rinsing were performed to remove tightly bound colloids removal the collector surfaces. Such extensive cleaning of the sand was necessary to eliminate convolution of the breakthrough signal

from any potential release of inherent colloids that are typically present in the as-received sand. The cleaned sand was then dried at 80 °C and stored in an airtight container. The cleaned sand was re-sieved with 20-25 mesh sieve, to attain a narrower grain size of 700-800 µm.

The Kontes columns were dry-packed[14] following a layer-by-layer packing process, where 1-cm layers were poured in and compacted with a wooden mullet. A vibrator was used to ensure uniform packing and eliminate stratification. Carbon dioxide gas was flowed through the column for 20 minutes to remove all the air from the pore spaces. Next the column was saturated by pumping DI water (Figure D-1) through the column for 8 h via an Ismatec precision variable-speed peristaltic pump purchased from IDEX Inc. (Wertheim, Germany). Porosity of the packed beds was determined gravimetrically weighing the column before and after DI saturation, and found to be 0.376 ±0.013. Right after saturating the column, tracer studies were performed using 4 pore volumes (PVs) of lithium bromide (LiBr) solution. The tracer was monitored continuously at 197.nm wavelength. Prior to introduction of the NMs, the packed column was flushed with at least 4 PVs of appropriate background solution. The approach velocity of the tracer and the carrier solution was adjusted to 0.003 cm s^{-1} (equivalent to a volumetric flow rate of ~1 mL min^{-1}). NMs were then introduced at the same background electrolyte concentration as a finite pulse (~4PV). The pulse was followed by the injection of respective electrolyte solution for 4 PV. Subsequent injection of DI water was made to observe NM release. For each new experiment, a cleaned and newly packed column was employed.

The eluent concentration was measured at the outlet using the pre-established calibration curves (Figure D-2) for AuNS, PA-SWNTs, and AuNS-PA-SWNT mixture. Dilution factors of 2, 4, 6, and 8 to the stock AuNS suspensions were used to obtain a calibration curve at 517 nm using a flow through cell (Agilent Technologies, Santa Clara, CA) of 300 µL volume. On the

other hand, 5, 10, 20, 40 dilution factors were used to generate a calibration curve for the PA-SWNTs at 235 nm. Calibration curve obtained for the AuNS and PA-SWNTs both resulted in a R^2 value of 0.9999. Similar calibration curve was obtained at 517 nm for the AuNS-PA-SWNT hetero-dispersion utilizing the same flow through cell with a R^2 value of 0.9998. For the NM transport studies, the column eluent concentration was monitored in every 15 s (approx. 0.02 pore volume) for the entire duration of the experiment.

To monitor single particle transport, AuNSs only were flowed through the saturated columns under relevant NaCl concentration. PA-SWNT (0.02%, 0.1%, 1%, and 5%) suspensions were flowed through the porous media in presence of 1mM NaCl and 100 mM NaCl. Such wide variation in salt concentration was used to reflect the effect of aggregation and extent of surface modification of SWNT on their transport behavior. At least one replicate run (through freshly packed column) was performed for each condition.

Co-transport experiments were performed flowing a hetero-dispersion of AuNS-SWNT (at a mass ratio of 1:5 for SWNT:AuNS). Also, sequential flow of PA-SWNT and AuNS was made, where PA-SWNTs was flowed through the sand packed column followed by AuNS injection. Such runs were made to assess the influence of SWNT pre-coating (of the collectors) on the mobility of the AuNS through the sand packed column. Co-transport and sequential-transport experiments were carried out at identical electrolyte concentrations, as utilized for the control "AuNS only" transport experiments.

5.3 Results and Discussions

5.3.1 Morphological and Chemical Properties

Figure D-3 shows representative HRTEM micrographs of AuNS and SWNTs. AuNSs show spherical morphology with an average diameter of 12.9±1.7 nm (Figure D-3a) determined from

imageJ particle size analysis. SWNTs are found to be well dispersed within the amorphous structure of PA (Figure D-3b). A significant number of dark spots are found in the PA-SWNT images, which are likely the metal catalysts used for SWNT synthesis. Elemental analysis (EDS) of the samples confirms the presence of iron (Fe) catalysts in the sample. EDS of the AuNS samples were also performed for elemental confirmation of the gold in the sample.

The elemental signature of the AuNS and surface properties of the PA-SWNTs were further evaluated using UV-vis spectroscopy and Raman Spectroscopy, respectively. AuNSs show a characteristics peak at 517 nm (Figure D-4a) with an absorbance of 0.347 a.u. at an AuNS concentration of 16.66 mg/L (DF of 3)[64]. Raman spectroscopy analysis of the SWNTs confirms characteristics defect or D and graphitic or G peaks at 1330 and 1595 cm^{-1}, respectively (Figure D-4b). The attenuation of the D/G ratio of SWNTs from 0.5580 to 0.1778 for pristine and PA-SWNTs (dispersed in 5% PA), respectively confirms the surface coverage of the SWNTs by PA. Similar attenuation of D/G has previously been reported in the literature[65].

The stability and size of the NMs were characterized by DLS (Figure D-5). The average hydrodynamic radii (HR) of the AuNSs in DI water and of PA-SWNTs are measured as 18.9±1.2 and 180.5±15.8 nm, respectively. However, the mixture of AuNS-SWNT demonstrates an average HR of 41.4±10.4 nm. The reduction of particle size in the hetero-dispersion is likely due to averaging of smaller AuNSs with relatively larger sized PA-SWNTs; as CONTIN algorithm provides intensity averaged particle sizes over the measurement period. On the other hand, higher particle size for the AuNSs and PA-SWNTs in the aqueous suspension compared to their TEM size can be attributed to the associated water molecules around the particles (or hydrated particles) during DLS measurement. Such differences between DLS and TEM size has been reported widely in the literature for colloids and ENMs[12, 55].

5.3.2 Electrokinetic Properties

EPMs of the NMs were measured as a function of ionic strength. NMs demonstrate a decreasing trend in the absolute values of the EPMs with the increase of electrolyte concentration (Figure D-6), supporting the classical electrokinetic behavior of charged particles[12, 14]. EPMs of AuNSs decreases from – (2.78±0.18) to – (1.63±0.23) × 10^{-8} m^2 V^{-1} S^{-1} for an increase in NaCl concentration from 1 to 100 mM. The origin of such surface potential is likely from the PAA polyelectrolytes (negative carboxyl moieties) and is consistent with previously reported literature values[34, 55, 66]. However, EPMs for both 0.02% and 5% PA-SWNTs doesn't vary substantially; demonstrating values from − (0.35 ± 0.03) and − (0.29 ± 0.03) × 10^{-8} m^2 V^{-1} S^{-1} to − (0.03 ± 0.03) and − (0.03 ± 0.02) × 10^{-8} m^2 V^{-1} S^{-1}, respectively for an increase in NaCl concentration from 1 to 100 mM. Since PA is a nonionic polymer, such low values of EPMs confirm effective coating of the SWNT surfaces with these polymers, and the likely stabilization has occurred from steric interaction between the sorbed polymer layers[67, 68]. For the hetero-dispersion of AuNSs and 5% PA-SWNTs, changes of background ionic strength from 1 to 100 mM results in an EPM decrease from −(1.02 ± 0.23) to −(0.18 ± 0.02) × 10^{-8} m^2 V^{-1} S^{-1}. These values are interestingly intermediate to the EPM values of AuNS and PA-SWNT homo-dispersions. Since EPM measurements are also presented as averages, the nonionic PA coated SWNTs (with low EPM) has likely reduced the overall electrokinetics of the hetero-dispersion.

5.3.3 Transport of AuNS Homo-dispersions

Mobility of the AuNS homo-dispersions is presented in Figure 1 as a function of NaCl concentration. Background electrolytes significantly influence the AuNS transport through the sand column, as their mobility decreases with the increase in electrolyte concentrations. The percent eluted of AuNSs is estimated as 96.9±4.6% of the influent mass for 1 mM NaCl case.

Such negligible deposition at lower ionic strength indicates strong electrostatic repulsion between AuNSs and collector surfaces. Other mechanisms of filtration, i.e., straining are not likely significant, because the size ratio of the AuNS and the sand grains (i.e., 0.0003) is much lower than literature reported favorable colloids/media diameter ratio (i.e., 0.005) for physical filtration[69]. Maximum C/C_0 value reduces to 0.91±0.06 and 0.79±0.02 for 10 mM and 30 mM, respectively, associated with 83.5±6.3% and 67.7±5.7% elution. AuNS mobility is the lowest in presence of 100 mM NaCl with a breakthrough plateau of 0.49±0.03 and elution of 40.0±2.3%. The decreasing trend of the elution of the AuNS homo-dispersion through the sand column with increasing ionic strength can be explained by corresponding reduction in electrostatic double layer interaction as evident from Figure D-6. Our results corroborate similar findings[12, 14] for other negatively charged ENMs.

Each breakthrough history was followed by a release curve obtained flowing DI water through the column. At low ionic strength, (i.e., 1 mM NaCl) no detachment of the AuNS was observed. Representative release curves for 10, 30 and 100 mM are presented in Figure D-7. Numerical integration of the release curves suggest that 57%, 87%, and 86% of the retained material has been released when the solution chemistry changed to DI from 10, 30, and 100 mM, respectively. Shape of the breakthroughs and the increasing release percentages with increased

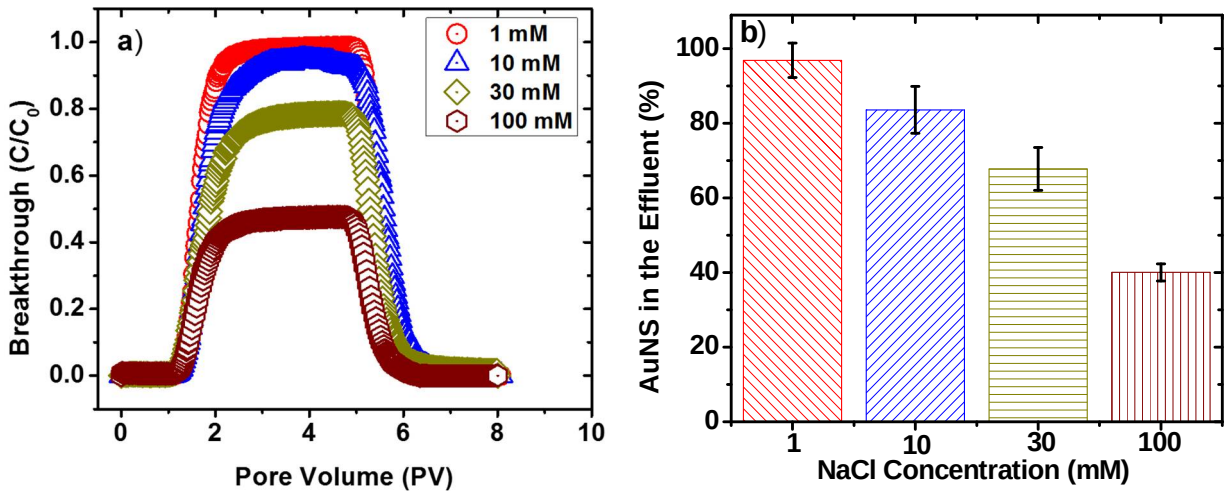

FIGURE 5.1. Transport of AuNS Homo-dispersion a) Breakthrough b) Percent Transport

mono-valent salt concentrations suggest that the AuNS depositions onto the sand surface are primarily electrostatic and at the secondary minima. Observed detachments of the particles can be attributed to removal of particles from the secondary energy well as observed earlier for the ENMs, i.e., SWNTs and CeO_2[14, 70].

5.3.4 Transport of PA-SWNT Homo-dispersions

SWNTs, dispersed in solutions of wide range of PA percentages (0.02-5%), were injected through the sand column in presence of low (1 mM) and high (100 mM) electrolyte concentrations. At low ionic strength, the effect PA functionalization on PA-SWNTs mobility is negligible (Figure D-8). Even though the EPMs of the PA-SWNTs slightly decreases (Figure D-6) with an increase in the amount of PA used in dispersion, their breakthrough plateau and retention percentage is similar for the entire range of the PA in such cases. Average retention of the PA-SWNTs, for the entire range (0.02-5%) of the PA, is 6.9±1.5 % at 1 mM NaCl as shown in Figure D-8. Filtration of PA-SWNTs at low ionic strength with no detectable releases can be attributed to physical removal mechanism for the PA-SWNTs, which are consistent with the previous findings[14, 71].

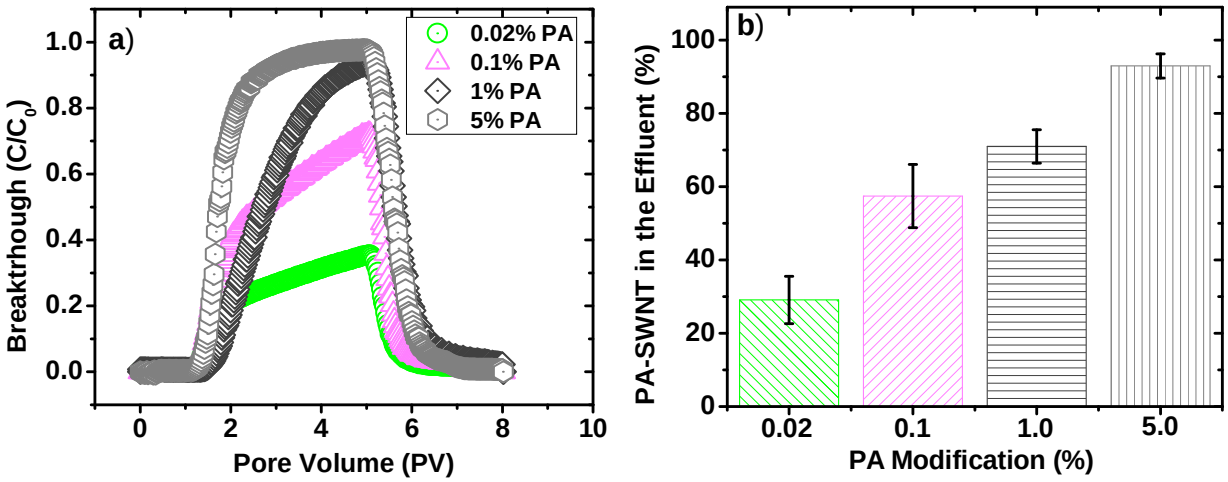

FIGURE 5.2. Transport of PA-SWNT Homo-dispersion at 100 mM NaCl a) Breakthrough b) Percent Transport

At 100 mM NaCl however, the amount of PA used in dispersing SWNTs demonstrates significant influence on their transport behavior. The percent breakthrough of PA-SWNTs increases with the increase in PA concentrations. The elution of 5 % PA-SWNTs is found to be 92.9±3.3 % compared to 29.1±6.4 % for the 0.02% PA-SWNTs. Percent eluted is estimated as 57.4±8.6 and 71±4.5 for 0.1 and 1% PA-SWNT, respectively. Similar effects on transport as a function of surface modification for SWNTs have been reported earlier[72, 73]. The shape of the PA-SWNT breakthrough curves at 100 mM NaCl do not follow the tracer or other PA-SWNT transport trends, rather show a gradual increase over time with no plateau at the end of the pulse injection. Such behavior can be attributed to blocking of available deposition sites as described in multiple previous studies[74, 75]. We believe that continual injection of PA-SWNTs blocks the available surface sites on the sand collectors via attachment of the SWNTs over time. Thus subsequent PA-SWNT injection results in SWNT-SWNT interaction between SWNTs in pore water and SWNTs that have already coated the collector grains. Thus these longer PV flushing causes complete recovery of these PA-SWNTs after 15 PV. Therefore, increased mobility of PA-SWNTs with the

increase in PA concentration likely has occurred from steric interaction from the attached nonionic macromolecules (i.e., PA) on the SWNTs[76] with the SWNTs in the porewater.

5.3.5 Transport of AuNS & PA-SWNT Hetero-dispersions

Role of the presence of PA-SWNTs on AuNS deposition was evaluated by performing transport experiments of AuNS-PA-SWNT hetero-dispersions. SWNTs dispersed in a 5% PA solution were used to prepare the hetero-dispersions (to ensure minimal deposition of PA-SWNTs only). Figure 3 presents the breakthrough curves (Figure 3a) and corresponding elution percentages (Figure 3b) determined from the co-transport experiments. The maximum C/C_0 values decreased (i.e., from 0.99±0.007 to 0.96±0.01) and % eluted (i.e., 98.0±1.2% to 79.1±3.2%) as the ionic strength was increased from 1 mM to 100 mM. Percent eluted for the AuNS-PA-SWNTs were 97.3±3.0 and 83.6±1.6 at 10 and 30 mM, respectively. Though the strength of the electrolytes showed minimal effect on the breakthrough plateau on the co-transport of AuNSs, the shape of the breakthrough histories showed significant differences between high and low electrolyte conditions. AuNS hetero-dispersion breakthroughs (Figure 3a) deviate from their homo-dispersion cases (Figure 1a), but closely resembles the shape of the breakthrough of 5% PA-SWNT (Figure 2a). Observed resemblance suggests that higher mobility of the AuNSs in presence of PA-SWNTs, under high ionic strength condition, may be attributed to their facilitated transport via highly mobile 5% PA-SWNTs. The filtration of AuNSs likely have occurred indirectly via facilitated removal of PA-SWNTs, where AuNSs nucleated at high ionic strength. Similar observations have been reported elsewhere for AuNS hetero-aggregation[55]. Similar transport mechanisms describing enhanced mobility of titanium dioxide (TiO_2) in presence of CNTs have been reported earlier[60]. Such preferential attachment of the negatively charged AuNSs onto the PA-SWNTs, instead of the sand grains, can be explained by unfavorable electrostatic interaction between charged AuNSs and

likely charged sand surfaces (i.e., -40 mV[77] to -25 mV[78]) compared to electrostatically favorable AuNS and PA-SWNTs interaction (with PA-SWNT EPM values of -3.5 mV to -0.6 mV, Figure D-6) for ionic strength ranging from 1 mM to 100 mM at pH ~7. Furthermore, order of magnitude smaller sizes of the SWNTs provided with additional (by an approx. factor of 1.5) higher surface area for the AuNSs to attach (Table D-1 to D-3).

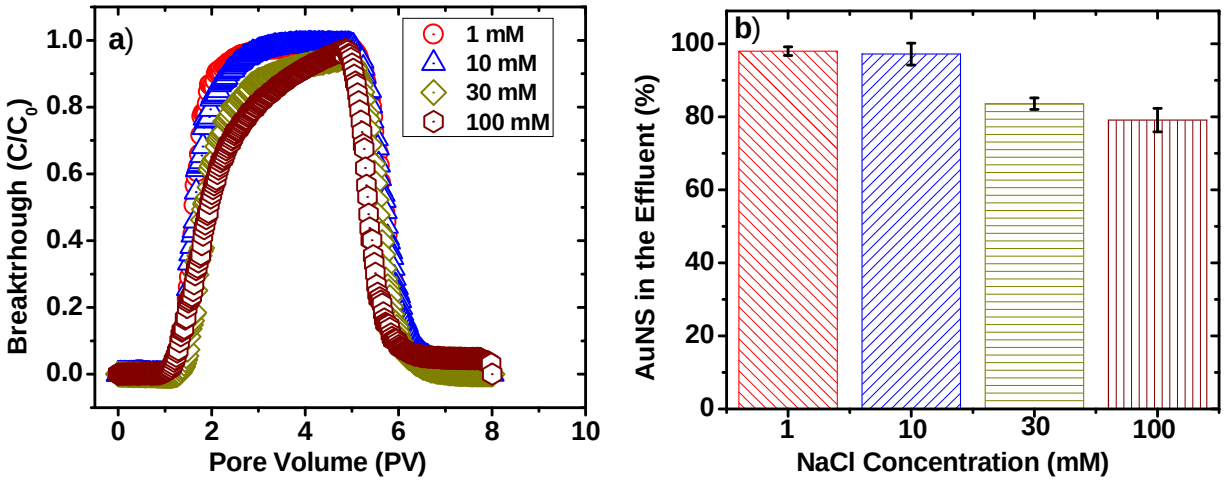

FIGURE 5.3. Transport of AuNS- SWNT Hetero-dispersion a) Breakthrough b) Percent Transport

Release curves of the co-deposited AuNSs in presence 30 and 100 mM NaCl are presented in Figure D-9. No significant release has been observed for AuNSs deposited at 1 or 10 mM NaCl when hetero-dispersed. The % release of AuNSs (Figure D-8) are found to be 59% and 55% for 30 and 100 mM ionic strength, respectively. Comparison of the amount of release of AuNS for hetero-dispersion case (Figure D-9) with the homo-dispersion (Figure D-7) suggests that presence of PA-SWNTs increases the irreversible attachment of the AuNSs at high ionic strength conditions. Such reduced % release can also be attributed to facilitated removal of AuNS via physical filtration[14] of PA-SWNTs, as described in the transport behavior of PA-SWNT homo-dispersion earlier (Figure D-8).

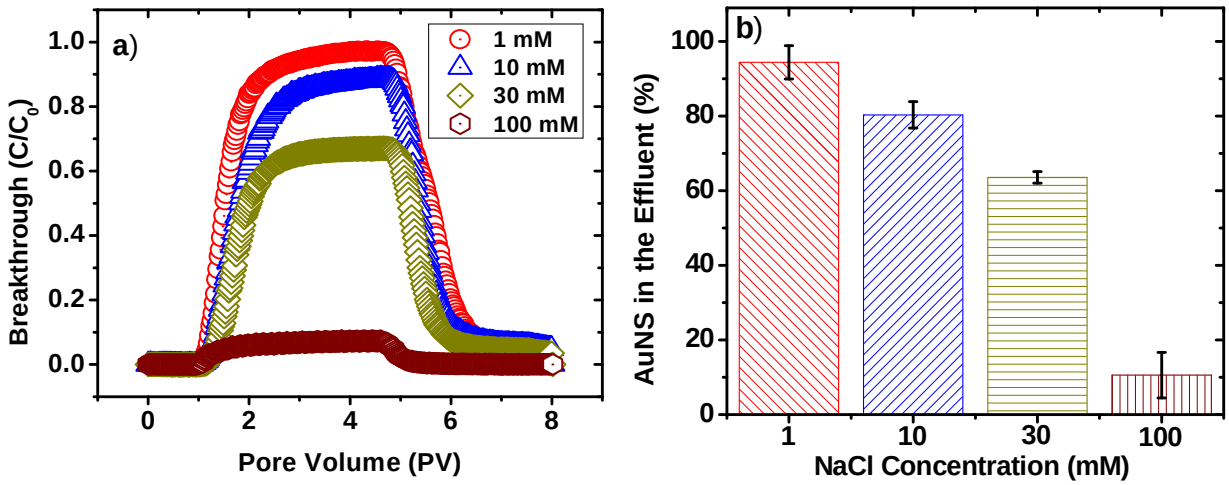

FIGURE 5.4. Transport of AuNS Homo-dispersion through SWNT Coated Column a) Breakthrough b) Percent Transport

5.3.6 Transport of AuNS through PA-SWNT Coated Sand

The breakthrough curves of AuNS homo-dispersions through PA-SWNTs (0.02 % PA) coated sand columns are presented in Figure 4. Average eluted AuNS is found to be 94.4±4.5% and 90.3±3.5% for 1 and 10 mM NaCl, respectively. The mobility of the AuNSs deceases significantly at higher NaCl concentration, resulting in 63.6±1.6% and 10.6±6.1% elution under 30 and 100 mM ionic strength, respectively. Comparing Figure 4 (i.e., pre-coated sand condition) with Figure 1 (un-coated sand) reveals that the AuNS breakthrough is strongly influenced by the presence of PA-SWNTs on the sand grains. Average % elution is lower for the pre-coated surfaces, but such influence is minor at low ionic strength. Differences between pre-coated and un-coated sand in terms of AuNS elution is also insignificant for 30 mM case; i.e., 63.6±1.6% for pre-coated condition vs. 67.7±5.7% for un-coated sand packed columns. However, at 100 mM NaCl such differences are more profound, resulting only 10.6±6.1% of elution of the AuNSs through the pre-coated sand compared to 40.0±2.3% through un-coated sand at an identical ionic strength. Increased filtration of AuNSs through PA-SWNT coated sand surfaces supports our earlier hypothesis regarding preferential attachment of the AuNS onto the PA-SWNTs. AuNS prefers the

PA-SWNT coated sand surfaces to the bare sand surfaces that results higher retention for the pre-coated case. Contribution of similar mechanism, e.g., preferential binding of biological particles (i.e., *E. coli)* with the CNTs has been reported earlier[59] in presence of high ionic strength.

5.4 Environmental Implications

Interaction of the ENMs (e.g., AuNSs) with the other nanoparticles (e.g., PA-SWNTs) upon environmental release and transport is highly likely. Such interactions may occur while the secondary particles are in suspension (co-transport) or already deposited onto the porous media (pre-coating). The study results show that although the presence of PA-SWNTs does not affect filtration of AuNS at low ionic strength (equivalent to fresh pore-water condition), AuNSs are significantly more mobile and thus will travel further in the porous media at elevated ionic strengths (e.g., in saline pore-water environment) when secondary particles (e.g., PA-SWNTs) are present. On the contrary, the pre-deposited SWNTs on the porous media will likely enhance filtration of AuNS at both low and high ionic strength conditions.

The findings of this study indicate that the coexistence of the ENMs may significantly influence their fate and transport in the natural environment. Using clean-bed filtration theory the estimated transport distances of 0.1% AuNS (i.e., C/C_0= 0.001) at 100 mM NaCl in homo-dispersion, hetero-dispersion, and pre-coated (with PA-SWNTs) were estimated as 0.6, 10.2, and 0.2 m respectively (Table D-4). In reality, however, the nature of such influences may become far more convoluted because of the additional complexity presented via the presence of multiple natural colloids and geo-macromolecules alongside with ENMs. ENM surface coatings and subsequent ligand exchange will also influence the transport behavior significantly. This is one of the first studies reporting co-transport of ENMs through porous media and highlights the importance of further research on such binary particulate conditions.

5.5 Literature Cited

1. Wagner, S.; Gondikas, A.; Neubauer, E.; Hofmann, T.; von der Kammer, F., Spot the Difference: Engineered and Natural Nanoparticles in the Environment—Release, Behavior, and Fate. *Angewandte Chemie International Edition* **2014,** *53*, (46), 12398-12419.
2. Nowack, B.; Bucheli, T. D., Occurrence, behavior and effects of nanoparticles in the environment. *Environmental pollution* **2007,** *150*, (1), 5-22.
3. Nowack, B.; Ranville, J. F.; Diamond, S.; Gallego-Urrea, J. A.; Metcalfe, C.; Rose, J.; Horne, N.; Koelmans, A. A.; Klaine, S. J., Potential scenarios for nanomaterial release and subsequent alteration in the environment. *Environmental Toxicology and Chemistry* **2012,** *31*, (1), 50-59.
4. Köhler, A. R.; Som, C.; Helland, A.; Gottschalk, F., Studying the potential release of carbon nanotubes throughout the application life cycle. *Journal of Cleaner Production* **2008,** *16*, (8), 927-937.
5. Khin, M. M.; Nair, A. S.; Babu, V. J.; Murugan, R.; Ramakrishna, S., A review on nanomaterials for environmental remediation. *Energy & Environmental Science* **2012,** *5*, (8), 8075-8109.
6. Morawska, L.; Ristovski, Z.; Jayaratne, E.; Keogh, D. U.; Ling, X., Ambient nano and ultrafine particles from motor vehicle emissions: Characteristics, ambient processing and implications on human exposure. *Atmospheric Environment* **2008,** *42*, (35), 8113-8138.
7. Walser, T.; Limbach, L. K.; Brogioli, R.; Erismann, E.; Flamigni, L.; Hattendorf, B.; Juchli, M.; Krumeich, F.; Ludwig, C.; Prikopsky, K., Persistence of engineered nanoparticles in a municipal solid-waste incineration plant. *Nature nanotechnology* **2012,** *7*, (8), 520-524.
8. Gottschalk, F.; Sonderer, T.; Scholz, R. W.; Nowack, B., Modeled Environmental Concentrations of Engineered Nanomaterials (TiO2, ZnO, Ag, CNT, Fullerenes) for Different Regions. *Environmental Science & Technology* **2009,** *43*, (24), 9216-9222.
9. Gottschalk, F.; Nowack, B., The release of engineered nanomaterials to the environment. *Journal of Environmental Monitoring* **2011,** *13*, (5), 1145-1155.
10. Lowry, G. V.; Gregory, K. B.; Apte, S. C.; Lead, J. R., Transformations of nanomaterials in the environment. *Environmental science & technology* **2012,** *46*, (13), 6893-6899.
11. Petosa, A. R.; Jaisi, D. P.; Quevedo, I. R.; Elimelech, M.; Tufenkji, N., Aggregation and deposition of engineered nanomaterials in aquatic environments: role of physico-chemical interactions. *Environmental science & technology* **2010,** *44*, (17), 6532-6549.
12. Saleh, N.; Sirk, K.; Liu, Y.; Phenrat, T.; Dufour, B.; Matyjaszewski, K.; Tilton, R. D.; Lowry, G. V., Surface modifications enhance nanoiron transport and NAPL targeting in saturated porous media. *Environmental Engineering Science* **2007,** *24*, (1), 45-57.
13. Lecoanet, H. F.; Wiesner, M. R., Velocity effects on fullerene and oxide nanoparticle deposition in porous media. *Environmental science & technology* **2004,** *38*, (16), 4377-4382.
14. Jaisi, D. P.; Saleh, N. B.; Blake, R. E.; Elimelech, M., Transport of single-walled carbon nanotubes in porous media: filtration mechanisms and reversibility. *Environmental science & technology* **2008,** *42*, (22), 8317-8323.
15. Fang, J.; Shan, X.-q.; Wen, B.; Lin, J.-m.; Owens, G., Stability of titania nanoparticles in soil suspensions and transport in saturated homogeneous soil columns. *Environmental pollution* **2009,** *157*, (4), 1101-1109.
16. Li, Y.; Wang, Y.; Pennell, K. D.; Abriola, L. M., Investigation of the transport and deposition of fullerene (C60) nanoparticles in quartz sands under varying flow conditions. *Environmental science & technology* **2008,** *42*, (19), 7174-7180.

17. Phenrat, T.; Kim, H.-J.; Fagerlund, F.; Illangasekare, T.; Tilton, R. D.; Lowry, G. V., Particle Size Distribution, Concentration, and Magnetic Attraction Affect Transport of Polymer-Modified Fe-0 Nanoparticles in Sand Columns. *Environmental science & technology* **2009,** *43*, (13), 5079-5085.
18. Solovitch, N.; Labille, J.; Rose, J.; Chaurand, P.; Borschneck, D.; Wiesner, M. R.; Bottero, J.-Y., Concurrent Aggregation and Deposition of TiO2 Nanoparticles in a Sandy Porous Media. *Environmental science & technology* **2010,** *44*, (13), 4897-4902.
19. Ben-Moshe, T.; Dror, I.; Berkowitz, B., Transport of metal oxide nanoparticles in saturated porous media. *Chemosphere* **2010,** *81*, (3), 387-393.
20. Liu, X.; Wazne, M.; Christodoulatos, C.; Jasinkiewicz, K. L., Aggregation and deposition behavior of boron nanoparticles in porous media. *Journal of Colloid and Interface Science* **2009,** *330*, (1), 90-96.
21. Jiang, X.; Tong, M.; Li, H.; Yang, K., Deposition kinetics of zinc oxide nanoparticles on natural organic matter coated silica surfaces. *Journal of Colloid and Interface Science* **2010,** *350*, (2), 427-434.
22. Li, Z.; Sahle-Demessie, E.; Hassan, A. A.; Sorial, G. A., Transport and deposition of CeO2 nanoparticles in water-saturated porous media. *Water Research* **2011,** *45*, (15), 4409-4418.
23. Fatisson, J.; Domingos, R. F.; Wilkinson, K. J.; Tufenkji, N., Deposition of TiO2 Nanoparticles onto Silica Measured Using a Quartz Crystal Microbalance with Dissipation Monitoring. *Langmuir* **2009,** *25*, (11), 6062-6069.
24. Quevedo, I. R.; Tufenkji, N., Influence of Solution Chemistry on the Deposition and Detachment Kinetics of a CdTe Quantum Dot Examined Using a Quartz Crystal Microbalance. *Environmental science & technology* **2009,** *43*, (9), 3176-3182.
25. Jiang, X.; Wang, X.; Tong, M.; Kim, H., Initial transport and retention behaviors of ZnO nanoparticles in quartz sand porous media coated with Escherichia coli biofilm. *Environmental pollution* **2013,** *174*, 38-49.
26. Chowdhury, I.; Duch, M. C.; Mansukhani, N. D.; Hersam, M. C.; Bouchard, D., Deposition and Release of Graphene Oxide Nanomaterials Using a Quartz Crystal Microbalance. *Environmental science & technology* **2014,** *48*, (2), 961-969.
27. Chang, X.; Bouchard, D. C., Multiwalled Carbon Nanotube Deposition on Model Environmental Surfaces. *Environmental science & technology* **2013,** *47*, (18), 10372-10380.
28. Li, W.; Liu, D.; Wu, J.; Kim, C.; Fortner, J. D., Aqueous Aggregation and Surface Deposition Processes of Engineered Superparamagnetic Iron Oxide Nanoparticles for Environmental Applications. *Environmental science & technology* **2014,** *48*, (20), 11892-11900.
29. Lin, S.; Wiesner, M. R., Deposition of Aggregated Nanoparticles - A Theoretical and Experimental Study on the Effect of Aggregation State on the Affinity between Nanoparticles and a Collector Surface. *Environmental science & technology* **2012,** *46*, (24), 13270-13277.
30. Yi, P.; Chen, K. L., Influence of Surface Oxidation on the Aggregation and Deposition Kinetics of Multiwalled Carbon Nanotubes in Monovalent and Divalent Electrolytes. *Langmuir* **2011,** *27*, (7), 3588-3599.
31. Thio, B. J. R.; Zhou, D.; Keller, A. A., Influence of natural organic matter on the aggregation and deposition of titanium dioxide nanoparticles. *Journal of Hazardous Materials* **2011,** *189*, (1-2), 556-563.
32. Petosa, A. R.; Brennan, S. J.; Rajput, F.; Tufenkji, N., Transport of two metal oxide nanoparticles in saturated granular porous media: Role of water chemistry and particle coating. *Water Research* **2012,** *46*, (4), 1273-1285.

33. Godinez, I. G.; Darnault, C. J. G., Aggregation and transport of nano-TiO2 in saturated porous media: Effects of pH, surfactants and flow velocity. *Water Research* **2011,** *45*, (2), 839-851.
34. Afrooz, A. R. M. N.; Sivalapalan, S. T.; Murphy, C. J.; Hussain, S. M.; Schlager, J. J.; Saleh, N. B., Spheres vs. rods: The shape of gold nanoparticles influences aggregation and deposition behavior. *Chemosphere* **2013,** *91*, (1), 93-98.
35. El Badawy, A. M.; Aly Hassan, A.; Scheckel, K. G.; Suidan, M. T.; Tolaymat, T. M., Key Factors Controlling the Transport of Silver Nanoparticles in Porous Media. *Environmental science & technology* **2013,** *47*, (9), 4039-4045.
36. Chowdhury, I.; Cwiertny, D. M.; Walker, S. L., Combined factors influencing the aggregation and deposition of nano-TiO2 in the presence of humic acid and bacteria. *Environmental science & technology* **2012,** *46*, (13), 6968-6976.
37. Tripathi, S.; Champagne, D.; Tufenkji, N., Transport Behavior of Selected Nanoparticles with different Surface Coatings in Granular Porous Media coated with Pseudomonas aeruginosa Biofilm. *Environmental science & technology* **2011,** *46*, (13), 6942-6949.
38. Hong, Y.; Honda, R. J.; Myung, N. V.; Walker, S. L., Transport of Iron-Based Nanoparticles: Role of Magnetic Properties. *Environmental science & technology* **2009,** *43*, (23), 8834-8839.
39. Mattison, N. T.; O'Carroll, D. M.; Rowe, R. K.; Petersen, E. J., Impact of Porous Media Grain Size on the Transport of Multi-walled Carbon Nanotubes. *Environmental science & technology* **2011,** *45*, (22), 9765-9775.
40. Cai, L.; Zhu, J.; Hou, Y.; Tong, M.; Kim, H., Influence of Gravity on Transport and Retention of Representative Engineered Nanoparticles in Quartz Sand. *Journal of Contaminant Hydrology* **2015**.
41. He, F.; Zhang, M.; Qian, T.; Zhao, D., Transport of carboxymethyl cellulose stabilized iron nanoparticles in porous media: Column experiments and modeling. *Journal of Colloid and Interface Science* **2009,** *334*, (1), 96-102.
42. Kanel, S.; Goswami, R.; Clement, T.; Barnett, M.; Zhao, D., Two dimensional transport characteristics of surface stabilized zero-valent iron nanoparticles in porous media. *Environmental science & technology* **2007,** *42*, (3), 896-900.
43. Hotze, E. M.; Phenrat, T.; Lowry, G. V., Nanoparticle aggregation: challenges to understanding transport and reactivity in the environment. *Journal of environmental quality* **2010,** *39*, (6), 1909-1924.
44. Song, L.; Elimelech, M., Transient Deposition of Colloidal Particles in Heterogeneous Porous Media. *Journal of Colloid and Interface Science* **1994,** *167*, (2), 301-313.
45. Saiers, J. E.; Ryan, J., Colloid deposition on non-ideal porous media: The influences of collector shape and roughness on the single-collector efficiency. *Geophysical research letters* **2005,** *32*, (21).
46. Song, L.; Johnson, P. R.; Elimelech, M., Kinetics of Colloid Deposition onto Heterogeneously Charged Surfaces in Porous Media. *Environmental Science & Technology* **1994,** *28*, (6), 1164-1171.
47. Joo, S. H.; Al-Abed, S. R.; Luxton, T., Influence of Carboxymethyl Cellulose for the Transport of Titanium Dioxide Nanoparticles in Clean Silica and Mineral-Coated Sands. *Environmental science & technology* **2009,** *43*, (13), 4954-4959.

48. Kim, H.-J.; Phenrat, T.; Tilton, R. D.; Lowry, G. V., Effect of kaolinite, silica fines and pH on transport of polymer-modified zero valent iron nano-particles in heterogeneous porous media. *Journal of Colloid and Interface Science* **2012,** *370*, 1-10.
49. Elimelech, M.; Nagai, M.; Ko, C.-H.; Ryan, J. N., Relative Insignificance of Mineral Grain Zeta Potential to Colloid Transport in Geochemically Heterogeneous Porous Media. *Environmental Science & Technology* **2000,** *34*, (11), 2143-2148.
50. Johnson, P. R.; Sun, N.; Elimelech, M., Colloid Transport in Geochemically Heterogeneous Porous Media: Modeling and Measurements. *Environmental Science & Technology* **1996,** *30*, (11), 3284-3293.
51. Wang, D.; Su, C.; Zhang, W.; Hao, X.; Cang, L.; Wang, Y.; Zhou, D., Laboratory assessment of the mobility of water-dispersed engineered nanoparticles in a red soil (Ultisol). *Journal of Hydrology* **2014,** *519, Part B*, (0), 1677-1687.
52. Wang, Y.; Li, Y.; Kim, H.; Walker, S. L.; Abriola, L. M.; Pennell, K. D., Transport and retention of fullerene nanoparticles in natural soils. *Journal of environmental quality* **2010,** *39*, (6), 1925-1933.
53. Cornelis, G.; Pang, L.; Doolette, C.; Kirby, J. K.; McLaughlin, M. J., Transport of silver nanoparticles in saturated columns of natural soils. *Science of The Total Environment* **2013,** *463–464*, (0), 120-130.
54. Tong, M.; Ding, J.; Shen, Y.; Zhu, P., Influence of biofilm on the transport of fullerene (C-60) nanoparticles in porous media. *Water Research* **2010,** *44*, (4), 1094-1103.
55. Afrooz, A. N.; Khan, I. A.; Hussain, S. M.; Saleh, N. B., Mechanistic Hetero-aggregation of gold nanoparticles in a wide range of solution chemistry. *Environmental science & technology* **2013,** *47*, (4), 1853-1860.
56. Cerbelaud, M.; Videcoq, A.; Abélard, P.; Pagnoux, C.; Rossignol, F.; Ferrando, R., Hetero-aggregation between Al2O3 submicrometer particles and SiO2 nanoparticles: Experiment and simulation. *Langmuir* **2008,** *24*, (7), 3001-3008.
57. Huynh, K. A.; McCaffery, J. M.; Chen, K. L., Hetero-aggregation of multiwalled carbon nanotubes and hematite nanoparticles: Rates and mechanisms. *Environmental science & technology* **2012,** *46*, (11), 5912-5920.
58. Wang, Y.; Gao, B.; Morales, V. L.; Tian, Y.; Wu, L.; Gao, J.; Bai, W.; Yang, L., Transport of titanium dioxide nanoparticles in saturated porous media under various solution chemistry conditions. *Journal of Nanoparticle Research* **2012,** *14*, (9), 1-9.
59. Yang, H.; Tong, M.; Kim, H., Effect of Carbon Nanotubes on the Transport and Retention of Bacteria in Saturated Porous Media. *Environmental science & technology* **2013,** *47*, (20), 11537-11544.
60. Wang, X.; Cai, L.; Han, P.; Lin, D.; Kim, H.; Tong, M., Cotransport of multi-walled carbon nanotubes and titanium dioxide nanoparticles in saturated porous media. *Environmental pollution* **2014,** *195*, 31-38.
61. Cai, L.; Tong, M.; Ma, H.; Kim, H., Cotransport of titanium dioxide and fullerene nanoparticles in saturated porous media. *Environmental science & technology* **2013,** *47*, (11), 5703-5710.
62. Bronikowski, M. J.; Willis, P. A.; Colbert, D. T.; Smith, K.; Smalley, R. E., Gas-phase production of carbon single-walled nanotubes from carbon monoxide via the HiPco process: A parametric study. *Journal of Vacuum Science & Technology A* **2001,** *19*, (4), 1800-1805.

63. Saleh, N. B.; Pfefferle, L. D.; Elimelech, M., Aggregation kinetics of multiwalled carbon nanotubes in aquatic systems: measurements and environmental implications. *Environmental science & technology* **2008,** *42*, (21), 7963-7969.
64. Soejima, T.; Oshiro, S.; Nakatsuji, Y.; Ito, S., Dense aqueous colloidal gold nanoparticles prepared from highly concentrated precursor solution. *Journal of colloid and interface science* **2011,** *362*, (2), 325-329.
65. Georgakilas, V.; Voulgaris, D.; Vazquez, E.; Prato, M.; Guldi, D. M.; Kukovecz, A.; Kuzmany, H., Purification of HiPCO carbon nanotubes via organic functionalization. *Journal of the American Chemical Society* **2002,** *124*, (48), 14318-14319.
66. Fresnais, J.; Yan, M.; Courtois, J.; Bostelmann, T.; Bée, A.; Berret, J. F., Poly(acrylic acid)-coated iron oxide nanoparticles: Quantitative evaluation of the coating properties and applications for the removal of a pollutant dye. *Journal of Colloid and Interface Science* **2013,** *395*, (0), 24-30.
67. Vaisman, L.; Wagner, H. D.; Marom, G., The role of surfactants in dispersion of carbon nanotubes. *Advances in colloid and interface science* **2006,** *128*, 37-46.
68. Moore, V. C.; Strano, M. S.; Haroz, E. H.; Hauge, R. H.; Smalley, R. E.; Schmidt, J.; Talmon, Y., Individually suspended single-walled carbon nanotubes in various surfactants. *Nano Letters* **2003,** *3*, (10), 1379-1382.
69. Bradford, S. A.; Bettahar, M.; Simunek, J.; Van Genuchten, M. T., Straining and attachment of colloids in physically heterogeneous porous media. *Vadose Zone Journal* **2004,** *3*, (2), 384-394.
70. Li, Z.; Sahle-Demessie, E.; Hassan, A. A.; Sorial, G. A., Transport and deposition of CeO 2 nanoparticles in water-saturated porous media. *Water research* **2011,** *45*, (15), 4409-4418.
71. Chowdhury, I.; Duch, M. C.; Gits, C. C.; Hersam, M. C.; Walker, S. L., Impact of synthesis methods on the transport of single walled carbon nanotubes in the aquatic environment. *Environmental science & technology* **2012,** *46*, (21), 11752-11760.
72. Tian, Y.; Gao, B.; Morales, V. L.; Wang, Y.; Wu, L., Effect of surface modification on single-walled carbon nanotube retention and transport in saturated and unsaturated porous media. *Journal of hazardous materials* **2012,** *239*, 333-339.
73. Bouchard, D.; Zhang, W.; Powell, T.; Rattanaudompol, U.-s., Aggregation kinetics and transport of single-walled carbon nanotubes at low surfactant concentrations. *Environmental science & technology* **2012,** *46*, (8), 4458-4465.
74. Bradford, S. A.; Bettahar, M., Concentration dependent transport of colloids in saturated porous media. *Journal of Contaminant Hydrology* **2006,** *82*, (1), 99-117.
75. Kasel, D.; Bradford, S. A.; Šimůnek, J.; Heggen, M.; Vereecken, H.; Klumpp, E., Transport and retention of multi-walled carbon nanotubes in saturated porous media: Effects of input concentration and grain size. *water research* **2013,** *47*, (2), 933-944.
76. Saleh, N. B.; Pfefferle, L. D.; Elimelech, M., Influence of Biomacromolecules and Humic Acid on the Aggregation Kinetics of Single-Walled Carbon Nanotubes. *Environmental Science & Technology* **2010,** *44*, (7), 2412-2418.
77. Johnson, P. R.; Sun, N.; Elimelech, M., Colloid transport in geochemically heterogeneous porous media: Modeling and measurements. *Environmental science & technology* **1996,** *30*, (11), 3284-3293.
78. Saiers, J. E.; Lenhart, J. J., Ionic-strength effects on colloid transport and interfacial reactions in partially saturated porous media. *Water Resources Research* **2003,** *39*, (9), 1256.

Chapter 6

Summary and Conclusions

6.1 Summary

The research presented in this dissertation focused on four primary data gaps. 1) Influence of AuNMs' shape on their aggregation and deposition; 2) Role of preliminary size on the aggregation behavior of AuNS; 3) Effect of presence of SWNT on the aggregation characteristics of AuNS (hetero-aggregation); and 4) Role of SWNT on the transport of AuNS (co-transport) in porous media. Alongside with classical characterization techniques (e.g., electron microscopy, optical microscopy, Raman and UV-vis spectroscopy, electro-kinetic methods, light scattering, quartz crystal microbalance), this research developed novel methods and applied new approaches to assess hetero-aggregation and co-transport of AuNS.

In an effort to address the first data gap, 12 nm diameter PAA coated AuNS and 12 × 60 nm AuNRs were procured and characterized by HRTEM, electrokinetic measurement, and UV-vis spectroscopy. Shape-dependent aggregation kinetics was investigated for a series of NaCl and $CaCl_2$ concentration. Aggregation histories (hydrodynamic radii vs. time) were obtained using time resolved DLS technique coupled with auto-correlation function and was analyzed via cumulant analysis. Attachment efficiencies were computed from the aggregation profiles followed by estimation of CCCs for the AuNSs and AuNRs using respective stability plots. Shape-dependent deposition behavior of the AuNMs onto a silica crystal was probed using a QCM-D setup in presence of a wide range of NaCl concentration. Deposition rates were plotted against the ionic strength to elucidate the effect of particle geometry on the deposition behavior of the AuNMs.

NIST reference materials, 30 nm and 60 nm diameter gold spheres, were used to address the second data gap. TEM and UV-vis spectroscopy were performed for the chemical and morphological analyses of both types of AuNSs. Electrokinetic measurements were performed on

the AuNSs. AuNSs were introduced into a biological culture media (RPMI solution with 1% streptomycin in presence of 10% fetal bovine serum, FBS) and their HR were continuously monitored in every 15 s for 24 h using DLS. Moreover, time-dependent aggregate structure information, (i.e., fractal dimensions) was obtained using SLS technique in every 2 h for a period of 24 h.

Hetero-aggregation kinetics of AuNS was probed using TEM and DLS in presence of PA-modified SWNTs (mix ratio of PA-SWNT: AuNS = 1:20) in an effort to address the third data gap. PA modification of the SWNT was performed through ultrasonication followed by centrifugation and functionalization the SWNTs with PA was confirmed using Raman spectroscopy, which eliminated SWNT-SWNT aggregation (via steric interaction) for a wide range of ionic strength and allowed formation of only AuNS homo- (AuNS-AuNS) and hetero-aggregates (AuNS-SWNT). Confirmation of a stable PA-SWNT dispersion was obtained by monitoring their unchanged HR in highly saline conditions. Electrokinetic measurements of the NMs, in presence of the chosen range of NaCl and $CaCl_2$, were performed. Homo- and hetero-aggregation rates (nm/s) were computed from the linear regression of the initial aggregation portion (time takes to reach 1.3 times of the HR at t=0 s) of the aggregation history plots. Mechanistic understanding of AuNS hetero-aggregation was facilitated by HRTEM imaging of the hetero-dispersions at high and low electrolyte conditions.

Final data gap was addressed by performing column experiments that involved injection of AuNS and PA-SWNTs through a saturated porous media. Ottawa sand (600-700 μm) packed glass columns were configured in up-flow condition and the eluent AuNSs were detected by a UV-vis spectrophotometer. Breakthrough curves (time or PV vs. normalized eluent concentration, C/C_0) were generated for AuNSs in presence of 1, 10, 30, and 100 mM NaCl. PA modification of the

SWNTs for a series of PA concentrations was performed and transport experiments were carried out to determine the role of PA percentages on SWNT mobility through the packed column under a range of ionic strength (1-100 mM). This allowed to determine the role of PA concentration on SWNT deposition and aided in selection of appropriate PA conditions to perform co-transport of collector pre-coating. AuNSs were transported under a range of ionic strength conditions in single-particle systems (i.e., AuNS) and on presence of secondary PA-SWNTs (either in hetero-dispersion or through pre-coated collectors). Effects of NOM on AuNS transport was also investigated.

6.2 Conclusions

The major conclusions of this research are summarized below:

6.2.1 Spheres vs. Rods: The Shape of Gold Nanoparticles Influences Aggregation and Deposition Behavior

- Uniform sized and shaped AuNSs showed higher aggregation propensity compared to AuNRs for the same surface coating; i.e., PAA.
- Attachment efficiencies of the AuNS at a certain ionic strength in presence of $CaCl_2$ was higher than that in presence of NaCl.
- Reaction limited and diffusion limited regimes were more pronounced for the AuNS than that for the AuNRs.
- CCCs for AuNS were found to be 50 mM for NaCl and 1.8 mM for $CaCl_2$
- CCCs for AuNR were found to be 250 mM for NaCl and 7 mM for $CaCl_2$
- The higher stability of the AuNRs has likely resulted from steric interaction of PAA polyelectrolyte coatings with extended conformation compared to the AuNSs.

- AuNRs also showed less deposition propensity compared to AuNSs, particularly in low electrolyte conditions.
- AuNMs can manifest shape-dependent fate, transport, and biological interaction.

6.2.2 Aggregate size and structure determination of nanomaterials in physiological media: Importance of dynamic evolution

- Both of the AuNS (i.e., 30 nm and 60 nm) showed significant aggregation over time in the culture media.
- Although AuNS particles' aggregation was gradual up to 6 h period, beyond 6 h time DLS detected multi-micron sized particles.
- Multi-micron sized particle could possibly be attributed to a snapshot of a large particle network formed by facilitated nucleation.
- There were significant differences between the aggregate structures of the 30 nm and 60 nm particles, more likely resulted from their preliminary size
- Although D_f in both particles demonstrated time dependent variation, experimental data lacked a defined trend of D_f over time.
- Continuous measurement of the aggregate size and aggregate structures of the nanoparticles is necessary for accurate interpretation of the nanotoxicity data and effective dose calculation in toxicity assays.

6.2.3 Mechanistic Hetero-aggregation of Gold Nanoparticles in a Wide Range of Solution Chemistry

- Presence of PA-SWNT influenced AuNS aggregation kinetics under a wide range of NaCl and $CaCl_2$ concentration.
- AuNS demonstrated slower hetero-aggregation at low electrolyte conditions compared to

their homo-aggregation rate under identical ionic strength

- At high electrolyte concentration, AuNS demonstrated enhanced aggregation in presence of SWNT compared to their homo-aggregation rates.
- In addition to being function of the ionic strength, homo- and hetero-aggregation rates of the AuNS depends on the valence of the electrolyte in suspension.
- Presence of NOM increases, in both homo- and hetero-dispersion state, the aggregation rate of the AuNS at environmentally relevant condition.
- It has been hypothesised from the TEM images that the decrease of the hetero-rates could be associated with obstruction of the AuNS aggregation induced by the suspended PA-SWNTs.
- Enhanced hetero-aggregation rates at favourable aggregation regime was assumed to be a result of facilitated attachment of AuNS on the PA-SWNT surfaces.
- DLS technique can be used in combination of SPR to investigate hetero-aggregation behaviour of the ENMs.

6.2.4 Co-transport of Gold Nanospheres with Single-walled Carbon Nanotubes in Saturated Porous Media

- Transport of AuNS through a sand packed column was strongly dependent on the background ionic strength
- Almost perfect mobility of the AuNS at 1 mM condition and substantial release at higher ionic strengths suggested that straining didn't affect AuNS transport through porous media.
- Amount of PA used to disperse a certain mass of SWNTs influence PA-SWNTs mobility: mobility increases with increasing PA amount.
- AuNS demonstrated increased transport behaviour in presence of PA-SWNT in the

suspension.

- Coating of the sand grains by PA-SWNTs decreased the mobility of the AuNS through the column.
- Co-transport of AuNS in presence of PA-SWNTs and the transport of AuNS through PA-SWNT coated sand column, both were influenced by the background ionic strengths.
- Increased mobility of the AuNS in presence of PA-SWNT can be attributed to facilitated transport, where highly mobile PA-SWNTs act as a courier of the AuNS
- Increased retention of the AuNS onto the PA-SWNT coated sand surfaces can be attributed to the facilitated deposition in presence of additional attachment sites.

6.3 Environmental Implications of the Research

Use of anisotropic ENMs in various applications makes their environmental releases very likely, and literature bears evidence of their significant antimicrobial and toxic potential alongside with proportionate human health concerns. Understanding the fate and transport of the anisotropic ENMs in the environment is a key to evaluate their risk and safety. This research assessed the aggregation and deposition of rod shaped AuNM, and demonstrated that the interfacial interaction of the anisotropic ENMs may significantly vary from the fate and transport behavior of their spherical counterpart. Experimental results indicates that PAA coated AuNR will show higher stability, thereby high mobility, at both low (equivalent to freshwater condition) and high (marine or estuarine environment) ionic strength conditions. Such shape dependent behavior of the ENMs also implies unique interaction of the anisotropic nanomaterials with the biological entities in the typical background chemistries.

In vitro toxicity assays are surrogates in evaluating ENMs' interaction in the biological environment, and such interactions greatly depend on the effective ENM dose of administered to

cells. ENMs' aggregation propensity is exacerbated by cellular exposure media (with elevated ionic strength) and thus is known to influence the effective dose of these ENMs. Along with the unique shape dependent interaction, size of the ENMs may significantly influence the effective dosage. This research delineated the importance of time-dependent characterization of the ENM hydrodynamic radii and aggregate structure in a cell culture media. The key findings indicated that evolution of the ENMs' aggregate size and shape should be taken into consideration in interpreting any size dependent toxicity data. The effect of size may diminish over time (during the exposure duration) as aggregation of the nano-scale entities surpasses the preliminary differences in size. Results of this research will likely improve the design of nano-toxicity assays.

This research not only evaluates the role of material attribute in their fate and transport but also extends to assess the role of environmental complexities on the same. Presence of secondary particles in the form of natural colloids, geo-macro molecules or pre-existing ENMs (i.e., PA-SWNTs) are very likely in the natural environment, and their presence may invalidate the fate and transport data obtained from controlled experiments in singular system. Influence of secondary particulate matter in the aggregation of AuNS is also systematically evaluated. The experimental findings indicate that hetero-aggregation of the AuNSs would be slower at low electrolyte conditions (e.g., surface water bodies; ~3-10 mM) compared to their homo-aggregation rates. However, in presence of elevated electrolyte conditions (e.g., groundwater, marine and estuarine environments; 100-700 mM), hetero-aggregation will be faster, potentially indicating to lesser mobility in such environmental systems compared to AuNS homo-dispersons. Additionally, increased aggregation rates in presence of NOM, indicates slower mobility of the AuNSs in the typical natural aquatic conditions. The method developed in this study can be extended to a wider

set of ENMs, and will likely serve as the first step to systematically evaluate hetero-aggregation behavior in a wide range of environmental conditions.

Finally, the co-transport study of the AuNS in presence of PA-SWNTs presented in this dissertation complements the findings concerning the effects of coexistence of ENMs in their fate and transport. This is the first study that investigates the transport behavior of the AuNSs in presence of PA-SWNTs under a wide range of ionic strength. The findings of this study show that presence of secondary particles will enhance AuNS mobility while in hetero-dispersions via facilitated transport, thus indicating to longer travel distances through sediments and aquifers. However, pre-coating of the natural soil media by secondary particles (i.e., PA-SWNTs) will likely reduce AuNS mobility by providing increased number of favorable attachment sites for deposition to occur on the coated collectors. These result indicate that the order of addition of the secondary particles in the aquatic system will have a strong influence on their transport through porous media.

6.4 Recommendations for Future Research

The research presented in the dissertation focused on assessing the roles of the anisotropy and environmental complexity on fate and transport of ENMs. The future research recommendations are laid out in two sections; i.e., research needs to evaluate (a) the effects of shape and (b) the role of environmental complexity.

6.4.1 Effect of Shape and Size of the ENMs on Aggregation and Deposition of the ENMs

Differences between the fate and transport of AuNS and AuNR as presented in this study, poses further questions to better understand the role of aspect ratio of the rod-shaped ENMs on their aggregation behavior. ENM fate and transport literature lacks in a detailed data set in regard to the effects of length of the metallic nano-rods on their aggregation and deposition in environmentally relevant solution chemistries. Moreover, theoretical interpretation of the

observed behavior in terms of mathematical modelling has not been addressed in the current research. Therefore, investigating the efficacy of DLVO theory on the anisotropic ENMs and developing appropriate modification to the classical model is highly important.

The research concerning the time evolution of AuNS size in RPMI media needs to be extended to investigate the effect of various common biological culture media (i.e., DMEM, EMB, MSA). As described in the chapter 3, such time evolution would likely affect the effective dose of the ENMs to the cells during *in vitro* studies. Further studies are needed to develop a way to accurately estimate effective dosage in a bioassay from the size and shape evolution of the ENMs in the culture media.

6.4.2 Role of Environmental Complexity on Aggregation and Deposition of the ENMs

Hetero-aggregation of AuNSs in presence of PA-SWNTs, as presented in chapter 4, provides evidence of altered aggregation behavior compared to homo-aggregation scenario. However, further studies and development of novel experimental techniques are needed that could distinguish between homo- and hetero-aggregates formed during the hetero-aggregation process. PA modification of the SWNTs followed by DLS measurements though confirms elimination of the homo-aggregation of the secondary particles, cannot differentiate between AuNS-AuNS and AuNS-PA-SWNT aggregates. Such differentiation could potentially lead to better mechanistic understanding of the hetero-aggregation process. Moreover, the reasoning of the absence of a favourable region for hetero-aggregation requires theoretical validation by theoretical modelling. Additionally, effects of % PA used in dispersing SWNTs and the ratio of the AuNS/PA-SWNT on hetero-aggregation of the AuNS is worth investigating. New techniques are desired to assess hetero-aggregation in presence of natural colloids (e.g., clay, bio-colloids). The zwitterionic nature of clay particles and heterogeneity in natural bio-colloids present complexities, which the

controlled hetero-aggregation studies developed here cannot address.

In addition to the study presented in Chapter 5, it is necessary to understand the effect of the ratio of the secondary/primary ENMs on their co-transport behavior; as the ratio of the co-existing ENMs may widely vary in the sediment/porewater in natural environment. Chapter 5 also lacks assessment of the efficacy of classical CFT model in capturing comparison behavior of AuNSs. Moreover, construction of individual depth profile for the secondary and primary ENMs in their co-transport studies may potentially help in better understanding of the filtration mechanisms. Methods to assess co-transport in presence of natural colloids are also desired.

Altered interfacial interaction of ENMs in presence of secondary entities also calls for evaluation of ENMs toxicity in similar binary system. Physico-chemical interaction of ENMs are widely reported to have significant effect on their toxic response. Therefore, toxic potential of a certain nanomaterial may be influenced by the presence of other colloids/ENMs in suspension. Systematic evaluation of the toxicity of ENMs hetero-dispersion may reveal the exact nature of such influences.

Appendix A: Supplemental Information for Chapter 2

Spheres vs. Rods: The Shape of Gold Nanoparticles Influences Aggregation and Deposition Behavior

A-1. Detailed Aggregation Kinetics Study Protocol

The aggregation kinetics data was analyzed using classical colloidal approach. Measured hydrodynamic radii of the AuNM were plotted with time as aggregation profiles. Analyses of the data were performed by estimation of initial aggregation rate; i.e. aggregation of AuNM up to ~1.3 times the initial hydrodynamic radius (R_0). The rate of aggregation is known to be proportional to the rate of change of R_0 with time and can be expressed as equation 1 as follows.

$$k \propto \frac{1}{N}\left[\frac{dR_0(t)}{dt}\right]_{\{t\to 0\}} \quad \text{(1)}$$

where, k is the initial aggregation rate, and N is the AuNM particle concentration.

To eliminate influence of particle concentration that can vary between samples, a normalized unit less quantity, known as attachment efficiency or 'α', was determined from the ratio of initial aggregation rate at each electrolyte condition with that of the favorable aggregation condition. Attachment efficiency 'α' is represented using equation 2 as follows.

$$\alpha = \frac{\left[\frac{dR_0(t)}{dt}\right]_{\{t \to 0\}}}{\left[\frac{dR_0(t)}{dt}\right]_{\{t \to 0, fav\}}} \quad \text{(2)}$$

where, α is the attachment efficiency, and t is the time of aggregation.

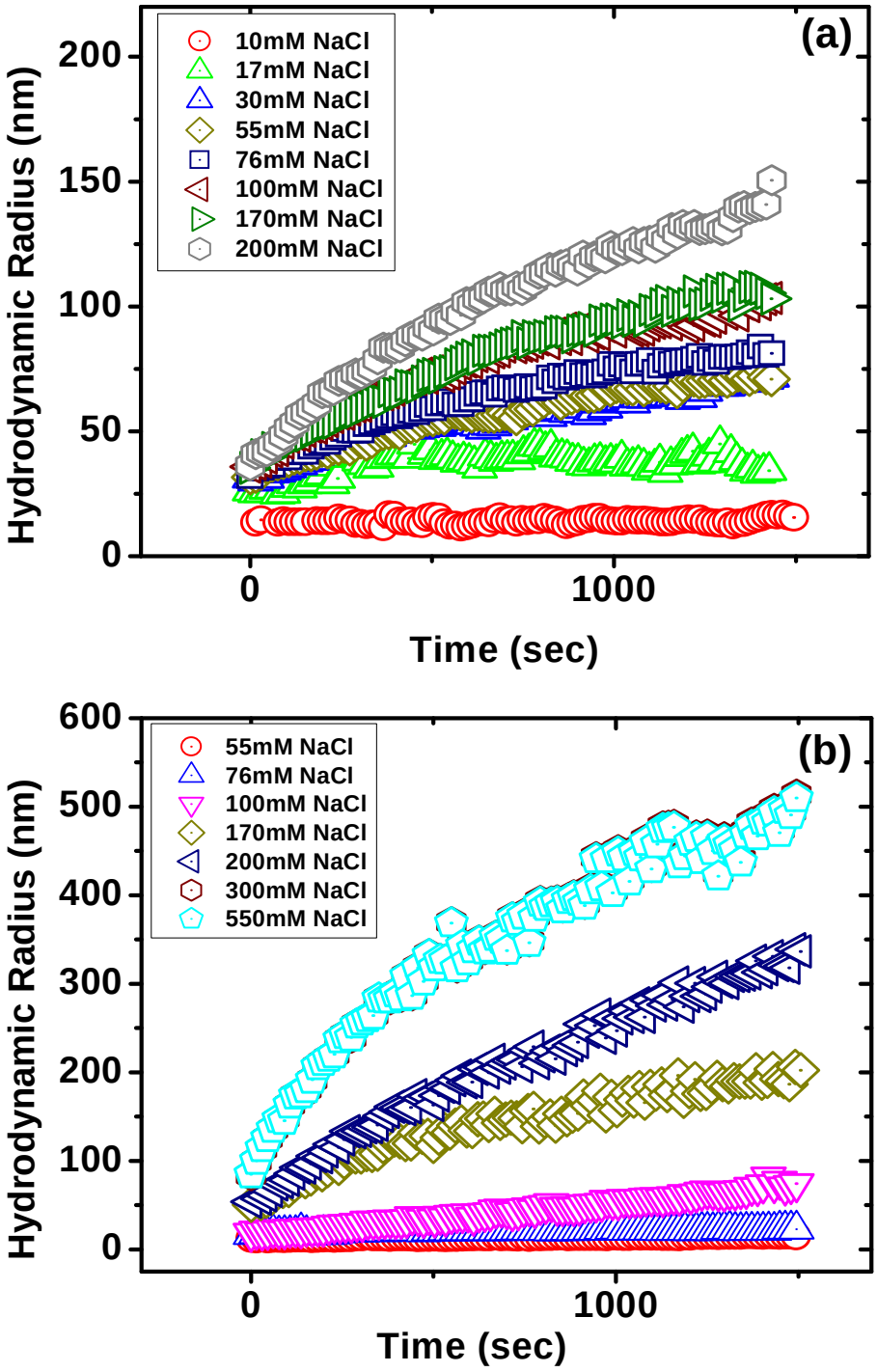

FIGURE A-1: Aggregation profile in presence of mono-valent NaCl of (a) AuNS and (b) AuNR. Measurements were carried out at 20 °C.

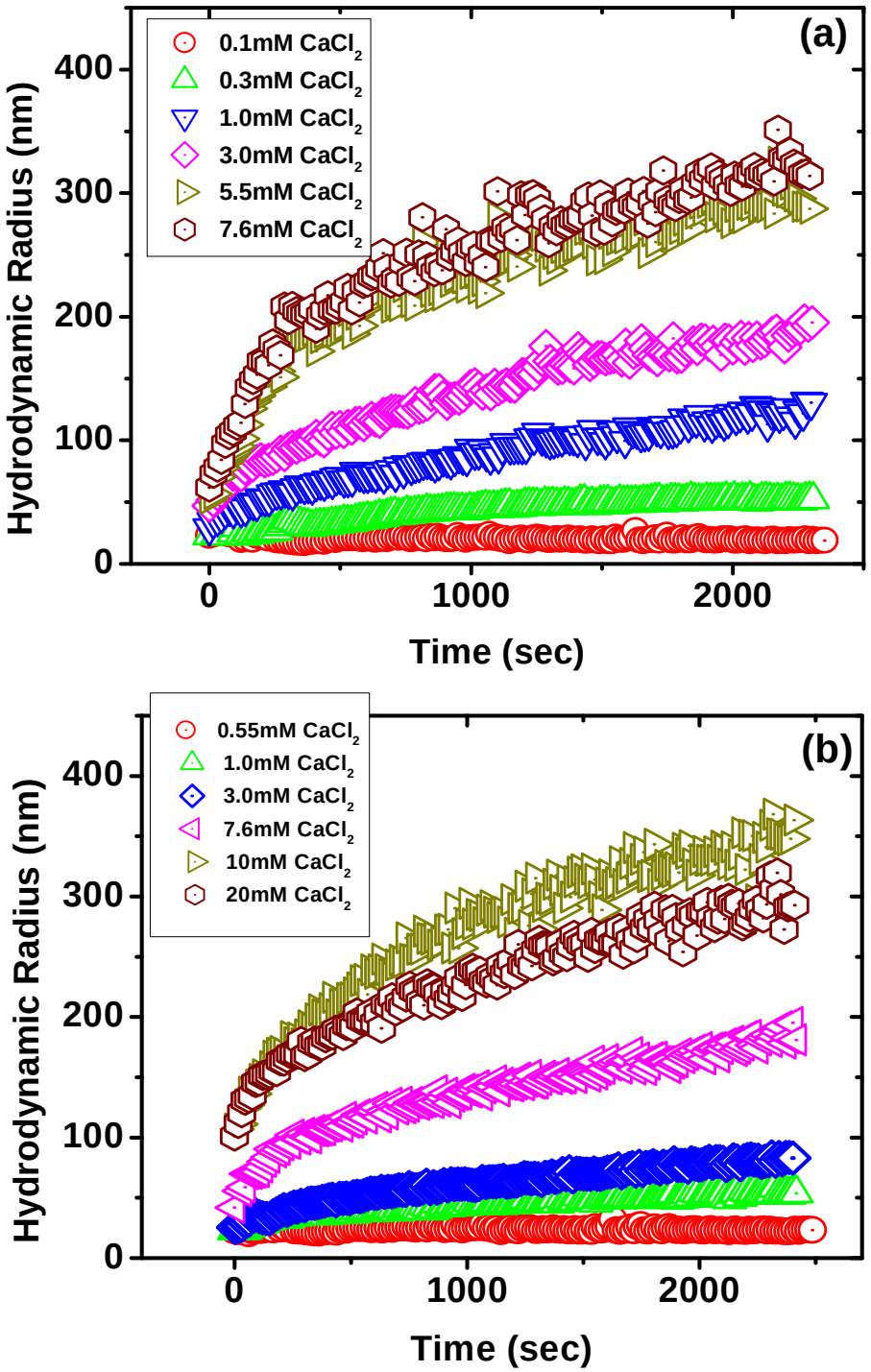

FIGURE A-2: Aggregation profile in presence of di-valent $CaCl_2$ of (a) AuNS and (b) AuNR. Measurements were carried out at 20 °C.

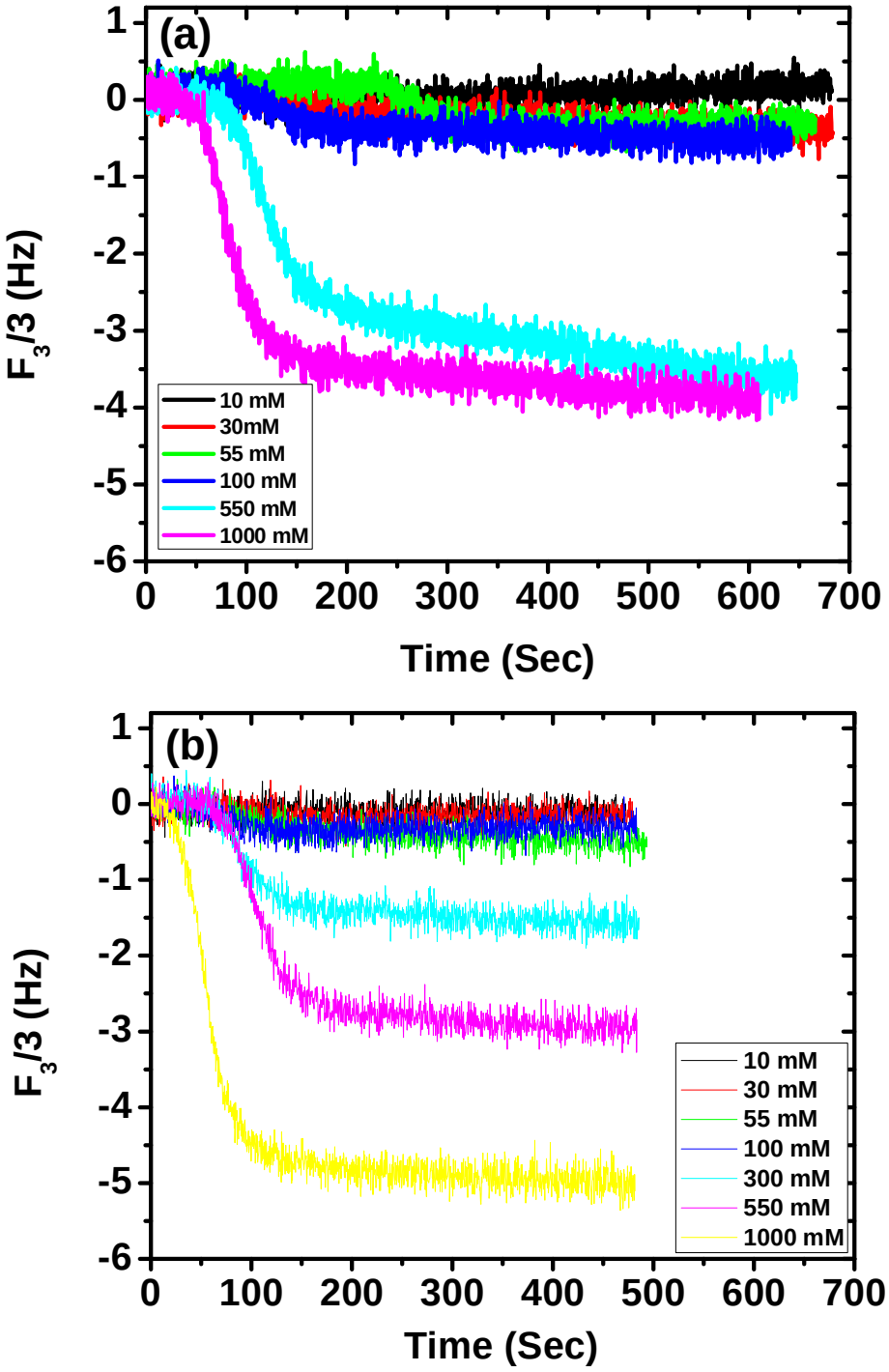

FIGURE A-3: Frequency profiles of (a) AuNS and (b) AuNR onto a silica coated quartz crystal as a function of NaCl concentrations. Changes in normalized frequency shift at the third overtone (F_3) reflect on AuNM attachment on quartz crystal surfaces. Measurements were carried out at 20^0 C

Appendix B: Supplemental Information for Chapter 3

Aggregate size and Structure Determination of Nanomaterials in Physiological Media: Importance of Dynamic Evolution

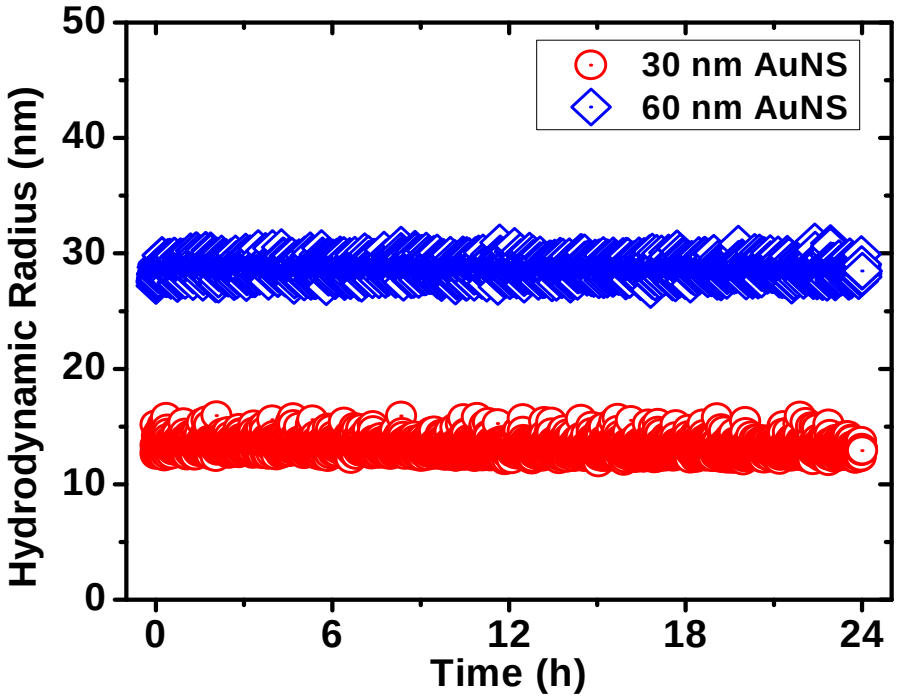

FIGURE B-1: Hydrodynamic radii of 2 different gold nanoparticles sample in DI water. Measurement was carried out at 37 °C

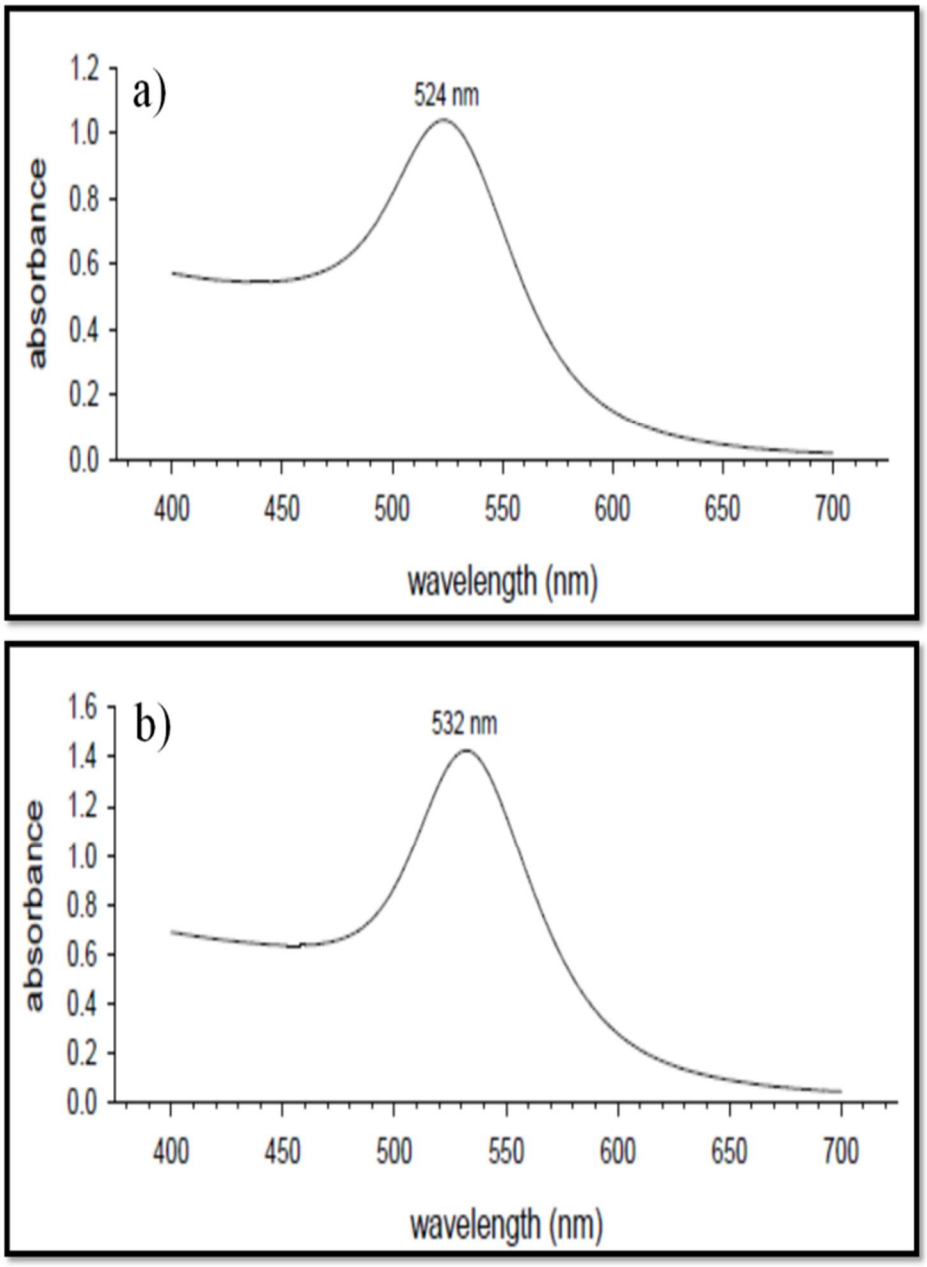

FIGURE B-2: UV-Vis spectra of Au NSs. a) 30 nm sample, b) 60 nm sample. Characteristic peak maxima for each spectra shift is based upon primary AuNS size; 524nm to 532nm for 30nm and 60nm Au NSs, respectively

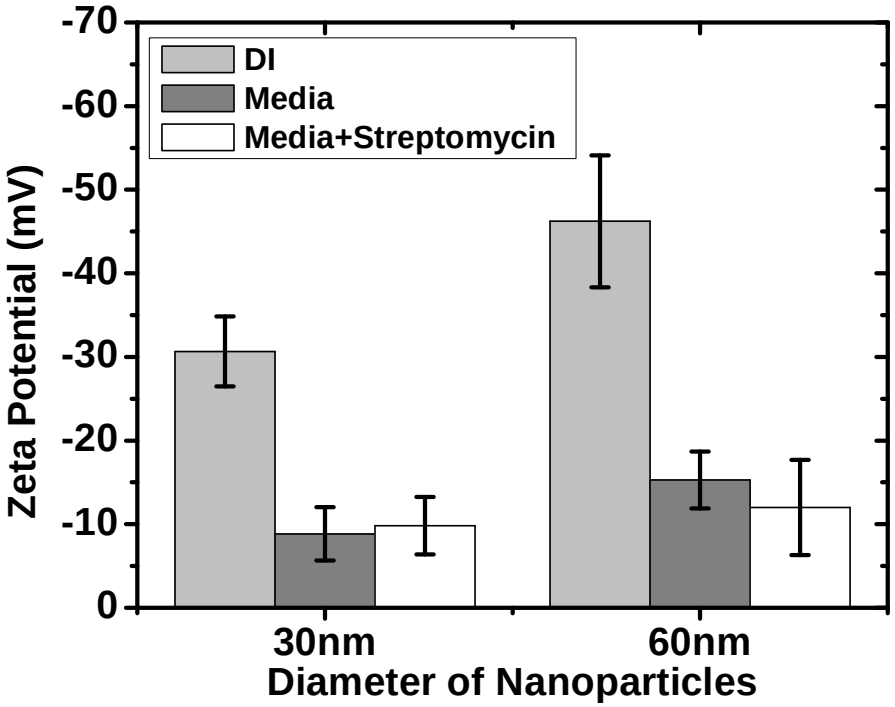

FIGURE B-3: Electrokinetic surface properties of gold nanoparticles in different solution chemistry

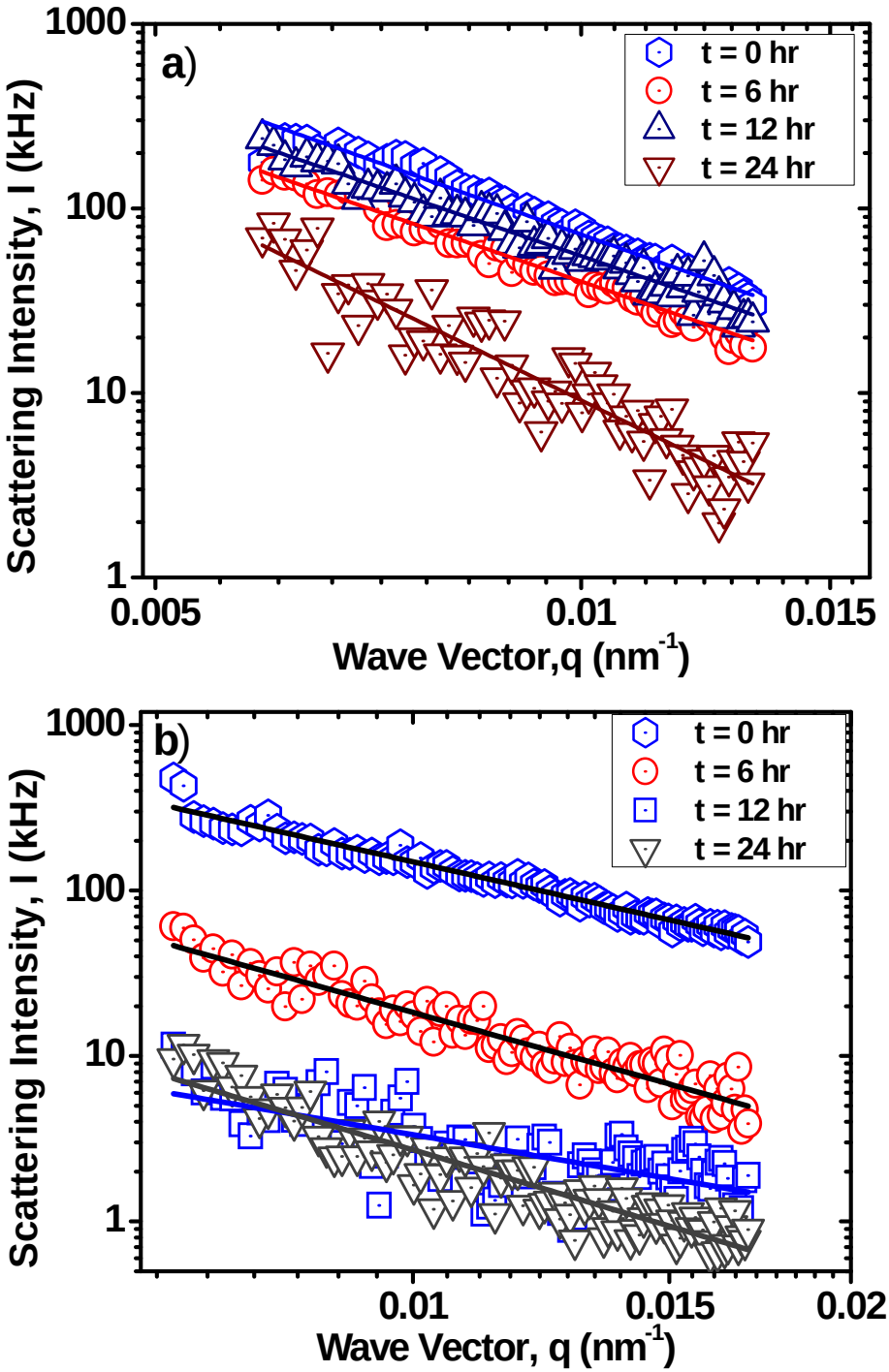

FIGURE B-4: Static light scattering (SLS) plot for gold nanoparticles in relevant physiological condition. a) 30 nm sample, b) 60 nm sample

Two-way (two-factor) ANOVA model fitting

Table B-1: Fractal Dimension Data for 30 nm Particle

Time (hrs)	D_f Run 1	D_f Run 2	D_f Run 3	Average D_f	Standard Deviation
0	2.78	2.78	2.8	2.786667	0.011547
6	2.61	2.6	2.69	2.633333	0.049329
12	2.59	2.61	2.65	2.616667	0.030551
24	2.72	2.69	2.75	2.72	0.03

Table B-2: Fractal Dimension Data for 60 nm Particle

Time (hrs)	D_f Run 1	D_f Run 2	D_f Run 3	Average D_f	Standard Deviation
0	2.01	1.86	2.11	1.993333	0.125831
6	2.51	2.19	2.64	2.446667	0.231589
12	1.48	1.44	1.59	1.503333	0.077675
24	2.61	2.61	2.64	2.62	0.017321

Assuming, The level of significance, $\alpha = 0.05$ (95% confidence level)

Table B-3: Effect of Time and Size Factor on D_f

Source	Degrees of Freedom	Type I Sum of Square	Mean Square	F-distribution Value	p Value
Time Points	3	1.24380000	0.41460000	6.42	0.0035
Particle size	1	1.80401667	1.80401667	27.94	<.0001

Hypothesis testing for the factor,Size:

We are testing

H_0: $\mu_1 = \mu_2$

H_a: $\mu_1 \neq \mu_2$

Where μ_1 = mean measurements for 30nm particles

μ_2 = mean measurements for metal 60nm particles

Decision: reject the null hypothesis, because p-value (<.0001) is less than α.
Conclusion: The factor, particle size, has significant effects on measurements. That is, the 30nm particles differ significantly from the 60nm particle in terms of the mean measurements.

Hypothesis testing for the factor, Time: we are testing

H_0: $\mu_1 = \ldots = \mu_4$

H_a: at least one mean is different from the rest

Where μ_1 = mean measurements at time '0' and so on…….

Decision: reject the null hypothesis, because p-value is 0.0035, which is less than α.
Conclusion: The factor, time of the measurement, has significant effects on the mean measurements

Appendix C: Supplemental Information for Chapter 4

Mechanistic Hetero-aggregation of Gold Nanoparticles for a Wide Range of Solution Chemistries

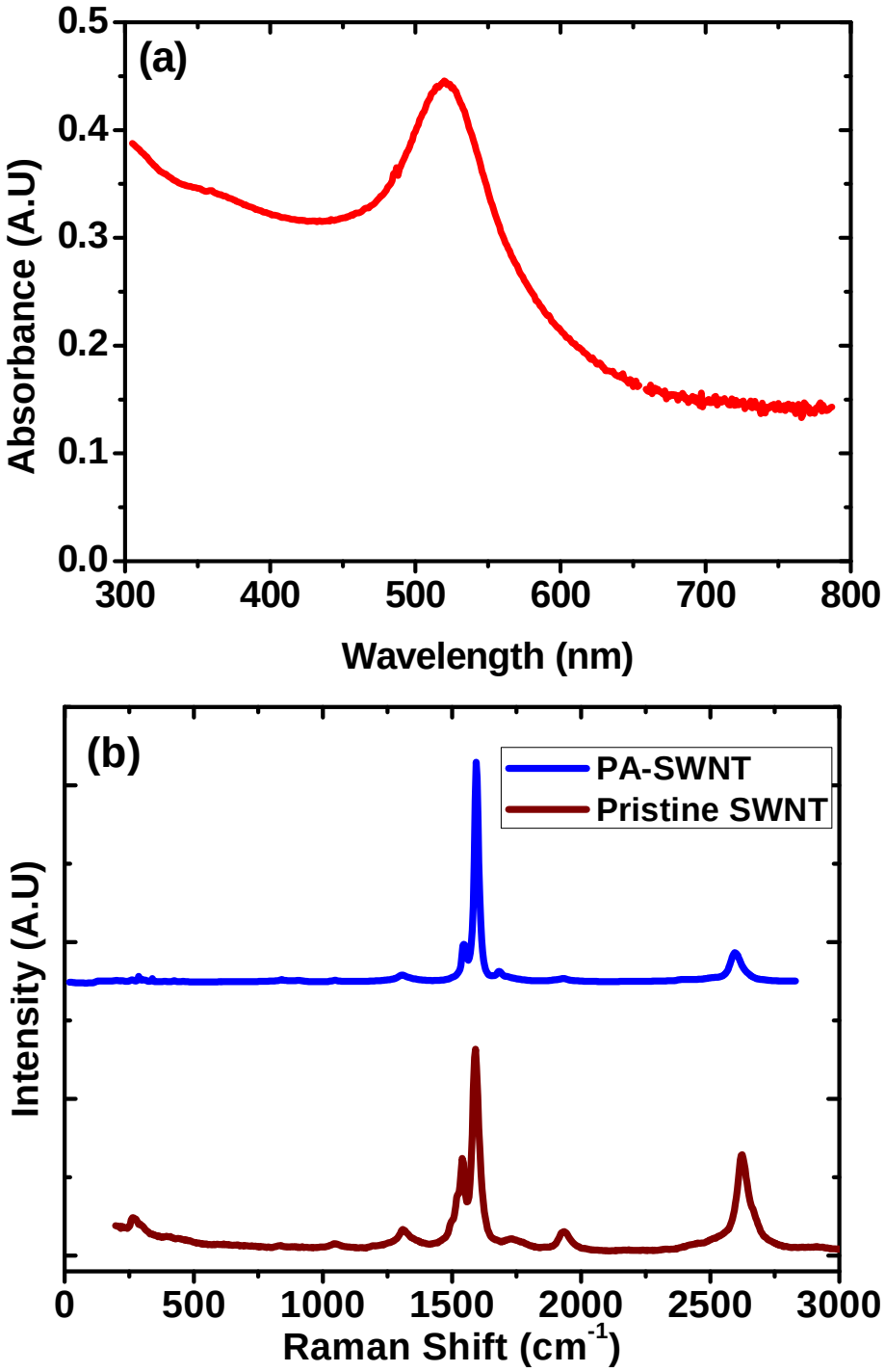

FIGURE C-1: Representative (a) UV-vis spectrum of AuNS and (b) Raman spectra of pristine and PA modified SWNTs.

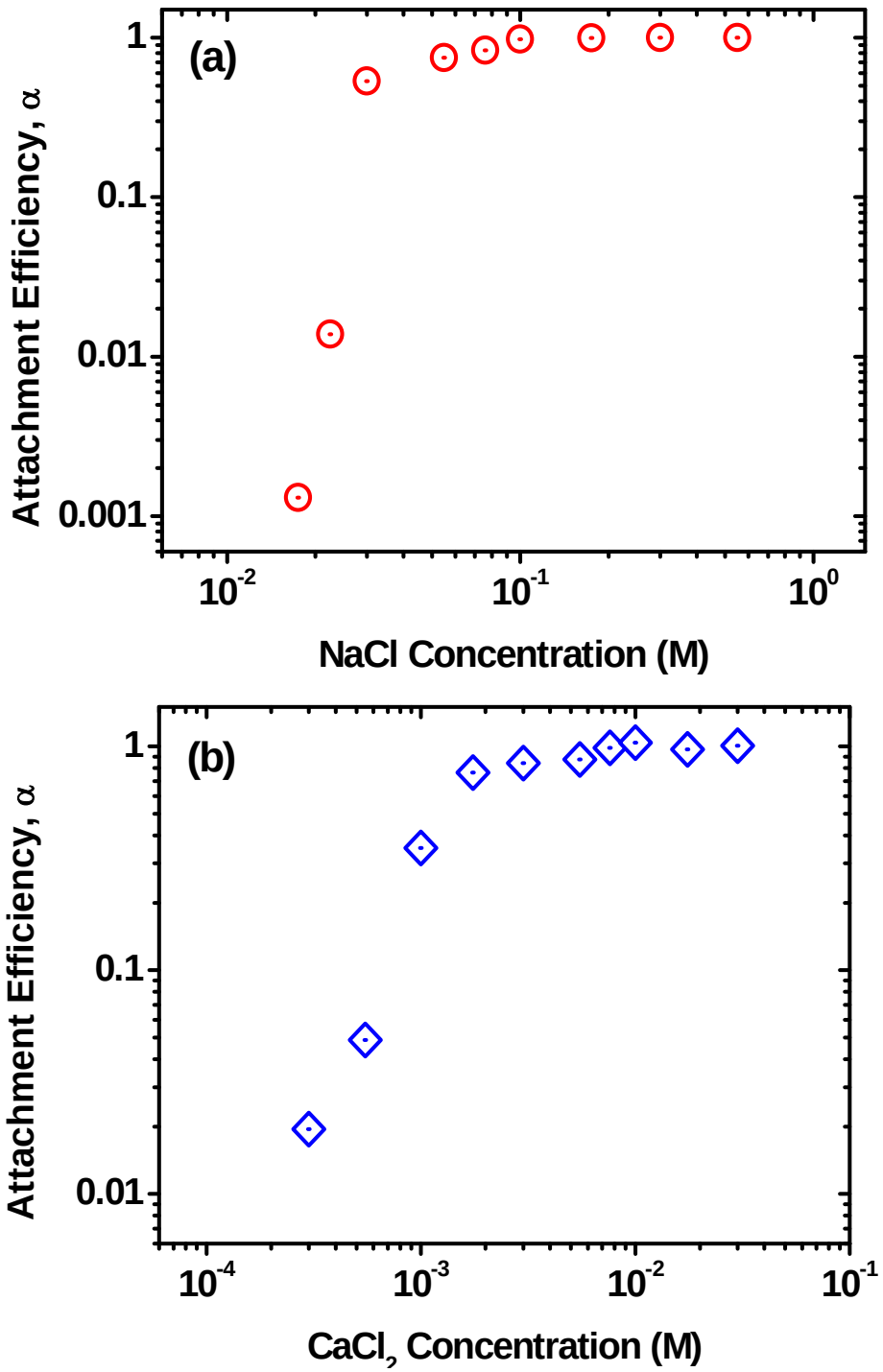

FIGURE C-2: Attachment efficiencies of AuNS as a function of (a) NaCl and (b) $CaCl_2$. Measurements were carried out at pH of ~6.5 and a temperature of 20 °C.

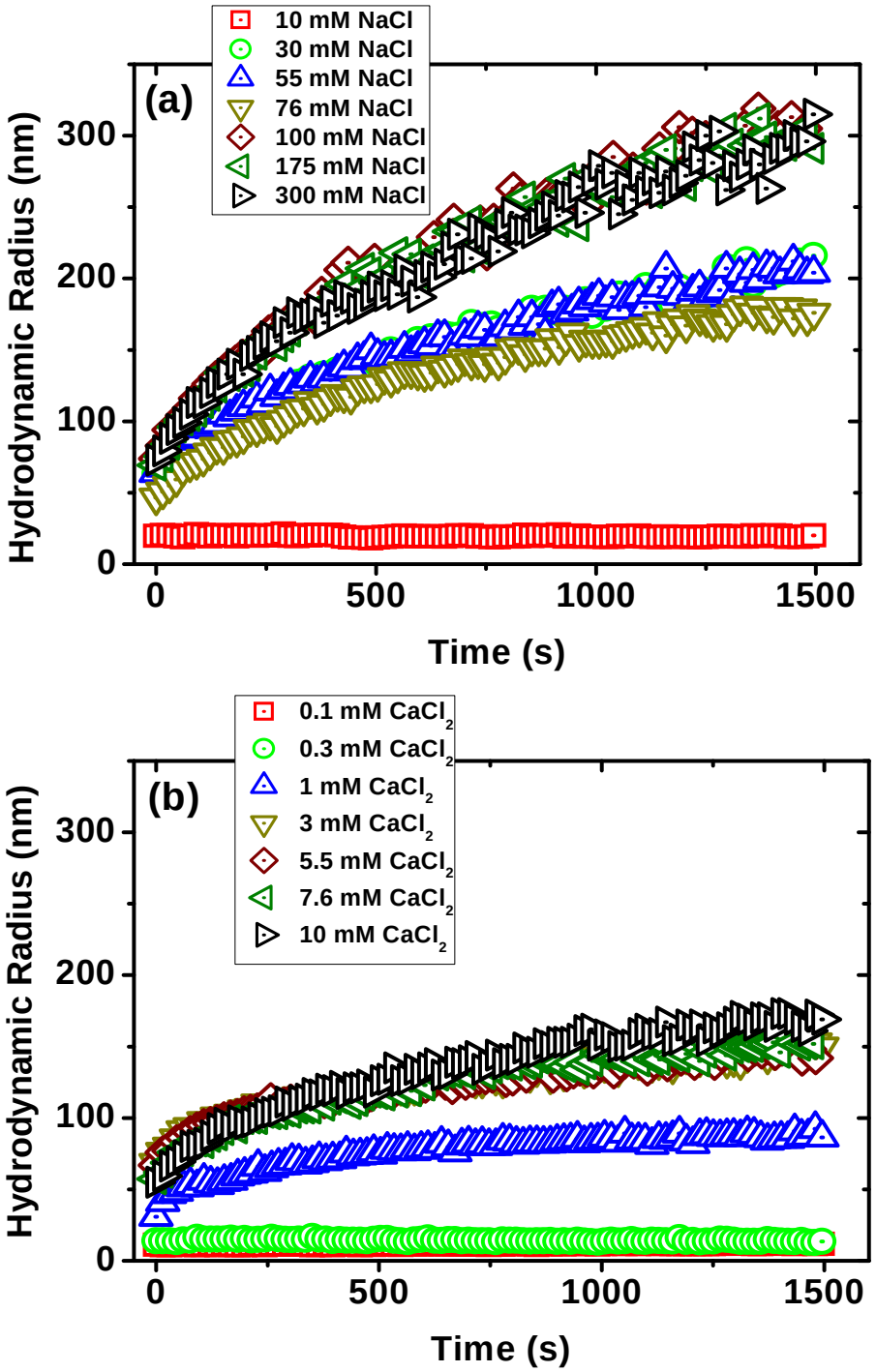

FIGURE C-3: Homo-aggregation profiles of AuNS in presence of (a) NaCl and (b) $CaCl_2$. Measurements were carried out at a temperature of 20°C.

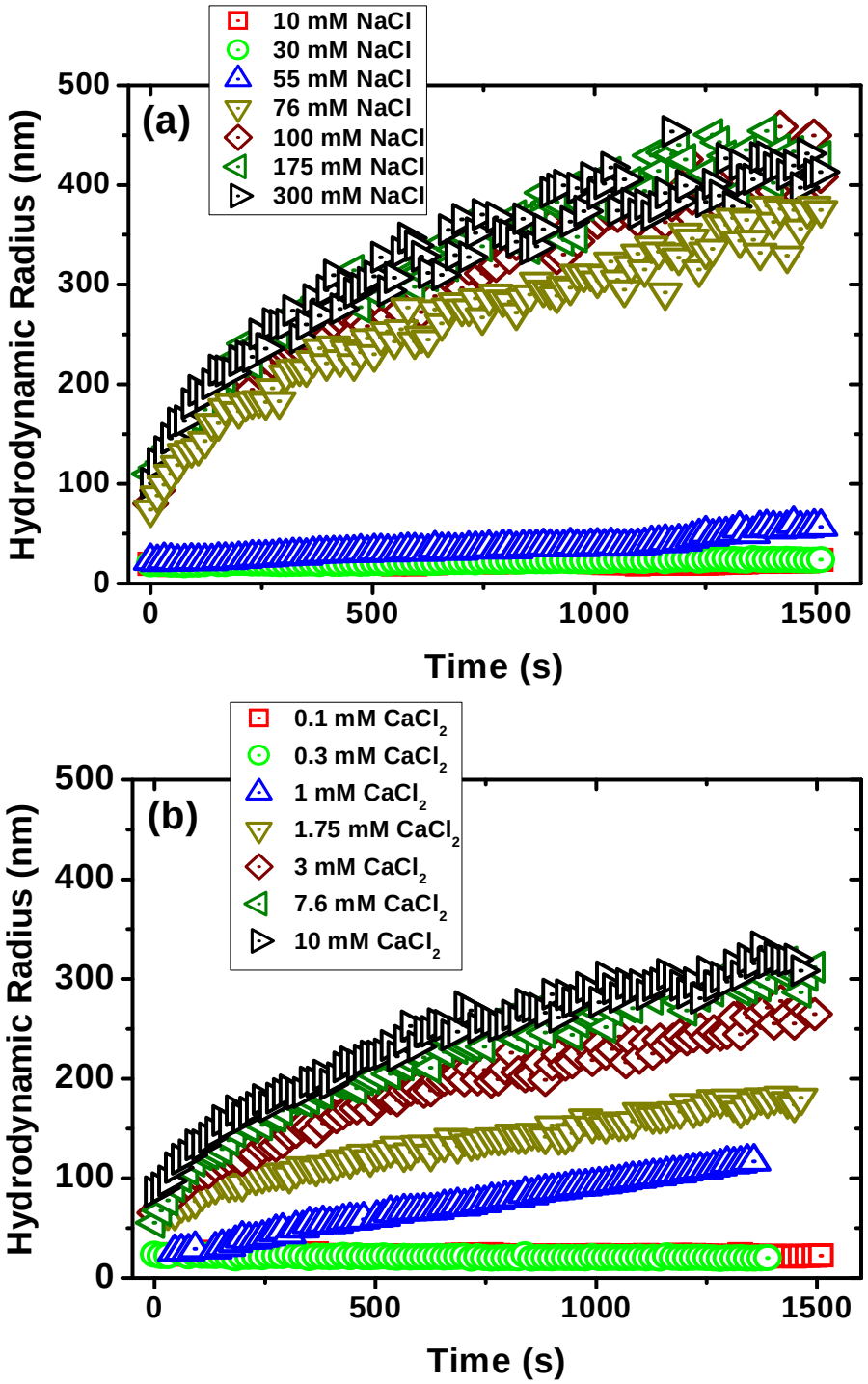

FIGURE C-4: Hetero-aggregation profiles of AuNS in presence of (a) NaCl and (b) $CaCl_2$. Measurements were carried out at a temperature of 20°C.

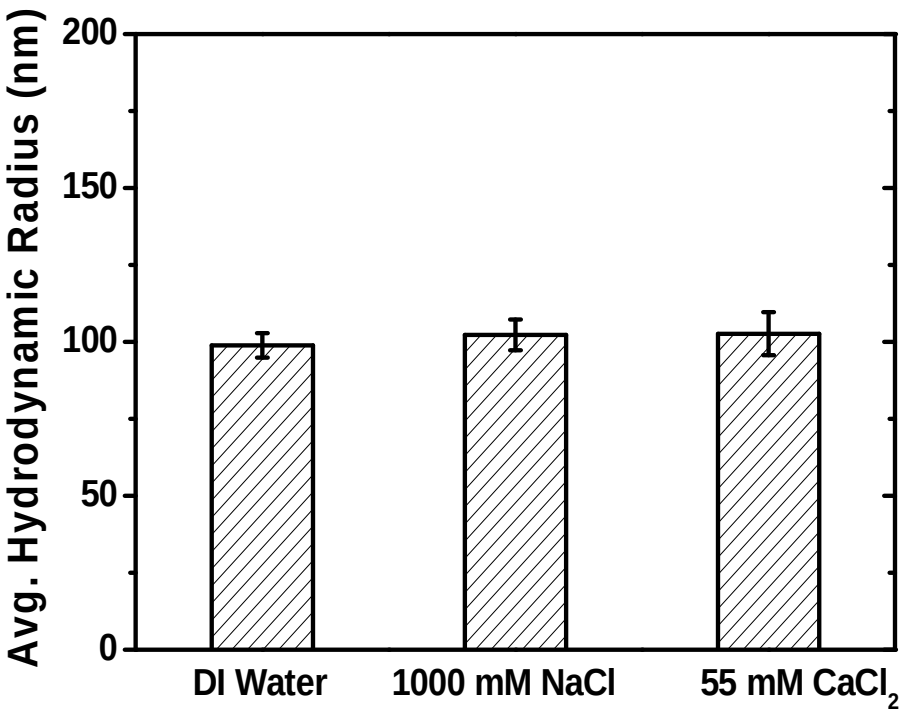

FIGURE C-5: Average hydrodynamic radii of PA-SWNTs in DI water and with high NaCl and $CaCl_2$ concentrations.

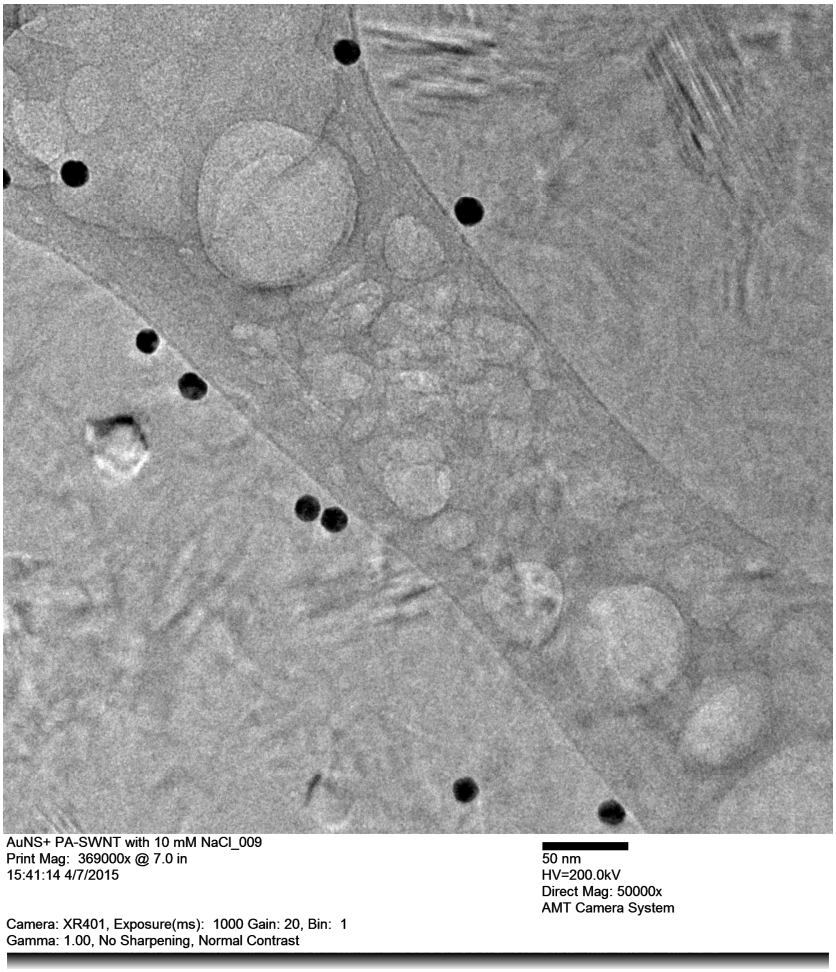

FIGURE C-6: Cryo-TEM images of AuNS and PA-SWNT heterodispersion under 10 mM NaCl.

Imaging Method: Cryo-TEM imaging of the vitrified sample of hetero-dispersion was performed utilizing a Jeol Jem 2100-TEM (Peabody, MA) in a specially cooled stage (Gatan Inc, Pleasanton, CA). The vitrification of the sample was accomplished with the help of a vitrobot (FEI, Hillsboro, OR) at a controlled temperature (25° C) and humidity (100%) under desired solution chemistry. A Quantifoil grids carbon on copper mesh (Electron Microscopy Center, Hartfield, CA) was plunged into the dispersion and blotted to have a thin TEM specimen. Resulting specimen was vitrified first using liquid ethane and then with the help of liquid nitrogen.

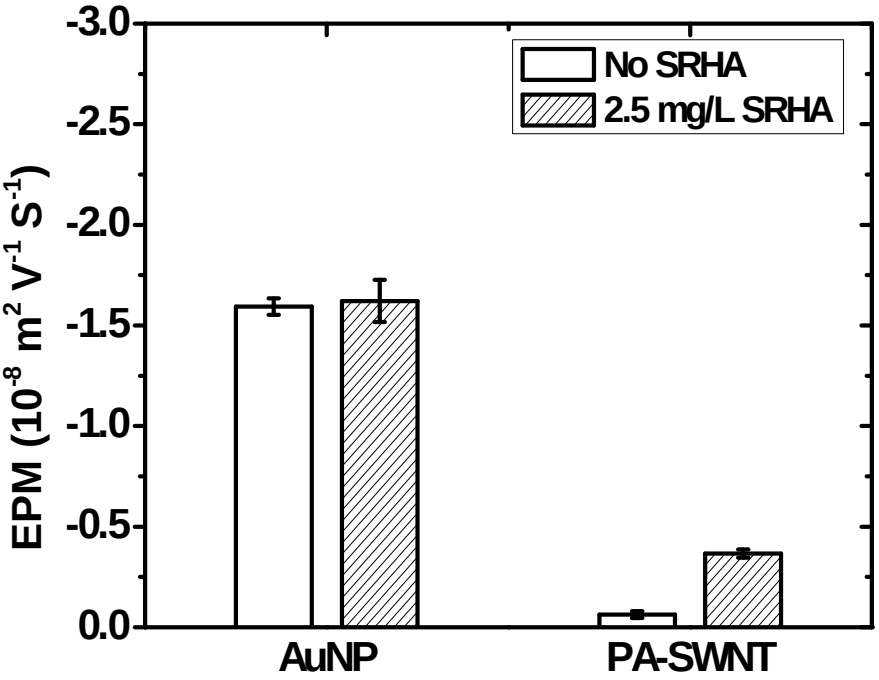

FIGURE C-7: Electrophoretic mobilities (EPM) of AuNS and PA-SWNTs under 7 mM NaCl and 1 mM $CaCl_2$ electrolyte mixture with and without the presence of Suwannee River humic acid (SRHA). Measurements were carried out at a pH of ~6.5 and a temperature of 20 °C.

Appendix D: Supplemental Information for Chapter 5

Gold Nanoparticles' Transport Through Saturated Porous Media in Presence of Single-walled Carbon Nanotubes

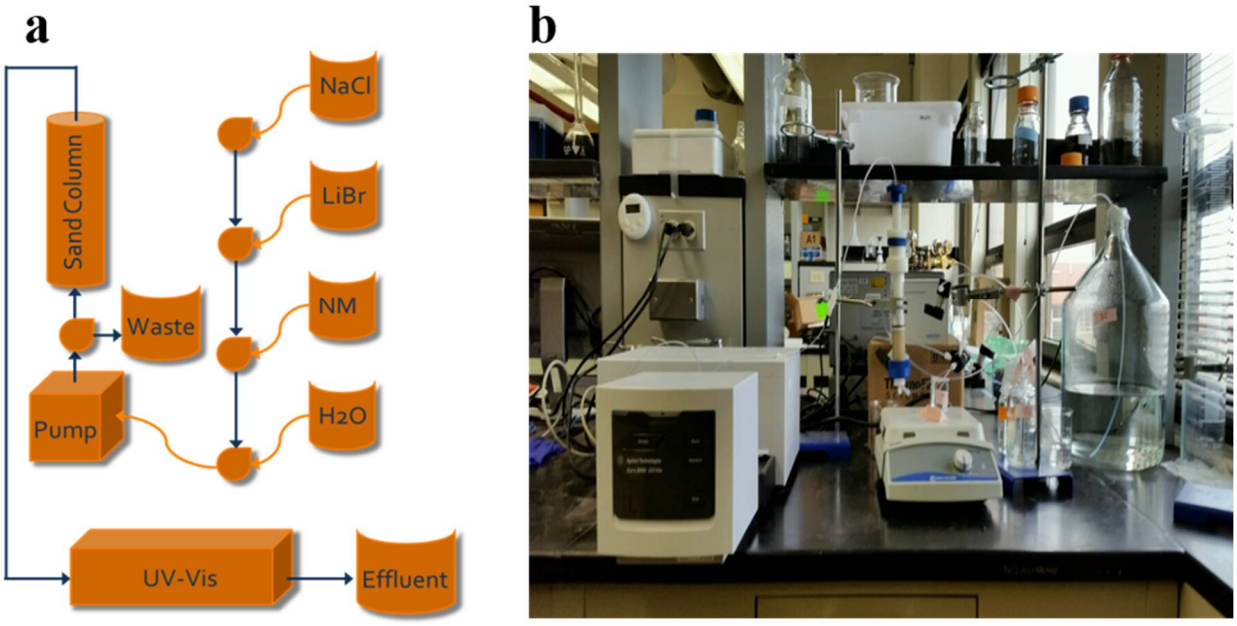

FIGURE D-1: Setup of the column experiments a) Schematic b) Picture

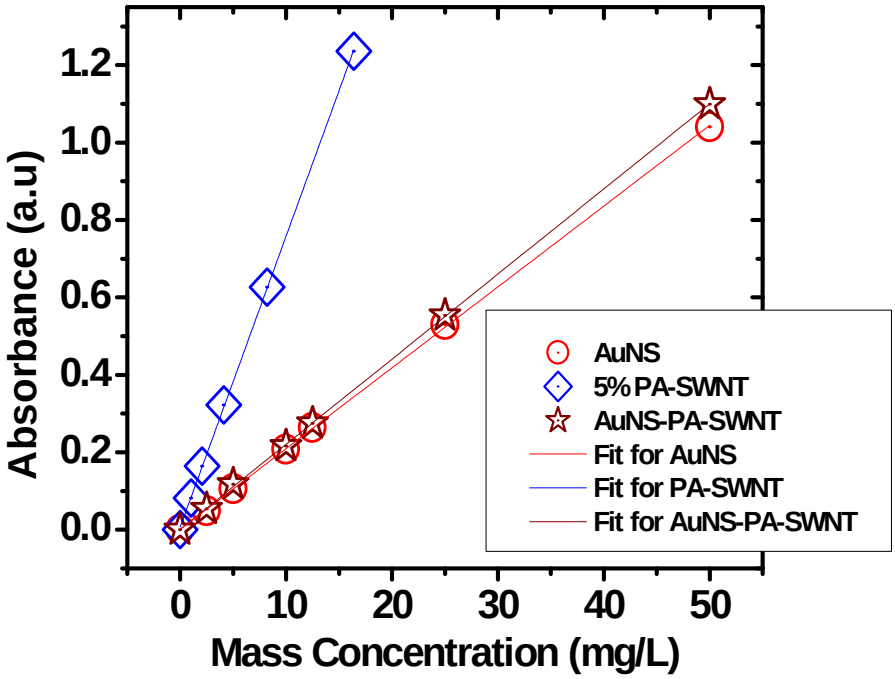

FIGURE D-2: Calibration curves obtained for the nanoparticles using linear regression

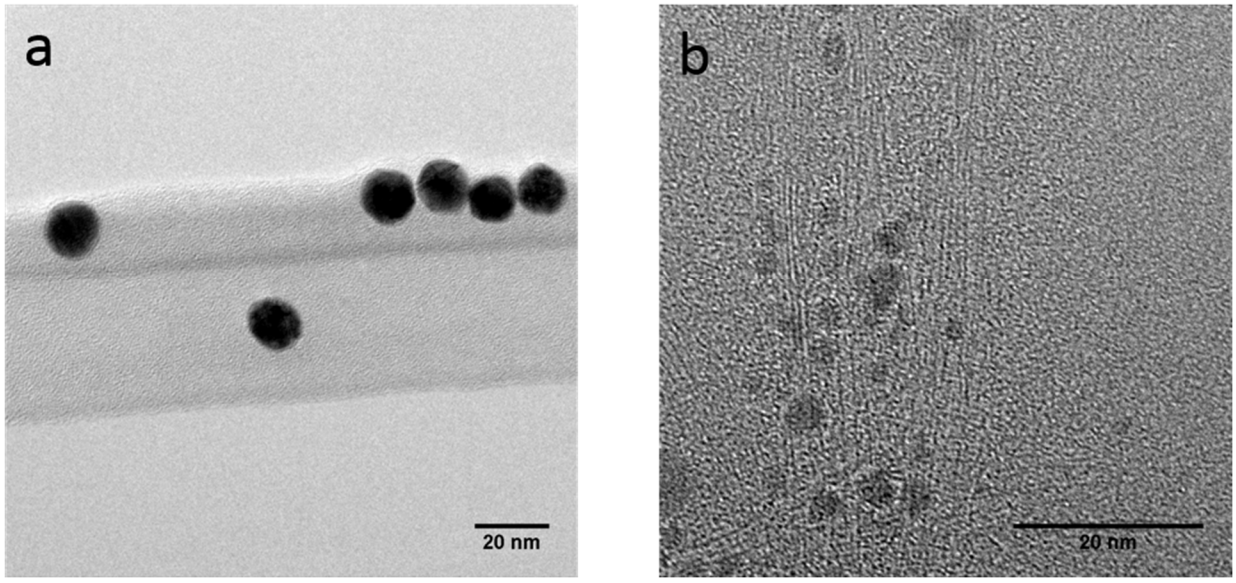

FIGURE D-3: Transmission electron microscopy images of a) AuNS b) PA-SWNT

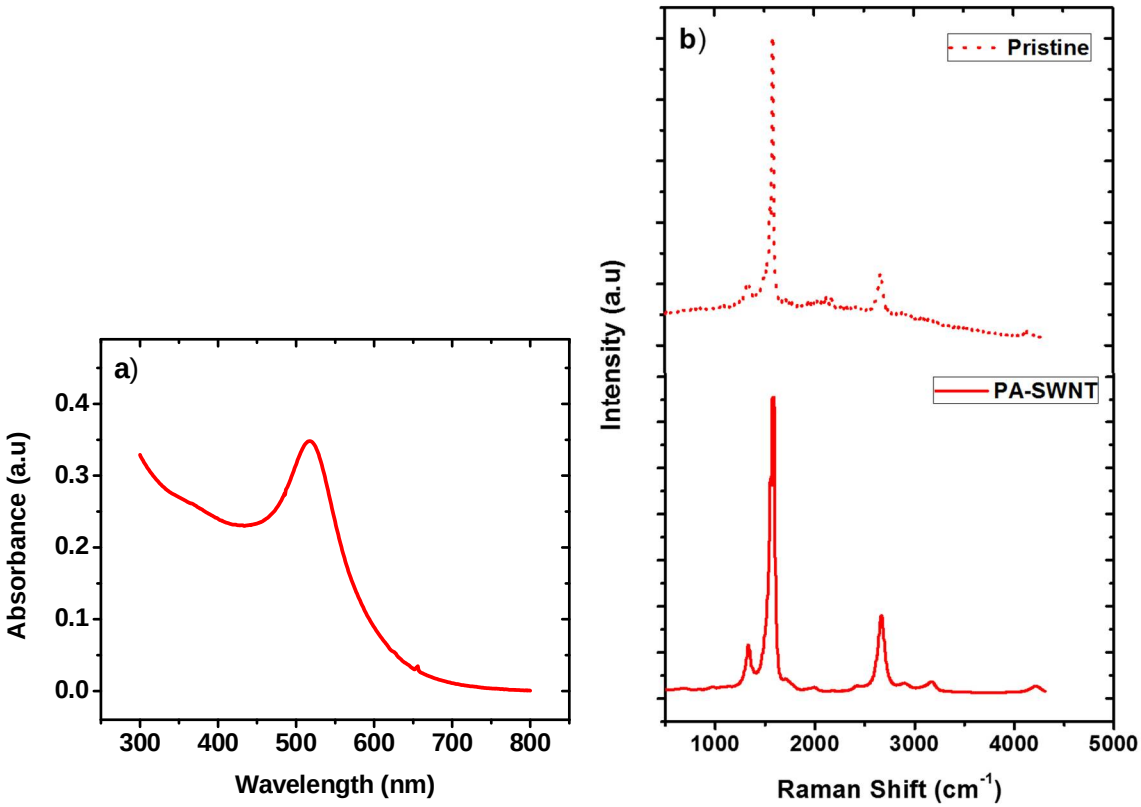

FIGURE D-4: a) UV-Vis spectra for AuNS b) Raman spectra for PA-SWNT

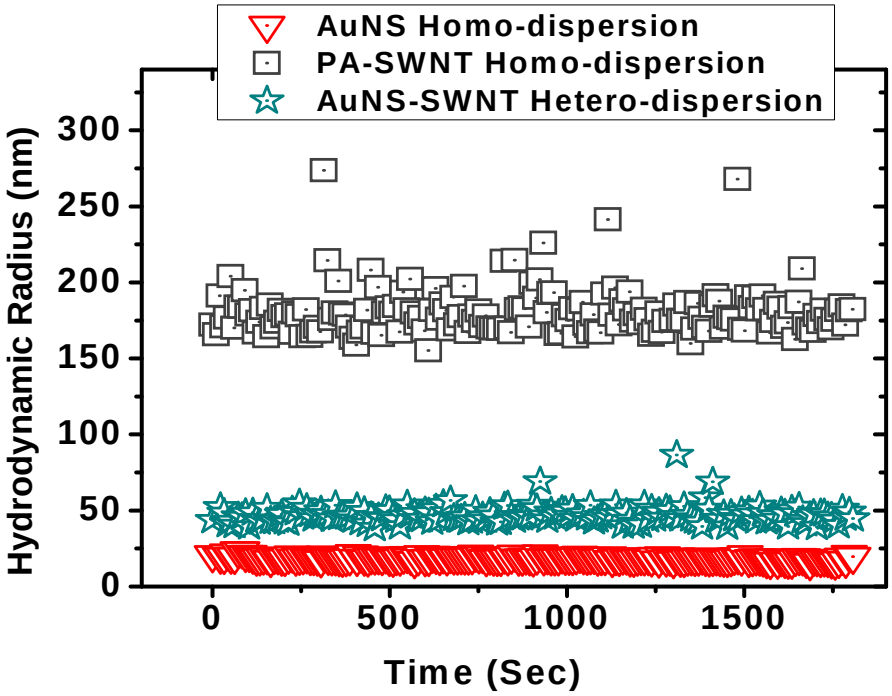

FIGURE D-5: Hydrodynamic radii of the nanoparticle suspensions in DI

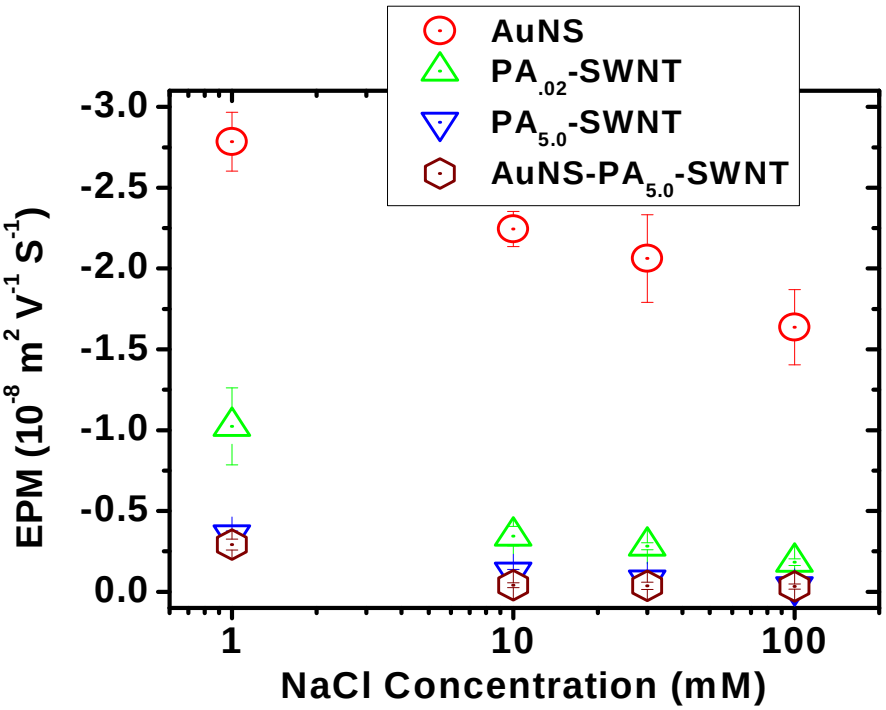

FIGURE D-6. Electrophoretic mobility of the nanoparticles under 1-100 mM of NaCl

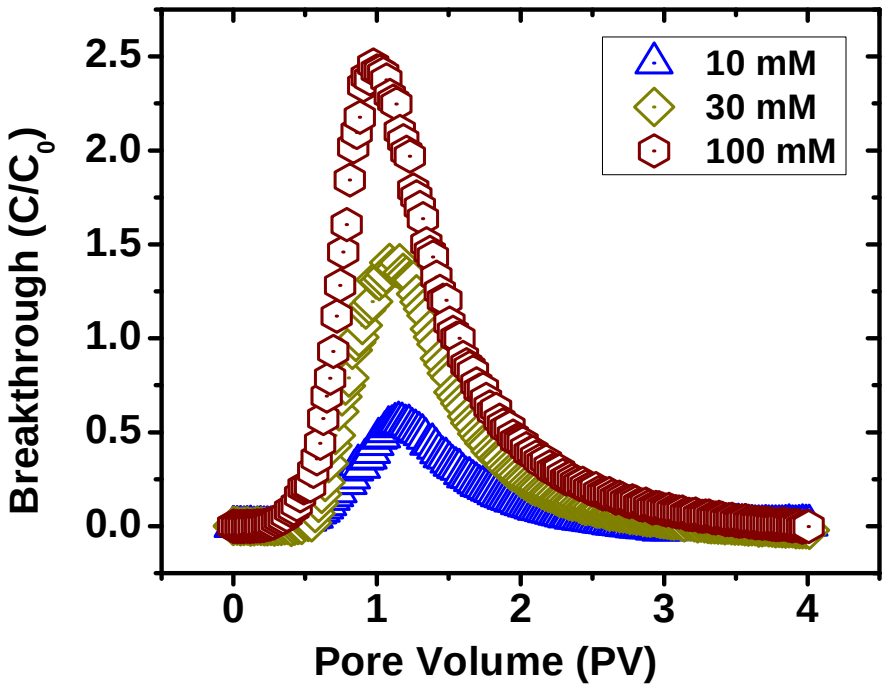

FIGURE D-7: Release of the AuNS homo-dispersion deposited under 10, 30, and 100 mM of NaCl

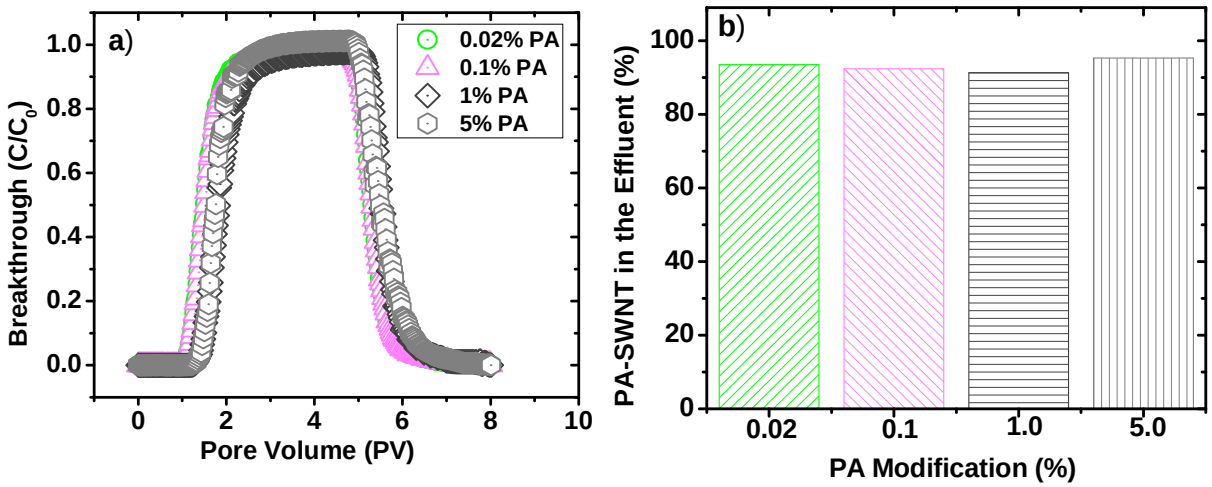

FIGURE D-8: Transport of PA-SWNT homo-dispersion at 1 mM NaCl a) Breakthrough b) Percent transport

Table D-1: Total Surface Area of Sand

Radius m	Volume per Particle m^3	Density kg/m^3	Mass per Particle kg	Number of Grains per Gram	Total Number of Grains	Surface Area/particle m^2	Total Surface Area in Column m^2
0.000325	1.43684E-10	2650	4E-07	2626	131315	1.3267E-06	0.17420901

Table D-2: Total Exposed Surface Area of Sand for Deposition

Porosity, n	Grain Diameter, d_p m	Specific Surface Area, $A_s = \frac{6*(1-n)}{d_p}$ (m^2/m^3)	Volume of Sand in the Column m^3	Total Surface Area Available for Deposition m^2
0.38	0.00065	5723.076923	2.94375E-05	0.168473077

Table D-3: Surface Area of Hipco SWNT

Material	Concentration mg/L	Volume Injected mL	Mass gm	Average Surface Area m^2/gm	Total Surface Area in column m^2
SWNT	2.5	44	0.000005	900	0.099

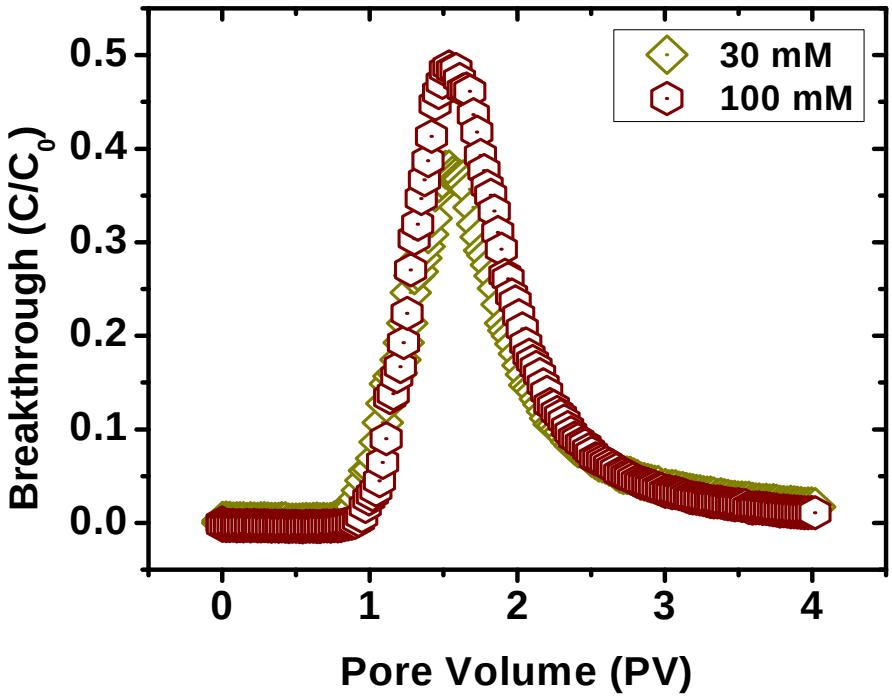

FIGURE D-9: Release of the AuNS deposited under 30 and 100 mM of NaCl

Table D-4: Computation of Travel Distances

Suspension	Kd (1/s)	U/f (m/s)	Estimated Travel Length (m)
AuNS Only	0.0010586	9E-05	0.581013
Co-transport	6.058E-05	9E-05	10.15299
AuNS Only through SWNT Coated Sand	0.0031463	9E-05	0.195478

Assumed,

Solution Chemistry = 100 mM NaCl

Velocity, U = 3.38E-05 ms^{-1}

Column Length, L= 0.06 m

Porosity, f = 0.38

$(C/C_0) = 0.01$

Appendix E

Scholarly Contributions

E-1: Peer Reviewed Journal Articles **(**first or second author: 7**)**

(1) **Afrooz, A. R. M. N**.; Das, D.; Murphy, C.J.; Vikesland, P.; Saleh, N. B. Co-transport of gold nanoparticles through saturated porous media in presence of single-walled carbon nanotube (in preparation)

(2) **Afrooz, A. R. M. N.**; Hussain, S. M.; Saleh, N. B. Aggregate size and structure determination of nanomaterials in physiological media: Importance of dynamic evolution. *Journal of Nanoparticle Research* 2014, 16(12), 1-7.

(3) **Afrooz, A. R. M. N.**; Sivalapalan, S. T.; Murphy, C. J.; Hussain, S. M.; Schlager, J. J.; Saleh, N. B. Spheres vs. rods: The shape of gold nanoparticles influences aggregation and deposition behavior. *Chemosphere* 2013, 91, 93-98.

(4) **Afrooz, A. R. M. N.**; Khan, I. A.; Hussain, S. M.; Saleh, N. B. Mechanistic heteroaggregation of gold nanoparticles in a wide range of solution chemistry. *Environmental Science & Technology* 2013, 47, 1853-1860.

(5) Saleh, N. B.; **Afrooz, A. R. M. N.;** Aich, N.; Bisesi J.; Tuttle, J. P.; Sabo-Attwood, T. Emergent properties and toxicological considerations for nanohybrid materials. *Journal of Nanomaterials* 2014, *4*, 372-407.

(6) Khan, I. A.; **Afrooz, A. R. M. N.**; Flora, J. R. V.; Schierz, P. A.; Ferguson, P. L.; Sabo-Attwood, T.; Saleh, N. B. Chirality affects aggregation kinetics of single-walled carbon nanotubes. *Environmental Science & Technology* 2013, 47, 1844-1852.

(7) Chambers, B. A.; **Afrooz, A. R. M. N.**; Bae, S.; Aich, N.; Katz, L.; Saleh, N. B.; Kirisits, M. J. Effects of chloride and ionic strength on physical morphology, dissolution, and bacterial toxicity of silver nanoparticles. *Environmental Science & Technology* 2013, 48, 761-769.

E-2: Peer Reviewed Journal Articles **(**co-author: 10**)**

(1) Khan, I. A.; Flora, J. R. V.; **Afrooz, A. R. M. N.**; Aich, N.; Schierz, P. A.; Ferguson, P. L.; Sabo-Attwood, T.; Saleh, N. B. Change in chirality of semiconducting single-walled carbon nanotubes can overcome anionic surfactant stabilization: A systematic study of aggregation kinetics. *Environmental Chemistry* 2014 (in press)

(2) Sanpui, P.; Zheng , X.; Loeb, J.; Bisesi , J.; Khan, I.; **Afrooz , A. R. M. N.;** Liu , K.; Badireddy, A.; Wiesner, M.; Ferguson, L.; Saleh, N. B.; Lednicky, J.; Sabo-Attwood, T. Single-walled carbon nanotubes increase pandemic influenza A H1N1 virus infectivity of lung epithelial cells. *Particle and Fibre Toxicology* 2014, 11:66.

(3) Saleh, N. B.; Caicedo, J. M.; Johnson, A.; **Afrooz, A. R. M. N.**; Khan, I. A. Nano in a global context: modular course design with integrated ethics improves core knowledge in nanotechnology. *Journal of Nano Education* 2014, 6(2), 124-131.

(4) Bisesi, J. H.; Merten, J.; Liu, K.; Parks, A. N.; **Afrooz, A. R. M. N.;** Glenn, J. B.; Klaine, S. J.; Kane, A.; Saleh, N. B.; Ferguson, L.; Sabo-Attwood, T. Tracking and quantification of single-walled carbon nanotubes in fish using near infrared fluorescence. *Environmental Science & Technology* 2014, 48 (3), 1973-1983.

(5) Schrand, A. M.; Lin, J. B.; Garrett, C. M.; Brownheim, S. V.; Hussain, S. M.; Cubadda, F.; **Afrooz, A. R. M. N.**; Saleh, N. B., Nanoparticle dynamics in the presence and absence of a cellular uptake altering chemical. *Il Nuovo Cimento C* 2013, 36, 117-129.

(6) Khan, I. A.; Aich, N.; **Afrooz, A. R. M. N.**; Flora, J. R. V.; Schierz, P. A.; Ferguson, P. L.; Sabo-Attwood, T.; Saleh, N. B. Fractal structures of single-walled carbon nanotubes in biologically relevant conditions: Role of chirality vs. media conditions. *Chemosphere* 2013, 93, 1997-2003.

(7) Schaeublin, N. M.; Braydich-Stolle, L. K.; Maurer, E. I.; Park, K.; MacCuspie, R. I.; **Afrooz, A. R. M. N.**; Vaia, R. A.; Saleh, N. B.; Hussain, S. M. Does shape matter? Bioeffects of gold nanomaterials in a human skin cell model. *Langmuir* 2012, 28, 3248-3258.

(8) Mukhopadhyay, A.; Grabinski, C.; **Afrooz, A. R. M. N.**; Saleh, N.; Hussain, S. Effect of gold nanosphere surface chemistry on protein adsorption and cell uptake in vitro. *Appl Biochem Biotechnol* 2012, 167, 327-337.

(9) Philbrook, N. A.; Winn, L. M.; **Afrooz, A. R. M. N.**; Saleh, N. B.; Walker, V. K. The effect of TiO_2 and Ag nanoparticles on reproduction and development of *Drosophila melanogaster* and CD-1 mice. *Toxicology and Applied Pharmacology* 2011, 257, 429-436.

(10) Philbrook, N. A.; Walker, V. K.; **Afrooz, A. R. M. N.**; Saleh, N. B.; Winn, L. M. Investigating the effects of functionalized carbon nanotubes on reproduction and development in *Drosophila melanogaster* and CD-1 mice. *Reproductive Toxicology* 2011, 32, 442-448.

E-3: Book Chapters (co-author:2)

(1) Saleh, N. B.; **Afrooz, A. R. M. N**.; Aich, N; Plazas-Tuttle, J. "Aggregation kinetics and fractal dimensions of nanomaterials in environmental systems" in *Engineered Nanoparticles and the Environment: Biophysico-chemical Processes and Biotoxicity*, 2015, IUPAC. (In Press)

(2) Saleh, N. B.; **Afrooz, A. R. M. N**.; Plazas-Tuttle, J.; Khan, I. A.; Hussain, S. M., "Aggregation rate and aggregate structure determination of nanomaterials under biological exposure conditions" in *Advances in Characterization Techniques for Nanotoxicology*, Eds Hussain, S.M., 2015, Willey-Blackwell. (In Press)

E-4: Conference Proceedings (first Author: 3)

(1) **Afrooz, A.R.M.N.**, Khan, I., Hussain, SM., Saleh, N. B. "Mechanistic hetero−aggregation of gold nanoparticles in presence of nonionic polymer modified single−walled carbon nanotubes". ACS National Meeting, Apr 7-11, 2013, New Orleans, LA.

(2) **Afrooz, A.R.M.N.**, Saleh, N. B. "Aggregation kinetics of gold nanorods in aquatic systems: Role of aspect ratio". ACS National Meeting, Mar 27-31, 2011, Anaheim, CA.

(3) **Afrooz, A.R.M.N.**, Zaib, Q., Decho, A. W., Saleh, N. B. "Role of nanoparticle geometry on Nano-bio interaction: A quest to separate physics from chemistry". ACS National Meeting, Aug 22-26, 2010, Boston, MA.

E-5: Conference Proceedings (co-author: 6)

(1) Saleh, N. B., Aich, N., Chambers, B.A., **Afrooz, A.R.M.N.,** Kirisits, M.J., "Influence of tin doping on environmental interactions of nano indium oxides in aqueous systems". 247th ACS National Meeting, Mar 16-20, 2014, Dallas, TX.

(2) Saleh, N. B., Hussain, SM., **Afrooz, A.R.M.N.** "Dynamic aggregation and fractal structure determination of gold nanoparticles in biological media conditions". ACS National Meeting, Apr 7-11, 2013, New Orleans, LA.

(3) Saleh, N. B., **Afrooz, A.R.M.N.**, Khan, I., Hussain, SM. "Mechanistic hetero-aggregation of gold nanoparticles in a wide range of solution chemistry". Sustainable Nanotechnology Organization Conference, Nov 4, 2012, Arlington, VA.

(4) Sabo-Attwood T, Bisesi J. H., Saleh N. B., **Afrooz, A.R.M.N**, Parks AN, Ferguson PL, Merten, J. "Dynamics of SWNT distribution and aggregate structure during aquatic exposures". Sustainable Nanotechnology Organization Conference, Nov 4, 2012, Arlington, VA.

(5) Shah, V., Haiduk, B., Collins, D., **Afrooz, A.R.M.N.**, Aich, N., Rispoli, F., Saleh, N. B. "Aggregation and antimicrobial activity of copper nanoparticle suspension". ACS National Meeting, Mar 25-29, 2012, San Diego, CA.

(6) Aich, N., **Afrooz, A.R.M.N.**, Khan, I, Saleh, N. B. "Deposition behavior of anisotropic nanomaterials". ACS National Meeting, Aug 22-26, 2010, Boston, MA.

REFERENCES

Chapter 1

1. Research, B. *Nanotechnology: A Realistic Market Assessment*; 2014.
2. CPI Nanoparticle consumer products inventory http://www.nanotechproject.org/cpi/browse/categories/ (Feb 26),
3. Pérez, J.; Bax, L.; Escolano, C. *Roadmap Report on Nanoparticles*; Willems & van den Wildenberg sl: Barcelona, Spain, 2005; pp 26-28.
4. Salem, A. K.; Searson, P. C.; Leong, K. W., Multifunctional nanorods for gene delivery. *Nat Mater* **2003,** *2*, (10), 668-671.
5. Murphy, C. J.; Thompson, L. B.; Alkilany, A. M.; Sisco, P. N.; Boulos, S. P.; Sivapalan, S. T.; Yang, J. A.; Chernak, D. J.; Huang, J., The Many Faces of Gold Nanorods. *The Journal of Physical Chemistry Letters* **2010**, 2867-2875.
6. Richter, G.; Hillerich, K.; Gianola, D. S.; MoÌˆnig, R.; Kraft, O.; Volkert, C. A., Ultrahigh Strength Single Crystalline Nanowhiskers Grown by Physical Vapor Deposition. *Nano Letters* **2009,** *9*, (8), 3048-3052.
7. Yang, P.; Yan, R.; Fardy, M., Semiconductor Nanowire: What's Next? *Nano Letters* **2010,** *10*, (5), 1529-1536.
8. Yuzvinsky, T. D.; Mickelson, W.; Aloni, S.; Begtrup, G. E.; Kis, A.; Zettl, A., Shrinking a Carbon Nanotube. *Nano Letters* **2006,** *6*, (12), 2718-2722.
9. Khan, I. A.; Ferguson, P. L.; Sabo-Attwood, T.; Saleh, N. B. In *Systematic change in chirality affects aggregation kinetics of single-walled carbon nanotubes* 240th ACS National Meeting, Boston, MA, 2010; Boston, MA, 2010.
10. Murphy, C. J.; San, T. K.; Gole, A. M.; Orendorff, C. J.; Gao, J. X.; Gou, L.; Hunyadi, S. E.; Li, T., Anisotropic metal nanoparticles: Synthesis, assembly, and optical applications. *J. Phys. Chem. B* **2005,** *109*, (29), 13857-13870.
11. Pérez-Juste, J.; Pastoriza-Santos, I.; Liz-Marzán, L. M.; Mulvaney, P., Gold nanorods: Synthesis, characterization and applications. *Coordination Chemistry Reviews* **2005,** *249*, (17-18), 1870-1901.
12. Yang, B.; Han, Z. H., Temperature-dependent thermal conductivity of nanorod-based nanofluids. *Appl. Phys. Lett.* **2006,** *89*, (8), 3.
13. Kwak, C. H.; Kim, B. H.; Park, C. I.; Seo, S. Y.; Kim, S. H.; Han, S. W., Structural and electrical properties of ZnO nanorods and Ti buffer layers. *Appl. Phys. Lett.* **2010,** *96*, (5), 3.
14. Wan, Q.; Lin, C. L.; Yu, X. B.; Wang, T. H., Room-temperature hydrogen storage characteristics of ZnO nanowires. *Appl. Phys. Lett.* **2004,** *84*, (1), 124-126.
15. Huynh, W. U.; Dittmer, J. J.; Alivisatos, A. P., Hybrid nanorod-polymer solar cells. *Science* **2002,** *295*, (5564), 2425-2427.
16. Chang, W.-S.; Ha, J. W.; Slaughter, L. S.; Link, S., Plasmonic nanorod absorbers as orientation sensors. *Proceedings of the National Academy of Sciences* **2010,** *107*, (7), 2781-2786.
17. Iijima, S.; Ichihashi, T., Single-shell carbon nanotubes of 1-nm diameter. *Nature* **1993,** *363*, (6430), 603-605.
18. Mani, R. C.; Li, X.; Sunkara, M. K.; Rajan, K., Carbon Nanopipettes. *Nano Letters* **2003,** *3*, (5), 671-673.
19. *Consumer product inventories*; Woodrow Wilson International Center for Scholars: Washington, DC, 2010.

20. De Volder, M. F.; Tawfick, S. H.; Baughman, R. H.; Hart, A. J., Carbon nanotubes: present and future commercial applications. *Science* **2013,** *339*, (6119), 535-539.
21. Beigbeder, A.; Degee, P.; Conlan, S. L.; Mutton, R. J.; Clare, A. S.; Pettitt, M. E.; Callow, M. E.; Callow, J. A.; Dubois, P., Preparation and characterisation of silicone-based coatings filled with carbon nanotubes and natural sepiolite and their application as marine fouling-release coatings. *Biofouling* **2008,** *24*, (4), 291-302.
22. Wu, Z.; Chen, Z.; Du, X.; Logan, J. M.; Sippel, J.; Nikolou, M.; Kamaras, K.; Reynolds, J. R.; Tanner, D. B.; Hebard, A. F., Transparent, conductive carbon nanotube films. *Science* **2004,** *305*, (5688), 1273-1276.
23. Ionescu, A. M.; Riel, H., Tunnel field-effect transistors as energy-efficient electronic switches. *Nature* **2011,** *479*, (7373), 329-337.
24. Dai, L.; Chang, D. W.; Baek, J. B.; Lu, W., Carbon nanomaterials for advanced energy conversion and storage. *Small* **2012,** *8*, (8), 1130-1166.
25. De La Zerda, A.; Zavaleta, C.; Keren, S.; Vaithilingam, S.; Bodapati, S.; Liu, Z.; Levi, J.; Smith, B. R.; Ma, T.-J.; Oralkan, O., Carbon nanotubes as photoacoustic molecular imaging agents in living mice. *Nature nanotechnology* **2008,** *3*, (9), 557-562.
26. Xiang, J.; Lu, W.; Hu, Y.; Wu, Y.; Yan, H.; Lieber, C. M., Ge/Si nanowire heterostructures as high-performance field-effect transistors. *Nature* **2006,** *441*, (7092), 489-493.
27. Tian, B.; Zheng, X.; Kempa, T. J.; Fang, Y.; Yu, N.; Yu, G.; Huang, J.; Lieber, C. M., Coaxial silicon nanowires as solar cells and nanoelectronic power sources. *Nature* **2007,** *449*, (7164), 885-889.
28. Akhavan, O.; Ghaderi, E., Enhancement of antibacterial properties of Ag nanorods by electric field. *Sci. Technol. Adv. Mater.* **2009,** *10*, (1).
29. Dev, A.; Kar, S.; Chakrabarti, S.; Chaudhuri, S., Optical and field emission properties of ZnO nanorod arrays synthesized on zinc foils by the solvothermal route. *Nanotechnology* **2006,** *17*, (5), 1533-1540.
30. Yoon, S. H.; Yang, H.; Kim, Y. S., Synthesis of ZnO nanorods and their application to hybrid plasma display panels for reduction of discharge voltages. *J. Ceram. Process. Res.* **2007,** *8*, (4), 261-265.
31. Jiang, X. X.; Chen, F.; Xu, H.; Yang, L. G.; Qiu, W. M.; Shi, M. M.; Wang, M.; Chen, H. Z., Template-free synthesis of vertically aligned CdS nanorods and its application in hybrid solar cells. *Sol. Energy Mater. Sol. Cells* **2010,** *94*, (2), 338-344.
32. Na, S. I.; Kim, S. S.; Hong, W. K.; Park, J. W.; Jo, J.; Nah, Y. C.; Lee, T.; Kim, D. Y., Fabrication of TiO2 nanotubes by using electrodeposited ZnO nanorod template and their application to hybrid solar cells. *Electrochim. Acta* **2008,** *53*, (5), 2560-2566.
33. Yin, Z. Y.; Wu, S. X.; Zhou, X. Z.; Huang, X.; Zhang, Q. C.; Boey, F.; Zhang, H., Electrochemical Deposition of ZnO Nanorods on Transparent Reduced Graphene Oxide Electrodes for Hybrid Solar Cells. *Small* **2010,** *6*, (2), 307-312.
34. Fang, F.; Futter, J.; Markwitz, A.; Kennedy, J., UV and humidity sensing properties of ZnO nanorods prepared by the arc discharge method. *Nanotechnology* **2009,** *20*, (24).
35. Fulati, A.; Ali, S. M. U.; Riaz, M.; Amin, G.; Nur, O.; Willander, M., Miniaturized pH Sensors Based on Zinc Oxide Nanotubes/Nanorods. *Sensors* **2009,** *9*, (11), 8911-8923.
36. Ogata, K.; Koike, K.; Sasa, S.; Inoue, M.; Yano, M., ZnO nanorod arrays on n-type Si(111) substrates for pH measurements. *J. Vac. Sci. Technol. B* **2009,** *27*, (3), 1684-1687.
37. Water, W.; Chen, S. E., Using ZnO nanorods to enhance sensitivity of liquid sensor. *Sens. Actuator B-Chem.* **2009,** *136*, (2), 371-375.

38. Adachi, M.; Jiu, J.; Isoda, S., Synthesis of morphology-controlled titania nanocrystals and application for dye-sensitized solar cell's. *Curr. Nanosci.* **2007,** *3*, (4), 285-295.
39. Bao, S. J.; Bao, Q. L.; Li, C. M.; Dong, Z. L., Novel porous anatase TiO2 nanorods and their high lithium electroactivity. *Electrochem. Commun.* **2007,** *9*, (5), 1233-1238.
40. Kislyuk, V. V.; Dimitriev, O. P., Nanorods and nanotubes for solar cells. *J. Nanosci. Nanotechnol.* **2008,** *8*, (1), 131-148.
41. Wei, Q. S.; Hirota, K.; Tajima, K.; Hashimoto, K., Design and synthesis of TiO2 nanorod assemblies and their application for photovoltaic devices. *Chem. Mat.* **2006,** *18*, (21), 5080-5087.
42. Yao, Q. H.; Liu, J. F.; Peng, Q.; Wang, X.; Li, Y. D., Nd-doped TiO2 nanorods: Preparation and application in dye-sensitized solar cells. *Chem.-Asian J.* **2006,** *1*, (5), 737-741.
43. Chanda, N.; Shukla, R.; Katti, K. V.; Kannan, R., Gastrin releasing protein receptor specific gold nanorods: Breast and prostate tumor avid nanovectors for molecular imaging. *Nano Lett.* **2009,** *9*, (5), 1798-1805.
44. Ding, H.; Yong, K. T.; Roy, I.; Pudavar, H. E.; Law, W. C.; Bergey, E. J.; Prasad, P. N., Gold nanorods coated with multilayer polyelectrolyte as contrast agents for multimodal imaging. *J. Phys. Chem. C* **2007,** *111*, (34), 12552-12557.
45. Durr, N. J.; Larson, T.; Smith, D. K.; Korgel, B. A.; Sokolov, K.; Ben-Yakar, A., Two-photon luminescence imaging of cancer cells using molecularly targeted gold nanorods. *Nano Lett.* **2007,** *7*, (4), 941-945.
46. Eghtedari, M.; Liopo, A. V.; Copland, J. A.; Oraevslty, A. A.; Motamedi, M., Engineering of Hetero-Functional Gold Nanorods for the in vivo Molecular Targeting of Breast Cancer Cells. *Nano Lett.* **2009,** *9*, (1), 287-291.
47. El-Sayed, I. H.; Huang, X. H.; El-Sayed, M. A., Surface plasmon resonance scattering and absorption of anti-EGFR antibody conjugated gold nanoparticles in cancer diagnostics: Applications in oral cancer. *Nano Lett.* **2005,** *5*, (5), 829-834.
48. Huff, T. B.; Tong, L.; Zhao, Y.; Hansen, M. N.; Cheng, J. X.; Wei, A., Hyperthermic effects of gold nanorods on tumor cells. *Nanomedicine* **2007,** *2*, (1), 125-132.
49. Kawano, T.; Niidome, Y.; Mori, T.; Katayama, Y.; Niidome, T., PNIPAM Gel-Coated Gold Nanorods, for Targeted Delivery Responding to a Near-Infrared Laser. *Bioconjugate Chem.* **2009,** *20*, (2), 209-212.
50. Mueller, N. C.; Nowack, B., Exposure modeling of engineered nanoparticles in the environment. *Environmental Science & Technology* **2008,** *42*, (12), 4447-4453.
51. Ibanez, J. G.; Hernandez-Esparza, M.; Doria-Serrano, C.; Fregoso-Infante, A.; Singh, M. M., *Environmental chemistry: fundamentals*. Springer Science & Business Media: 2010.
52. Saleh, N. B.; Afrooz, A. R. M. N.; Aich, N.; Plazas-Tuttle, J., Aggregation kinetics and fractal dimensions of nanomaterials in environmental systems. In *Engineered nanoparticles and the environment: Biophysico-chemical processes and biotoxicity*, 2015.
53. Lawler, D.; Benjamin, M., *Water Quality Engineering: Physical-Chemical Treatment Processes*. McGraw-Hill: 2003.
54. Hotze, E. M.; Phenrat, T.; Lowry, G. V., Nanoparticle aggregation: challenges to understanding transport and reactivity in the environment. *Journal of environmental quality* **2010,** *39*, (6), 1909-1924.
55. Borm, P.; Klaessig, F. C.; Landry, T. D.; Moudgil, B.; Pauluhn, J.; Thomas, K.; Trottier, R.; Wood, S., Research strategies for safety evaluation of nanomaterials, part V: role of dissolution in biological fate and effects of nanoscale particles. *Toxicological Sciences* **2006,** *90*, (1), 23-32.

56. Petosa, A. R.; Jaisi, D. P.; Quevedo, I. R.; Elimelech, M.; Tufenkji, N., Aggregation and deposition of engineered nanomaterials in aquatic environments: role of physico-chemical interactions. *Environmental science & technology* **2010,** *44*, (17), 6532-6549.
57. Lowry, G.; Casman, E., Nanomaterial transport, transformation, and fate in the environment. In *Nanomaterials: risks and benefits*, Springer: 2009; pp 125-137.
58. Chen, K. L.; Elimelech, M., Aggregation and deposition kinetics of fullerene (C-60) nanoparticles. *Langmuir* **2006,** *22*, (26), 10994-11001.
59. Chen, K. L.; Elimelech, M., Influence of humic acid on the aggregation kinetics of fullerene (C-60) nanoparticles in monovalent and divalent electrolyte solutions. *J. Colloid Interface Sci.* **2007,** *309*, (1), 126-134.
60. Chen, K. L.; Mylon, S. E.; Elimelech, M., Aggregation kinetics of alginate-coated hematite nanoparticles in monovalent and divalent electrolytes. *Environ. Sci. Technol.* **2006,** *40*, (5), 1516-1523.
61. Chen, K. L.; Smith, B. A.; Ball, W. P.; Fairbrother, D. H., Assessing the colloidal properties of engineered nanoparticles in water: case studies from fullerene C-60 nanoparticles and carbon nanotubes. *Environ. Chem.* **2009,** *7*, (1), 10-27.
62. Chen, Q.; Saltiel, C.; Manickavasagam, S.; Schadler, L. S.; Siegel, R. W.; Yang, H. C., Aggregation behavior of single-walled carbon nanotubes in dilute aqueous suspension. *J. Colloid Interface Sci.* **2004,** *280*, (1), 91-97.
63. Saleh, N.; Kim, H. J.; Phenrat, T.; Matyjaszewski, K.; Tilton, R. D.; Lowry, G. V., Ionic strength and composition affect the mobility of surface-modified Fe-0 nanoparticles in water-saturated sand columns. *Environ. Sci. Technol.* **2008,** *42*, (9), 3349-3355.
64. Saleh, N. B.; Pfefferle, L. D.; Elimelech, M., Aggregation kinetics of multiwalled carbon nanotubes in aquatic systems: Measurements and environmental implications. *Environ. Sci. Technol.* **2008,** *42*, (21), 7963-7969.
65. Saleh, N. B.; Pfefferle, L. D.; Elimelech, M., Influence of Biomacromolecules and Humic Acid on the Aggregation Kinetics of Single-Walled Carbon Nanotubes. *Environmental Science & Technology* **2010,** *44*, (7), 2412-2418.
66. Puisto, A.; Illa, X.; Mohtaschemi, M.; Alava, M., Modeling the viscosity and aggregation of suspensions of highly anisotropic nanoparticles. *The European Physical Journal E: Soft Matter and Biological Physics* **2012,** *35*, (1), 1-7.
67. Mohraz, A.; Moler, D. B.; Ziff, R. M.; Solomon, M. J., Effect of Monomer Geometry on the Fractal Structure of Colloidal Rod Aggregates. *Physical Review Letters* **2004,** *92*, (15), 155503.
68. Bradford, S. A.; Yates, S. R.; Bettahar, M.; Simunek, J., Physical factors affecting the transport and fate of colloids in saturated porous media. *Water Resour. Res.* **2002,** *38*, (12).
69. Klein, R.; Meakin, P., Universality in colloid aggregation. *Nature* **1989,** *339*.
70. Okubo, T.; Aotani, S., Microscopic observation of ordered colloids in sedimentation equilibrium and the importance of Debye-screening length. 8. Unsymmetrical ordering and inclusion of anisotropic particles. *Colloid and Polymer Science* **1988,** *266*, (11), 1049-1057.
71. Vold, M. J., Van der Waals' attraction between anisometric particles. *Journal of Colloid Science* **1954,** *9*, (5), 451-459.
72. Youngren, G.; Acrivos, A., Stokes flow past a particle of arbitrary shape: a numerical method of solution. *Journal of fluid Mechanics* **1975,** *69*, (02), 377-403.

73. Saleh, N. B.; Pfefferle, L. D.; Elimelech, M., Influence of biomacromolecules and humic acid on the aggregation kinetics of single-walled carbon nanotubes. *Environ. Sci. Technol.* **2010,** *44*, (7), 2412-2418.
74. Jaisi, D. P.; Elimelech, M., Single-walled carbon nanotubes exhibit limited transport in soil columns. *Environ. Sci. Technol.* **2009,** *43*, (24), 9161-9166.
75. Liu, X. Y.; O'Carroll, D. M.; Petersen, E. J.; Huang, Q. G.; Anderson, C. L., Mobility of multiwalled carbon nanotubes in porous media. *Environ. Sci. Technol.* **2009,** *43*, (21), 8153-8158.
76. Smith, B.; Wepasnick, K.; Schrote, K. E.; Bertele, A. H.; Ball, W. P.; O'Melia, C.; Fairbrother, D. H., Colloidal properties of aqueous suspensions of acid-treated, multi-walled carbon nanotubes. *Environ. Sci. Technol.* **2009,** *43*, (3), 819-825.
77. Smith, B.; Wepasnick, K.; Schrote, K. E.; Cho, H. H.; Ball, W. P.; Fairbrother, D. H., Influence of surface oxides on the colloidal stability of multi-walled carbon nanotubes: A structure-property relationship. *Langmuir* **2009,** *25*, (17), 9767-9776.
78. Tian, Y.; Gao, B.; Batista, C. S.; Ziegler, K. J., Transport of engineered nanoparticles in saturated porous media. *J Nanopart Res* **2010,** *12*, 2371-2380.
79. Keller, A. A.; Wang, H.; Zhou, D.; Lenihan, H. S.; Cherr, G.; Cardinale, B. J.; Miller, R.; Ji, Z., Stability and aggregation of metal oxide nanoparticles in natural aqueous matrices. *Environmental Science & Technology* **2010,** *44*, (6), 1962-1967.
80. Zhou, D.; Keller, A. A., Role of morphology in the aggregation kinetics of ZnO nanoparticles. *Water research* **2010,** *44*, (9), 2948-2956.
81. Islam, A.; Chowdhry, B.; Snowden, M., Hetero-aggregation in colloidal dispersions. *Advances in colloid and interface science* **1995,** *62*, (2), 109-136.
82. Lin, W.; Kobayashi, M.; Skarba, M.; Mu, C.; Galletto, P.; Borkovec, M., Hetero-aggregation in binary mixtures of oppositely charged colloidal particles. *Langmuir* **2006,** *22*, (3), 1038-1047.
83. Yates, P. D.; Franks, G. V.; Jameson, G. J., Orthokinetic Hetero-aggregation with nanoparticles: Effect of particle size ratio on aggregate properties. *Colloids and Surfaces a-Physico-chemical and Engineering Aspects* **2008,** *326*, (1-2), 83-91.
84. Kim, A. Y.; Berg, J. C., Fractal Hetero-aggregation of Oppositely Charged Colloids. *Journal of Colloid and Interface Science* **2000,** *229*, (2), 607-614.
85. James, R. O.; Homola, A.; Healy, T. W., Heterocoagulation of amphoteric latex colloids. *Journal of the Chemical Society, Faraday Transactions 1: Physical Chemistry in Condensed Phases* **1977,** *73*, 1436-1445.
86. Kitano, H.; Iwai, S.; Ise, N.; Okubo, T., Kinetic analysis of association processes between oppositely charged polymer latex particles. *Journal of the American Chemical Society* **1987,** *109*, (22), 6641-6644.
87. Fern; aacute; ndez-Barbero, A.; Vincent, B., Charge Hetero-aggregation between hard and soft particles. *Physical Review E* **2000,** *63*, (1), 011509.
88. Saleh, N.; Phenrat, T.; Sirk, K.; Dufour, B.; Ok, J.; Sarbu, T.; Matyjaszewski, K.; Tilton, R. D.; Lowry, G. V., Adsorbed Triblock Copolymers Deliver Reactive Iron Nanoparticles to the Oil/Water Interface. *Nano Letters* **2005,** *5*, (12), 2489-2494.
89. Sun, N.; Elimelech, M.; Sun, N.-Z.; Ryan, J. N., A novel two-dimensional model for colloid transport in physically and geochemically heterogeneous porous media. *Journal of Contaminant Hydrology* **2001,** *49*, (3-4), 173-199.

90. Chowdhury, I.; Cwiertny, D. M.; Walker, S. L., Combined factors influencing the aggregation and deposition of nano-TiO2 in the presence of humic acid and bacteria. *Environmental science & technology* **2012,** *46*, (13), 6968-6976.
91. Yang, H.; Tong, M.; Kim, H., Effect of Carbon Nanotubes on the Transport and Retention of Bacteria in Saturated Porous Media. *Environmental science & technology* **2013,** *47*, (20), 11537-11544.
92. Tong, M.; Ding, J.; Shen, Y.; Zhu, P., Influence of biofilm on the transport of fullerene (C 60) nanoparticles in porous media. *water research* **2010,** *44*, (4), 1094-1103.
93. Lerner, R. N.; Lu, Q.; Zeng, H.; Liu, Y., The effects of biofilm on the transport of stabilized zerovalent iron nanoparticles in saturated porous media. *Water research* **2012,** *46*, (4), 975-985.
94. Murphy, C. J. S., T. K.; Gole, A.; Orendorff, C. J.; Gao, J.; Gou, L.; Hunyadi, S. Li, T, Anisotropic Metal Nanoparticles: Synthesis, Assembly, and Optical Applications, . [a Top Five ACS article by citations, National Chemistry Week, 2007]. *J. Phys. Chem. B* **2005,** *109*, 13857-13870.
95. Gou, L. M., C. J., Fine-Tuning the shape of gold nanorods *Chem. Mat.* **2005,** *17*, 3668-3672.
96. Cho, W. S.; Kim, S.; Han, B. S.; Son, W. C.; Jeong, J., Comparison of gene expression profiles in mice liver following intravenous injection of 4 and 100 nm-sized PEG-coated gold nanoparticles. *Toxicol. Lett.* **2009,** *191*, (1), 96-102.
97. Akiyama, Y.; Mori, T.; Katayama, Y.; Niidome, T., The effects of PEG grafting level and injection dose on gold nanorod biodistribution in the tumor-bearing mice. *J. Control. Release* **2009,** *139*, (1), 81-84.
98. Goodman, C. M.; McCusker, C. D.; Yilmaz, T.; Rotello, V. M., Toxicity of gold nanoparticles functionalized with cationic and anionic side chains. *Bioconjugate Chem.* **2004,** *15*, (4), 897-900.
99. Merchant, B., Gold, the Noble Metal and the Paradoxes of its Toxicology. *Biologicals* **1998,** *26*, (1), 49-59.
100. Pan, Y.; Neuss, S.; Leifert, A.; Fischler, M.; Wen, F.; Simon, U.; Schmid, G.; Brandau, W.; Jahnen-Dechent, W., Size-dependent cytotoxicity of gold nanoparticles. *Small* **2007,** *3*, (11), 1941-1949.
101. Tong, L.; Cheng, J. X., Gold nanorod-mediated photothermolysis induces apoptosis of macrophages via damage of mitochondria. *Nanomedicine* **2009,** *4*, (3), 265-276.
102. Root, S. W.; Andrews, G. A.; Kniseley, R. M.; Tyor, M. P., The distribution and radiation effects of intravenously administered colloidal Au198 in man. *Cancer* **1954,** *7*, (5), 856-866.
103. Alkilany, A. M.; Murphy, C. J., Toxicity and cellular uptake of gold nanoparticles: what we have learned so far? *J Nanopart Res* **2010,** *12*, (7), 2313-2333.
104. Kang, S.; Mauter, M. S.; Elimelech, M., Microbial Cytotoxicity of Carbon-Based Nanomaterials: Implications for River Water and Wastewater Effluent. *Environmental Science & Technology* **2009,** *43*, (7), 2648-2653.
105. Kang, S.; Pinault, M.; Pfefferle, L. D.; Elimelech, M., Single-walled carbon nanotubes exhibit strong antimicrobial activity. *Langmuir* **2007,** *23*, (17), 8670-8673.
106. Vecitis, C. D.; Zodrow, K. R.; Kang, S.; Elimelech, M., Electronic-Structure-Dependent Bacterial Cytotoxicity of Single-Walled Carbon Nanotubes. *Acs Nano* **2010,** *ASAP*.

107. Hauck, T. S.; Ghazani, A. A.; Chan, W. C. W., Assessing the effect of surface chemistry on gold nanorod uptake, toxicity, and gene expression in mammalian cells. *Small* **2008,** *4*, (1), 153-159.
108. Patra, C. R.; Moneim, S. S. A.; Wang, E.; Dutta, S.; Patra, S.; Eshed, M.; Mukherjee, P.; Gedanken, A.; Shah, V. H.; Mukhopadhyay, D., In vivo toxicity studies of europium hydroxide nanorods in mice. *Toxicol. Appl. Pharmacol.* **2009,** *240*, (1), 88-98.
109. Wang, S. G.; Lu, W. T.; Tovmachenko, O.; Rai, U. S.; Yu, H. T.; Ray, P. C., Challenge in understanding size and shape dependent toxicity of gold nanomaterials in human skin keratinocytes. *Chem. Phys. Lett.* **2008,** *463*, (1-3), 145-149.
110. Goodman, C. M.; Chari, N. S.; Han, G.; Hong, R.; Ghosh, P.; Rotello, V. M., DNA-binding by functionalized gold nanoparticles: Mechanism and structural requirements. *Chemical Biology & Drug Design* **2006,** *67*, (4), 297-304.
111. Colvin, V. L., The potential environmental impact of engineered nanomaterials. *Nature Biotech* **2003,** *21*, 166-1170.
112. Wiesner, M. R.; Bottero, J.-Y., *Environmental Nanotechnology: Applications and Impacts of Nanomaterials*. McGraw-Hill Companies: New York, NY, 2007.
113. Afrooz, A. R. M. N.; Sivalapalan, S. T.; Murphy, C. J.; Hussain, S. M.; Schlager, J. J.; Saleh, N. B., Spheres vs. rods: The shape of gold nanoparticles influences aggregation and deposition behavior. *Chemosphere* **2013,** *91*, (1), 93-98.
114. Afrooz, A. R. M. N.; Hussain, S.; Saleh, N., Aggregate size and structure determination of nanomaterials in physiological media: importance of dynamic evolution. *Journal of Nanoparticle Research* **2014,** *16*, (12), 1-7.
115. Afrooz, A. R. M. N.; Khan, I. A.; Hussain, S. M.; Saleh, N. B., Mechanistic Hetero-aggregation of Gold Nanoparticles in a Wide Range of Solution Chemistry. *Environmental Science & Technology* **2013,** *47*, (4), 1853-1860.

Chapter 2

1. Murphy, C. J.; Thompson, L. B.; Alkilany, A. M.; Sisco, P. N.; Boulos, S. P.; Sivapalan, S. T.; Yang, J. A.; Chernak, D. J.; Huang, J., The many faces of gold nanorods. *J. Phys. Chem. Lett.* **2010**, 2867-2875.
2. Salem, A. K.; Searson, P. C.; Leong, K. W., Multifunctional nanorods for gene delivery. *Nat. Mater.* **2003,** *2*, (10), 668-671.
3. Pérez-Juste, J.; Pastoriza-Santos, I.; Liz-Marzán, L. M.; Mulvaney, P., Gold nanorods: Synthesis, characterization and applications. *Coordin. Chem. Rev.* **2005,** *249*, (17-18), 1870-1901.
4. Yang, B.; Han, Z. H., Temperature-dependent thermal conductivity of nanorod-based nanofluids. *Appl. Phys. Lett.* **2006,** *89*, (8), 3.
5. Kwak, C. H.; Kim, B. H.; Park, C. I.; Seo, S. Y.; Kim, S. H.; Han, S. W., Structural and electrical properties of ZnO nanorods and Ti buffer layers. *Appl. Phys. Lett.* **2010,** *96*, (5), 3.
6. Iijima, S.; Ichihashi, T., Single-shell carbon nanotubes of 1-nm diameter. *Nature* **1993,** *363*, (6430), 603-605.
7. Tian, B.; Zheng, X.; Kempa, T. J.; Fang, Y.; Yu, N.; Yu, G.; Huang, J.; Lieber, C. M., Coaxial silicon nanowires as solar cells and nanoelectronic power sources. *Nature* **2007,** *449*, (7164), 885-889.

8. Huff, T. B.; Hansen, M. N.; Zhao, Y.; Cheng, J.-X.; Wei, A., Controlling the cellular uptake of gold nanorods. *Langmuir* **2007,** *23*, (4), 1596-1599.
9. Huang, X.; Neretina, S.; El-Sayed, M. A., Gold nanorods: From synthesis and properties to biological and biomedical applications. *Adv. Mater.* **2009,** *21*, (48), 4880-4910.
10. Jain, P. K.; Lee, K. S.; El-Sayed, I. H.; El-Sayed, M. A., Calculated absorption and scattering properties of gold nanoparticles of different size, shape, and composition: Applications in biological imaging and biomedicine. *J. Phy. Chem. B.* **2006,** *110*, (14), 7238-7248.
11. Hauck, T. S.; Ghazani, A. A.; Chan, W. C. W., Assessing the effect of surface chemistry on gold nanorod uptake, toxicity, and gene expression in mammalian cells. *Small* **2008,** *4*, (1), 153-159.
12. Patra, C. R.; Moneim, S. S. A.; Wang, E.; Dutta, S.; Patra, S.; Eshed, M.; Mukherjee, P.; Gedanken, A.; Shah, V. H.; Mukhopadhyay, D., In vivo toxicity studies of europium hydroxide nanorods in mice. *Toxicol. Appl. Pharmacol.* **2009,** *240*, (1), 88-98.
13. Pan, Y.; Neuss, S.; Leifert, A.; Fischler, M.; Wen, F.; Simon, U.; Schmid, G.; Brandau, W.; Jahnen-Dechent, W., Size-dependent cytotoxicity of gold nanoparticles. *Small* **2007,** *3*, (11), 1941-1949.
14. Leunissen, M. E.; Christova, C. G.; Hynninen, A. P.; Royall, C. P.; Campbell, A. I.; Imhof, A.; Dijkstra, M.; van Roij, R.; van Blaaderen, A., Ionic colloidal crystals of oppositely charged particles. *Nature* **2005,** *437*, (7056), 235-240.
15. Vanzanten, J. H.; Elimelech, M., Determination of absolute coagulation rate constants by multiangle light-scattering. *J. Colloid Interf. Sci.* **1992,** *154*, (1), 1-7.
16. Onsager, L., The effects of shape on the interaction of colloidal particles. *Ann. NY. Acad. Sci.* **1949,** *51*, (4), 627-659.
17. Bhattacharjee, S.; Chen, J. Y.; Elimelech, M., DLVO interaction energy between spheroidal particles and a flat surface. *Colloids and Surfaces A.* **2000,** *165*, (1-3), 143-156.
18. Hunter, R. J., *Foundations of colloid science*. Oxford University Press: New York, NY, 1995; Vol. 1.
19. Petosa , A. R.; J aisi, D.; Q ue vedo , I.; E limelech , M.; T ufenkji , N., Aggregation and deposition of engineered nanomaterials in aquatic environments: Role of physico-chemical interactions. *Environ. Sci. Technol.* **2010,** *44*, 6532–6549.
20. Mulvihill, M. J.; Habas, S. E.; Jen-La Plante, H.; Wan, J.; Mokari, T., Influence of size, shape, and surface coating on the stability of aqueous suspensions of CdSe nanoparticles. *Chem. Mater.* **2010,** *22*, (18), 5251-5257.
21. Zhou, D. X.; Keller, A. A., Role of morphology in the aggregation kinetics of ZnO nanoparticles. *Water Res.* **2010,** *44*, (9), 2948-2956.
22. Jana, N. R.; Gearheart, L.; Murphy, C. J., Seed-mediated growth approach for shape-controlled synthesis of spheroidal and rod-like gold nanoparticles using a surfactant template. *Adv. Mater.* **2001,** *13*, (18), 1389-1393.
23. Jana, N. R.; Gearheart, L.; Murphy, C. J., Seeding growth for size control of 5-40 nm diameter gold nanoparticles. *Langmuir* **2001,** *17*, (22), 6782-6786.
24. Jana, N. R.; Gearheart, L.; Murphy, C. J., Wet chemical synthesis of high aspect ratio cylindrical gold nanorods. *J. Phys. Chem. B.* **2001,** *105*, (19), 4065-4067.
25. Gao, J. X.; Bender, C. M.; Murphy, C. J., Dependence of the gold nanorod aspect ratio on the nature of the directing surfactant in aqueous solution. *Langmuir* **2003,** *19*, (21), 9065-9070.

26. Saleh, N. B.; Pfefferle, L. D.; Elimelech, M., Aggregation kinetics of multiwalled carbon nanotubes in aquatic systems: Measurements and environmental implications. *Environ. Sci. Technol.* **2008,** *42*, (21), 7963-7969.
27. Saleh, N. B.; Pfefferle, L. D.; Elimelech, M., Influence of biomacromolecules and humic acid on the aggregation kinetics of single-walled carbon nanotubes. *Environ. Sci. Technol.* **2010,** *44*, (7), 2412-2418.
28. Saleh, N.; Kim, H.-J.; Phenrat, T.; Matyjaszewski, K.; Tilton, R. D.; Lowry, G. V., Ionic strength and composition affect the mobility of surface-modified Fe-0 nanoparticles in water-saturated sand columns. *Environ. Sci.Technol.* **2008,** *42*, (9), 3349-3355.
29. Haiss, W.; Thanh, N. T. K.; Aveyard, J.; Fernig, D. G., Determination of size and concentration of gold nanoparticles from UV-Vis spectra. *Anal. Chem.* **2007,** *79*, (11), 4215-4221.
30. Murphy, C. J.; San, T. K.; Gole, A. M.; Orendorff, C. J.; Gao, J. X.; Gou, L.; Hunyadi, S. E.; Li, T., Anisotropic metal nanoparticles: Synthesis, assembly, and optical applications. *J. Phys. Chem. B* **2005,** *109*, (29), 13857-13870.
31. Deng, Z.; Liang, M.; Toth, I.; Monteiro, M.; Minchin, F., Molecular interaction of Poly(acrylic acid) gold nanoparticles with human fibrinogen. *ACS Nano* **2012**.
32. Wang, J.; Dong, B.; Chen, B.; Jiang, Z.; Song, H., Selective photothermal therapy for breast cancer with targeting peptide modified gold nanorods. *Dalton T.* **2012,** *41*, (36), 11134-11144.
33. Liu, J. F.; Legros, S.; Ma, G. B.; Veinot, J. G. C.; von der Kammer, F.; Hofmann, T., Influence of surface functionalization and particle size on the aggregation kinetics of engineered nanoparticles. *Chemosphere* **2012,** *87*, (8), 918-924.
34. Yang, Y. I.; Choi, I.; Hong, S.; Lee, S.; Kang, T.; Lee, H.; Yi, J., Selective aggregation of polyanion-coated gold nanorods induced by divalent metal ions in an aqueous solution. *J. Nanosci. Nanotechno.* **2010,** *10*, (5), 3538-3542.
35. Furusawa, K.; Shou, Z.; Nagahashi, N., Polymer adsorption on fine particles - the effects of particle-size and its stability. *Colloid Polym. Sci.* **1992,** *270*, (3), 212-218.
36. Kyrylyuk, A. V.; Philipse, A. P., Effect of particle shape on the random packing density of amorphous solids. *Phys. Status Solidi A.* **2011,** *208*, (10), 2299-2302.
37. Kyrylyuk, A. V. W., Alan. Philipse Albert P. In *Random packings of Rod-Sphere mixtures simulated by mechanical contraction method* 6th International Conference on Micromechanics of Granular Media, Golden, Colorado., 2009; M. Nakagawa, S. L., Ed. 2009.
38. Rudge, J. F.; Holness, M. B.; Smith, G. C., Quantitative textural analysis of packings of elongate crystals. *Contrib. Mineral. Petr.* **2008,** *156*, (4), 413-429.
39. Chen, K. L.; Elimelech, M., Aggregation and deposition kinetics of fullerene (C-60) nanoparticles. *Langmuir* **2006,** *22*, (26), 10994-11001.

Chapter 3

1. Oberdorster, G.; Maynard, A.; Donaldson, K.; Castranova, V.; Fitzpatrick, J.; Ausman, K.; Carter, J.; Karn, B.; Kreyling, W.; Lai, D.; Olin, S.; Monteiro-Riviere, N.; Warheit, D.; Yang, H.; Toxicity, I. R. F. R. S. I. N.; Screening Working, G., Principles for characterizing the potential human health effects from exposure to nanomaterials: elements of a screening strategy. *Particle and fibre toxicology* **2005,** *2*, 8-8.

2. Kante, B.; Couvreur, P.; Dubois-Krack, G.; De Meester, C.; Guiot, P.; Roland, M.; Mercier, M.; Speiser, P., Toxicity of polyalkylcyanoacrylate nanoparticles I: Free nanoparticles. *Journal of pharmaceutical sciences* **1982,** *71*, (7), 786-790.
3. Allison, A. C., Lysosomes and toxicity of particulate pollutants. *Archives of Internal Medicine* **1971,** *128*, (1), 131-&.
4. Nel, A. E.; Maedler, L.; Velegol, D.; Xia, T.; Hoek, E. M. V.; Somasundaran, P.; Klaessig, F.; Castranova, V.; Thompson, M., Understanding biophysico-chemical interactions at the nano-bio interface. *Nature Materials* **2009,** *8*, (7), 543-557.
5. Pasquini, L. M.; Hashmi, S. M.; Sommer, T. J.; Elimelech, M.; Zimmerman, J. B., Impact of Surface Functionalization on Bacterial Cytotoxicity of Single-Walled Carbon Nanotubes. *Environmental Science & Technology* **2012,** *46*, (11), 6297-6305.
6. Nel, A.; Xia, T.; Madler, L.; Li, N., Toxic potential of materials at the nanolevel. *Science* **2006,** *311*, (5761), 622-627.
7. POTOČNIK, J., Commission Recommendation of 18 October 2011 on the definition of nanomaterial Text with EEA relevance. *Official Journal of the European Union* **2011,** *275*, 38-40.
8. Oberdorster, G.; Oberdorster, E.; Oberdorster, J., Nanotoxicology: An emerging discipline evolving from studies of ultrafine particles. *Environmental Health Perspectives* **2005,** *113*, (7), 823-839.
9. Oberdorster, G.; Stone, V.; Donaldson, K., Toxicology of nanoparticles: A historical perspective. *Nanotoxicology* **2007,** *1*, (1), 2-25.
10. Cho, E. C.; Zhang, Q.; Xia, Y., The effect of sedimentation and diffusion on cellular uptake of gold nanoparticles. *Nature Nanotechnology* **2011,** *6*, (6), 385-391.
11. Lison, D.; Thomassen, L. C. J.; Rabolli, V.; Gonzalez, L.; Napierska, D.; Seo, J. W.; Kirsch-Volders, M.; Hoet, P.; Kirschhock, C. E. A.; Martens, J. A., Nominal and effective dosimetry of silica nanoparticles in cytotoxicity assays. *Toxicol. Sci.* **2008,** *104*, (1), 155-162.
12. Kim, T.-H.; Kim, M.; Park, H.-S.; Shin, U. S.; Gong, M.-S.; Kim, H.-W., Size-dependent cellular toxicity of silver nanoparticles. *Journal of Biomedical Materials Research Part A* **2012,** *100A*, (4), 1033-1043.
13. Clément, L.; Hurel, C.; Marmier, N., Toxicity of TiO2 nanoparticles to cladocerans, algae, rotifers and plants – Effects of size and crystalline structure. *Chemosphere* **2013,** *90*, (3), 1083-1090.
14. Zhou, D.; Keller, A. A., Role of morphology in the aggregation kinetics of ZnO nanoparticles. *Water Research* **2010,** *44*, (9), 2948-2956.
15. Phenrat, T.; Saleh, N.; Sirk, K.; Kim, H.-J.; Tilton, R. D.; Lowry, G. V., Stabilization of aqueous nanoscale zerovalent iron dispersions by anionic polyelectrolytes: adsorbed anionic polyelectrolyte layer properties and their effect on aggregation and sedimentation. *Journal of Nanoparticle Research* **2008,** *10*, (5), 795-814.
16. Saleh, N. B.; Pfefferle, L. D.; Elimelech, M., Influence of Biomacromolecules and Humic Acid on the Aggregation Kinetics of Single-Walled Carbon Nanotubes. *Environmental Science & Technology* **2010,** *44*, (7), 2412-2418.
17. Weitz, D. A.; Oliveria, M., Fractal structures formed by kinetic aggregation of aqueous gold colloids. *Physical Review Letters* **1984,** *52*, (16), 1433-1436.
18. Hauck, T. S.; Ghazani, A. A.; Chan, W. C., Assessing the effect of surface chemistry on gold nanorod uptake, toxicity, and gene expression in mammalian cells. *Small* **2008,** *4*, (1), 153-159.

19. Shukla, R.; Bansal, V.; Chaudhary, M.; Basu, A.; Bhonde, R. R.; Sastry, M., Biocompatibility of gold nanoparticles and their endocytotic fate inside the cellular compartment: a microscopic overview. *Langmuir* **2005,** *21*, (23), 10644-10654.
20. Afrooz, A. R. M. N.; Khan, I. A.; Hussain, S. M.; Saleh, N. B., Mechanistic Hetero-aggregation of Gold Nanoparticles in a Wide Range of Solution Chemistry. *Environmental Science & Technology* **2013,** *47*, (4), 1853-1860.
21. Pecora, R., *Dynamic light scattering: Applications of photon correlation spectroscopy*. Springer-Verlag New York, LLC: 1985.
22. Lin, M. Y.; Lindsay, H. M.; Weitz, D. A.; Ball, R. C.; Klein, R.; Meakin, P., Universality in colloid aggregation. *Nature* **1989,** *339*, (6223), 360-362.
23. Shields, S. P.; Richards, V. N.; Buhro, W. E., Nucleation control of size and dispersity in aggregative nanoparticle growth. A study of the coarsening kinetics of thiolate-capped gold nanocrystals. *Chemistry of Materials* **2010,** *22*, (10), 3212-3225.
24. Lamer, V. K.; Dinegar, R. H., Theory, production and mechanism of formation of monodispersed hydrosols. *Journal of the American Chemical Society* **1950,** *72*, (11), 4847-4854.
25. Wu, H., Lattuada, M., Morbidelli, M., Dependence of fractal dimension of DLCA clusters on size of primary particles. *Advances in Colloid and Interface Science* **2013**.

Chapter 4

1. Klaine, S. J.; Alvarez, P. J. J.; Batley, G. E.; Fernandes, T. F.; Handy, R. D.; Lyon, D. Y.; Mahendra, S.; McLaughlin, M. J.; Lead, J. R., Nanomaterials in the environment: Behavior, fate, bioavailability, and effects. *Environmental Toxicology and Chemistry* **2008,** *27*, (9), 1825-1851.
2. Nel, A. E.; Maedler, L.; Velegol, D.; Xia, T.; Hoek, E. M. V.; Somasundaran, P.; Klaessig, F.; Castranova, V.; Thompson, M., Understanding biophysico-chemical interactions at the nano-bio interface. *Nature Materials* **2009,** *8*, (7), 543-557.
3. Denkov, N. D.; Velev, O. D.; Kralchevsky, P. A.; Ivanov, I. B.; Yoshimura, H.; Nagayama, K., Mechanism of formation of 2-dimensional crystals from latex-particles on substrates. *Langmuir* **1992,** *8*, (12), 3183-3190.
4. Grabar, K. C.; Smith, P. C.; Musick, M. D.; Davis, J. A.; Walter, D. G.; Jackson, M. A.; Guthrie, A. P.; Natan, M. J., Kinetic control of interparticle spacing in Au colloid-based surfaces: Rational nanometer-scale architecture. *Journal of the American Chemical Society* **1996,** *118*, (5), 1148-1153.
5. Halperin, A.; Tirrell, M.; Lodge, T. P., Tethered chains in polymer microstructures. *Advances in Polymer Science* **1992,** *100*, 31-71.
6. Mattoussi, H.; Mauro, J. M.; Goldman, E. R.; Anderson, G. P.; Sundar, V. C.; Mikulec, F. V.; Bawendi, M. G., Self-assembly of CdSe-ZnS quantum dot bioconjugates using an engineered recombinant protein. *Journal of the American Chemical Society* **2000,** *122*, (49), 12142-12150.
7. Mukhopadhyay, A.; Grabinski, C.; Afrooz, A. R. M. N.; Saleh, N. B.; Hussain, S., Effect of Gold Nanosphere Surface Chemistry on Protein Adsorption and Cell Uptake In Vitro. *Applied Biochemistry and Biotechnology* **2012,** *167*, (2), 327-337.
8. Gustafsson, O.; Gschwend, P. M., Aquatic colloids: Concepts, definitions, and current challenges. *Limnology and Oceanography* **1997,** *42*, (3), 519-528.
9. Means, J. C.; Wijayaratne, R., Role of natural colloids in the transport of hydrophobic pollutants. *Science* **1982,** *215*, (4535), 968-970.

10. Petosa, A. R.; Jaisi, D. P.; Quevedo, I. R.; Elimelech, M.; Tufenkji, N., Aggregation and Deposition of Engineered Nanomaterials in Aquatic Environments: Role of Physico-chemical Interactions. *Environmental Science & Technology* **2010,** *44*, (17), 6532-6549.
11. Nowack, B.; Bucheli, T. D., Occurrence, behavior and effects of nanoparticles in the environment. *Environmental Pollution* **2007,** *150*, (1), 5-22.
12. Buffle, J.; Wilkinson, K. J.; Stoll, S.; Filella, M.; Zhang, J. W., A generalized description of aquatic colloidal interactions: The three-colloidal component approach. *Environmental Science & Technology* **1998,** *32*, (19), 2887-2899.
13. Li, D.; Kaner, R. B., Shape and aggregation control of nanoparticles: Not shaken, not stirred. *Journal of the American Chemical Society* **2006,** *128*, (3), 968-975.
14. Lin, M. Y.; Lindsay, H. M.; Weitz, D. A.; Klein, R.; Ball, R. C.; Meakin, P., Universal diffusion-limited colloid aggregation. *Journal of Physics-Condensed Matter* **1990,** *2*, (13), 3093-3113.
15. Bagwe, R. P.; Hilliard, L. R.; Tan, W. H., Surface modification of silica nanoparticles to reduce aggregation and nonspecific binding. *Langmuir* **2006,** *22*, (9), 4357-4362.
16. Saleh, N. B.; Pfefferle, L. D.; Elimelech, M., Aggregation Kinetics of Multiwalled Carbon Nanotubes in Aquatic Systems: Measurements and Environmental Implications. *Environmental Science & Technology* **2008,** *42*, (21), 7963-7969.
17. Saleh, N. B.; Pfefferle, L. D.; Elimelech, M., Influence of Biomacromolecules and Humic Acid on the Aggregation Kinetics of Single-Walled Carbon Nanotubes. *Environmental Science & Technology* **2010,** *44*, (7), 2412-2418.
18. Bradley, M., Mat Lazim, A., Eastoe, J., Stimulus-Responsive Hetero-aggregation of colloidal dispersions: Reversible systems and composite materials. *Polymers* **2011,** *3*, 1036-1050.
19. Lin, W.; Kobayashi, M.; Skarba, M.; Nu, C. D.; Galletto, P.; Borkovec, M., Hetero-aggregation in binary mixtures of oppositely charged colloidal particles. *Langmuir* **2006,** *22*, (3), 1038-1047.
20. Lopez-Lopez, J. M.; Schmitt, A.; Moncho-Jorda, A.; Hidalgo-Alvarez, R., Electrostatic Hetero-aggregation regimes in colloidal suspensions. *Advances in Colloid and Interface Science* **2009,** *147-48*, 186-204.
21. Rubio, J.; Souza, M. L.; Smith, R. W., Overview of flotation as a wastewater treatment technique. *Minerals Engineering* **2002,** *15*, (3), 139-155.
22. Ouali, L.; Stoll, S.; Pefferkorn, E.; Elaissari, A.; Lanet, V.; Pichot, C.; Mandrand, B., Coagulation of antibody-sensitized latexes in the presence of antigen. *Polymers for Advanced Technologies* **1995,** *6*, (7), 541-546.
23. Ito, H.; Hayashi, H.; Sasaki, H., Rapid separation of oil particles from low-concentrated O/W emulsions in the presence of anionic surfactants using fibrous slag. *Journal of Colloid and Interface Science* **2002,** *252*, (1), 214-221.
24. Bandini, P.; Prestidge, C. A.; Ralston, J., Colloidal iron oxide slime coatings and galena particle flotation. *Minerals Engineering* **2001,** *14*, (5), 487-497.
25. DiFeo, A.; Finch, J. A., Sphalerite/silica interactions: model predictions. *International Journal of Mineral Processing* **2002,** *64*, (4), 219-227.
26. Derjaguin, B.; Landau, L., Theory of the stability of strongly charged lyophobic sols and of the adhesion of strongly charged-particles in solutions of electrolytes. *Progress in Surface Science* **1993,** *43*, (1-4), 30-59.

27. Verwey, E. J. W., Theory of the stability of lyophobic colloids. *Journal of Physical and Colloid Chemistry* **1947,** *51*, (3), 631-636.
28. Elimelech, M.; Omelia, C. R., Effect of electrolyte type on the electrophoretic mobility of polystyrene latex colloids. *Colloids and Surfaces* **1990,** *44*, 165-178.
29. Findlay, A. D.; Thompson, D. W.; Tipping, E., The aggregation of silica and haematite particles dispersed in natural water samples. *Colloids and Surfaces a-Physico-chemical and Engineering Aspects* **1996,** *118*, (1-2), 97-105.
30. Holthoff, H.; Schmitt, A.; FernandezBarbero, A.; Borkovec, M.; CabrerizoVilchez, M. A.; Schurtenberger, P.; HidalgoAlvarez, R., Measurement of absolute coagulation rate constants for colloidal particles: Comparison of single and multiparticle light scattering techniques. *Journal of Colloid and Interface Science* **1997,** *192*, (2), 463-470.
31. Islam, A. M.; Chowdhry, B. Z.; Snowden, M. J., Hetero-aggregation in colloidal dispersions. *Advances in Colloid and Interface Science* **1995,** *62*, (2-3), 109-136.
32. Lopez-Lopez, J. M.; Moncho-Jorda, A.; Schmitt, A.; Hidalgo-Alvarez, R., Formation and structure of stable aggregates in binary diffusion-limited cluster-cluster aggregation processes. *Physical Review E* **2005,** *72*, (3).
33. Puertas, A. M.; Fernandez-Barbero, A.; de las Nieves, F. J., Kinetics of colloidal Hetero-aggregation . *Physica a-Statistical Mechanics and Its Applications* **2002,** *304*, (3-4), 340-354.
34. Puertas, A. M.; Maroto, J. A.; Fernandez-Barbero, A.; De las Nieves, F. J., On the kinetics of Hetero-aggregation versus electrolyte concentration: comparison between simulation and experiment. *Colloids and Surfaces a-Physico-chemical and Engineering Aspects* **1999,** *151*, (3), 473-481.
35. Yu, W. L.; Borkovec, M., Distinguishing Hetero-aggregation from homoaggregation in mixed binary particle suspensions by multiangle static and dynamic light scattering. *Journal of Physical Chemistry B* **2002,** *106*, (51), 13106-13110.
36. Yu, W. L.; Matijevic, E.; Borkovec, M., Absolute Hetero-aggregation rate constants by multiangle static and dynamic light scattering. *Langmuir* **2002,** *18*, (21), 7853-7860.
37. Jia, J.; Jia, Z.; Iwata, S., Bimodal colloidal mixtures: From fast to slow aggregation regions. *Journal of Colloid and Interface Science* **2011,** *362*, (2), 633-637.
38. Puertas, A. M.; Fernandez-Barbero, A.; De Las Nieves, F. J., Charged colloidal Hetero-aggregation kinetics. *Journal of Chemical Physics* **2001,** *114*, (1), 591-595.
39. Hall, R. J.; Pinkrah, V. T.; Chowdhry, B. Z.; Snowden, M. J., Hetero-aggregation studies of mixed cationic co-polymer/anionic homopolymer microgel dispersions. *Colloids and Surfaces a-Physico-chemical and Engineering Aspects* **2004,** *233*, (1-3), 25-38.
40. Bouyer, F.; Robben, A.; Yu, W. L.; Borkovec, M., Aggregation of colloidal particles in the presence of oppositely charged polyelectrolytes: Effect of surface charge heterogeneities. *Langmuir* **2001,** *17*, (17), 5225-5231.
41. Huynh, K. A., McCaffery,J.M, Chen, K.L., Hetero-aggregation of multiwalled Carbon nanotubes and hematite nanoparticles: rates and mechanisms. *Environ. Sci. Technol.* **2012**.
42. Chefetz, B.; Deshmukh, A. P.; Hatcher, P. G.; Guthrie, E. A., Pyrene sorption by natural organic matter. *Environmental Science & Technology* **2000,** *34*, (14), 2925-2930.
43. Torrents, A.; Jayasundera, S., The sorption of nonionic pesticides onto clays and the influence of natural organic carbon. *Chemosphere* **1997,** *35*, (7), 1549-1565.
44. Seo, J.-W. T.; Green, A. A.; Antaris, A. L.; Hersam, M. C., High-Concentration Aqueous Dispersions of Graphene Using Nonionic, Biocompatible Block Copolymers. *The Journal of Physical Chemistry Letters 2*, (9), 1004-1008.

45. Haiss, W.; Thanh, N. T. K.; Aveyard, J.; Fernig, D. G., Determination of Size and Concentration of Gold Nanoparticles from UV-Vis Spectra. *Analytical Chemistry* **2007,** *79*, (11), 4215-4221.
46. Shen, K.; Curran, S.; Xu, H.; Rogelj, S.; Jiang, Y.; Dewald, J.; Pietrass, T., Single-Walled Carbon Nanotube Purification, Pelletization, and Surfactant-Assisted Dispersion:A Combined TEM and Resonant Micro-Raman Spectroscopy Study. *The Journal of Physical Chemistry B* **2005,** *109*, (10), 4455-4463.
47. Vaisman, L.; Wagner, H. D.; Marom, G., The role of surfactants in dispersion of carbon nanotubes. *Advances in Colloid and Interface Science* **2006,** *128â€“130*, (0), 37-46.
48. Wu, T.; Gong, P.; Szleifer, I.; VlcÌŒek, P.; Å ubr, V.; Genzer, J., Behavior of Surface-Anchored Poly(acrylic acid) Brushes with Grafting Density Gradients on Solid Substrates: 1. Experiment. *Macromolecules* **2007,** *40*, (24), 8756-8764.
49. Treat, N. D.; Ayres, N.; Boyes, S. G.; Brittain, W. J., A Facile Route to Poly(acrylic acid) Brushes Using Atom Transfer Radical Polymerization. *Macromolecules* **2005,** *39*, (1), 26-29.
50. Liu, J.; Legros, S.; Ma, G.; Veinot, J. G. C.; von der Kammer, F.; Hofmann, T., Influence of surface functionalization and particle size on the aggregation kinetics of engineered nanoparticles. *Chemosphere* **2012,** *87*, (8), 918-924.
51. Murphy, R. J.; Pristinski, D.; Migler, K.; Douglas, J. F.; Prabhu, V. M., Dynamic light scattering investigations of nanoparticle aggregation following a light-induced pH jump. *Journal of Chemical Physics* **2010,** *132*, (19).
52. White, B.; Banerjee, S.; O'Brien, S.; Turro, N. J.; Herman, I. P., Zeta-potential measurements of surfactant-wrapped individual single-walled carbon nanotubes. *Journal of Physical Chemistry C* **2007,** *111*, (37), 13684-13690.
53. Carpineti, M.; Ferri, F.; Giglio, M.; Paganini, E.; Perini, U., Salt-induced fast aggregation of polystyrene latex. *Phys Rev A* **1990,** *42*, (12), 7347-7354.
54. Wang, Y.; Combe, C.; Clark, M. M., The effects of pH and calcium on the diffusion coefficient of humic acid. *J. Membr. Sci.* **2001,** *183*, (1), 49-60.
55. Xu, H.; Schlenoff, J. B., Kinetics, isotherms, and competition in polymer adsorption using the quartz crystal microbalance. *Langmuir* **1994,** *10*, (1), 241-245.
56. Yoon, S. H.; Lee, C.-H.; Kim, K.-J.; Fane, A. G., Effect of calcium ion on the fouling of nanofilter by humic acid in drinking water production. *Water Res* **1998,** *32*, 2180-2186.

Chapter 5

1. Wagner, S.; Gondikas, A.; Neubauer, E.; Hofmann, T.; von der Kammer, F., Spot the Difference: Engineered and Natural Nanoparticles in the Environment—Release, Behavior, and Fate. *Angewandte Chemie International Edition* **2014,** *53*, (46), 12398-12419.
2. Nowack, B.; Bucheli, T. D., Occurrence, behavior and effects of nanoparticles in the environment. *Environmental pollution* **2007,** *150*, (1), 5-22.
3. Nowack, B.; Ranville, J. F.; Diamond, S.; Gallego-Urrea, J. A.; Metcalfe, C.; Rose, J.; Horne, N.; Koelmans, A. A.; Klaine, S. J., Potential scenarios for nanomaterial release and subsequent alteration in the environment. *Environmental Toxicology and Chemistry* **2012,** *31*, (1), 50-59.
4. Köhler, A. R.; Som, C.; Helland, A.; Gottschalk, F., Studying the potential release of carbon nanotubes throughout the application life cycle. *Journal of Cleaner Production* **2008,** *16*, (8), 927-937.

5. Khin, M. M.; Nair, A. S.; Babu, V. J.; Murugan, R.; Ramakrishna, S., A review on nanomaterials for environmental remediation. *Energy & Environmental Science* **2012,** *5*, (8), 8075-8109.
6. Morawska, L.; Ristovski, Z.; Jayaratne, E.; Keogh, D. U.; Ling, X., Ambient nano and ultrafine particles from motor vehicle emissions: Characteristics, ambient processing and implications on human exposure. *Atmospheric Environment* **2008,** *42*, (35), 8113-8138.
7. Walser, T.; Limbach, L. K.; Brogioli, R.; Erismann, E.; Flamigni, L.; Hattendorf, B.; Juchli, M.; Krumeich, F.; Ludwig, C.; Prikopsky, K., Persistence of engineered nanoparticles in a municipal solid-waste incineration plant. *Nature nanotechnology* **2012,** *7*, (8), 520-524.
8. Gottschalk, F.; Sonderer, T.; Scholz, R. W.; Nowack, B., Modeled Environmental Concentrations of Engineered Nanomaterials (TiO2, ZnO, Ag, CNT, Fullerenes) for Different Regions. *Environmental Science & Technology* **2009,** *43*, (24), 9216-9222.
9. Gottschalk, F.; Nowack, B., The release of engineered nanomaterials to the environment. *Journal of Environmental Monitoring* **2011,** *13*, (5), 1145-1155.
10. Lowry, G. V.; Gregory, K. B.; Apte, S. C.; Lead, J. R., Transformations of nanomaterials in the environment. *Environmental science & technology* **2012,** *46*, (13), 6893-6899.
11. Petosa, A. R.; Jaisi, D. P.; Quevedo, I. R.; Elimelech, M.; Tufenkji, N., Aggregation and deposition of engineered nanomaterials in aquatic environments: role of physico-chemical interactions. *Environmental science & technology* **2010,** *44*, (17), 6532-6549.
12. Saleh, N.; Sirk, K.; Liu, Y.; Phenrat, T.; Dufour, B.; Matyjaszewski, K.; Tilton, R. D.; Lowry, G. V., Surface modifications enhance nanoiron transport and NAPL targeting in saturated porous media. *Environmental Engineering Science* **2007,** *24*, (1), 45-57.
13. Lecoanet, H. F.; Wiesner, M. R., Velocity effects on fullerene and oxide nanoparticle deposition in porous media. *Environmental science & technology* **2004,** *38*, (16), 4377-4382.
14. Jaisi, D. P.; Saleh, N. B.; Blake, R. E.; Elimelech, M., Transport of single-walled carbon nanotubes in porous media: filtration mechanisms and reversibility. *Environmental science & technology* **2008,** *42*, (22), 8317-8323.
15. Fang, J.; Shan, X.-q.; Wen, B.; Lin, J.-m.; Owens, G., Stability of titania nanoparticles in soil suspensions and transport in saturated homogeneous soil columns. *Environmental pollution* **2009,** *157*, (4), 1101-1109.
16. Li, Y.; Wang, Y.; Pennell, K. D.; Abriola, L. M., Investigation of the transport and deposition of fullerene (C60) nanoparticles in quartz sands under varying flow conditions. *Environmental science & technology* **2008,** *42*, (19), 7174-7180.
17. Phenrat, T.; Kim, H.-J.; Fagerlund, F.; Illangasekare, T.; Tilton, R. D.; Lowry, G. V., Particle Size Distribution, Concentration, and Magnetic Attraction Affect Transport of Polymer-Modified Fe-0 Nanoparticles in Sand Columns. *Environmental science & technology* **2009,** *43*, (13), 5079-5085.
18. Solovitch, N.; Labille, J.; Rose, J.; Chaurand, P.; Borschneck, D.; Wiesner, M. R.; Bottero, J.-Y., Concurrent Aggregation and Deposition of TiO2 Nanoparticles in a Sandy Porous Media. *Environmental science & technology* **2010,** *44*, (13), 4897-4902.
19. Ben-Moshe, T.; Dror, I.; Berkowitz, B., Transport of metal oxide nanoparticles in saturated porous media. *Chemosphere* **2010,** *81*, (3), 387-393.
20. Liu, X.; Wazne, M.; Christodoulatos, C.; Jasinkiewicz, K. L., Aggregation and deposition behavior of boron nanoparticles in porous media. *Journal of Colloid and Interface Science* **2009,** *330*, (1), 90-96.

21. Jiang, X.; Tong, M.; Li, H.; Yang, K., Deposition kinetics of zinc oxide nanoparticles on natural organic matter coated silica surfaces. *Journal of Colloid and Interface Science* **2010,** *350*, (2), 427-434.
22. Li, Z.; Sahle-Demessie, E.; Hassan, A. A.; Sorial, G. A., Transport and deposition of CeO2 nanoparticles in water-saturated porous media. *Water Research* **2011,** *45*, (15), 4409-4418.
23. Fatisson, J.; Domingos, R. F.; Wilkinson, K. J.; Tufenkji, N., Deposition of TiO2 Nanoparticles onto Silica Measured Using a Quartz Crystal Microbalance with Dissipation Monitoring. *Langmuir* **2009,** *25*, (11), 6062-6069.
24. Quevedo, I. R.; Tufenkji, N., Influence of Solution Chemistry on the Deposition and Detachment Kinetics of a CdTe Quantum Dot Examined Using a Quartz Crystal Microbalance. *Environmental science & technology* **2009,** *43*, (9), 3176-3182.
25. Jiang, X.; Wang, X.; Tong, M.; Kim, H., Initial transport and retention behaviors of ZnO nanoparticles in quartz sand porous media coated with Escherichia coli biofilm. *Environmental pollution* **2013,** *174*, 38-49.
26. Chowdhury, I.; Duch, M. C.; Mansukhani, N. D.; Hersam, M. C.; Bouchard, D., Deposition and Release of Graphene Oxide Nanomaterials Using a Quartz Crystal Microbalance. *Environmental science & technology* **2014,** *48*, (2), 961-969.
27. Chang, X.; Bouchard, D. C., Multiwalled Carbon Nanotube Deposition on Model Environmental Surfaces. *Environmental science & technology* **2013,** *47*, (18), 10372-10380.
28. Li, W.; Liu, D.; Wu, J.; Kim, C.; Fortner, J. D., Aqueous Aggregation and Surface Deposition Processes of Engineered Superparamagnetic Iron Oxide Nanoparticles for Environmental Applications. *Environmental science & technology* **2014,** *48*, (20), 11892-11900.
29. Lin, S.; Wiesner, M. R., Deposition of Aggregated Nanoparticles - A Theoretical and Experimental Study on the Effect of Aggregation State on the Affinity between Nanoparticles and a Collector Surface. *Environmental science & technology* **2012,** *46*, (24), 13270-13277.
30. Yi, P.; Chen, K. L., Influence of Surface Oxidation on the Aggregation and Deposition Kinetics of Multiwalled Carbon Nanotubes in Monovalent and Divalent Electrolytes. *Langmuir* **2011,** *27*, (7), 3588-3599.
31. Thio, B. J. R.; Zhou, D.; Keller, A. A., Influence of natural organic matter on the aggregation and deposition of titanium dioxide nanoparticles. *Journal of Hazardous Materials* **2011,** *189*, (1-2), 556-563.
32. Petosa, A. R.; Brennan, S. J.; Rajput, F.; Tufenkji, N., Transport of two metal oxide nanoparticles in saturated granular porous media: Role of water chemistry and particle coating. *Water Research* **2012,** *46*, (4), 1273-1285.
33. Godinez, I. G.; Darnault, C. J. G., Aggregation and transport of nano-TiO2 in saturated porous media: Effects of pH, surfactants and flow velocity. *Water Research* **2011,** *45*, (2), 839-851.
34. Afrooz, A. R. M. N.; Sivalapalan, S. T.; Murphy, C. J.; Hussain, S. M.; Schlager, J. J.; Saleh, N. B., Spheres vs. rods: The shape of gold nanoparticles influences aggregation and deposition behavior. *Chemosphere* **2013,** *91*, (1), 93-98.
35. El Badawy, A. M.; Aly Hassan, A.; Scheckel, K. G.; Suidan, M. T.; Tolaymat, T. M., Key Factors Controlling the Transport of Silver Nanoparticles in Porous Media. *Environmental science & technology* **2013,** *47*, (9), 4039-4045.
36. Chowdhury, I.; Cwiertny, D. M.; Walker, S. L., Combined factors influencing the aggregation and deposition of nano-TiO2 in the presence of humic acid and bacteria. *Environmental science & technology* **2012,** *46*, (13), 6968-6976.

37. Tripathi, S.; Champagne, D.; Tufenkji, N., Transport Behavior of Selected Nanoparticles with different Surface Coatings in Granular Porous Media coated with Pseudomonas aeruginosa Biofilm. *Environmental science & technology* **2011,** *46*, (13), 6942-6949.
38. Hong, Y.; Honda, R. J.; Myung, N. V.; Walker, S. L., Transport of Iron-Based Nanoparticles: Role of Magnetic Properties. *Environmental science & technology* **2009,** *43*, (23), 8834-8839.
39. Mattison, N. T.; O'Carroll, D. M.; Rowe, R. K.; Petersen, E. J., Impact of Porous Media Grain Size on the Transport of Multi-walled Carbon Nanotubes. *Environmental science & technology* **2011,** *45*, (22), 9765-9775.
40. Cai, L.; Zhu, J.; Hou, Y.; Tong, M.; Kim, H., Influence of Gravity on Transport and Retention of Representative Engineered Nanoparticles in Quartz Sand. *Journal of Contaminant Hydrology* **2015**.
41. He, F.; Zhang, M.; Qian, T.; Zhao, D., Transport of carboxymethyl cellulose stabilized iron nanoparticles in porous media: Column experiments and modeling. *Journal of Colloid and Interface Science* **2009,** *334*, (1), 96-102.
42. Kanel, S.; Goswami, R.; Clement, T.; Barnett, M.; Zhao, D., Two dimensional transport characteristics of surface stabilized zero-valent iron nanoparticles in porous media. *Environmental science & technology* **2007,** *42*, (3), 896-900.
43. Hotze, E. M.; Phenrat, T.; Lowry, G. V., Nanoparticle aggregation: challenges to understanding transport and reactivity in the environment. *Journal of environmental quality* **2010,** *39*, (6), 1909-1924.
44. Song, L.; Elimelech, M., Transient Deposition of Colloidal Particles in Heterogeneous Porous Media. *Journal of Colloid and Interface Science* **1994,** *167*, (2), 301-313.
45. Saiers, J. E.; Ryan, J., Colloid deposition on non-ideal porous media: The influences of collector shape and roughness on the single-collector efficiency. *Geophysical research letters* **2005,** *32*, (21).
46. Song, L.; Johnson, P. R.; Elimelech, M., Kinetics of Colloid Deposition onto Heterogeneously Charged Surfaces in Porous Media. *Environmental Science & Technology* **1994,** *28*, (6), 1164-1171.
47. Joo, S. H.; Al-Abed, S. R.; Luxton, T., Influence of Carboxymethyl Cellulose for the Transport of Titanium Dioxide Nanoparticles in Clean Silica and Mineral-Coated Sands. *Environmental science & technology* **2009,** *43*, (13), 4954-4959.
48. Kim, H.-J.; Phenrat, T.; Tilton, R. D.; Lowry, G. V., Effect of kaolinite, silica fines and pH on transport of polymer-modified zero valent iron nano-particles in heterogeneous porous media. *Journal of Colloid and Interface Science* **2012,** *370*, 1-10.
49. Elimelech, M.; Nagai, M.; Ko, C.-H.; Ryan, J. N., Relative Insignificance of Mineral Grain Zeta Potential to Colloid Transport in Geochemically Heterogeneous Porous Media. *Environmental Science & Technology* **2000,** *34*, (11), 2143-2148.
50. Johnson, P. R.; Sun, N.; Elimelech, M., Colloid Transport in Geochemically Heterogeneous Porous Media: Modeling and Measurements. *Environmental Science & Technology* **1996,** *30*, (11), 3284-3293.
51. Wang, D.; Su, C.; Zhang, W.; Hao, X.; Cang, L.; Wang, Y.; Zhou, D., Laboratory assessment of the mobility of water-dispersed engineered nanoparticles in a red soil (Ultisol). *Journal of Hydrology* **2014,** *519, Part B*, (0), 1677-1687.

52. Wang, Y.; Li, Y.; Kim, H.; Walker, S. L.; Abriola, L. M.; Pennell, K. D., Transport and retention of fullerene nanoparticles in natural soils. *Journal of environmental quality* **2010,** *39*, (6), 1925-1933.
53. Cornelis, G.; Pang, L.; Doolette, C.; Kirby, J. K.; McLaughlin, M. J., Transport of silver nanoparticles in saturated columns of natural soils. *Science of The Total Environment* **2013,** *463–464*, (0), 120-130.
54. Tong, M.; Ding, J.; Shen, Y.; Zhu, P., Influence of biofilm on the transport of fullerene (C-60) nanoparticles in porous media. *Water Research* **2010,** *44*, (4), 1094-1103.
55. Afrooz, A. N.; Khan, I. A.; Hussain, S. M.; Saleh, N. B., Mechanistic Hetero-aggregation of gold nanoparticles in a wide range of solution chemistry. *Environmental science & technology* **2013,** *47*, (4), 1853-1860.
56. Cerbelaud, M.; Videcoq, A.; Abélard, P.; Pagnoux, C.; Rossignol, F.; Ferrando, R., Hetero-aggregation between Al2O3 submicrometer particles and SiO2 nanoparticles: Experiment and simulation. *Langmuir* **2008,** *24*, (7), 3001-3008.
57. Huynh, K. A.; McCaffery, J. M.; Chen, K. L., Hetero-aggregation of multiwalled carbon nanotubes and hematite nanoparticles: Rates and mechanisms. *Environmental science & technology* **2012,** *46*, (11), 5912-5920.
58. Wang, Y.; Gao, B.; Morales, V. L.; Tian, Y.; Wu, L.; Gao, J.; Bai, W.; Yang, L., Transport of titanium dioxide nanoparticles in saturated porous media under various solution chemistry conditions. *Journal of Nanoparticle Research* **2012,** *14*, (9), 1-9.
59. Yang, H.; Tong, M.; Kim, H., Effect of Carbon Nanotubes on the Transport and Retention of Bacteria in Saturated Porous Media. *Environmental science & technology* **2013,** *47*, (20), 11537-11544.
60. Wang, X.; Cai, L.; Han, P.; Lin, D.; Kim, H.; Tong, M., Cotransport of multi-walled carbon nanotubes and titanium dioxide nanoparticles in saturated porous media. *Environmental pollution* **2014,** *195*, 31-38.
61. Cai, L.; Tong, M.; Ma, H.; Kim, H., Cotransport of titanium dioxide and fullerene nanoparticles in saturated porous media. *Environmental science & technology* **2013,** *47*, (11), 5703-5710.
62. Bronikowski, M. J.; Willis, P. A.; Colbert, D. T.; Smith, K.; Smalley, R. E., Gas-phase production of carbon single-walled nanotubes from carbon monoxide via the HiPco process: A parametric study. *Journal of Vacuum Science & Technology A* **2001,** *19*, (4), 1800-1805.
63. Saleh, N. B.; Pfefferle, L. D.; Elimelech, M., Aggregation kinetics of multiwalled carbon nanotubes in aquatic systems: measurements and environmental implications. *Environmental science & technology* **2008,** *42*, (21), 7963-7969.
64. Soejima, T.; Oshiro, S.; Nakatsuji, Y.; Ito, S., Dense aqueous colloidal gold nanoparticles prepared from highly concentrated precursor solution. *Journal of colloid and interface science* **2011,** *362*, (2), 325-329.
65. Georgakilas, V.; Voulgaris, D.; Vazquez, E.; Prato, M.; Guldi, D. M.; Kukovecz, A.; Kuzmany, H., Purification of HiPCO carbon nanotubes via organic functionalization. *Journal of the American Chemical Society* **2002,** *124*, (48), 14318-14319.
66. Fresnais, J.; Yan, M.; Courtois, J.; Bostelmann, T.; Bée, A.; Berret, J. F., Poly(acrylic acid)-coated iron oxide nanoparticles: Quantitative evaluation of the coating properties and applications for the removal of a pollutant dye. *Journal of Colloid and Interface Science* **2013,** *395*, (0), 24-30.

67. Vaisman, L.; Wagner, H. D.; Marom, G., The role of surfactants in dispersion of carbon nanotubes. *Advances in colloid and interface science* **2006,** *128*, 37-46.
68. Moore, V. C.; Strano, M. S.; Haroz, E. H.; Hauge, R. H.; Smalley, R. E.; Schmidt, J.; Talmon, Y., Individually suspended single-walled carbon nanotubes in various surfactants. *Nano Letters* **2003,** *3*, (10), 1379-1382.
69. Bradford, S. A.; Bettahar, M.; Simunek, J.; Van Genuchten, M. T., Straining and attachment of colloids in physically heterogeneous porous media. *Vadose Zone Journal* **2004,** *3*, (2), 384-394.
70. Li, Z.; Sahle-Demessie, E.; Hassan, A. A.; Sorial, G. A., Transport and deposition of CeO 2 nanoparticles in water-saturated porous media. *Water research* **2011,** *45*, (15), 4409-4418.
71. Chowdhury, I.; Duch, M. C.; Gits, C. C.; Hersam, M. C.; Walker, S. L., Impact of synthesis methods on the transport of single walled carbon nanotubes in the aquatic environment. *Environmental science & technology* **2012,** *46*, (21), 11752-11760.
72. Tian, Y.; Gao, B.; Morales, V. L.; Wang, Y.; Wu, L., Effect of surface modification on single-walled carbon nanotube retention and transport in saturated and unsaturated porous media. *Journal of hazardous materials* **2012,** *239*, 333-339.
73. Bouchard, D.; Zhang, W.; Powell, T.; Rattanaudompol, U.-s., Aggregation kinetics and transport of single-walled carbon nanotubes at low surfactant concentrations. *Environmental science & technology* **2012,** *46*, (8), 4458-4465.
74. Bradford, S. A.; Bettahar, M., Concentration dependent transport of colloids in saturated porous media. *Journal of Contaminant Hydrology* **2006,** *82*, (1), 99-117.
75. Kasel, D.; Bradford, S. A.; Šimůnek, J.; Heggen, M.; Vereecken, H.; Klumpp, E., Transport and retention of multi-walled carbon nanotubes in saturated porous media: Effects of input concentration and grain size. *water research* **2013,** *47*, (2), 933-944.
76. Saleh, N. B.; Pfefferle, L. D.; Elimelech, M., Influence of Biomacromolecules and Humic Acid on the Aggregation Kinetics of Single-Walled Carbon Nanotubes. *Environmental Science & Technology* **2010,** *44*, (7), 2412-2418.
77. Johnson, P. R.; Sun, N.; Elimelech, M., Colloid transport in geochemically heterogeneous porous media: Modeling and measurements. *Environmental science & technology* **1996,** *30*, (11), 3284-3293.
78. Saiers, J. E.; Lenhart, J. J., Ionic-strength effects on colloid transport and interfacial reactions in partially saturated porous media. *Water Resources Research* **2003,** *39*, (9), 1256.